Validation of the shear capacity of a CRC console without stirrups

T.S. Jaspers Focks

Pieters BOUWTECHNIEK

HiCON HIGH PERFORMANCE CONCRETE

TU Delft

Validation of the shear capacity of a CRC console without stirrups

by

T.S. Jaspers Focks

to obtain the degree of Master of Science
at the Delft University of Technology,

to be defended publicly on Friday March 1, 2019 at 13.45 PM.

Student number:	4158393	
Project duration:	February 26, 2018 – March 1, 2019	
Thesis committee:	Prof. dr. ir. D.A. Hordijk,	TU Delft, chairman
	Dr. ir. Drs. C.R. Braam,	TU Delft, main supervisor
	Dr. ir. M.A.N. Hendriks,	TU Delft, supervisor
	Ir. L.J.M. Houben,	TU Delft, coordinator
	Ir. C.F. Bosveld,	Pieters Bouwtechniek, supervisor

This thesis is confidential and cannot be made public until March 1, 2024.

TU Delft Delft University of Technology

HiCON HIGH PERFORMANCE CONCRETE

Pieters BOUWTECHNIEK

Abstract

Engineering firm Pieters Bouwtechniek Delft has designed many cantilevering elements in *Compact Reinforced Composite* over the past years. This material, often abbreviated as CRC, is an UHPFRC developed by Hi-Con Denmark and the material distinguishes itself from other concretes as it incorporates large volumes of steel fibres and reinforcement steel. As a result it is a ductile concrete type with outstanding crack controlling properties. One of the challenges met during designing with CRC is the fact that the Eurocode does not implement the improved properties of the material, such as the improved post-cracking response which is a result of the addition of fibres. This results in designs often requiring stirrups in order to comply with the Eurocode with regard to the shear capacity and the prevention of brittle failure.

An example case where this problem was faced, is in the design of the landing platform in a staircase for the Raqtan project, engineered by Pieters Bouwtechniek. This design consist of a cantilevered platform, connected to a wall via a console. The Eurocode requires the addition of stirrups, while it is expected that these stirrups are not required in order to provide a sufficiently safe design. Therefore the following question was raised: *Were stirrups required in the console in the design of the Raqtan landing platform in order to obtain a level of safety as required by the Eurocode?* This report researched the structural response of the element without the application of stirrups in order to answer this question and determine whether the safety standards as stated in the Eurocode are met.

The design without the stirrups is validated in three ways. The first method is by application of multiple design standards which incorporate a contribution by the fibres, such as the *Model Code 2010* and the renewed French annex to the Eurocode. Most codes did not validate the design and predicted shear failure before the design load was reached. The French annex did validate the application of the design without stirrups. This is a result of the underlying principles used for this approach: the French guideline bases the tensile behaviour of the UHPFRC on the uni-axial tensile curve, while the other guidelines are based on the flexural tensile curve.

The second validation method was through the Finite Element Method. Multiple tensile models were validated against previous experiments and were then used to determine the structural response and ultimate capacity of the Raqtan element. The models failed in bending at a capacity above the design load, thus validating the design. After the results were analytically validated, a variation study was performed on the influence of certain model properties on the structural response. The variations, such as the boundary conditions and mesh configuration, did not significantly influence the ultimate capacity. This analysis validated the application of the design without stirrups.

The third and last validation was performed by testing multiple elements in the lab to find the actual capacity. Both elements without and with stirrups were tested to compare the resulting change in structural response. Some elements were reinforced to increase the bending capacity by at least 50%, as the FE models predicted failure in bending even when mean material properties were applied. The reinforced elements did not fail in shear as well, which demonstrated that the bending moment capacity was not only governing, but also significantly lower than the shear capacity. The derived design values for the ultimate load resulted in sufficient capacity for the element to resist the design loads.

Combining the performed validations, it is concluded that the element's shear capacity was not governing for the ultimate resistance as it was at least 50% higher than the found the bending moment capacity. This bending moment capacity was sufficient according to all applied codes. When this capacity is taken as the total capacity of the element, it can be stated that the element complies with the codes and therefore provides a level of safety as required by the Eurocode.

keywords: Compact Reinforced Composite, CRC, Ultra High Performance Fibre Reinforced Concrete, UHPFRC, stirrups, shear, Raqtan, design validation, design codes, FRC, Fibre Reinforced Concrete

”Stay hungry, stay foolish.”

- Steve Jobs, 2005

Preface

The research subject for this thesis is found in cooperation with Pieters Bouwtechniek and their Danish partner Hi-Con. Together they design and construct elements, such as balconies and stairs, in Compact Reinforced Composite (CRC). This innovative material is developed by Hi-con and possesses superior properties compared to traditional concrete. The incorporation of a large amount of steel fibres and reinforcement steel combined with a micro-mechanically tailored matrix results not only in a high compressive strength, but also in a remarkable ductility and durability, making this material fit for a broad scope of structural applications. Researching such a material and its structural behaviour allowed me to gain better understanding of the mechanical properties of concrete. Therefore I would like to thank Pieters Bouwtechniek and Hi-Con for providing me with this opportunity. Both parties supported me throughout the research, both in knowledge, space and time and welcomed me like any other employee. Thanks for answering all my questions, providing a critical opinion regarding my work and investing in me to enable the lab experiments.

I also have to express my gratitude to everyone from the TU lab who helped me in the preparation of, and during, the experiments. In this context Albert Bosman deserves a special note for his patience and help with all my requests. I really enjoyed my time in the laboratory and learned much about the practical approach required to perform experiments and retrieve useful data from them. Thanks also to Rempt van der Donk and his colleagues for taking the time to meet with me and discuss their view on the Raqtan project and design.

I would also like to thank the members of my committee individually. Chris Bosveld, who always had time for my questions, which reached from execution basics to the explaining the design codes used during the engineering of elements such as in the Raqtan project. René Braam, for his valuable insights and taking the time to discuss the questions I had, both theoretical and practical in preparation for the experiments. Max Hendriks, for always having time for me to drop by and shortly discuss the challenges I faced. Dick Hordijk, for providing critial, but constructive feedback to my research, which forced me to be more critical myself and therefore kept me challenged to perform the best I could.

Finally I would like to thank my friends and family, for listening to my endless stories about my obsession with concrete, large structures and my research.

Thank you all for providing me with a great opportunity to perform the thesis research as I had my in mind.

T.S. (Thijmen) Jaspers Focks
Delft, February 2019

Contents

1

Introduction

Engineering firm Pieters Bouwtechniek (PBT) cooperates with the Danish company Hi-Con to design and construct with the material CRC®, or Compact Reinforced Composite. This innovative material is developed by Hi-Con and possesses superior properties compared to traditional concrete. The incorporation of a large amount of steel fibers and reinforcement steel combined with a micro-mechanically tailored matrix results not only in a high compressive strength, but also in a remarkable ductility and durability, making this material is fit for a broad scope of structural applications.

In 2017 Pieters Bouwtechniek designed a CRC staircase for a project named Raqtan in Dammen, Saudi Arabia, as shown in Figure 1.1. This design included a CRC landing platform, which was clamped in the wall via two consoles. Part of the design is shown in Figure 1.2, where the landing platform is the centre element. The elements are only connected to the central spine (an elevator shaft) and are unsupported in the other directions.

The design was made in compliance with the Dutch design codes (the Eurocode with the Dutch annex) to obtain a sufficient level of safety. The landing platform was designed to be connected to the wall using two 250 mm wide consoles and according to the used code the shear forces resulted in the requirement of shear reinforcement, also called stirrups. The application of the stirrups is shown in Figure 1.3 and in Figure 1.4.

The engineers from Pieters expected a design without the stirrups to meet the level of redundancy that the Eurocode tries to accomplish as well. This expectation is based on previous experience with the material CRC in other projects and test loadings, and it is further fuelled by the neglect of the effect

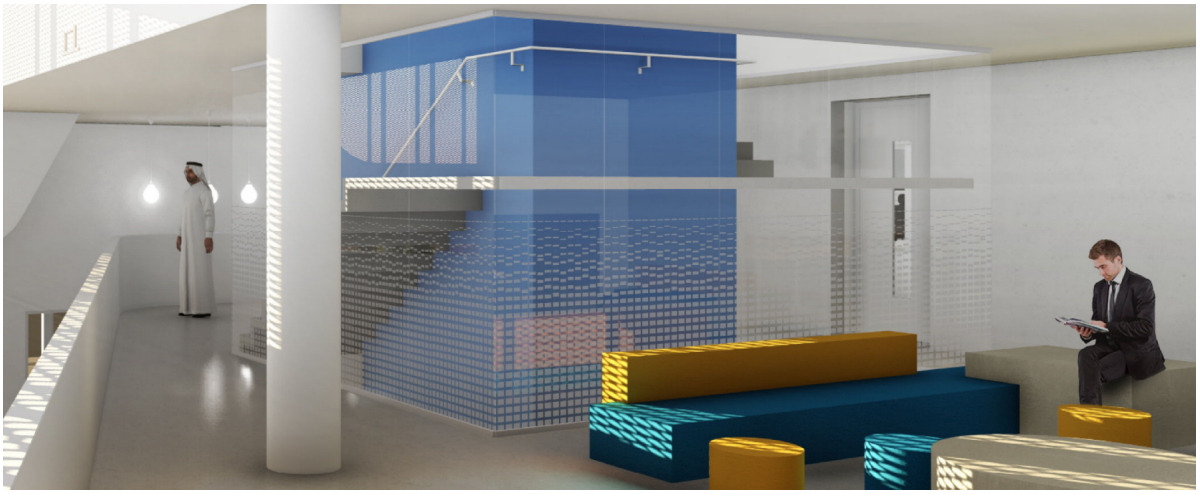

Figure 1.1: Impression of the CRC stairs as designed by Pieters and Hi-Con. (source: Rempt van der Donk)

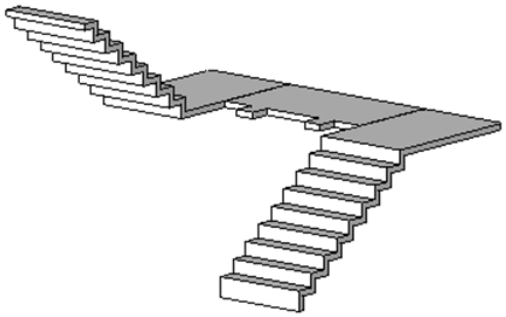

Figure 1.2: General overview of the Raqtan design. The landing platform is the centre element.

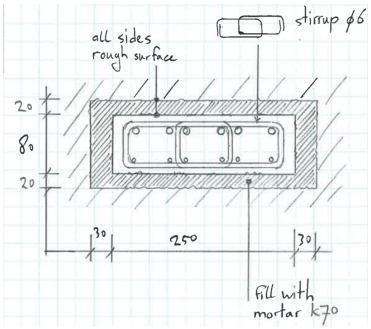

Figure 1.3: Cross section of the console connected to the wall. Dimensions in *mm*. (source: [27, p.121])

of steel fibres in the Eurocode, while they play a major role in the structural behaviour of CRC. The application of stirrups in such a slender design also results in dense reinforcement designs, with in this case 10 stirrups within 200 mm. The bend radius of the stirrups also influences the placement of the main reinforcement, raising the question whether or not the stirrups are actually activated properly after crack initiation, due to their small size and close centre-to-centre distance (45 mm).

Knowing the true capacity can result in a better understanding of the actual structural behaviour of an element. It helps with predicting the expected failure mechanism and can result in more efficient designs with reduced material usage. It also allows for the construction of even more slender structures, while maintaining an accepted level of structural integrity.

The idea that the Eurocode underestimates the shear capacity of CRC is also met during the design of other cantilevering elements in CRC, such as stairs or balconies. Therefore it was decided to research the actual capacity of such elements, in this case with a specific focus on CRC element as it was designed for the Raqtan project.

State of the art

Research into usage of fibres as minimal shear reinforcement [21], shows good potential and over the past decades many experiments have been performed to determine a relation between the application of steel fibres and the shear capacity of beams without stirrups [19]. Some design codes, such as the *fib* Model Code 2010 [20] and German guidelines [44] have incorporated methods to determine the shear capacity while including a fibre component. Research into the structural effects of steel fibres is ongoing and the quality of the models to predict the enhanced properties, such as cracking [16] and shear response [15], is still improving.

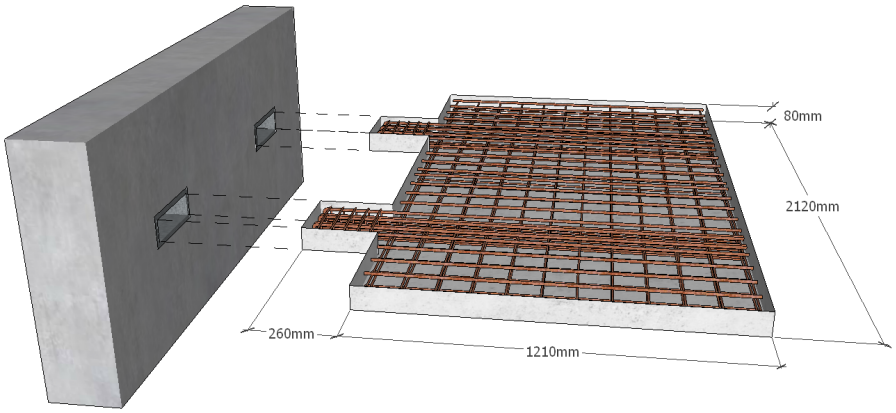

Figure 1.4: General overview of the dimensions of the landing platform with the rebar design.

2

Research definition

The aim of the research is to determine whether the design of the Raqtan landing platform without stirrups can be used while maintaining a level of safety which meets the modern standards. The boundary conditions of the slab are investigated and multiple structural models are considered to determine the capacity. Within this study, the Raqtan landing platform refers to the CRC element, consisting of a plate with two consoles, and the connection to the wall is considered as a boundary condition.

Research subject:
A case study on the requirement of stirrups in the console of a cantilevering CRC element: The Raqtan landing platform.

Problem definition:
The Raqtan landing platform is designed according to the Dutch design codes, which resulted in the requirement of stirrups in the console. This results in dense and complex reinforcement details, while it is expected that the structure will meet the level of safety required by the code, even if the stirrups are not added.

Purpose of this thesis:
The purposes of this thesis are:

- Gain more insight in the shear capacity of the Raqtan landing platform as predicted by the Dutch design codes, the Eurocode and alternative codes in relation to the actual capacity.
- Determine the actual capacity of the Raqtan landing platform in ULS with and without stirrups.
- Determine which design code predicts this capacity most realistic, based on the results of the actual capacity and the structural models used for the codes.
- Determine the design resistance of the elements without stirrups by *Design by testing*.
- Make recommendations regarding further research.

This can be summarised in the main purpose:

> *Determine whether the application of stirrups in the Raqtan case is required to obtain a level of safety as required by the Eurocode.*

Research question:
The purpose of this research will be fulfilled by answering the following main research question:

> *Were stirrups required in the console in the design of the Raqtan landing platform in order to obtain a level of safety as required by the Eurocode?*

This question will be answered using the by means of answering the sub-questions:

1. Is shear failure the governing failure mechanism for the Raqtan landing platforms when no stirrups are applied?
2. What would the actual capacity of the Raqtan landing platform be if the stirrups are excluded from the design?
3. What is the actual capacity of the Raqtan landing platform without stirrups in relation to the capacity as predicted by multiple design codes?

2.1. Methodology

In this chapter the different elements of the research methodology will be elaborated on. The complete research can be split into three main parts: literature review, design validation, and conclusions. Figure 2.1 provides a schematic overview of the methodology.

Part I: Literature review
The first part will focus on the state of the art by means of a literature research, which should provide insight in the different fundamentals of this research. The researched topics are:

- The material: CRC. This part will focus on the history of this type of concrete and its structural behaviour. The focus will be on the properties in which CRC distinguishes itself from other types of concrete.
- The behavior: Shear. This part will focus on the shear capacity of structural elements, with a special focus on the models which have been developed for fibre reinforced concretes and the assumptions which are made to justify these models.
- The methods: Design codes. This part will focus on the way structural integrity is currently determined using design guides such as the Eurocode. The purpose and use of such documents will be elaborated on.
- The application: The Raqtan landing platform. This part will focus on the currently applied design methods as they are used by Pieters Bouwtechniek to design the element. This in done in order to be able to explain the current design process and the resulting limitations which are imposed on the design of the platform.

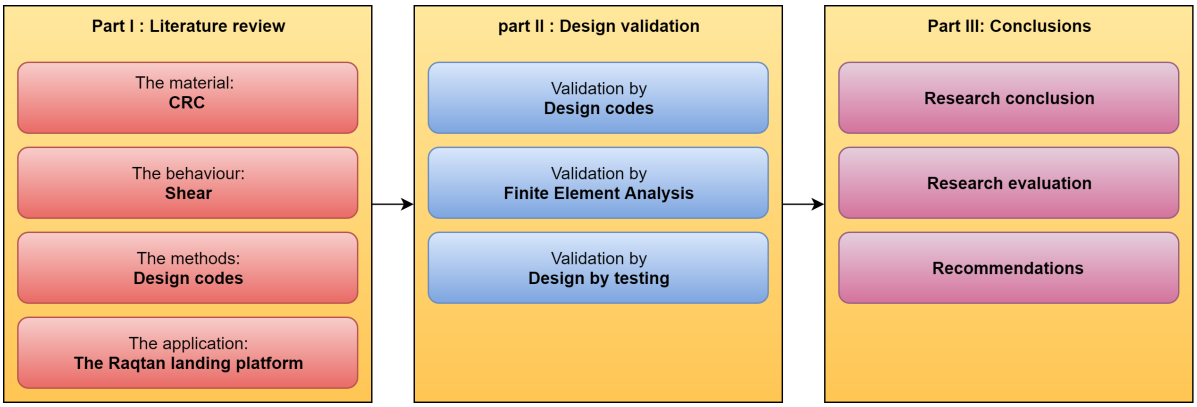

Figure 2.1: Schematic overview of the research methodology.

Part II: Design validation
The second part of the research is about the validation of the design without the stirrups in order to determine whether or not the stirrups are required to obtain a sufficient level of safety. The design load will be determined and compared to the design capacity, which is derived in three different ways:

- By design codes: different design codes have their own limitations and simplifications in order to be widely applicable. The design is verified by multiple codes and their models will be investigated in order to determine the applicability of the different codes. Multiple codes and guidelines will be used to determine the design capacity of the Raqtan landing platform.
- By numerical analysis according to the Finite Element Method (FEM): The design will be modelled in a FE application to study its response to the design loads and determine the limitations to load resistance. The different possibilities regarding model input will be analysed as well as their influence on the predicted failure load and failure behaviour. This give a more accurate prediction of the actual structural behaviour of the element compared to the analytical approach.
- By Design by Testing: The Eurocode also provides a method which allows the direct determination of the design capacity by means of experimental tests. This method involves the determination of the capacity with the proper safety margins based on experimental data.

These results from the experiment can be used to validate the outcome of the FEA as well, which is required as the application of such an analysis does not result in direct design values. This calibration is an important step in the application of FEA.

Part III: Conclusions
The final part of the research will focus on the results of the previous part and conclusions will be drawn regarding the validation of the design without the stirrups in comparison to the original design. The research itself will be evaluated and the research questions will be answered.

I

Background

3

The material: CRC

This chapter focusses on the properties of the material used for this research: Compact Reinforced Composite, often abbreviated as CRC. First a short history of the material is provided, followed by the most important material properties.

3.1. Development of CRC

The word concrete origins from the Latin word *concretus*, which can be translated as *shape by compaction* or *grown together* [34] and is often used to refer to a material that is created by the combination of multiple other materials. The first known application of such a material occurred in Israel, around 9000 years ago on the floor of a hut. The material was used during the the thousands of years that followed and the application allowed for example the Romans from 300BC onwards to create shapes which were hard to accomplish using other techniques such as stonecutting. After the fall of the Roman empire the knowledge on how to create concrete was forgotten for almost a millennium. It was not until 1678 that the process to create concrete was used again, as Joseph Moxom found a method to convert lime into a stone-like material. It then took another century for the possibilities of the material to be put to efficient use, as the famous British engineer John Smeaton used limestone to create a hydraulic cement and used it for the construction of the Eddystone Lighthouse in 1756. Fast-forward another century and the cement industry is growing and Joseph Aspdin patented a process of heating clay and chalk together and grinding it in 1824. The result is a material known as Portland cement. [39]

The properties of concrete are such that it performs well under compression, but not so well under tension. The understanding of this behaviour can be seen in the use of compression arches, such as Pont du Gard in France. A main improvement to these material properties is often credited to a French engineer and gardener, named Joseph Monier. He reinforced his pots with fine iron rods to prevent them from breaking. This allowed the composite material to resist tension stresses largely exceeding those of the concrete cracking stresses. The first proper use of reinforced concrete in construction is thought to be done by William Wilkinson in 1854, proven by his patents which strategically placed iron strips in concrete elements [41].

From here on the challenge became to improve and tailor the material properties, such as compressive strength. An important step was made by A. Abrams Duff in 1918 as he noted the relationship between the water/cement ratio (w/c ratio, also known as water/binder ratio) and compressive strength. Increasing the compressive strength by lowering the w/c ratio much far resulted in a concrete mix with a low workability, which is unsuitable from application. The invention of super-plasticiser in the 1970s resulted in a workable mixture while keeping the w/c ratio low. As a result it became possible to produce concrete with strength classes of C100/115 [10]. This solved the workability limit of HPC, but another problem arose: The decrease in w/c ratio resulted in an increase in brittleness of the concrete matrix [14]. This problem was tackled by H.H. Bache in 1986 by heavily increasing the amount of steel in the mixture. Not only increasing the amount of regular reinforcement steel, but also adding high volume percentage of steel fibres to the mix resulted in a mixture called Compact Reinforced Composite (CRC) [1].

Besides CRC there are multiple mixtures developed which have similar properties, such as RPC, which stand for Reactive Powder Concrete, developed by Bouygues in 1994; or Multi Scale Cement Composite (MSCC). The differences in these mixtures lie within the exact composition, the type and volume percentage of fibres used, but their general behaviour is not that different. This results in these type of mixtures being grouped under the label Ultra High Performance Fibre Reinforced Concrete, or UHPFRC. There is no precise definition of UHPFRC, but commonly accepted required material properties are [5]:

- A compressive strength exceeding 150 MPa
- Direct tensile strength exceeding 7 MPa
- w/c ratio lower than 0.25
- High content of binder, resulting in a dense matrix
- Fibres to ensure ductile behaviour

After the development of CRC in the 1980s it took some time to study the material properties and in 1995 the material became commercially available. This research is documented in multiple reports, of which the following are the most important:

- Final Technical Report - MINImal STRUCTures using ultra high strength concrete [22]
- MINISTRUCT - Task 5: Structural analysis [23]

The following sections are largely based on these documents.

3.2. Production and composition of CRC

The production of CRC starts with the mixing of the different components. Every component has its unique properties which influences the resulting concrete composition, also called the concrete matrix, and thereby the (mechanical) properties of CRC. A CRC mixture contains the following components: CRCbinder, water, aggregates, fibres, silica fume (SF) and super-plasticiser. The influence of the different components will be treated separately.

3.2.1. Production

The mixing procedure takes a total of 8 minutes and can subdivided in the following steps:

- **Dry mixing:** The coarse aggregates and the binder are mixed.
- **Addition of water:** The water is added to the mixture.
- **Fluidification:** The mixture is mixed for multiple minutes to fluidify the dry components.
- **Fibre introduction:** The fibres are added.
- **Homogenisation:** The mixture is homogenised by multiple minutes of mixing.

To further densify the concrete matrix it is possible to vibrate the mixture once poured in the mould. The required effort for vibration is reduced by the addition of super-plasticiser, which greatly improves the workability of the mixture. Due to a high viscosity of UHPFRC mixtures it is required to use smaller frequencies (80 Hz, or 4800 Vibrations Per Minute (VPM) instead of the more common range of 8500-12500 VPM [25]) and higher amplitudes to obtain optimal results.

3.2.2. Cement

Cement might be the most important component of concrete. This material hydrates in the presence of water, resulting in a cement paste which connects the other elements in the concrete matrix. Most of the concrete mixtures, including CRC, are based on Portland cement, as the proterties are competitive for most strength classes and the price is relatively low. The low Tricalcium aluminate (C_3A) content is advantageous as well, as this results in a lower water demand [5].

The concrete mixtures for UHPFRC contain about double the amount of cement as used for regular concretes. As not all the cement reacts during the hardening of the concrete, there is still cement left which can react when cracking occurs, providing for the self-healing properties of CRC.

In recent years the environmental discussion is gaining momentum. This is having an impact on the use of certain types of cement. The production of Portland cement is especially harmful for the environment. Per kilo of Portland concrete 0.82 kg of carbondioxide (CO_2) is emitted. This results in 5-7% of the global CO_2 emissions [43]. The consequences of the application of such cements should be kept in mind during the design process.

3.2.3. Water

Water is the component which activates the hydration process of the cement, which in turn results in the cement paste. The most important parameter regarding the water component is the w/c ratio. This ratio has, as previously mentioned, a large influence on the compressive strength which can be achieved. Lowering the water content of the mixture results in a higher viscosity, and therefore and lower workability. This again limits the application of the material. A typical CRCmixture has a w/c ratio in the range of 0.15-0.20.

3.2.4. Aggregates

In normal strength concretes the aggregates are used to provide volume to the mixture. With higher w/c ratios the strength of the concrete matrix is governed by the strength of the inter-facial transition zone (ITZ), this is the connection between the coarse aggregates and the cement paste. For lower w/c ratios the strength of the aggregates themselves become governing. Therefore it is important to use aggregates with a high mechanical strength [5]. In CRC this is Quartz.

The maximal aggregate size in UHPFRC is often smaller than for regular concrete, as the maximal aggregate size heavily influences the distribution of the fibres [17], as shown in Figure 3.1. The maximal aggregate size in UHPFRC is often 8 mm.

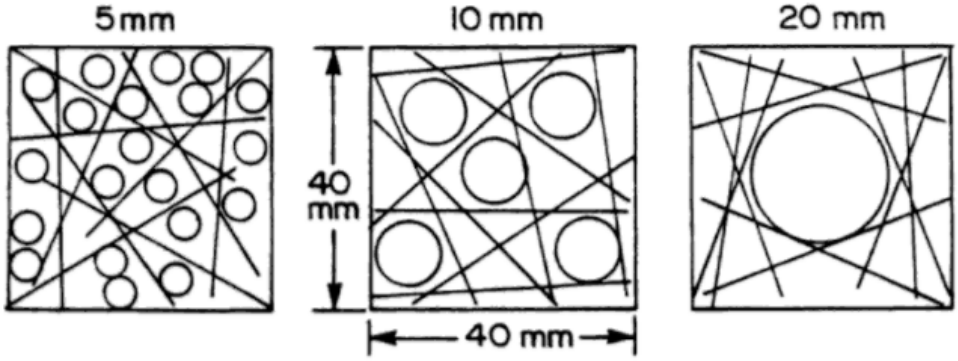

Figure 3.1: The effect of particle size on the fibre arrangement in the concrete matrix. (source [17, p.170])

3.2.5. Fibres

The large volume percentages of fibres which are added to the mixture have a large impact on the mechanical properties of the CRC. Without the fibres the mixture would be extremely brittle, which is a dangerous property as failure can occur without a warning. The addition of fibres results in a ductile material, while maintaining the high performance of other properties such as durability and strength.

Many different types of fibres became available over the past decades as experiments have been performed on many different materials for fibres, from natural (jute, bamboo) or mineral (rock-wool) to man-made (such as glass, Kevlar or steel). The most commonly used materials for fibres have a high tensile strength and modulus of elasticity. This combination results in a significant improvement of the post-cracking behaviour of the composite [26]. CRC is based on steel fibres as this is a well-known material with the required properties.

Another important property of the fibres is their shape. Besides the most commonly used straight fibres, there are also hooked and twisted fibres available. Figure 3.2 shows different types of fibres which are available. Most deviations from the straight shape are introduced to improve the bond stress. CRCuses the first generation of fibres, the straight fibres. Even though the bond stress might be lower than other

configuration, this fibre has the advantage of workability, as the straight fibre does influence flow the least. Another advantage of the straight fibre are the costs, as it is less (mechanical)labour intensive to produce the fibres.

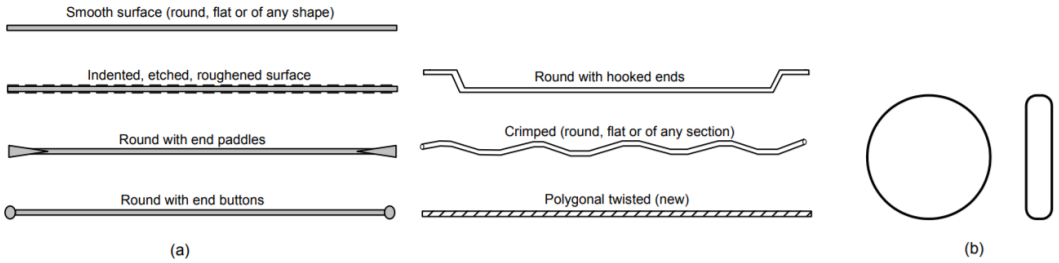

Figure 3.2: Different available fibres types: a) fibre shape; b) fibre cross-section. (source [26, p.241])

The fibre dimensions also greatly influence the structural effect it has on the concrete matrix. The diameter is usually between 0.4 and 0.8 mm and the length between 25-60 mm. The structural behaviour is often linked to the aspect ratio of the fibre, length/diameter, and usually ranges from 40-80. The fibres in CRC have a diameter of 0.4 mm and a short length of 12.5 mm, resulting in an aspect ratio of only 31.25. This short length has the advantage that the fibre orientation remains almost random. Longer fibres tend to follow the direction of the mold due to the wall effect [39], as shown in Figure 3.3. The final fibre orientation is also influenced by the flow direction of the concrete when being poured. This effect is also smaller for smaller fibres. These factors can play a major role when the dimensions of the cast elements are thin, resulting in a preferred orientation for the fibres.

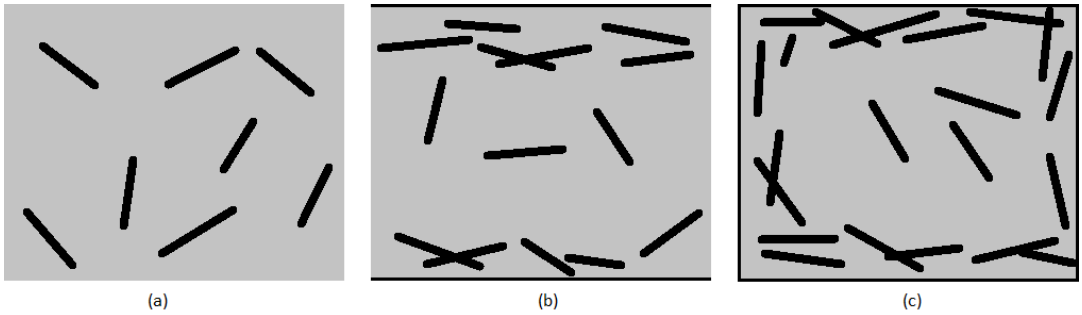

Figure 3.3: The wall effect for fibres: a) Random distribution due to the lack of boundaries; b) Bounded by the top and the bottom, resulting in a parallel orientation; c) Bounded at all sides, further altering the fibre orientation. (source: based on [39, p.34])

The last parameter regarding fibres which has a significant impact on the final material properties is the fibre content, usually measured in volume percentage, V_f. Increasing the fibre content does increase the ductility of the material, but the maximal fibre content is often limited by the workability. Short straight fibres allow for a maximum fibre content of up to 20% for specific concretes such as SIFCON (slurry-infiltrated-fibred concrete), but the limit for premixed concrete is around 11%. Longer and more complex fibres result in a maximum fibre content of 2-3%. The fibre content for CRCis around 2%, which results in a tough material.

3.2.6. Silica fume

Silica fume (SF) is added to the mixture to act as a micro filler. With a diameter in the range of 0.1-0.2 μm, the average particle size of SF is about 1/100 of a cement particle (1-50 μm) and about 20 times smaller than the average ITZ thickness. As a result the SF is able to fill the voids between the larger elements and therefore improving the ITZ between the cement, the aggregates and the fibres, as shown in Figure 3.4 [12]. This reduction in voids results in a significant increase in strength. A further increase in strength is achieved as SF reacts with calcium hydroxide (CH) and forms CHS, Calcium-Silicates-Hydrates, which are significantly stronger [5].

Filling the voids in the matrix with particles in stead of water, results in a lower demand for water and also reduces the porosity of the concrete matrix, which improves the durability of the material. It becomes harder, or even impossible, for water and chloride molecules to intrude the material. Which results in a reduction of the required concrete cover.

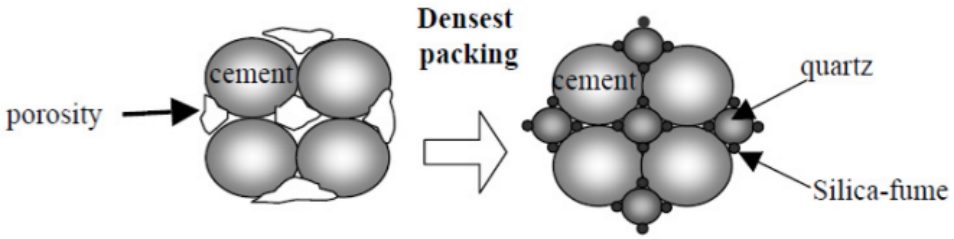

Figure 3.4: The effect of particle size on packing density. (source [5, p.12])

3.2.7. Super-plasticiser

Reducing the water/binder ratio is beneficial for the mechanical strength of the hardened material, but during the casting it imposes some practical challenges as the workability is reduced. This is due to an increase in viscosity and it prevents the concrete from flowing and properly distributing throughout the form work. Super-plasticiser is added to the mixture as it prevents the cement particles from joining together during the casting and therefore increases the liquidity of the mix [36].

3.3. Material properties of CRC

The following section focusses on the material properties of CRC. Special attention is given to the differences in performance between regular concrete and this type of UHPFRC.

3.3.1. Uniaxial Compressive behaviour

The previously provided definition of UHPFRC states a uniaxial compression strength in the order of magnitude of 150 MPa or higher. The increasing compressive strength resulted in brittle failure as soon as the limit value was achieved when te concrete was not reinforced. This is clearly shown in the results of an experiment performed by Hassan et al.[13] as shown in Figure 3.5. The same figure also shows the difference when fibres with similar properties as those used in CRC (straight steel fibres, $L = 13$ and $d = 0.2$) are added to the mixture with a fibre content of 2%.

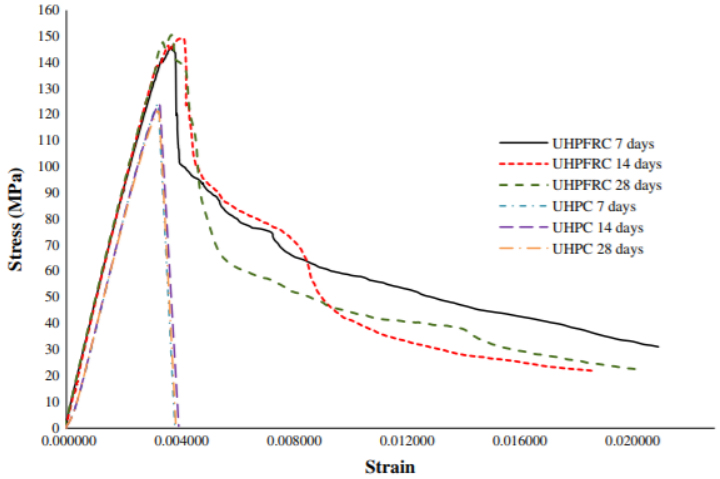

Figure 3.5: Compressive stress-strain curve for UHPC and UHPFRC. (source [13, p.879])

The addition of fibres resulted in a an increased ultimate stress, in this case with 10% to 20%, but the most significant change is in the post-peak behaviour. The fibres allow the concrete to absorb

energy when crack propagation initiates, resulting in a more ductile behaviour of the material. The type of fibre used in the mixture influences the descending branch of the compressive stress-stain curve. The combination of fibre content, length, diameter and orientation determine the energy which can be absorbed [9].

The mean compressive strength of CRC is determined based on multiple experiments. At a maturity of 28 days it has a value of $f_{cm} = 130$ MPa. The following formula is derived in order to determine the value at varying maturities ($M_{20} < 200$ days), based on curing temperature of $20°$:

$$f_{cm}(M_{20}) = 130 + 32 \cdot log(\frac{M_{20}}{28}) \text{ MPa} \tag{3.1}$$

The coefficient of variance (COV) for the uniaxial compressive strength is empirically determined to be 7%. The characteristic value, f_{ck} for a 5% fractile can then be determined:

$$f_{ck} = (1 - 1.64 \cdot 0.07) \cdot f_{cm} \approx 115 \text{ MPa} \tag{3.2}$$

It should be noted that these values are found for cylindrical test samples, which means that should be divided by 0.9 to get the cubical strengths. The addition of fibres to the mixture results in a ductile failure, as can be seen in Figure 3.6, similar to the behaviour in Figure 3.5.

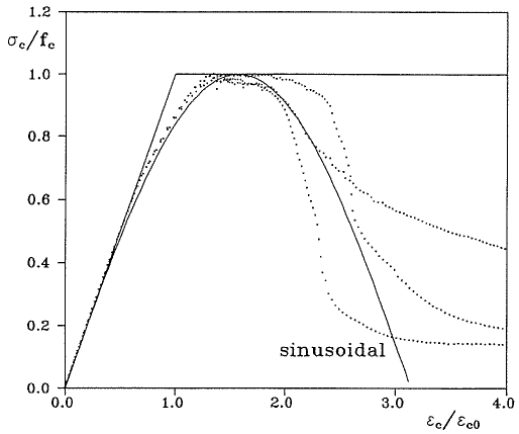

Figure 3.6: Normalised stress-strain relation for CRC. (source [23, p.6])

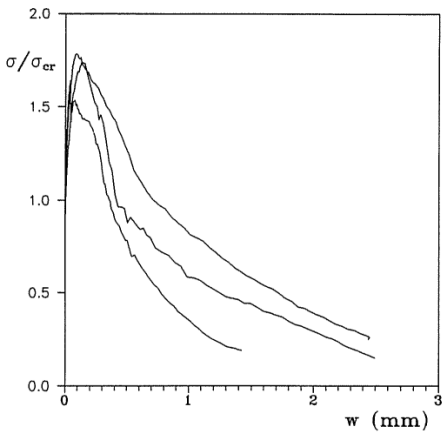

Figure 3.7: Normalised stress-displacement curve for CRC. (source [23, p.7])

3.3.2. Tensile behaviour

The addition of fibres also greatly improves the tensile behaviour of UPHC. The brittle failure of UHPC is replaced by a more ductile response. The UHPC matrix fails at the occurrence of the first crack and is unable to provide any resistance afterwards, while in the fibre reinforced material the fibres can still resist a significant stress, sometime almost double that of of the unreinforced UHPC [13].

The stress-crackwidth curve of a typical UHPFRC is described by three phases, as visible in Figure 3.8:

- **Phase 1, The uncracked response:** In this phase the concrete is in a linear-elastic state. The material behaves stiffer then it would without the fibres as the modulus of elasticity can be increased by $6 - 10\%$ [13].
- **Phase 2, Cracking formation:** As the exposed stress exceeds the cracking stress of the concrete matrix the steel fibres are activated. While bridging the cracks, these fibres keep the cracks small and allow for further spreading of the cracks. The composite action between the fibres and the concrete matrix is responsible for the concrete residual strength during this phase. The post-cracking behaviour is again mainly determined by the type and amount of fibres used [9].
- **Phase 3, Fibre action:** In the last phase the fibres are solely responsible for the residual strength. An increase in stress results in elongation of the fibres and finally in pulling out of the fibres, as the bond stress is exceeded.

The CRC matrix has a crack stress of $\sigma_{cr} = 7.0$ MPa, while the fibres allow for a maximal stress increase of $50\% - 75\%$, as seen in Figure 3.7. After the ultimate stress is reached the curve immediately shows softening, as a result of the short fibres which are used. These fibres do no have to ability to bridge the crack for long.

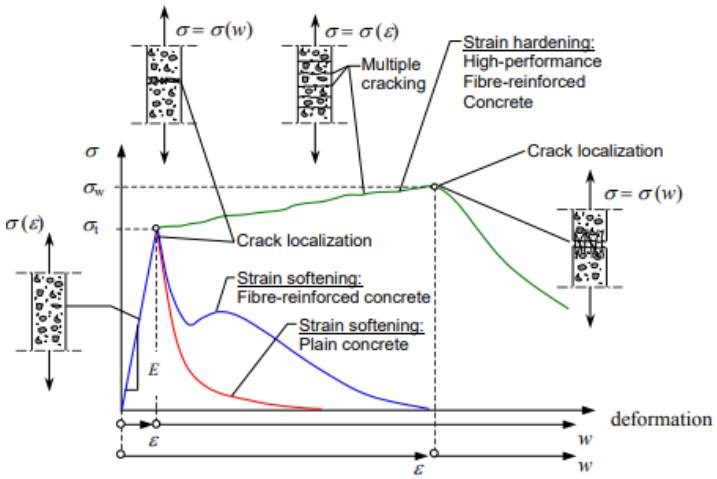

Figure 3.8: Stress-displacement curve for UHPC. (source [16, p.2])

3.3.3. Flexural behaviour

The flexural behaviour of UHPFRC can be split in to four phases [39], as visualized in Figure 3.9:

- **Phase 1, The uncracked phase:**. During this phase the flexural member behaves as it would without fibres. The entire concrete cross-section is effective. As the load is increased the tensile stresses in the bottom section will increase up until the cracking stress of the concrete matrix.
- **Phase 2, The linear-elastic cracked phase:** In this phase the first micro-cracks occur at the bottom section as the stresses in the matrix exceed the cracking stress. The fibres are activated as soon as the crack occurs and take over the tensile stresses which were previously transferred through the concrete matrix. As the load is further increased the cracks propagate to the centre of the element and the formed cracks widen. The neutral axis starts to move towards the compression zone. The maximum crack width in this phase ranges from 0.1 to 0.3mm.
- **Phase 3, The non-linear cracked phase:** As the load is further increased the elements starts to show non-linear, plastic behaviour. This is caused by increasing width of the cracks, which results in loss of bridging fibres as the anchor length becomes too small. There are still enough fibres crossing the crack to transfer the load, but as the load increases, the number of activated fibres decreases.
- **Phase 4, The fibre pull-out phase:**. During this phase the outer tensile section contains cracks which are too wide for any fibres to bridge. The loss of activated fibres results in the tensile capacity of these cracks to be reduced to zero and the neutral axis moves further up. This process continues until failure, as the element becomes unable to resist the opposed load.

Different matrix configurations can result in completely different shapes of the load-deflection curve. Two such curves for notched CRC beams ($100 \times 100 \times 420$ mm, notch$= 50$ mm) are shown in Figure 3.10. These curves clearly show the ductile behaviour of CRC.

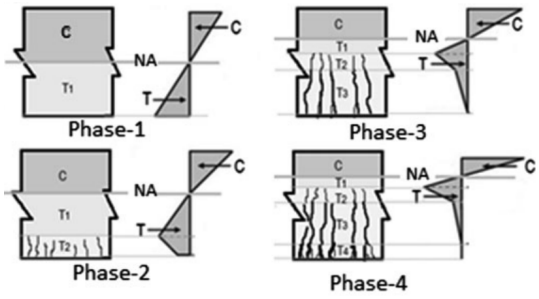

Figure 3.9: Different phases of UHPC under flexural loading. (source [39, p.62])

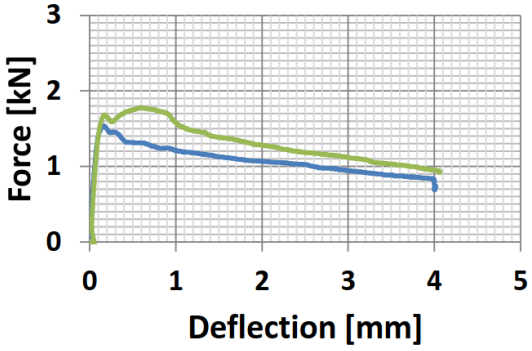

Figure 3.10: Flexural behaviour of CRC. (source [40, p.18])

3.3.4. Bond

There are two types of bond of importance in CRC: bond between the concrete matrix and the fibres and bond between concrete matrix and the conventional reinforcement.

Bond with conventional reinforcement. The bond with the conventional reinforcement determines the minimal anchor length required for the reinforcement bars to be able to transfer the stresses from the reinforcing steel to the concrete member. Analysis of experimental data showed that CRC has an improved bondage behaviour compared to regular concrete. The resulting ratio for anchorage length between C75/85 and CRC is shown in Figure 3.11.

The experiment showed that the required anchor length was dependent on three factors when ribbed bars were used. The first factor is constant and is based on the adhesion to the bar. The second factor is dependent on the concrete cover and the third factor is dependent on the usage of transverse reinforcement, which prevents the development of splitting cracks [22]. This resulted in the empirically derived Formula 3.3 [23]:

$$\frac{\tau_u}{\sqrt{f_c}} = 0.5 + 0.7\frac{c}{d}\sqrt{\frac{d}{L}} + 17\phi_t \tag{3.3}$$

Bond with fibres. A proper bond with the fibres is the main reason for the improved material properties of UHPFRC. As the regular concrete matrix is cracked, the bond with the fibres becomes the mechanism to transfer tensile stresses. An unreinforced crack is able to transfer some tensile stress in the tip of the crack due to aggregate interlocking, but this mechanism is lost as soon as the crack is opened too far. This mechanism is mainly dependent on the type of fibre used and the specific configuration of the concrete matrix [26].

3.3.5. Shrinkage

Shrinkage in maturing concrete is the result of two different time dependent processes: autogenous shrinkage and drying shrinkage. Autogenous shrinkage is the result of the chemical reaction of the cement, where the water in the mixture reacts. This process results in a decreasing pressure and therefore a decrease in volume of the mixture. The speed of this process depends on the amount of cement which reacts and stops over time. The second type of shrinkage is a result of the extraction of unreacted water out of the pores in the concrete matrix. As the water pressure in the pores is lowered, this results in a negative pressure in the material. This also results in shrinkage. This process depends on the relative humidity of the surroundings and an increase in humidity can even results in a negative shrinkage. This is a process which never stops, as the humidity can always change.

The influence of shrinkage in UHPFRC differs from regular concrete for both types. As UHPFRC contains larger quantities of cement per volume than regular concrete, the effect of autogenous shrinkage is increased up to 1.2μm/mm. As this process is based on the mixture type, it is predictable. The influence of drying shrinkage is reduced in comparison to regular concrete. This a result of the low porosity of UHPFRC [5]. All in all, the shrinkage of UHPFRC is much less dependent of the surroundings and better predictable than for regular concrete.

The shrinkage behaviour for CRC for the first 150 days after casting (stored at $20°$ and a relative humidity of 50%) is shown in Figure 3.12. It can be seen that the process of autogenous shrinkage almost stops after 28 days, while the drying shrinkage becomes significant after this period. This is a result of the hardening of the concrete.

3.3.6. Creep

While the increased cement volume has a positive impact on the shrinkage, it influences the creep negatively [5]. Experiments on CRC regarding creep resulted a creep factor $\Phi(2days, \infty) = 2.18$ when the load is applied 2 days after casting. Most of the CRC element are precast, which results in the loads being applied later on. When the load is applied after 28 days, the creep factor is already reduced to $\Phi(2days, \infty) = 1.16$ [23].

3.3.7. Durability

The durability of CRC is largely improved when compared to regular concrete. Due to the low water/cement ratio the hydration rate is only 30%, which results in sufficient unreacted cement particles. As a result capillary water can react with the cement and the pores which contained water will be further closed. Due to this process the largest pores in CRC have a diameter of less than 60 Angström and capillary porosity has not been measured. Another aspect which enhances the durability is in unconnectivity of the micro-cracks, which is partly due to the large fibre content of CRC [23].

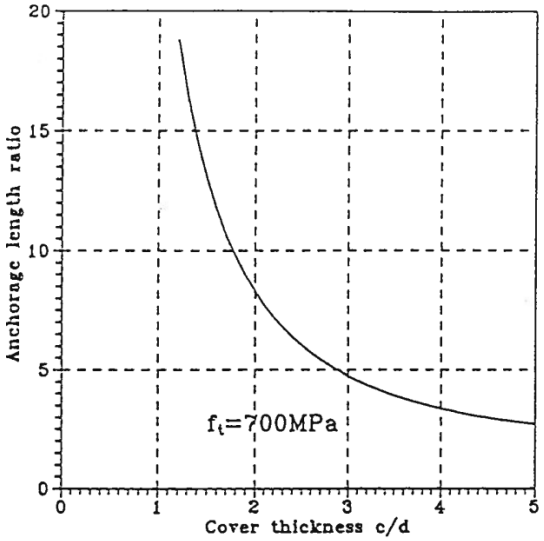

Figure 3.11: Anchor length ratio C75/85. (source [22, p.13])

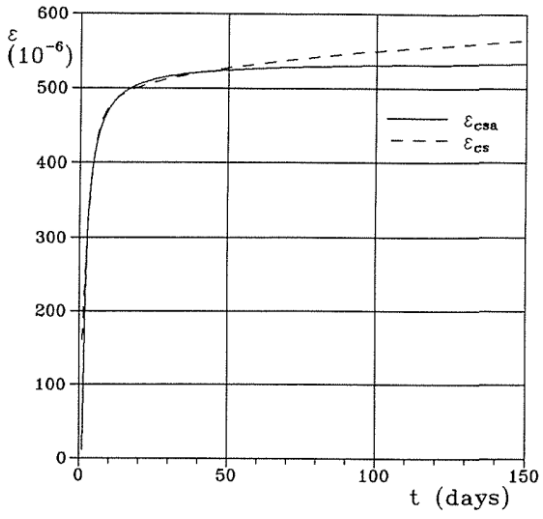

Figure 3.12: Shinkage for CRC. ϵ_{csa} is autogenous shrinkage and ϵ_{cs} the total shrinkage. (source [23, p.9])

4

The behaviour: Shear

This chapter focusses on the failure behaviour which is investigated in this research: Shear. Firstly a description of shear is provided, followed by a short summary of the history of modelling and prediction this behaviour. Special attention will be given to the models regarding UHPFRC elements. Finally some notes will be added regarding exceptions or other points which might require extra attention.

4.1. Observations on shear

The shear reinforcement is required by design codes to prevent shearfailure. This type of failure can often occur without a warning, which makes it a dangerous failure mechanism. Preventing the occurrence of such brittle mechanisms should have a high priority, but this is this is where shearfailure poses a challenge: the fundamentals of this mechanism are still not fully understand [48]. Multiple models have been derived over the past century to predict the shear capacity of concrete elements, but they include a conservative underestimation of the capacity [3].

4.1.1. Types of shear

Multiple shear types can be distinguished, but for this research the following are the most important:

Pure shear is the type of shear when two faces are forced in opposite directions without the occurrence of a bending moment on the interface, as shown in Figure 4.1a. Pure shear does not occur often in practise, but is essential in the understanding the mechanics behind other types of shear.

Flexural shear is a type of shear which combines the actions of pure shear and bending moment. Flexural shear occurs most often in vertically loaded elements, such as shown in Figure 4.1b.

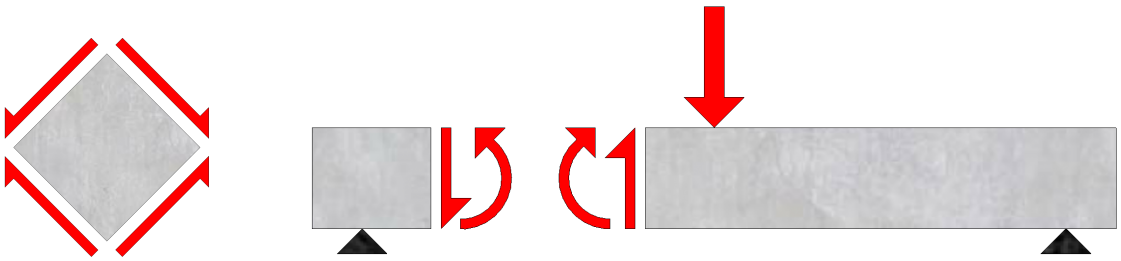

(a) A free body under pure shear. (b) A beam under flexural shear.

Figure 4.1: Different types of shear.

4.1.2. phases in shear failure

Beams loaded under flexural shear, such a shown in Figure 4.2, go through multiple stages as the load is increased. This is best described by the relation between the crack angle or concrete strut angle, θ and the applied load, in this case denoted as V. The general behaviour can be visualized by four stages [8]:

Phase 1: Uncracked (or micro-cracked)

Phase 2: Cracking (macro-cracked)

Phase 3: Fully developed crackpattern

Phase 4: Failure

A general relation is shown in Figure 4.3. In the first stage the concrete is uncracked and the compression struts at the heart of the beam make an angle of $\theta = 45°$ with the longitudinal direction of the span. As the load is increased, the beams start to show cracks at the bottom and stage two is entered. The newly formed cracks are initialized by the tension stresses in the bottom fibre which are caused by the bending moment and often start at a $90°$ angle, but follow the principle tension force as the reach the heart of the beam. These cracks result in rotation of the compression angle and θ start to drop. A minimal value for theta which is proven to be almost always reached is $21.9°$. After a while the crack angle is stabilized as a new equilibrium is found. In the last stage the beam starts to display plastic behaviour, as the shear reinforcement starts to yield or the concrete fails under compression.

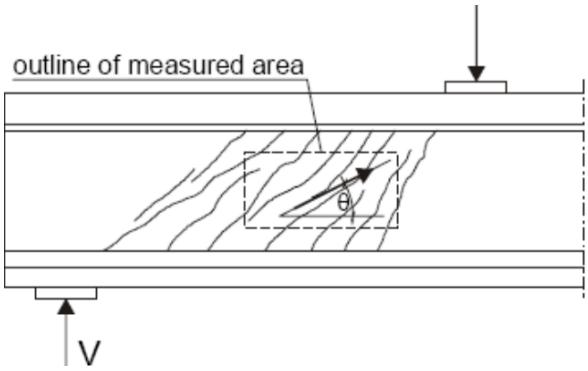

Figure 4.2: (source [8, p.6-22])

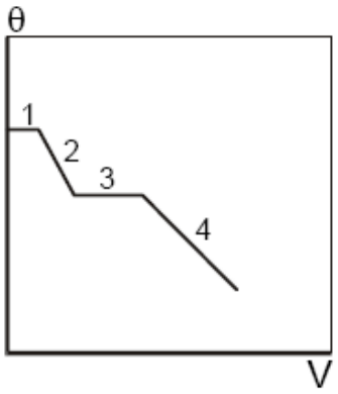

Figure 4.3: The stages during flexural shear failure. (source [8, p.6-22])

4.1.3. Failure types in flexural shear

A beam loaded in shear can fail in multiple ways, depending on the design properties and dimensions. The following methods can be distinguished:

Diagonal tension failure, shown in Figure 4.4a, if a mechanism which is often initiated with a bending crack. This crack reduces the capacity to transfer shear forces over the cross-section and causes a crack over the complete cross-section. The dowel action, caused by the reinforcement is insufficient to resist the remaining load.

Shear compression failure, shown in Figure 4.4b, where a (semi)diagonal crack develops from a bending crack. As the load is increased the crack is widened and the reinforcement start yielding.

Shear tension failure, shown in Figure 4.4c, is a failure type which is initiated similar to the shear compression failure, but the reinforcement does not yield. Instead the local influence of the reinforcements separates the surrounding concrete.

Web crushing failure, or compressive diagonal crushing failure, is shown in Figure 4.4d. The concrete zone which is under compression can fail as the applied stress exceeds the compressive strength of the concrete.

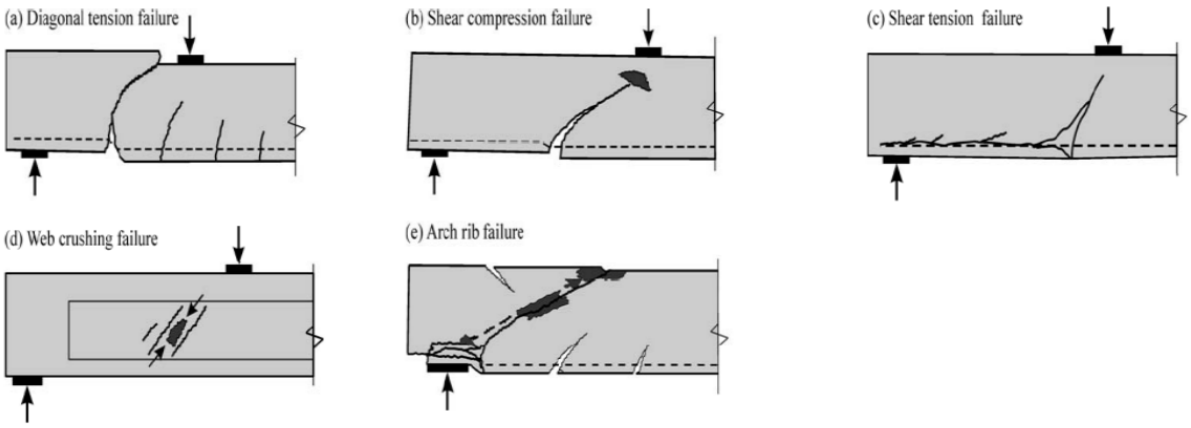

Figure 4.4: Types of shear failure. (source [35, p.117])

Arch-rib failure, shown in Figure 4.4e, is initiated at the support. The compressive arch starts rotating and collapses. Note that, in contrast to *web crushing failure*, does not require crushing of the concrete.

4.1.4. Shear reinforcement

Designs for concrete beams and, to a lesser extend, slabs, often require the implementation of shear reinforcement. Depending on the applied design codes this reinforcement type can consist of stirrups and/or bend anchors. Some design codes even allow the use of the steel fibre capacity as a minimum shear reinforcement. It is however always necessary to understand the argumentation for application of minimal reinforcement. There are multiple advances of this application:

Prevention of brittle failure: This is the first and most important reason to apply minimal reinforcement. A structural element should always provide a warning before failure to allow for appropriate action, be it evacuation of reparation. These warnings can be provided in multiple manners, such as a significant deflection while maintaining the structural integrity or occurrence of large cracks. As regular concrete itself does not posses the properties, it is required to add reinforcing steel which results in a composite action where a proper warning can be given.

Shear resistance: The application of shear reinforcement can also increase the load-bearing capacity of the element. As the reinforcement allows stresses to be transferred over the cracks in the concrete matrix it provides capacity the beyond the point of initial cracking.

Crack width control: The cracking of concrete is wanted as a sign of oncoming failure, but is unwanted when the structure is not loaded to its ultimate capacity. This point is not only aesthetic, but also has great influence on the durability of the element. Cracks allow the intrusion in the concrete of harmful chemical elements, such as chlorides or acids. A proper reinforcement design can decrease the crack width and spread the cracks.

4.2. History of methods to determine shear capacity

Before a model can be chosen or derived to determine the shear capacity of CRC elements, it is useful to take a look at the history of such models and the available methods. This is done in this section.

4.2.1. Strut and tie model (Mörsch, 1908)

The first accurate model to predict the shear capacity of beams is created by Mörsch [2] at the beginning of the 20^{th} century. He used a truss analogy to describe how the applied load is transfered to the supports. In this model the concrete act as a compressive strut at a 45° angle, while the shear reinforcement and the lateral reinforcement act as tension ties, as shown in Figure 4.7. As a results the capacity was limited to the shear which can be transfered by the shear reinforcement over an effective

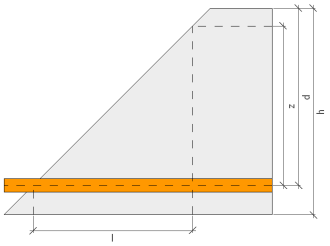

Figure 4.5: Effective length of the reinforcement.

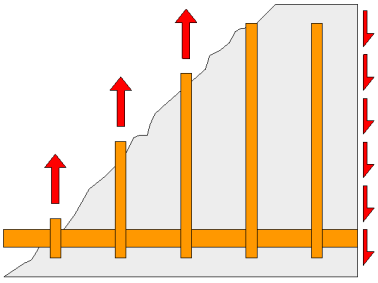

Figure 4.6: Shear resistance of the shear reinforcement: V_s.

length. This effective length is determined via geometry as shown in Figure 4.5:

$$l_{eff} = z \cdot cot(\theta) \tag{4.1}$$

For an angle of $45°$ this results in $l_{eff} = z$. With this effective length the capacity is determined by the average shear area per unit of length:

$$V_s = l_{eff} \cdot \rho_{sr} \cdot b \cdot f_y \tag{4.2}$$

This shear component is shown in Figure 4.6.

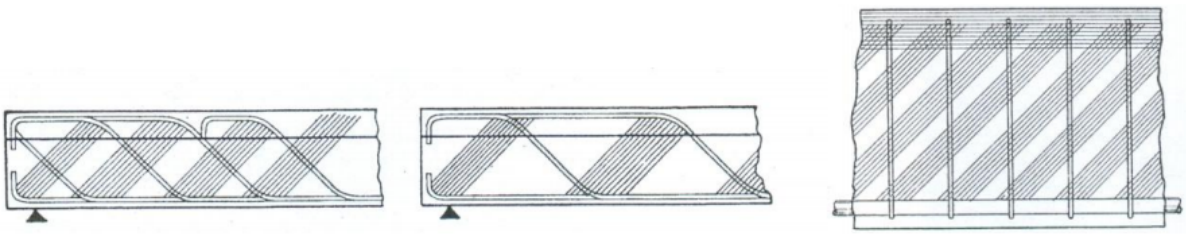

Figure 4.7: Simple or multiple truss system as proposed by Mörsch (1908). (source [2, p.3])

4.2.2. Variable strut inclination method (Kupfer, 1962)

Half a century later this strut and tie model was improved by allowing the angle θ between the lateral direction and the concrete strut to change withing the limits $0.25 \leq \tan\theta \leq 1.00$. Which results in an angle of $14° \leq \theta \leq 45°$. The actual inclination can be determined using the principle of minimum deformation work [2]. In the same year Walther published a design method which uses the Möhr circles to determine the shear capacity.
In 1964 Kani [18] developed a method which explained the shear failure of a beam as being the combination of two different mechanisms: failure of the concrete “teeth”, the concrete between the cracks at the bottom of the beam, and the failure of the arch, which is the uncracked concrete between the load and the support. The relation $a/d = 2.5$ was shown to be critical. Which results in the angle θ to often be restricted to 21.8° as this results in $\tan\theta = 2.5$.

4.2.3. Upper limit (Leonhardt and Mönig, 1973)

Further research into shear failure by Leonhardt and Mönig in 1973 regarding the increased shear reinforcement ratio, ρ_{sr}, showed the influence of this ratio on the crack angle, θ. As the amount of shear reinforcement was increased, Leonhardt and Mönig also revealed a new failure mechanism: failure of the compressive concrete struts. These struts were unable to transfer the load to the supports, even though the reinforcement was not yielding. This resulted in an upper limit of shear resistance. The effective width of the compressive struts is determined as shown in Figure 4.8 via geometry:

$$l_{eff} = z \cdot cos(\theta) \cdot sin(\theta) \tag{4.3}$$

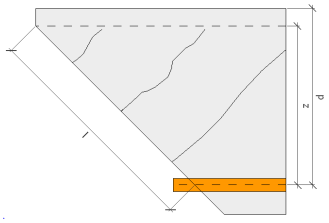

Figure 4.8: Effective length of compressive struts.

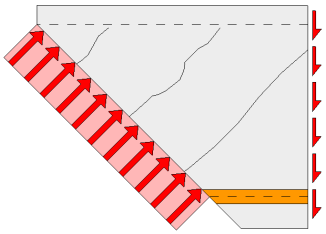

Figure 4.9: Shear resistance of compressive struts: V_{max}.

4.2.4. Compression Field Theory (Collins, 1978)

This model is the first model that focusses on the material properties rather than the structural response. Collins developed the next step in shear models as he derived a model for pure shear, while the previous models were based on flexural shear in beams under bending [6]. For this model a stress-strain relation is derived, based on the composite action of the concrete and the reinforcement. This model does not yet subscribe any tensile capacity to the concrete [4] and is therefore unable to model stirrups.

4.2.5. Modified Compression Field Theory (Vecchio and Collins, 1986)

Vecchio and Collins [45] improved the CFT model. With the the new testing rig it became much easier to distinguish the important parameters for shear tests. Figure 4.10 shows the model which was used. This new model allowed stresses to be transferred over the crack through aggregate interlocking. The formulas for this new mechanism are empirically fitted to previous experiments.

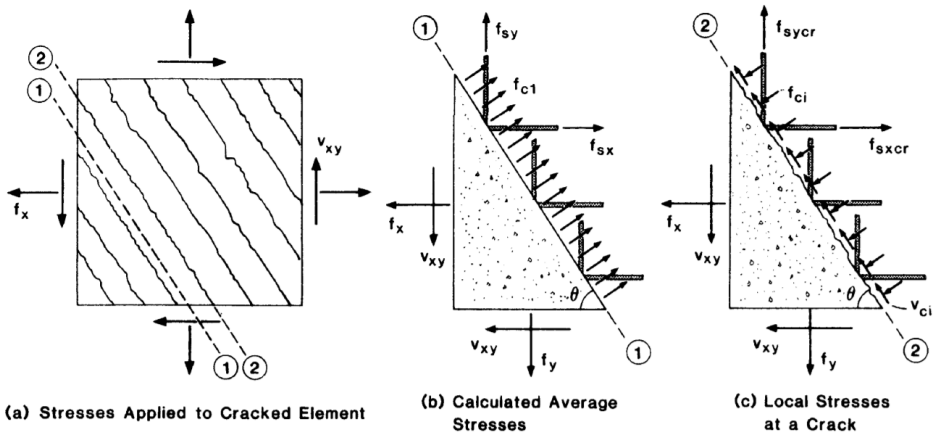

Figure 4.10: Stresses over an uncracked(1) and a cracked(2) plane. (source [45, p.226])

4.2.6. Generalized Stress Field Approach (Sigrist, 2011)

This approach is a combination of the MCFT and the Limit Analysis of the Theory of Plasticity. Sigrist found equilibrium while considering the steel, concrete and shear forces in a crack. This combined with empirically derived results in a relation between the average strain longitudinal strain and the crack inclination angle:

$$20^\circ + 5000\epsilon_x \leq \theta \leq 35^\circ + 5000\epsilon_x \tag{4.4}$$

Where the longitudinal strain can be derived based on the internal forces (Bending moment M, shear force V and normal force N) and some properties (Youngs modulus of steel E_s, the longitudinal steel area A_{sx} and the effective height d). This model formed the base for the *fib* Model Code 2010 [32].

5

The method: guidelines

During the design of an element such as the Raqtan landing platform the structural safety is determined via the validation by design codes such as the Eurocode. The design codes or guidelines contain prescribed methods to predict the loads which the element can be subjected to during its lifespan and the load-bearing capacity of the element itself including required safety margins. This provides engineers with proven tools to create constructional elements. This chapter provides the information which is required to understand the development and application of such design tools.

5.1. Development of the current codes

The first widely available document which can be considered a design code is the *SP-3* by the American Concrete institute (ACI), which was published in 1939 [39]. It's purpose was to combine the available knowledge and provide means to engineers to apply proven methods for the validation of their designs. The purpose of design codes has not changed since, only their content and the subjects they cover.

In the subsequent decades many countries developed their own building codes. This often restricted engineers in Europe to their own country, as the rules differed across the border. The *European Union* decided in 1975 to remove these restrictions and create a guideline for the entire union. The first version was ready in 1980s and in 2010 the member states became obliged to implement the Eurocode. Member states were allowed to implement their own alternations to the Eurocode through the implementation of a National Application Document (NAD), often referred to as National Annexes. An example is the Dutch National Annex, or Nationale Bijlage [11].

The Eurocode is created based on consensus regarding the models and required safety levels for specific structure types. Implementing new innovations into the Eurocode can take up much time, while the desire to use the innovations is already there. In the Netherlands this is solved by creating an intermediate norm, the CUR. These type of codes are often accepted as prenormative and contain guidelines which can complement the Eurocodes. The acceptance of design codes can differ per authority. As deviating from the proven path often requires explanation. On an international scale there exist multiple alternatives to the Eurocode, such as the Modelcode or the codes developed by RILEM. The innovations in these alternatives are often incorporated into new versions of the Eurocode [8], as shown in Figure 5.1.

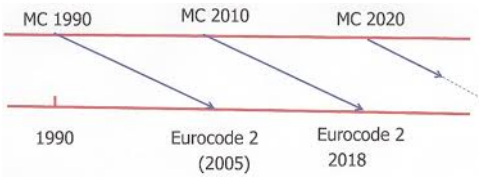

Figure 5.1: Relation between the Model Code and the Eurocode. (source [46, p.xvii])

5.2. Design approach

The available design codes may differ in their content, but this is mostly based on the topics they cover. The general approach to the validation of design is more or less the same. Some codes provide multiple methods to determine the validity of the structure. Most often the more complex models will result in more accurate results, as shown in Figure 5.2. This is a result of one of the challenges which de composers of design codes face: the trade-off between accuracy and complexity. The codes should be easy to use as they form the base for many designs.

5.2.1. Limit States

Most design codes prescribe the design to two types of loading: Servicability Limit State (SLS) and Ultimate Limit State (ULS):

- **Serviceability Limit State** is used to determine the usability of the structure. The structural validation in this state is mostly based on comfort demands, such as vibrations and deflections. Exceeding the maximal deflection might not results in structural failure, but the structure does not provide the service it was designed to do any more. [11]
- **Ultimate Limit State** refers to the state just before (partial) structural failure. The validation with respect to this state is mostly about structural safety and resistance [11].

Besides the above limit states their are also demands regarding durability and robustness to the design. These also depend on the general consensus of what is acceptable.

5.2.2. Loads and resistances

The validation of a design if done by describing a relation between the applied loads and the resulting reaction of the structure. But as the exact value of the loads and resistance is often unknown this imposes uncertainties to the models. The first step in most codes is to determine a characteristic value, denoted by X_k. This value is expected to be reached in 95% of the cases. As this value is still exceeded 5% of the time, it is required to determine a more appropriate value: the design value, X_d. There are multiple methods (also called levels of approximation) to do this and derive deterministic values:

- Level 0: using a deterministic value, which should always exceeds the expected values
- Level I: using a partial safety factor
- Level II: using a distribution

Most codes apply *Level I* to result in realistic, but safe loads and resistances. These values have to balanced based on the required level of safety. Lowering the resistance by using higher safety factors would result in a safer design, but in an increased material usage. These consideration are included in the codes to derive the values which meet the modern demands for safety and reliability.

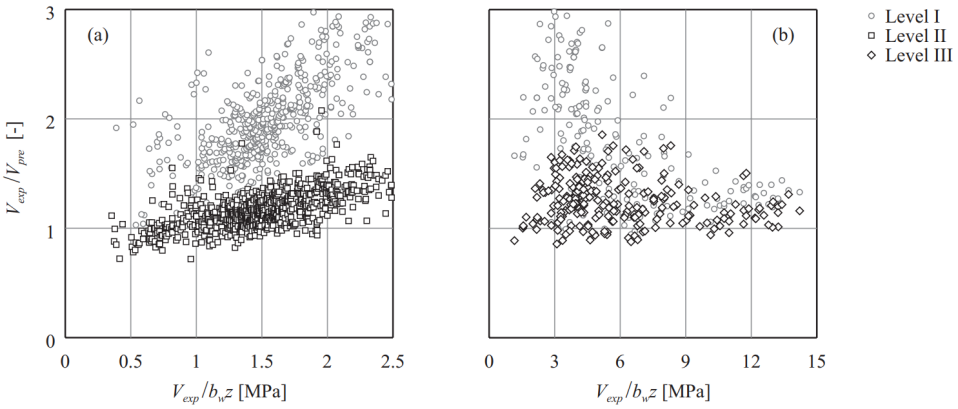

Figure 5.2: The relation between the experimentally derived resistance and the resistance as determined by multiple Levels of Approximation according to the Model code 2010. Increasing levels mean increasing complexity, but also result in increasing accuracy. The structural component is a shear beams with (b) and without (a) shear reinforcement. (source [37, p.197])

As the design values are derived, the next step is to derive the relation between the design loads, often denoted as $X_E d$, and the design resistance, $X_R d$. This comparison is often performed by an unity check:

$$UC = \frac{X_{Ed}}{X_{Rd}} \leq 1.0 \tag{5.1}$$

5.3. Safety

The guidelines have as a main purpose to ensure the structural integrity of the designs which they validate. This should be accomplished by providing clear methods to determine the relation between the load which act on the structure and the resistance the structure is able to offer. This relation is often not as absolute and safe or unsafe. Most of the times the loads are have a probability of occurrence and the resistance can be modelled with a distribution. This is a result of the materials properties containing a variance. An example of such variances in loading and resistance is shown in Figure 5.3.

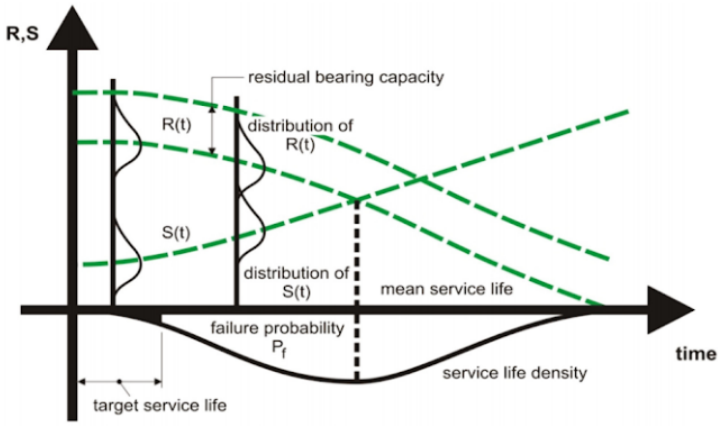

Figure 5.3: Relation between the structural resistance (R) and the load (S) over time, resulting in the probability of failure (P_f). (source [46, p.xx])

Structural safety depends on the overlap between the load distribution and the resistance distribution. Even when the probability is small, there is still a chance of the load exceeding the resistance. In order to be able to design safe structures, the codes define a required level of safety, or a probability of occurrence. The probability of failure in the Eurocode for example is coupled to the consequence class of the structure, the limit state and the length of the life span. For example a structure in consequence class R2 () with a lifespan of 50 years has an prescribed maximal failure probability of:

$$P_f = \Phi(-\beta_{50}) = \Phi(-3.8) = 0.000072 \tag{5.2}$$

As it it often hard to derive the statistical distribution for such parameters, the code often provides factors which can be used instead. An example of such a factor are the material factors ($\gamma_s = 1.15$ for steel and $\gamma_c = 1.5$ for concrete). Besides these requirements regarding the probability of failure, the codes often add other requirements. For example regarding the failure mechanism. Brittle failure is often prevented and a ductile failure is enforced, resulting in a warning as the structure is overloaded and providing the users a possibility to leave. As a result it should be able design the structures in such a way that the modern safety standards are met and it is considered safe to use the structures.

6

The application: The Raqtan landing platform

This chapter elaborates on the design of the Raqtan landing platform as it was originally designed. The design considerations and calculations will be discussed and their influence on the final design is shown.

6.1. The case study

The Raqtan project consists of a new office building and hall for the Raqtan company in Dammam. The city Dammam, also spelled Damman, is located at the west coast of Saudi Arabia, as shown in Figure 6.1. The project design was made by architect firm Rempt van der Donk. This project included the engineering of the stairs and and separation walls in CRC by Pieters Bouwtechniek. The elements would be cast by Hi-Con in Weert, the Netherlands, then transported to the harbour in Antwerp and from there on transported to Dammam by boat.

Figure 6.1: The project location in Saudi Arabia. (source: https://www.worldatlas.com/as/sa/5/where-is-dammam.html)

Figure 6.2: [Raqtan project impression. (source: Rempt van der Donk architecten)

The focus of this research is on the landingplatform, which is the bridge between two separate stair elements. It is a CRC slab of 1210×2120mm, with a thickness of 80mm. The platform is connected to the 250mm thick wall (C30/37) which encloses the elevator shaft. This connection is made via two consoles, shown in Figure 6.4, which are slid into a cut-out in the wall. This connection is filled with mortar of class K70. The connection between the landing platform and the stair elements is made via a dowel at 100mm from the edge. The consoles are 250mm wide and have a length of 260mm. As they are only slid in the wall for 240 mm, this leave a 20mm margin between the landingplatform and the wall.

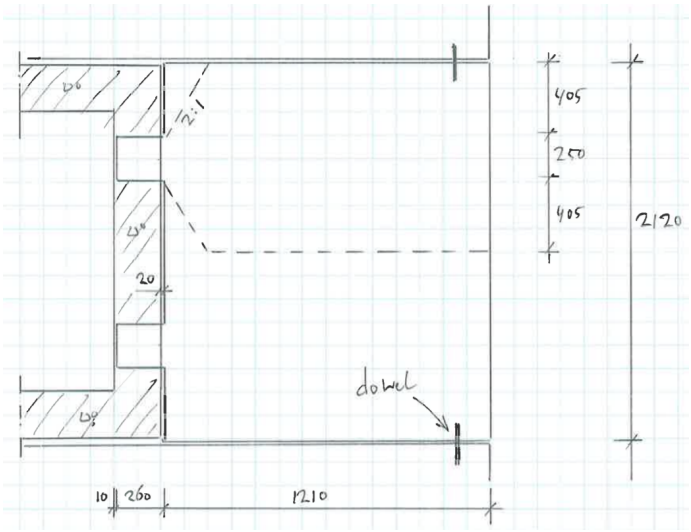

Figure 6.3: Overview of the landing platform in the project. (source [27, p.122])

Figure 6.4: The cast landingplatforms. (source: Rempt van der Donk)

6.2. The mechanical model

The exact stress distribution is often not known to an engineer. Instead the design capacity according to the applied design codes is based on a mechanical model which resembles the actual structure. The advantage of applying such simplifications is that the engineering becomes more apprehesable. It should however be kept in mind that these simplifications can also result in the neglect of import load-paths. This is the responsibility of the engineer to determine the applicability of a certain mechanical model. The first step in the creation of a model is to determine the supports. These provide information regarding the connections of the modeled element to its surroundings and the stiffness of these connections

6.2.1. Modelled construction

In the actual construction the landing platform is clamped in the wall as it is continuously supported at the top, bottom and sides of the consoles and has a connection to the stair elements, as shown in Figure 6.5.

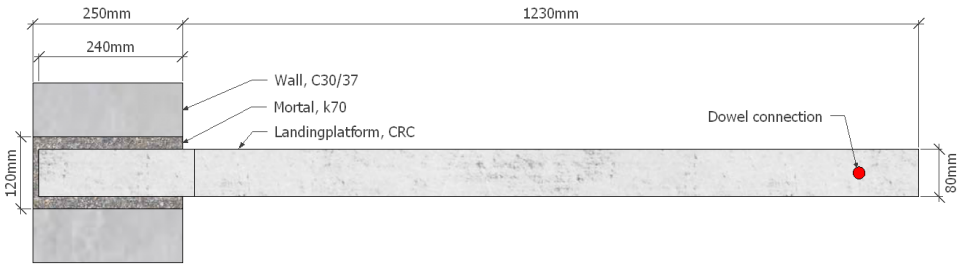

Figure 6.5: Actual connection of the Raqtan landing platform to the wall.

The model which is used to determine the capacity of the landing platform contains some simplifications. The first simplification is to reduce the dimensionality of the problem: instead of modelling the entire platform, only half is taken into consideration: a platform with a width of 1060mm with one console. The influence of the dowel connection is assumed to be on the same line (dimension) as the console. Due to this simplification the effect of torsion within the element are neglected.

The second simplification concerns the way the connection to the wall is made. Instead of modelling the connection as being clamped, which has a complex stress distribution, the connection is modelled as being pinned on two points. Each point represents a 20mm wide strip in the console which transfers

the load to the wall. The centre-to-centre distance of the supports is chosen to be a little smaller than the maximal possible in this configuration and is set to be 200mm. This model is shown in Figure 6.6 and a detail of its representation is provided in Figure 6.7.

Figure 6.6: Used model of the Raqtan landing platform to the wall. The red arrow indicates the influence of the dowel connection.

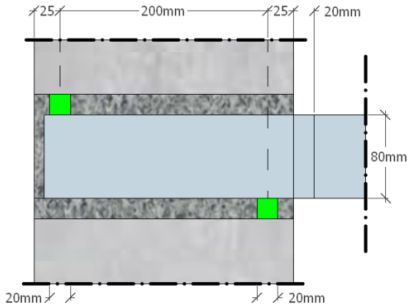

Figure 6.7: Representation of the used model of the Raqtan landing platform to the wall. The green zones indicate the considered compression zones.

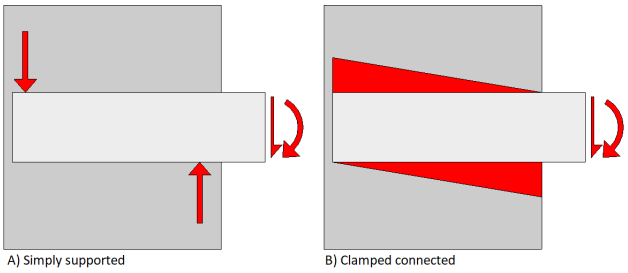

Figure 6.8: Models for the connection of the Raqtan landing platform.

The obtained model still contains a connection to the stairs. This connection results in a model where the mutual influences, such as deflection and resulting loads, have to be considered. This is simplified by assuming a 300mm slab of the stair is carried by the landing platform. This assumption is supported on calculations which showed the stiffness of the stair to be lower than the stiffness of the platform, resulting in a load-transfer from the stairs to the platform. As the stairs are about 1250mm wide, it is assumed that the loads (self-weight and applied) of this 300×1250mm slab have to be resisted by the platform. This results in 4 loads on the platform:

- q_G: The dead load of the platform. With a width of 1060mm, a height of 80mm and a density of 27 kN/m^3, this becomes $q_G = 1.06 \cdot 0.08 \cdot 27 = 2.29$kN/m.
- q_Q: A load of 3 kN/m^2 on the platform. This is the live load of the structure as defined in Eurocode 1990. As the considered section is 1060mm wide, this results in a load of $q_Q = 1.06 \cdot 3 = 3.18$kN/m.
- F_G: The dead load of the connected stair. The considered section is 1250×300 mm^2 and has a heigth of 80mm. This results in $f_G = 1.25 \cdot 0.3 \cdot 0.08 \cdot 27 = 0.81$kN.
- F_Q: The live load of the platform is also present on the considered stair slab, which results in a point load on the landing platform of $F_Q = 1.25 \cdot 0.3 \cdot 3 = 1.125$kN/m.

6.2.2. Remarks on the used model

In the design process the supports of the slab are chosen to be two supports, one at 15mm from the edge of the console, and one at 215mm. The result is a leverarm of 200mm which should resist the bending moment at the centre support. This model is shown in Figure 6.8A.

This type of connection is convenient for analytical purposes as the constraints on the model are minimal. With only two constraints in the vertical direction and one in the lateral direction, the structure become statically determined. It should however be noted that the actual behaviour of a clamped element can differ. When the concrete elements is assumed to be infinitely stiff, the actual stress distribution will be more as shown in Figure 6.8B.

This distribution of stresses will has to resist the same bending moment as the simply supported model. As the leverarm between the centre of the stresses is decreased (from 200mm to 1/3*240 = 80mm), the the equivalent force is increased by approximately 200/80=2.50. More detailed calculations, provided in Appendix C.1, show the actual shearforce can increase by a factor of 1.32. As the used design codes result in shear capacity being governing for the element capacity in the used loadcase, this results in an reduced capacity.

6.3. The design

For the design of the Raqtan landing platform Pieters Bouwtechniek chose to use the Eurocode in combination with the Dutch annex, instead of applying the local codes. This decision was made as the company has experience with this code, but not with the local design guidelines of Saudi Arabia and the Eurocode with Dutch annex results in a sufficient safety level to be allowed to be used. Some specific formulas in the code are replaced with formulas derived for CRC when allowed. This method is accepted through a second opinion written by *Prof.dr.ir. Dr.-Ing.h.c. J.C. Walraven*.

6.3.1. Loads

The EC prescribes a method to determine the load cases which the structure should be able to resist. The loads are determined according to EC0(6.10a) and EC0(6.10b), where the permanent load, respectively the live load, are governing:

$$\sum_{j\geq 1} \gamma_{G,j} G_{k,j} + \gamma_p P + \gamma_{Q,1} \phi_{0,1} Q_{k,1} + \sum_{i>1} \gamma_{Q_i} \phi_{0,i} Q_{k,i} \tag{6.1}$$

$$\sum_{j\geq 1} \xi_j \gamma_{G,j} G_{k,j} + \gamma_p P + \gamma_{Q,1} Q_{k,1} + \sum_{i>1} \gamma_{Q_i} \phi_{0,i} Q_{k,i} \tag{6.2}$$

For the exact meaning of all the parameters reference is made to the Eurocode 1990 section 6.4.3.2. Appendix A of the EC0 provide the factors which have to be used in the above formula for this design: a Category B building (office). The Dutch annex provides values as well. These factors increase the actual expected loads to translate them in to design loads, which should not be exceeded during the lifespan of the structure. With the determined loads it is possible to determine the shear and the bending moment though out the element. The results are shown in Figure 6.9. The exact calculations can be found in Appendix B.2.1

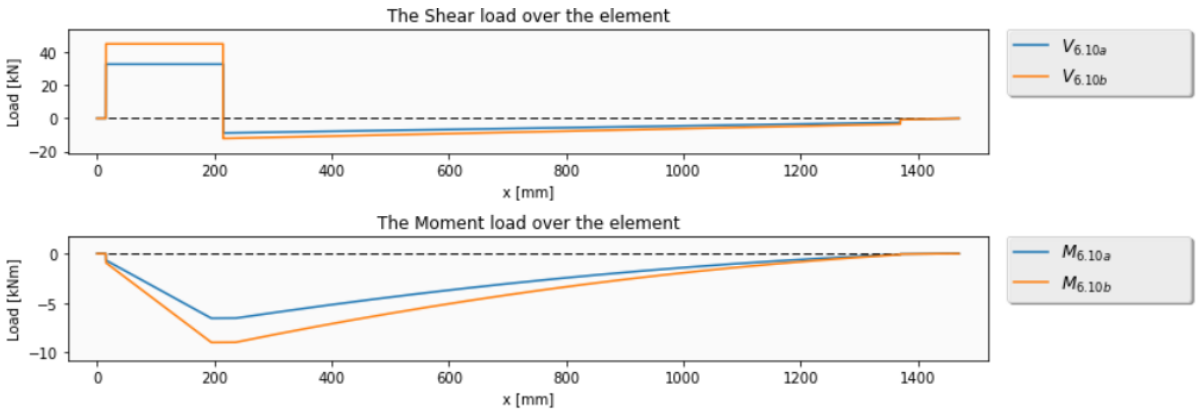

Figure 6.9: V_{Ed} and M_{Ed} over the element length.

It should be noted here that the Eurocode prescribes in EC2, section 6.2.2(6) and section 6.2.3(8) that V_{Ed} can be reduce by a factor β. In this research this factor is chosen to be applied to the resistance capacity V_{Rd} instead. As the result is the same, while the used shear load is now equal to the actual shear load.

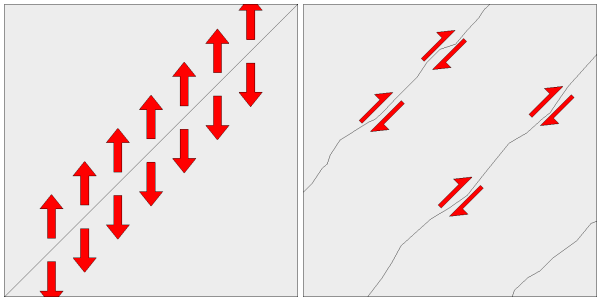

(a) $V_{Rd,min}$ (b) $V_{Rd,c}$

Figure 6.10: The different components for shear resistance according to the Eurocode: 6.10a) Shear tension component; 6.10b) Shear friction component.

6.3.2. Shear capacity without stirrups

The Eurocode has implemented multiple methods to determine the shear capacity. The first method is provided in Eurocode 1992 section 6.2.2. This method can be used to determine the shear resistance when the element does not require shear calculated reinforcement. This method uses the mechanisms shown in Figure 6.10), which is based on the friction that can be transferred of a shear crack, while the crack is kept small enough by the longitudinal reinforcement. The EC provide the following formula for this mechanism (EC2(6.2.a)):

$$V_{Rd,c} = \left[C_{Rd,c}k\left(100\rho_l f_{ck}\right)^{1/3} + k_1\sigma_{cp}\right]b_w d \tag{6.3}$$

For CRC the minimal value, v_{min}, is determined using a formula from the Danish annex:

$$v_{min} = f_{ctd}\left(0.7 - \frac{f_{ck}}{200}\right) \geq 0.45 f_{ctd} \tag{6.4}$$

The results of applying these formulas to the Raqtan landing platform are shown in Figure 6.11. The applied loads, as found in section 6.3.1, exceed the provided capacity, resulting in a Unity Check of 2.18. According to the applied design method, EC2, with Dutch annex and some modifications, the current structure does not meet the requirements regarding shear capacity. This means that the method as defined in EC2 section 6.2.3, *Elements requiring calculated shear reinforcement* has to be applied and shear reinforcement has to be added.

6.3.3. Minimum reinforcement

The next step is to determine the shear reinforcement design. The Eurocode states multiple requirements for the design in section 9.2.2. Even when the design does not require calculated shear reinforcement, there are still minimal requirements. The first requirement is stated in EC2F(9.5N), which regulates the minimum reinforcement ratio:

$$\rho_{w,min} = \frac{0.08\sqrt{f_{ck}}}{f_{yk}} \tag{6.5}$$

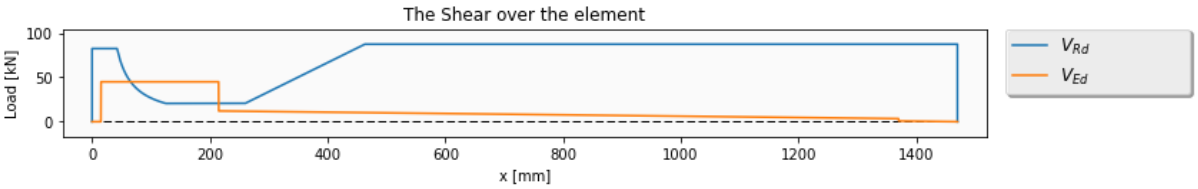

Figure 6.11: Design shear force(V_{Ed}) and shear force resistance (V_{Rd}) over the element length.

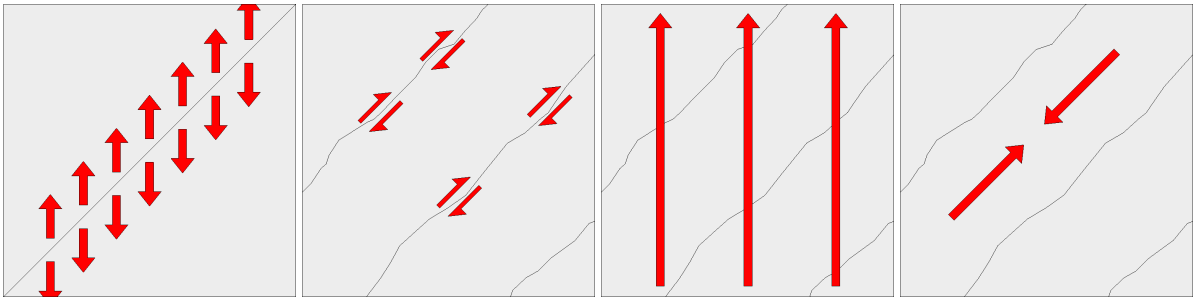

(a) $V_{Rd,min}$ (b) $V_{Rd,c}$ (c) $V_{Rd,s}$ (d) $V_{Rd,max}$

Figure 6.12: The different components for shear resistance according to the Eurocode section 6.2.3: 6.12a) Shear tension component; 6.12b) Shear friction component; 6.12c) Shear reinforcement component; 6.12d) Maximal compression strut component.

Other requirements regard the distance between the legs of the shear elements. In longitudinal direction this distance is limited by $s_{l,max}$ (NEN-EN 1992 9.2.2(6)) and in transverse direction by $s_{t,max}$ (NEN-EN 1992 9.2.3(5)):

$$s_{l,max} = 0.75d(1 + cot(\alpha)) \leq 300 \tag{6.6}$$

$$s_{t,max} = 0.75d(1 + b/2h) \leq 1.5d \leq 600mm \tag{6.7}$$

These limitation ensure that, as a shear crack occurs, there is at least one stirrups leg which crosses the crack. This way the crack does not result in brittle failure. In the Raqtan platform the value for d is equal to 60mm, which results in values of $s_{t,max} = 90$ and $s_{l,max} = 45$. The value for d is chosen to be without Δc_{dev}. This means that during construction of the element extra attention should be paid to this reinforcement. This results in a congestion of shear reinforcement in the console, but is still possible to create. The slenderness of the structure results in a low effective height and therefore in a low maximal distance between the stirrup legs.

6.3.4. Shear capacity with stirrups

As the resistance of the element without shear reinforcement was insufficient according to section 6.2.2 it is necessary to determine the actual capacity. This can be done using EC2 section 6.2.3 *Elements which require calculated shear reinforcement*. The method provided in this section is an expansion to the previous method and includes more components, as shown in Figure 6.12. A new component, shown in Figure 6.12c is the component of the shear reinforcement. As the concrete is cracked the reinforcement is able to transfer part of the load over the crack. This is limited by the yielding of the steel. The formula for this is (EC2(6.8)):

$$V_{Rd,s} = \frac{A_{sw}}{s} z f_{ywd} cot(\theta) \tag{6.8}$$

Which is analytically derived by taking the vertical force, $\frac{A_{sw} f_{ywd}}{s}$ per unit of length and multiplying this with the effective length of a crack $zcot(\theta)$. Combined with the shearforce which the crack was able to transfer, $V_{Rd,c}$, this results in the total shear capacity. This capacity should be checked against the limit $V_{Rd,max}$. This limit is shown in Figure 6.12d and is the shear load beyond which the concrete struts between the crack would fail in compression. This load is defined as (EC2(6.9)):

$$V_{Rd,max} = \frac{\alpha_{cw} b_w z v_1 f_{cd}}{cot(\theta) + tan(\theta)} \tag{6.9}$$

In this formula α_{cw} and v_1 are factors to include reduced concrete strength due to cracking and prestressing. $z/(cot(\theta) + tan(\theta)$ is the concrete area available over the cross-section (orthogonal to the crack). When these formulas are applied to the Raqtan loading platform this results in sufficient shear capacity, as shown in Figure 6.13.

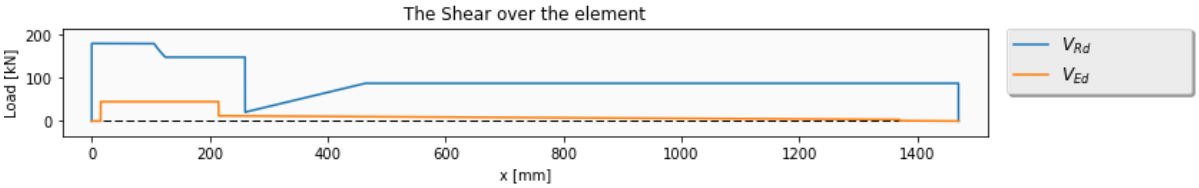

Figure 6.13: The shear capacity over the element for PBT-method with shear reinforcement

6.3.5. Completing the design

Creating sufficient shear capacity is only one of the requirements set by the Eurocode. Another import capacity to determine is the bending moment capacity. In the appendix this capacity, and other requirements are determined according the Eurocode. As the design meets all the requirements it is possible to apply it without further research.

7

Preliminary Conclusions

The application of CRC has numerous advantages over the use of normal strength concrete. The use of large quantities of reinforcement in combination with the addition of steel fibres results in an improved post-cracking behaviour. These improved properties can only be fully used when their capabilities are taken into account during the design phase. While the current Eurocode does not provide the means to do so, there are alternatives which subscribe the value and increased capacity that FRC materials have. These codes and guidelines are based on may years of research and are accepted by large communities, such as the *fib*, as they are implemented. This not only provides proven means to determine the capacity of FRC elements, but also results in a legitimate reason to apply them as these codes are widely accepted.

The Raqtan element is an example of a design which can be improved by the incorporation of a fibre contribution in the design calculations. The improvements are not only in costs, as a small amount of reinforcement steel is spared and the required labour is decreased, but also in practicality. The stirrups which are required by the Eurocode cause a congestion of the reinforcement, which not only makes the preparation of the reinforcement harder, but also has a negative effect on the concrete flow though the form work during casting.

II

Design validation

8

Validation by design codes

There are currently multiple design guidelines available, but governmental entities often prescribe which one has to be used for designing in their jurisdiction. As the structural behaviour of a structure does not depend on its location, it is interesting to compare the predicted capacity of the Raqtan landing platform according to multiple available codes. The purpose of this chapter is to investigate the structural models behind multiple available codes and their influence on the design capacity of the Raqtan landing platform. By including multiple codes which have implemented FRC models, it can be determined whether the design is considered sufficiently safe. The applied codes are:

Table 8.1: The used design codes.

Code	Abbr.	Full name	Reference
Eurocode	EC	NEN-EN 1992-1-1+C2:2011 (NL)	[30]
Dutch Eurocode	ECnl	NEN-EN 1992-1-1+C2:2011/NB:2016 (NL)	[31]
Modelcode 2010	MC2010		[20]
German guidelines	ECge	Ergänzungen und Änderungen zu DIN EN 1992-1-1	[44]
French guidelines	ECfr	NF P18-710:2016-04	[33]

There are three sections per code. The first section will describe the methods used by the code to determine the capacity of the Raqtan landing platform. The models behind the predictions will be provided. The discussed failure mechanisms will be those which are expected to be governing in ULS, as their influence can be verified in the laboratorial experiments. The second section is used to determine the design capacity according to the code. This section is used to determine whether there are guidelines which allow the design without stirrups. The third section provides some remarks on the applicability of the design method regarding the Raqtan landing platform.

The methods provided here are based on stirrups with a 90° angle to the longitudinal reinforcement and factors regarding prestressing are neglected as this is not applied in the Raqtan landing platform. The resistance is compared to the shear force based on the clamped connection, as basing it on the hinged connection might overestimate the actual capacity.

8.1. The Eurocode

The first code to use is the Eurocode without national annexes. This is the basis document for the European guidelines since 1997. The version used for this calculation is *NEN-EN 1992-1-1+C2:2011* [30]. Formulas in the section will be referred to as EC2-F(X), where X denotes the number as found in the codes themselves and references to section in the Eurocode will be made as EC2§X, where X refers to the actual section.

8.1.1. Design methods

The shear capacity is determined as a combination of different mechanisms. The main mechanism is the based on the assumption that the concrete is cracked and the shear reinforcement has to resist the remaining load. An underlimit is determined as the force required to start the cracking and an upperlimit is based on the crushing of the concrete diagonals. These mechanisms are shown in Figure 8.1. The methods to determine the shear capacity, V_{Rd}, according to the Eurocode are given in section EC2§6.2. The shear capacity is provided three main component: A steel component, a concrete component and an upper limit:

$$V_{Rd} = V_{Rd,s} + max\left(V_{Rd,c}, V_{Rd,min}\right) \leq V_{Rd,max} \tag{8.1}$$

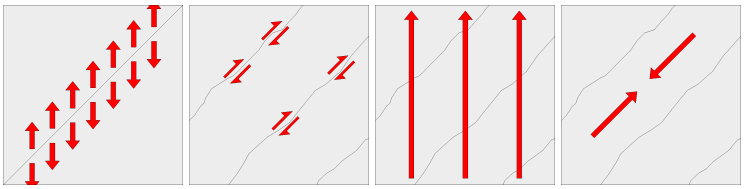

(a) $V_{Rd,min}$ (b) $V_{Rd,c}$ (c) $V_{Rd,s}$ (d) $V_{Rd,max}$

Figure 8.1: The different components which determine the shear resistance according to EC: 8.1a) Shear tension component; 8.1b) Shear friction component; 8.1c) Shear reinforcement component; 8.1d) Compressive strut component.

The concrete component consists of two different mechanisms: the shear force which can be resisted while maintaining uncracked and the resistance which is a result of aggregate interlocking. Both are empirically derived.
The shear reinforcement component is based on the earliest with regard to shear: the variable strut inclination method, as created by Kupfer (see §4.2.2) and the upper limit is based on the work done by Leonhardt and Mönig in 1973 (see §4.2.3). Both of these are based on analytic models, while being improved with fitted safety values. The upper limit for example contains reduction factors to include the cracking of the concrete and prestressing forces.

Minimal shear requirements Besides the requirement for shear capacity, which can result in a requirement for shear reinforcement, the Eurocode contains another requirement which always results in this reinforcement: Minimal shear reinforcement, as defined in section EC2§9.2 and EC2§9.3. These requirements result in shear reinforcement in all shear cracks and enforce a ductile failure mechanism.

The bending moment capacity in the Eurocode is based is based on the plasticity model shown in Figure 8.2, where the concrete is assumed to behave plastic in the compression zone and has no influence in the tension zone, as the tension strength is assumed to be negligible. When applying this model there are two failure mechanisms which have to be tested: The yielding of the reinforcement steel and the crushing of the concrete. The yielding of the steel is the preferred mechanism, as this results in ductile failure, while the crushing of the concrete is brittle.

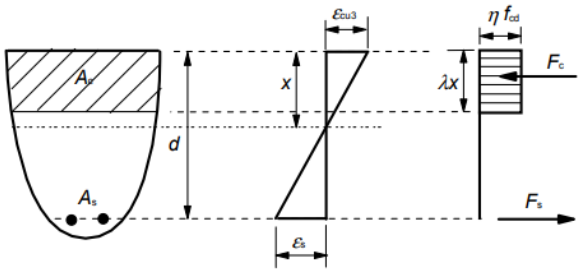

Figure 8.2: The model for bending used by the Eurocode. (source: based on [30, p.37])

8.1.2. Capacity

The methods in the previous sections are calculated in Appendix Appendix B.1. The Unity Check for the element shows that the console has insufficient capacity according to the Eurocode, as shown in Figure 8.3. An overview of the numerical result is shown in 8.2.
Performing the unity check over the element results in the plot shown in Figure 8.3. With a UC for shear of 2.88 it can be concluded that according to the Eurocode the element requires calculated stirrups. The result is a failure of this design to meet two of the design criteria stated by the Eurocode:

- $V_{Ed} \leq V_{Rd}$, which results in insufficient capacity.
- The requirement of minimal shear reinforcement as stated in section EC2§9.2.2 and §9.3.2.

8.1.3. Remarks

The shear capacity in the Eurocode is based on a mix of model based formulas and empirically fitted equations. Both of these have some properties which should be taken into account when extrapolating.

When considering the model based formulas, such as the formula for $V_{Rd,max}$ or $V_{Rd,s}$, it is important to know the limitations of the underlying models. The components which are taken in to account do not incorporate the fibre contribution. This has a major influence as the behaviour of the concrete matrix is and the material properties are largely effected by the addition of fibres.

The empirically fitted formulas have the advantage that they can be derived while the exact underlying mechanisms are not fully understood. This is useful when implementing complex features in to the Eurocode, but it has some well set limitations. The fitted formula is only fitted to a certain range of experimental data. Interpolation between these data points can be possible, but extrapolation can result in large errors. The formula for $V_{Rd,c}$ is fitted for regular concrete, but a compressive strength of 110 MPa is more than double that of the concrete classes which were used for fitting. The addition of fibres can result in even larger deviations from the actual capacity.

Although the Eurocode is accepted in the Netherlands as a design validation tool, it has some major shortcomings when applying in on CRC elements. As the deviations are expected to result in underestimation of the actual properties based on the material properties explained previously, it is considered safe to apply this code.

Table 8.2: Design requirements according to the Eurocode at the centre support. Green marking indicated that the requirement is met, red markings indicate the requirement is not met.

		Design load		**Design Resistance**		**Unity Check**	
		Ed		Rd		UC	
Shear	V	57.48	kN	19.92	kN	2.88	-
Min. shear reinforcement	$\rho_{sw,min}$						
Bending moment	M	9.00	kNm	10.12	kNm	0.89	-

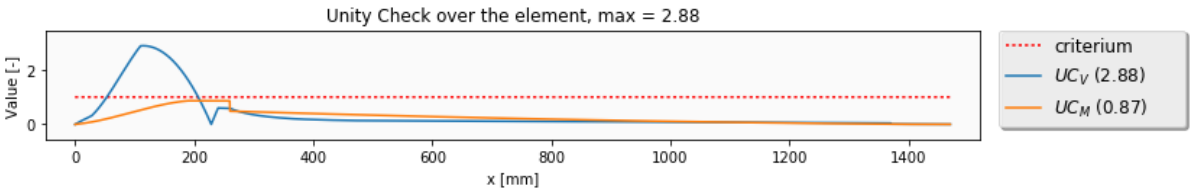

Figure 8.3: The unity check performed for method of EC for the element without stirrups.

8.2. The Dutch annex

The Netherlands have an annex to the Eurocode, which includes minor changes in values for parameters. The version used for the validation of the Raqtan landing platform according to the Dutch design code is *NEN-EN 1992-1-1+C2:2011/NB:2016* [31]. The differences do not influence the here performed calculated resistance and results. For the exact values reference is made to §8.1.

8.3. Method PBT

This section focuses on the methods which are used by Pieters Bouwtechniek to determine the capacity of the Raqtan landing platform and is based on internal design documents, calculation sheets and input from the engineers.

8.3.1. Design methods

Pieters Bouwtechniek uses some adaptations to the Dutch annex in order to model the behaviour of the CRC better. These changes are based on the application of the Danish national annex and the use of formulas which are fitted to experimental data. Their methods and results were provided to *Prof.dr.ir. Dr.-Ing.h.c. J.C. Walraven* for a second opinion to validate the usage, as mentioned in §6.3. The main difference with regard to the Raqtan landing platform is in the determination of the lower limit for the shear capacity. The Danish annex provides the following formula for as a substitution for v_{min} in EC2-S6.2.2:

$$v_{min} = f_{ctd} \cdot \left(0.7 - \frac{f_{ck}}{200}\right) \geq 0.45 \cdot f_{ctd} \tag{8.2}$$

For the properties of CRC this results in a value of $v_{min} = 1.50MPa$ instead of $1.04MPa$ as calculated according to the Dutch annex. This does not have an influence on the shear capacity as the lower limit was not governing.

8.3.2. Capacity

The exact capacity is determined in Appendix B.3 and the results are provided in table 8.3. Performing the unity check over the element results in the plot shown in Figure 8.4.

8.3.3. Remarks

The here applied modification to the lower limit has the same limitations as the original formula, as it is empirically fitted. The results is that the remarks made in §8.1.3 are still valid.

Table 8.3: Design requirements according to the method used by Pieters Bouwtechniek at the centre support. Green marking indicated that the requirement is met, red markings indicate the requirement is not met.

		Design load		**Design Resistance**		**Unity Check**	
		Ed		Rd		UC	
Shear	V	57.47	kN	20.63	kN	2.79	-
Min. shear reinforcement	$\rho_{sw,min}$						
Bending moment	M	9.00	kNm	10.12	kNm	0.89	-

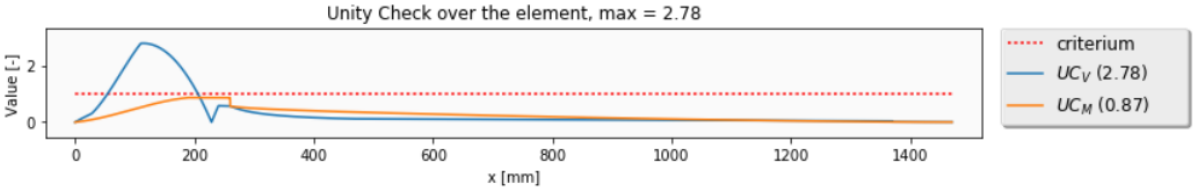

Figure 8.4: The Unity Check performed for method used by Pieters Bouwtechniek.

8.4. Method ModelCode 2010 LoAI

The latest version of the ModelCode, MC2010[20], is developed by the International Federation for Concrete (*fib*) and is the third edition after MC78 and MC90. These codes are developed by the concrete industry and most often support a wider range of application than the EC. The methods provided in the MC are often corporated into the next version of the EC, which makes this a good design code to apply on this case.

One of the significant differences with the EC is that the MC provides multiple methods to determine design values, The so called Level-of-Approximations (LoA) result in less conservative values as their complexity increases. This allows designers to use different methods depending the accuracy required. In this section the method as provided in section MC2010§7.7.3 is applied.

8.4.1. Design principles

The fibre behaviour is implemented in the ModelCode by means of an ultimate tension stress f_{Ftuk}. This value is based on the standard test as described in EN14651. The results of these tests can be interpret using a rigid plastic model or a linear model. The linear model is chosen as it provides a better approximation of the actual shape of the stress-CMOD graph. This model is shown in Figure 8.5.

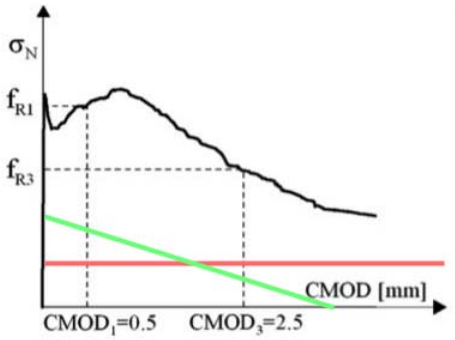

Figure 8.5: The model for fibre behaviour used by the ModelCode2010 with in red the rigid-plastic model and in green the linear model. (source: based on [20, p.148])

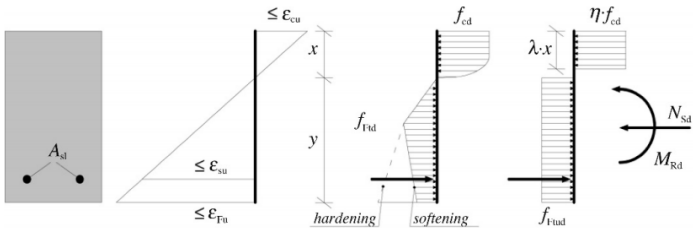

Figure 8.6: The model for bending capacity as used by the ModelCode2010. (source [20, p.298])

The shear capacity is adapted to include a fibre contribution as well. The design strength for element without shear, $V_{Rd,c}$, is replaced by MC-F(7.7-5):

$$V_{Rd,F} = \left[\frac{0.18}{\gamma_c} \cdot k \cdot \left(100 \cdot \rho_l \cdot \left\{1 + 7.5 \cdot \frac{f_{Ftuk}}{f_{ctk}}\right\} \cdot f_{ck}\right)^{1/3} + k_1 \sigma_{cp}\right] \cdot b_w \cdot d \tag{8.3}$$

This equation is empirically fitted, which requires a certain level of conservatism, as it should fit a wide range of applications. The new equation is formulated by adding a factor with the characteristic ultimate tensile stress of the fibres.

Minimal shear requirements are loosened in the MC2010 to allow the application of fibres as minimal reinforcement. This is requirement, MC10-F(7.7-15), is formulated such that the f_{Ftuk} is large enough to resist the stress at which the concrete matrix cracks:

$$f_{Ftuk} \geq 0.08\sqrt{f_{ck}} \tag{8.4}$$

The bending moment capacity is also increased as the fibres contribute. This means that there are now three mechanisms which have to be verified: Failure of the concrete in compression, the reinforcement in tension and the fibres in tension. The model used in the MC10 to determine the maximal capacity is shown in Figure 8.6. The fibre contribution is assumed to be a square stress block. The reduction which is applied on the compressive concrete stress block is not necessary as the value for f_{Ftud} is already significant lower than f_{fd}.

8.4.2. Capacity

The exact capacity is determined in Appendix B.6 and the results are provided in table 8.4. Performing the unity check over the element results in the plot shown in Figure 8.7. The application of this design code allows the use of fibres to replace the minimal shear reinforcement, but the shear resistance is not sufficient to result in a safe design. The inclusion of the fibre contribution does not result in a sufficient increase.

Table 8.4: Design requirements according to the Modelcode2010 at the centre support. Green marking indicated that the requirement is met, red markings indicate the requirement is not met.

		Design load		**Design Resistance**		**Unity Check**	
		Ed		Rd		UC	
Shear	V	57.47	kN	40.63	kN	1.41	-
Min. shear reinforcement	$\rho_{sw,min}$						
Bending moment	M	9.00	kNm	11.14	kNm	0.79	-

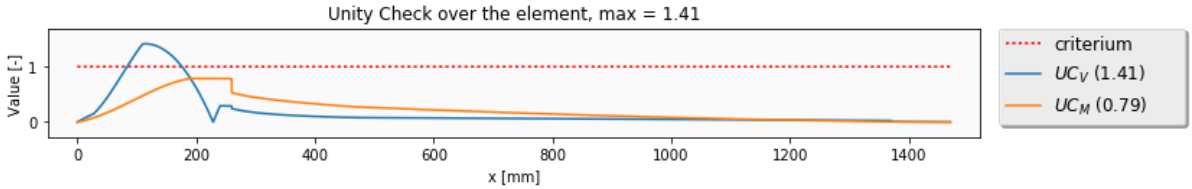

Figure 8.7: The Unity Check performed for the Modelcode2010

8.4.3. Remarks

The found shear resistance is based on empirical derivation, which has the same short comings as the previous design codes. Generalizing the tensile behaviour of all sorts of fibres into a single parameter, f_{Ftuk}, results in a simplification of the response. In order to obtain a sufficient safety while accommodating the huge variety of the FRC spectrum it is required to add conservative factors to the equation. The equation in Formula 8.3 results in a safe and easily calculated design value, but a more sophisticated approach might yield less conservative redundancy.

8.5. ModelCode 2010, Alternative Shear approach

The MC2010 provides a second method for fibre reinforced concrete to determine the capacity. This method is based on the same theory as the general shear part in the MC2010. The general shear part (MC2010§7.3.3) provides multiple levels of approximation (I-IV), where LoAIII is applicable for FRC with a small modification to include the fibre component. This method is requires more computational power as the process is iterative in order to obtain convergence in equilibrium.

8.5.1. Design principles

This method is based on the Level III approximation for shear capacity in MC2010, which is based on the generalized stress field approach [32]. Without a component for the shear reinforcement ($V_s = 0$) the follow equation becomes governing (MC-F(7.7-7)):

$$V_{Rd,F} = \frac{1}{\gamma_F}\left(k_v\sqrt{f_{ck}} + k_f f_{Ftuk} cot\theta\right) z b_w \tag{8.5}$$

$$k_v = \frac{0.4}{1 + 1500\epsilon_x}\frac{1300}{1000 + k_{dg}z} \tag{8.6}$$

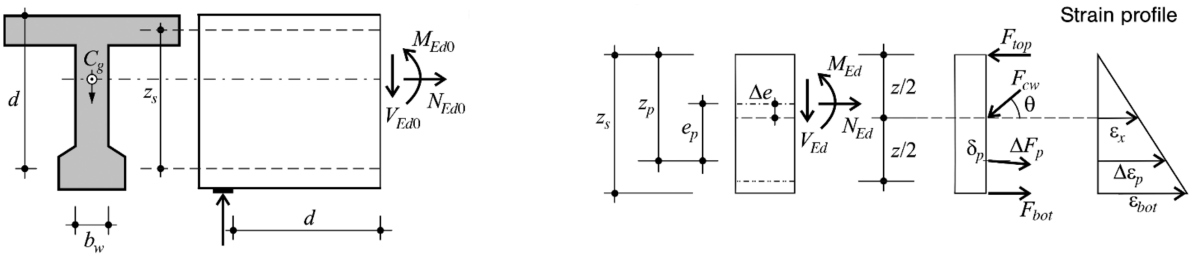

Figure 8.8: Strain profile according to the MC2010, (source: based on [20, p.219]).

Where $k_{dg} = 1.0$, k_v and $k_f = 0.8$ are reduction factors. The value of k_v is a factor to include the concrete contribution to the shear capacity and depends on the longitudinal strain at the neutral axis of the element. Finding the maximal value for Formula 8.5 is iterative, as this strain is a result of the applied forces, V_{Ed}, M_{Ed} and N_{Ed}. Under the assumption of a Bernoulli beam, resulting is Figure 8.8, the following relation is derived (MC-F(7.3-16)):

$$\epsilon_x = \frac{1}{2E_sA_s}\left(\frac{M_{Ed}}{z} + V_{Ed}\right) \tag{8.7}$$

By applying this relation is becomes possible to determine the area over which the fibres are activated and determine their contribution based on the model in Figure 8.5. The crack angle can be varied as well, but the minimal value is raised from 21.9° to $\theta \geq 29° + 7000\epsilon_x$. As the crack angle depends on the strain distribution over the cross-section.

8.5.2. Capacity

The exact capacity is determined in Appendix B.6 and the results are provided in table 8.5. Performing the unity check over the element results in the plot shown in Figure 8.9. The increased complexity of the applied model did not result in a significant increase in the design capacity and therefore the overall capacity is still not sufficient to validate the design.

Table 8.5: Design requirements according to the MC2010 (alternative method) at the centre support. Green marking indicated that the requirement is met, red markings indicate the requirement is not met.

		Design load		**Design Resistance**		**Unity Check**	
		Ed		Rd		UC	
Shear	V	57.47	kN	41.13	kN	1.22	-
Min. shear reinforcement	$\rho_{sw,min}$						
Bending moment	M	9.00	kNm	11.14	kNm	0.79	-

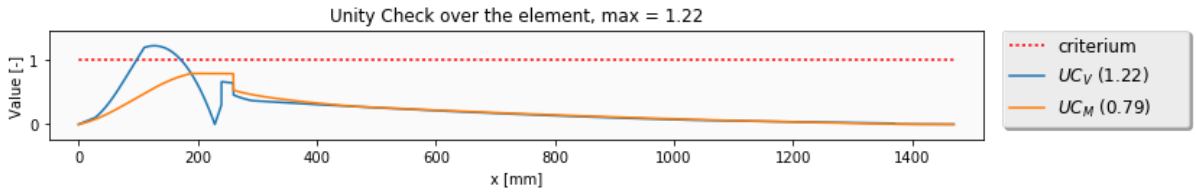

Figure 8.9: The Unity Check performed for the Modelcode2010 LoAIII

8.5.3. Remarks

This alternative approach is based on better understandable models, as the formulas are mostly based on analytical models, instead of the empirically fitted models used in the regular approach of the MC2010. As a result an engineer can better understand the relation between the input and the output. One of the downsides of this approach is the complexity: the shear capacity depends on a combination of other parameters, which make it harder to compare multiple loadcases and determine the actual capacity. This process does not allow for calculation by hand, but can be easily automated in spreadsheets or other programmable calculation tools.

8.6. The German Guideline for FRC

This guideline, DAfStb-Richtlinie Stahlfaserbeton, contains additional methods to include the steel fibre contribution in the Eurocode.

8.6.1. Design methods

These guidelines are an extension to the Eurocode and they do include a fibre contribution. This contribution is added to the concrete resistance, $V_{Rd,c}$:

$$V_{Rd,c}^{f} = V_{Rd,c} + V_{Rd,cf} \tag{8.8}$$

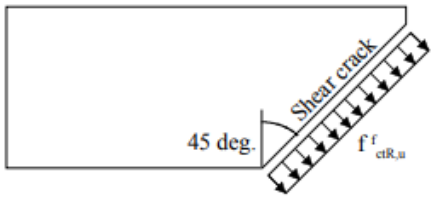

Figure 8.10: The model used for the fibre contribution in the German guidelines. (source [44, p.19])

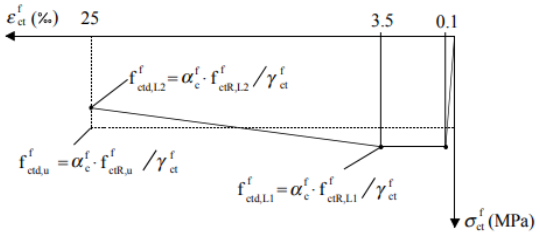

Figure 8.11: Tensile model for the German guidelines. (source [44, p.19])

The fibre contribution, $V_{Rd,cf}$, is based the ultimate resistance the fibres can offer over a crack with a $45°$ angle in ULS. The model is shown in Figure 8.10. The value for $V_{Rd,cf}$ is determined by multiplying the concrete cross section ($b_w \cdot h$) with the stress which the fibres can take over this area, $f_{ctR,u}^{f}$. This value for stress is based on a simplified stress-strain relation, as shown in Figure 8.11. The rectangular dashed relation is used. The used value for the ultimate stress is determined via tests as prescribed in EN14651, which are corrected for the applied structure. In this the case multiplied with:

$1/\gamma_{ct}^{f}$	$= 0.80$	A material factor for steel fibres.
α_{c}^{f}	$= 0.85$	A factor to take long-term effect of the steel fibres in to account.
κ_{F}^{f}	$= 0.80$	A factor to take in to account the fibre orientation relative to the fibre orientation factor in the EN14651 experiment. This value is element specific, but difficult to determine. A 3D random distribution results in a value of 1.07, while a 2D random distribution results in a value of 0.8. Due to the wall effect the value for this element will be somewhere in between these two values, but it is assumed to be 0.8 in order to be on the safe side.
κ_{G}^{f}	$= 1.01$	A factor to take member size in to account. This value is element specific: it is determined as $1.0 + 0.5 \cdot A_{ct}^{f} \leq 1.70$ with A_{ct}^{f} assumed to be $0.9A_c$

8.6.2. Capacity

The exact capacity is determined in Appendix B.4 and the results are provided in table 8.6. Performing the unity check over the element results in the plot shown in Figure 8.12.

Table 8.6: Design requirements according to the Eurocode with the German Guidelines at the centre support. Green marking indicated that the requirement is met, red markings indicate the requirement is not met.

		Design load		**Design Resistance**		**Unity Check**	
		Ed		Rd		UC	
Shear	V	57.47	kN	33.74	kN	1.70	-
Min. shear reinforcement	$\rho_{sw,min}$						
Bending moment	M	9.00	kNm	10.60	kNm	0.85	-

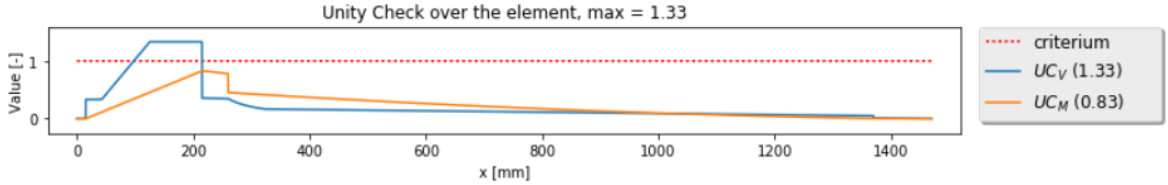

Figure 8.12: The Unity Check performed for the German Guidelines

8.6.3. Remarks

This approach is based on finding a reliable method which uses a simplified tension model. As a result the method is straight forward to apply, but compared to the Modelcode a significantly lower capacity is found.

8.7. The French Guidelines

France published a national addition to the Eurocode 2 with specific rules for UHPFRC in 2016: *NF P18-710* [33]. This document is the result of years of research and is the implementation of the previous Recommendations from AFGC[7]. The new document has an official status in France, making it easy to apply on new designs.

8.7.1. Design principles

The UHPFRCs are divided in to three categories based on their tensile behaviour: strain softening (T1), low strain hardening (T2) and strain hardening (T3). The last category contains the material where the peak tensile stress, f_{tu}, exceeds the cracking stress, $f_{t,cr}$, by more than $1.25\times$. CRC falls in the last category, as $f_{tu} \geq 1.5 f_{t,cr}$.

The shear capacity is implemented by introducing a fibre term. Where the previous methods determined certain characteristic values, the French appendix takes another route. A maximum value for the crack-width is determined, w^*. Under the assumption of a Bernoulli beam, this can be translated into an average stress over the crack. For T3 types the strain is used instead of the crack-width, and the equation is (ECFR-F(6.214)):

$$\sigma_{Rd,f} = \frac{1}{K\gamma_{cf}} \frac{1}{\epsilon^* - \epsilon_{el}} \int_{\epsilon_{el}}^{\epsilon^*} \sigma_f(\epsilon) d\epsilon \tag{8.9}$$

The found average stress is assumed to be active over the entire area in tension in a cross-section along the crack angle θ. The concrete and the steel contribution are tread separately, similar to the original Eurocode. The capacity is then determined according to ECFR§6.2.1.1(2):

$$V_{Rd} = V_{Rd,c} + V_{Rd,s} + V_{Rd,f} \leq V_{Rd,max} \tag{8.10}$$

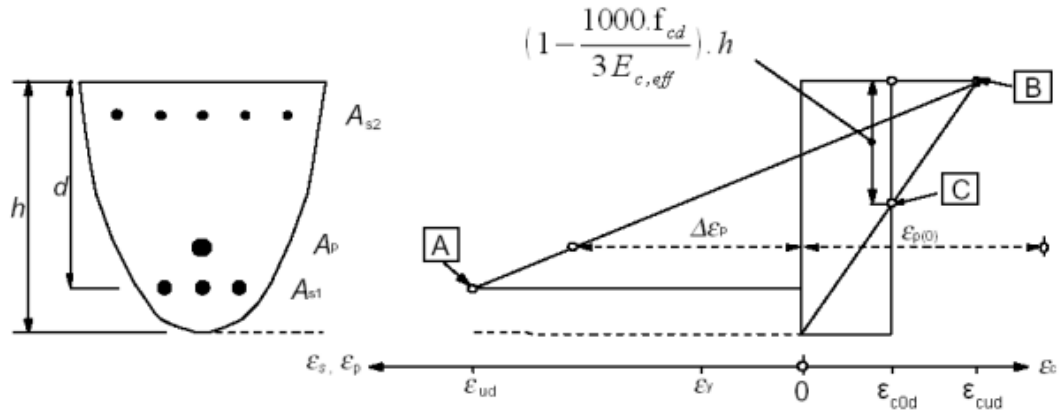

Figure 8.13: Stress model for the French guideline, (source: based on [7, p.101])

Minimal shear requirements is mend to enforce ductile failure. As a T3 category concrete already provides ductile failure it is no longer necessary to add minimal shear reinforcement. ECFR§7.3.2(1)P provides this exclusion.

The bending moment capacity is determined in relation with the model as provided in Figure 8.13. The fibre contribution is added to the equilibrium equations using the average stress.

8.7.2. Capacity

The exact capacity is determined in Appendix B.5 and the results are provided in table 8.7. Performing the unity check over the element results in the plot shown in Figure 8.14. According to the French annex there is sufficient capacity in the element to ensure the wanted level of redundancy. All requirements are met.

8.7.3. Applicability

This guideline uses the actual stress-strain curve as determined in an uni-axial tensile test. Usage of the actual curve instead of a simplified model curve results in a better fit for the unique properties which many types of FRC have. It does however take more information from experiments to be able to determine the resistance. A relation between the stress and the crack-width, or ultimate crack-width and average stress, is required.

Table 8.7: Design requirements according to the Eurocode with the French guidelines at the centre support. Green marking indicated that the requirement is met, red markings indicate the requirement is not met.

		Design load Ed		**Design Resistance** Rd		**Unity Check** UC	
Shear	V	57.47	kN	89.67	kN	0.65	-
Min. shear reinforcement	$\rho_{sw,min}$						
Bending moment	M	9.00	kNm	13.54	kNm	0.65	-

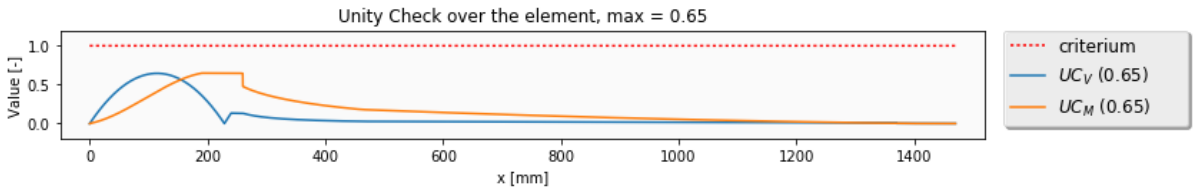

Figure 8.14: The unity check performed for method of the Eurocode with the French guidelines

8.8. Conclusions for the design predictions

Multiple design codes have been applied to the design in the previous sections to determine the whether the structure was sufficiently safe. An overview of the derived values is provided in Table 8.8. The design did not comply with most of the codes, as can be seen in Figure 8.15, where most codes have a UC above 1.0. According to these code the application of shear reinforcement in necessary. The figure also clearly shows the difference between the codes which include a fibre component and those which do not.

Deciding which design code to apply should not be a case of picking the most advantageous one. Most of the time the authorities decides which code should be applied. Deviation from this standard approach should only be done when the new codes are better fitted for the design. In this case this would mean neglecting the the EC, ECNL and PBT, as these methods do not include the fibre component. The more advanced the model was, the higher the predicted capacity. This can be explained by the fact that a more advanced model can be a closer approximation of the reality.

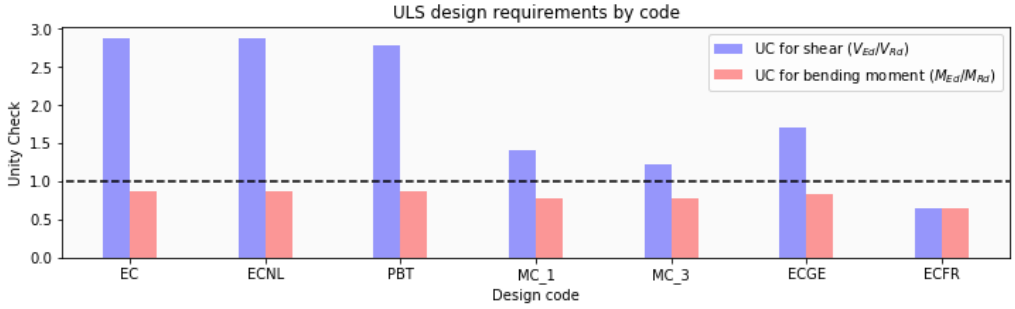

Figure 8.15: The Unity Check performed for the applied codes.

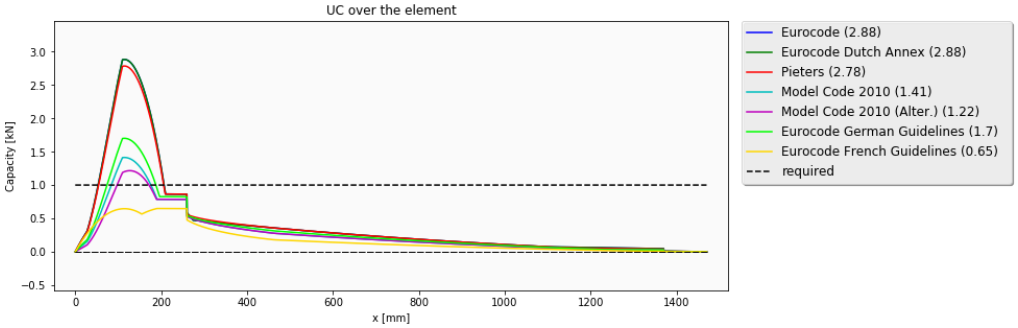

Figure 8.16: The Unity Check performed for the applied codes.

Table 8.8: Overview of all determined capacities.

Method		P_{Vu}		P_{Mu}		P_u		
		P_{Vm}	P_{Vd}	P_{Mm}	P_{Md}	P_{um}	P_{ud}	
Codes	EC	37.1	23.4	77.5	59.4	37.1	23.4	kN
	ECNL	37.1	23.4	77.5	59.4	37.1	23.4	kN
	ECPBT	45.7	24.2	77.5	59.4	45.7	23.4	kN
	ECFR	178.6	105.2	79.4	79.4	79.4	79.4	kN
	ECGE	76.6	39.6	85.0	62.2	76.6	39.6	kN
	MC2010	73.8	47.7	88.8	65.3	73.8	47.7	kN
	MC2010a	65.3	48.3	88.8	65.3	65.3	48.3	kN
Design load		-	52.8	-	52.8		52.8	kN

9

Validation by FEM

The predictions of the shear capacity in the previous chapter are based on generalised methods, which incorporate the combined structural behaviour. Another method which can be used to predict the structural capacity is the Finite Element Method (FEM). This method uses the material properties and element dimensions to create a stiffness matrix of the structure. This matrix can be used to numerically determine the reaction forces given a certain displacement, or vice versa. This method will be applied on the Raqtan landing platform. The advantage of FEM is the possibility to include non-linear behaviour, such as cracking or yielding, which can provide useful information regarding the structural response.

The Finite Element Analysis (FEA) is performed using the software DIANA 10.2. This software is preferred over other packages such as ATENA, as the researcher has more experience with DIANA and DIANA provides the required means to incorporate the fibres properties in the material behaviour. Another factor in this decision was the programmability of DIANA, as it allows the use of Python code to fully automate the model creation and analysis. The use of Python also results in a less error-prone model building than using the regular interface, as the input is better controllable.

The first section of this chapter discusses the tensile model which is used to model the FRC behaviour. Previous experiments from Hi-Con will be used to calibrate the tensile model. The next section focusses on the basic model for the Raqtan platform, which is used for a first insight. Then multiple alterations to this model, such as tension models or element size, will be made to determine the influence on the result. Finally conclusions from these analyses will be drawn.

9.1. The tensile material model

The material property which deviates the most from the regular concrete behaviour is the tensile behaviour. This property defines the post cracking response and should resemble the actual behaviour in order for the FE model to be representative. This post-cracking response of different tensile models are compared to the experimental response in the set-up as determined in Eurocode 14651 [28].

9.1.1. The EN-14651 experiment

This experiment is a three-point-bending test to determine the relation between the Crack-Mouth-Opening-Displacement (CMOD) and required load. This load is used to derive the residual tensile stresses of the material in relation to the strain. The experiment set-up is shown in Figure 9.1. The experimental data is used to derive the mean, characteristic (90% interval) and design values for the P-CMOD curve. The resulting curves are shown in Figure 9.2. These curves are used to derive the tensile stress at 5 point. The Limit of Proportionality (f_{LOP}), at the peak value before a strain of 0.05, and the stress $f_R i$ for i 1 to 4 at respectively at a displacement of 0.5, 1.5, 2.5 and 3.5 mm.

The model The experiment is modelled in DIANA in 2D, with a main mesh-size of 25mm and above the notch the element size is decreased to 5mm. The resulting model is shown in Figure 9.3. The

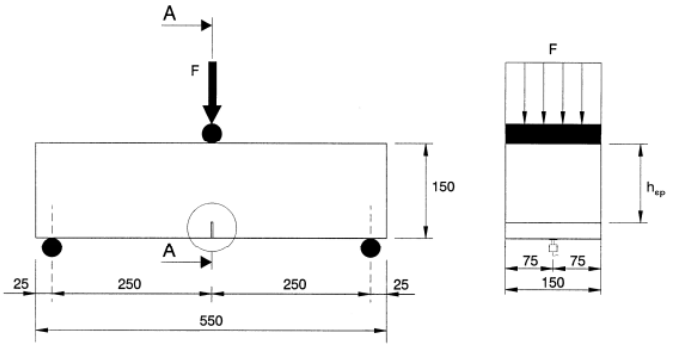

Figure 9.1: The experiment set-up according to EN-14651. (source [28, p.9])

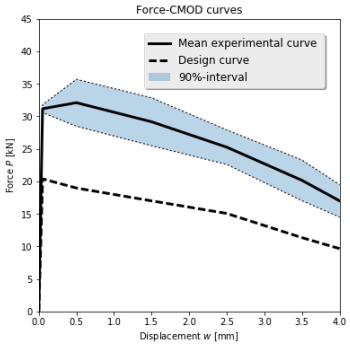

Figure 9.2: The derived P-CMOD curves.

elements are *CQ16M* elements, 8-noded quadrilateral isoparametric plane stress element, as shown in Figure 9.4. Which means that the stress over the third dimension, z in this model, is assumed to be zero. The default integration scheme for this element is 2x2 Gauss integration, but the element allows the use of a 3x3 integration scheme. This is used as it can accommodate more complex structural responses.

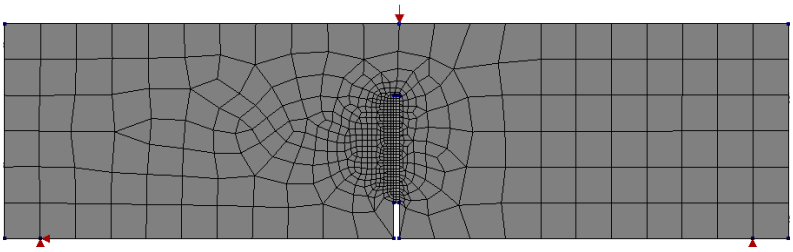

Figure 9.3: The EC14651 model in DIANA.

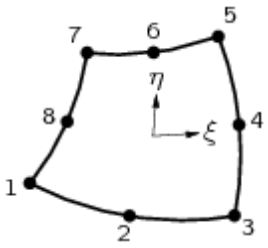

Figure 9.4: Representation of the used element: CQ16M. [1]

The applied non-linear analysis is *displacement controlled*. This means that the boundary condition is chosen in such a way that the displacement of the centre support is fixed per step and the required load P is determined to impose this deformation. *Displacement controlled* is preferred over *force controlled* as this allows to model the post peak behaviour as well. Non-linear analyses require convergence of the solution towards an equilibrium state for every step made. This convergence is tried to be found by the application of the *Modified Newton-Raphson* method, which scales down the computational power required compared to the *Regular Newton-Raphson* method. Another method which is used and brings down the computational power required is *line search*, which is especially useful for finding the post-peak response of a structure.

The earlier mentioned convergence determines when a load step is finished, even though the equilibrium is not fully met. The convergence criteria is set as a combination of both displacement and force norms (norm tolerance is 1% of the initial difference), which ensures a valid response for every load step. The amount of iterations per step is increased from the default value of DIANA to 1000, to accommodate for large differences in the stiffness matrix per step.

The material properties The CRC is modelled using the *Concrete and masonry* material class in DIANA, which allows the use of the *total strain based cracking* model. The values used for this model are the mean values, as the goal is to recreate the original experiment. The compressive behaviour is modelled as prescribed in the *Eurocode 2 EN 1992-1-1* and is shown in Figure 9.5. For the tensile curve multiple options were evaluated:

- **FRCCMD033** and **FRCCMD045**: These models use a FRC model provided by DIANA (FRCCON). The input is directly derived from the EC14651 experiment. The experiment provide mul-

[1] source:*dianafea.com/manuals/d944/ElmLib/node113.html*

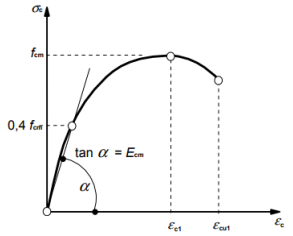

Figure 9.5: The compressive model as proposed in EC1992. (source [30, p.35])

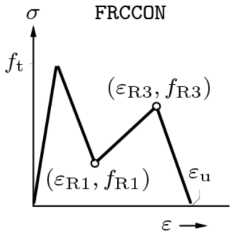

Figure 9.6: Tension model from fib for FRC in DIANA. [2]

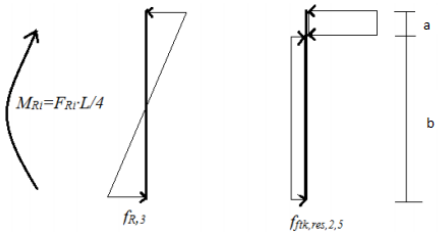

Figure 9.7: Assumed relation between $f_{fl,res}$ and $f_{ten,res}$. (source: based on [24, p.24])

tiple values for the residual flexural strength, $f_{fl,res}$, which have to be multiplied by a factor to convert them in to the residual tensile strength, $f_{t,res}$, before they can be used in this DIANA model. This depends on the assumed height of the compressive zone, a in Figure 9.7. The relation, determined through equal resulting moments, then becomes:

$$f_{fl,res} \cdot \frac{h^2}{6} = f_{ten,res} \cdot b \cdot 0.5(a+b) \tag{9.1}$$

With $b = \alpha \cdot h$ this can be rewritten as:

$$f_{ten,res} = \frac{1}{3 \cdot \alpha} \cdot f_{fl,res} \tag{9.2}$$

As $\alpha \to 1$, this results in a lower limit for the multiplication factor of 0.33. A reasonable upper value is determined with $\alpha = 0.75$, resulting in a factor of 0.45. Using these to factors the residual tensile stresses for the DIANA model are determined.

- **FRCEPS033** and **FRCEPS045**: These models also use the FRCCON model as provided by DIANA, but they use the strain-residual tensile stress relation as input, while the previous models used the CMOD-residual tensile stress as input. The strain values are derived under the assumption of a Bernoulli beam:

$$\epsilon = \frac{0.5 \cdot 125}{25 + 0.5 \cdot 125} \cdot \frac{CMOD}{5} = 0.14 \cdot CMOD \tag{9.3}$$

- **MC2010RIG** This is a stress - crack-width relation provided by the Modelcode, which uses the value for f_{R3} to determine a rigid relation: $f_{Fts} = f_{R3}/3$. This relation is converted to a stress-strain relation using the previously provided relation between CMOD and strain. The implementation in DIANA is achieved using the multi-linear tensile model MULTLN.

- **MC2010LIN** This is a stress - crack-width relation provided by the Modelcode, which uses the values f_{R1} and f_{R3} to determine a linear relation. The initial value, at $w = 0$ is determined with $f_{Fts} = 0.45 f_{R1}$. The other point on the line is determined by:

$$F_{Ftu} = f_{Fts} - \frac{w_u}{CMOD_3}(f_{Fts} - 0.5 f_{R3} + 0.2 f_{R1}) \geq 0 \tag{9.4}$$

  This relation is converted to a stress-strain relation using the previously provided relation between CMOD and strain. The implementation in DIANA is achieved using the multi-linear tensile model MULTLN.

- **MULTI_TEN** This model is based on experimental results from uniaxial tensile tests. The MULTLN model in DIANA is used again for the implementation.

The stress-strain relations from the used models are shown in Figure 9.8. It should again be noted that all used values are based on the mean material properties in order to simulate the actual experiment. The other used material properties are provided in Table 9.1.1

[2] source: *dianafea.com/manuals/d96/MatLib/node84.html*

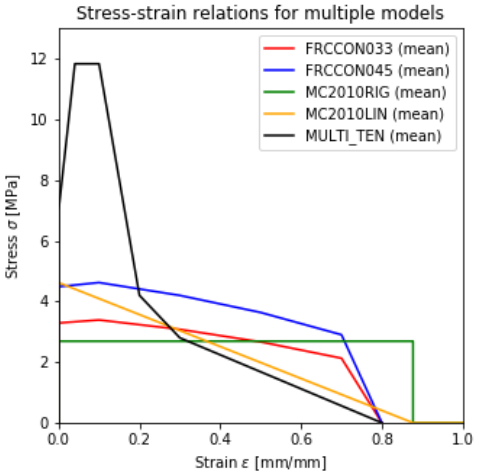

Figure 9.8: The stress-strain relations for the implemented models.

Property		Value	
Young's Modulus	E_{cm}	50000	MPa
poisson's ratio	ν	0.20	-
crack orientation		rotating	
Tensile curve		Variable	
compressive curve		*Eurocode 2*	
Compressive strength	f_{cm}	130	MPa
Strain at f_{cm}	ϵ_{c1}	0.0028	mm/mm
Max strain	ϵ_{cu}	0.0028	mm/mm
Young's at $0.4f_{cm}$	E_{cm}	50000	MPa

Table 9.1: Material properties for te EC14651 DIANA model.

9.1.2. The model output

The model is run with all the tensile models and compared to the experimentally derived curve. The result is shown in Figure 9.9. In order to determine the usability of the different tensile models, it is useful to compare their output values for the EC14651 test to the experimental results. When these values are within the 90% domain they are likely to be found during experiments as well and therefore admissible for further DIANA models. As seen in the graph and quantified in Table 9.2, the difference in behaviour between the models and the experiments is significant and none of the tensile model provide a close resemblance with the target curve.

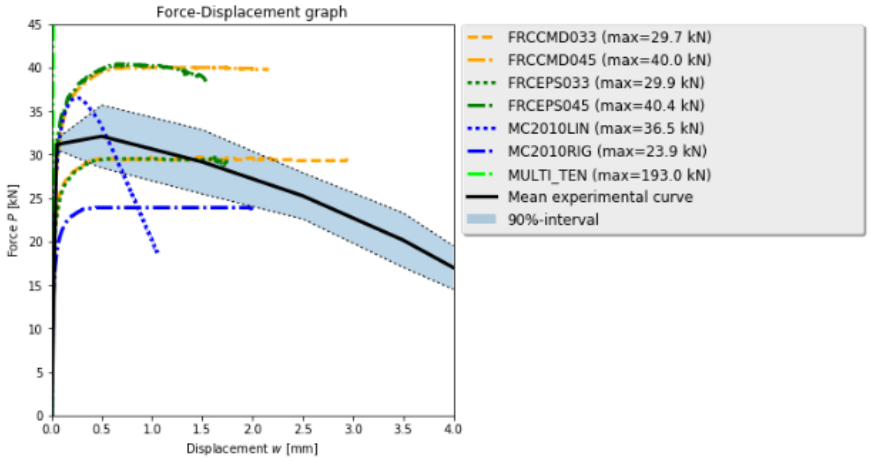

Figure 9.9: The Unity Check performed for the applied codes.

The deviation in structural response can be explained by the simplifications which are made to most models in order to be widely applicable. This might neglect the actual, more complex, behaviour. The curves do tell something about the required stress-strain relation. The height of the peak value in the P-CMOD is governed by the peak value in the $\sigma - \epsilon$ relation and the post-peak behaviour is determined by the drop in capacity as the peak stress is past.

9.1.3. Inverse analysis I

Another method to find a satisfying stress-strain relationship is the inverse analysis. When this method is applied, an attempt is made to determine a stress-strain relation which satisfies a target curve. This is often done for FRC [42, 47] as the exact tensile behaviour can be rather complex. A curve with multiple variables is fitted and the best values for the variables are searched. An example is provided

Table 9.2: Validation of the tensile models. Green cells indicate that the value is in the desired domain, red cell indicate otherwise.

	f_{LOP} [MPa]	f_{R1} [MPa]	f_{R2} [MPa]	f_{R3} [MPa]	f_{R4} [MPa]
90% lowerlimit	9.78	9.11	8.15	7.23	5.45
90% upperlimit	10.17	11.42	10.51	8.93	7.45
FRCCMD033	7.23	9.44	9.50	9.38	-
FRCCMD045	8.86	12.64	12.80	-	-
FRCEPS033	7.10	9.41	9.41	-	-
FRCEPS045	9.22	12.70	12.48	-	-
MC2010LIN	8.86	10.66	-	-	-
MC2010RIG	5.73	7.65	7.65	-	-
MULTI_TEN	28.58	-	-	-	-

in Figure 9.10. This curve contains multiple variable, including the stress at the Failure point and the coordinates for the points 2,3 and 4.

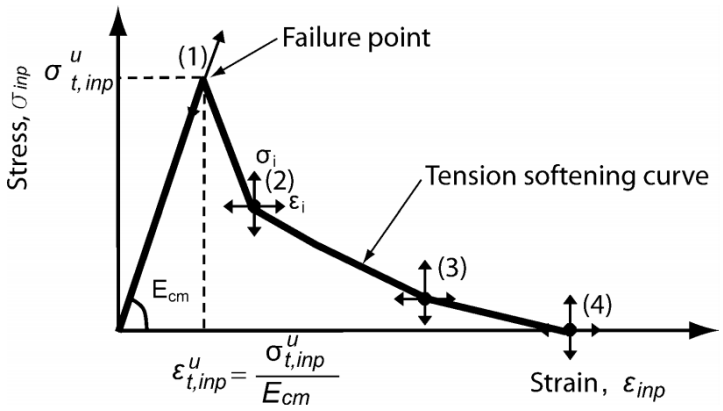

Figure 9.10: An initial curve for inverse analysis. (source [42, p.224])

The process can be automated with the use of *Machine Learning*. The experimental mean curve is used as a target curve and a relation between input stress-strain relation and P-CMOD curve is implemented. The relation is based on the assumption of a Bernoulli beam. The following steps are taken to find the optimal stress strain relation:

1. Learning rates for each parameter are set at 0.2. This determines the rate of convergence.
2. An initial guess is made for the parameters and a stress-strain curve is determined
3. For 1000 points on the interval between 0 and 4mm CMOD the height of the compression zone is determined based on horizontal force equilibrium. With the height of the compression zone known, it is possible to determine the bending moment in the cross-section. Which results in the load. A P-CMOD curve has been found for the provided stress-strain curve.
4. The Root Mean Square Error (RMSE) is determined using all the defined points in the P-CMOD curve.
5. A random parameter is updated with its learning rate in both directions, which results in two new stress-strain curves. For each curve the new RMSE is determined.
6. If an improvement is found, the new curve is stored and the step 5 is repeated until a convergence criteria is reached. Otherwise the learning rate is halved and then step 5 is repeated.

Performing this operation multiple times until the decrease of the RMSE was not significant any more, resulted in a stress-strain relation and the corresponding, analytically determined, P-CMOD relation are shown in Figure 9.11.

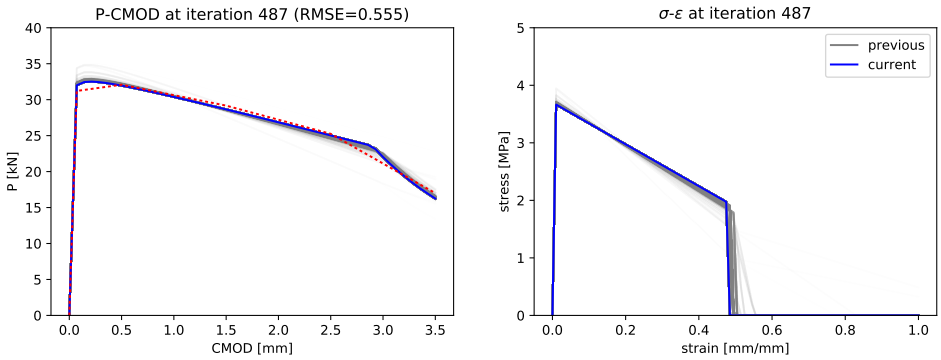

Figure 9.11: The fitted P-CMOD and stress-strain curves for inverse analysis.

This stress-strain relation is used for a DIANA model, MULTI_FIT. The resulting curve is shown in 9.12. The curve does reach an equal peak value, but starts to drop rapidly afterwards. This is a result of the non-linear strain distribution over the cross-section of the element, which is observed in the DIANA model (see Figure 9.13). The evaluation of the curve is provided in Table 9.3. Inverse analysis using the analytical approach does not result in a satisfying curve as only one of the 5 default values is within the 90% range.

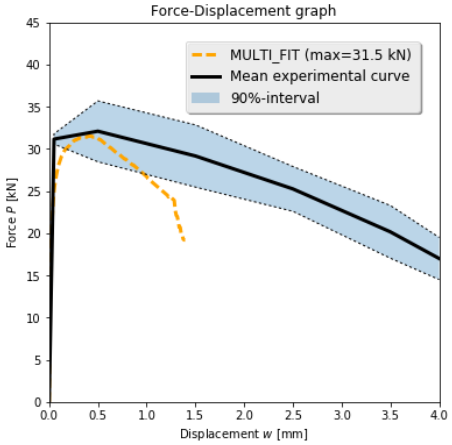

Figure 9.12: P-CMOD curve for the fitted stress-strain relation.

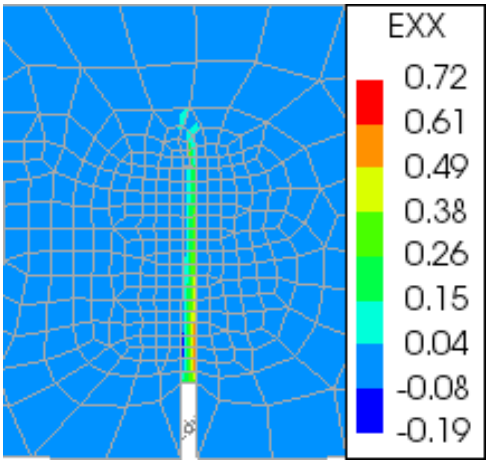

Figure 9.13: The strain in x-direction (ϵ_{xx}) in the last converging step (d=1.41mm).

Table 9.3: Validation of the Inverse analysis model. Green cells indicate that the value is in the desired domain, red cell indicate otherwise.

	f_{LOP} [MPa]	f_{R1} [MPa]	f_{R2} [MPa]	f_{R3} [MPa]	f_{R4} [MPa]
90% lowerlimit	9.78	9.11	8.15	7.23	5.45
90% upperlimit	10.17	11.42	10.51	8.93	7.45
MULTI_FIT	7.97	10.02	-	-	-

9.1.4. Inverse analysis II

The inverse analysis can also be applied directly to the DIANA model. This requires less knowledge of the actual response, which makes it more prone to over-fitting. This happens when the tensile model is optimized for this particular experiment, but does not represent the behaviour in other settings. As the previous methods did not provide a satisfying result it is chosen to perform this type of direct inverse analysis. The stress-strain relation is modified and the fitted curves for the mean, characteristic and the design curves are shown in Figure 9.14.

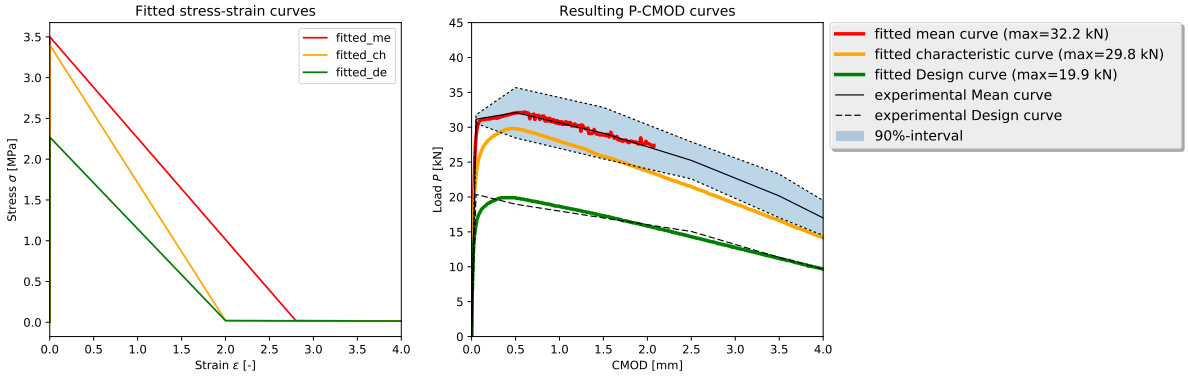

Figure 9.14: The directly fitted curves in relation to the experimental results.

These curves satisfy the 90% range, but with a larger RMSE than the analytically fitted curves. Improving the curves is time consuming, while the expected increase in result is small. The found curves can be used for the Raqtan model, but the influence of over-fitting should be examined. This can be done when comparing the experiments results with the DIANA models.

9.2. The Raqtan model

The initial model is mechanically based on the methods used by the previous design steps and the connection is modelled as a three-point-bending test. The clamped connection would result in different behaviour and in an expected increase in shear stress. This increase is already included in the design load, which will be compared to the design resistance. The clamped connection will be investigated as one of the variants in order to be able to compare the results of both connections types.

9.2.1. The model settings

The initial model is chosen to be straight forward and simple, as this allows the verification of the output. It is a 2D analysis which includes physical non-linearities, such as yielding of the reinforcement and cracking of the concrete. The reinforcement is added as a 1D bar with the area property set to the combined area of the main reinforcement. The tensile behaviour is implemented using the previously defined models. Not only the fitted curves will be used, but the other models will be used as well. The comparison between the different models can provide insight in the importance of the proper tensile model.

The design values are used as input values for the material properties. This way the model output can be used as a design output. For the fitted curve the characteristic curve is used as well. In that case the material factors (1.5 for both γ_c and γ_{cf}) will be applied on the output to determine the design response.

The initial mesh is chosen to have an element size of 20mm, which results in 4 elements over the height of the element. Later on different element sizes will be investigated in relation to the structural response. The elements are *CQ16M* elements, the same elements as in the EC14651 model.

The boundary conditions are applied by adding steel plates and restraining these from translation to create a simply supported system. This results in a spread area for the introduction of forces and reduces the impact of these singularities. The code which is used to create the model is provided in Appendix D.1 and results in the model as shown in Figure 9.15.

The material properties which are used for this model are provided in Table 9.4 and 9.5. The reinforcement is modelled with *uniaxial nonlinear elasticity*. Which allows the implementation of yielding of the steel.

Table 9.4: Material properties for the EC14651 DIANA

Property		**Value**	
Concrete			
Young's Modulus	E_c	42000	MPa
poisson's ratio	ν_c	0.20	-
crack orientation		*rotating*	
Tensile curve		*Variable*	
compressive curve		*Eurocode 2*	
Compressive strength	f_{cd}	73.33	MPa
Strain at f_{cd}	ϵ_{c1}	0.0017	-
Max strain	ϵ_{cu}	0.0017	-
Young's at $0.4f_{cd}$	E_c	42000	MPa

Table 9.5: Material properties for the EC14651 DIANA

Property		**Value**	
Reinforcement			
Young's Modulus	E_s	210000	MPa
poisson's ratio	ν_s	0.25	-
yield strength	f_{yd}	435	MPa
cross-section area	A_s	471;628	mm^2
Support Plates			
Young's Modulus	E_{ss}	210000	MPa
poisson's ratio	ν_{ss}	0.25	-
yield strength	f_{syd}	435	MPa

The analysis is similar to the one used for the EC14651 model. It is *displacement controlled* and the convergence method is the *Modified Newton-Raphson* method. The convergence criteria is strict, which means it is a combination of force and displacement equilibrium which both have to be satisfied. The tolerances are set to 1% and the maximum number of iterations is again increased to 1000, as the stiffness matrix can be subjected to significant modifications during the cracking of the material.

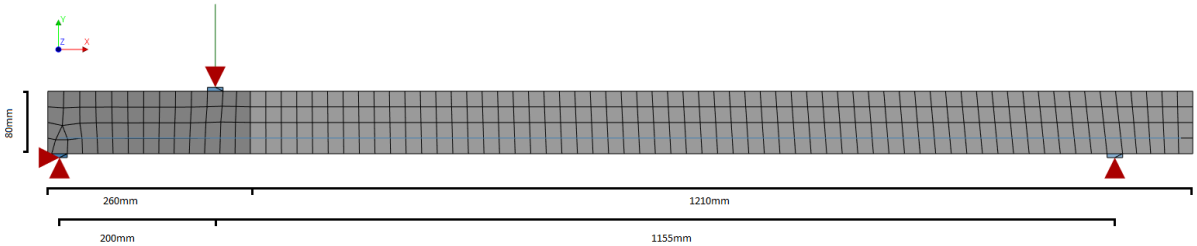

Figure 9.15: The mesh for a meshsize of 20mm.

9.2.2. The model output

The model provides the displacement in relation to the applied force at the centre support. This output is plotted for all tensile models in Figure 9.16. The peak value is an 80kN, as the tensile model based on the uni-axial tensile test has proven to be inaccurate. This force is significantly exceeding the design load of 57.5 kN. This indicates the validity of the model, but a number of parameters of the model has to be verified in order to ensure the proper behaviour.

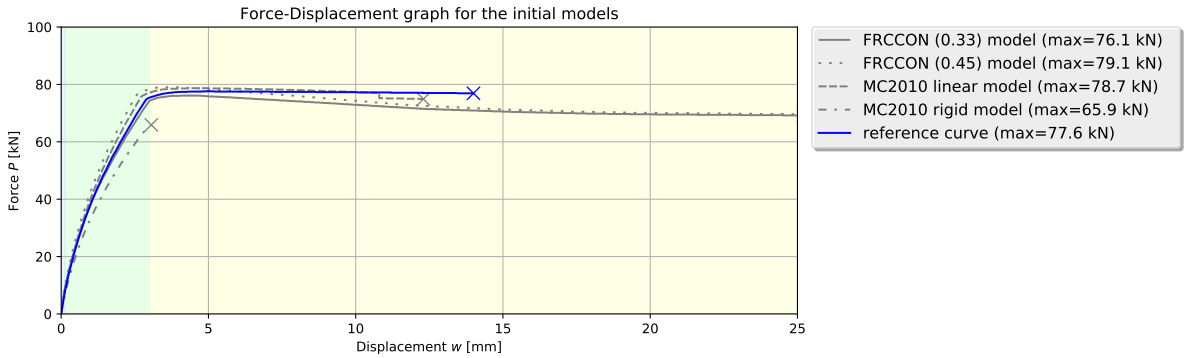

Figure 9.16: The force-displacement curve for the initial models.

The first analysis is the force-displacement curve. This curve is often used for visualization of the structural response, as it provides information regarding the different resistance mechanisms which together provide the structural response. This curve can be dissected in to three zones with three transition zones, as shown in Figure 9.17. The background colours of the graph indicate the different phases during the deformation. The model based on the uni-axial tensile test is neglected from this point onwards. This models was inaccurate in the EN14651 experiment model and results in an overcapacity of the model. As the purpose of this analysis is to determine a safe lower limit of the capacity the information gained by the tensile model is not fit for usage.

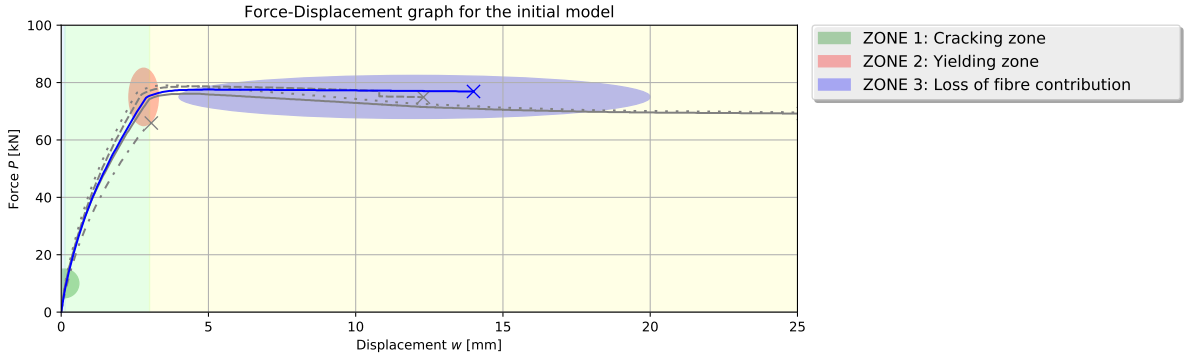

Figure 9.17: The mesh for a mesh-size of 20mm. Points of attention are marked: *(1)* cracking occurs; *(2)* main reinforcement yields; *(3)* loss of fibre contribution; *(4)* plastically hinged.

Phase I (Blue) - Uncracked During this phase the concrete matrix is uncracked and and the behaviour can be assumed to be elastic. At point transition-zone 1 the stiffness of the element changes, as the cracks change the material properties and the fibres are activated. This phase is marked blue in the graph.

Phase II (Green) - Fibre activation As the load is increased further after the initial cracking, the stiffness of the element keeps slowly going down. This is a result of the expanding cracks. This phase ends with a sudden change of the stiffness as the reinforcement starts to yield. This point is marked in the graph as the second transition zone.

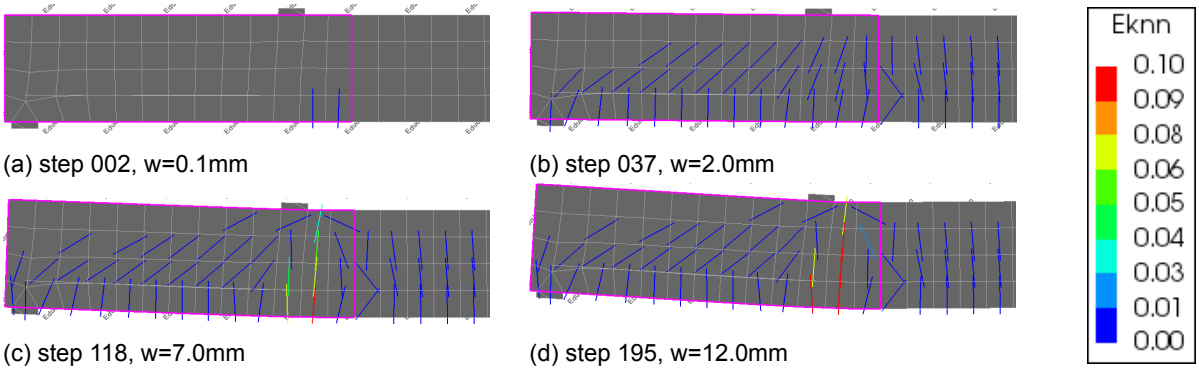

(a) step 002, w=0.1mm (b) step 037, w=2.0mm

(c) step 118, w=7.0mm (d) step 195, w=12.0mm

Figure 9.18: The crack pattern at multiple deformation stages. The console is marked in pink.

Phase III (Yellow) - Loss of fibre contribution After the yielding of the main reinforcement, the resistance is created by a combination of the yielding reinforcement and a fibre contribution. The fibre contribution changes as the cracks are widening: The fibres at the lower side of the tensile zone have past their peak stress, F_{LOP} and start losing their resistance. At the same time, due to crack widening, the fibres in the centre of the element are activated further. This first results in an increase of resistance, as the second mechanisms is stronger than the first, but as the crack is widened further (in the third transition zone), the balance goes the other way. At this point the capacity starts going down towards a value which is reached by a plastic hinge, a case when the fibres are not contributing any more. This phase goes on until the compression zone is so small that it is not able to resist the stresses and fails. This value was not reached in the models. The transitions between these two mechanisms is smooth and therefore this phase can not be split up.

The behaviour and the phases mentioned above have to be validated by the actual output of the model. The first validation is the determination of the first crack occurrence. Going through the output step by step this is found already at step 2, with a displacement of 0.10mm. This step, along with steps in other stages (2,7 and 12mm displacement), is shown in Figure 9.18. The first crack occurs at the last element of the console. This is not the location of the highest bending moment or the highest shear force, but the crack occurs here as the cantilevering platform is significantly stiffer than the console. The width (1060mm) is more than four times the width of the console, resulting in a four time higher moment of inertia. As stiffer elements attract more stresses, the connecting elements are heavier loaded. In this case the first row of elements of the console.

The second transition is marked by the first occurrence of yielding in the main reinforcement. This happens at a displacement of 2.65mm. The strain in the reinforcement is shown in Figure 9.19. It can be seen that the peak strain is localized in the main crack.

The transitions within phase III can be visualised by determining the strain state in which the elements are during the different loading steps. This is done in Figure 9.20 for the marked steps. It can be seen that the strain are localized after yielding, but the fibres spanning the main crack still have some resistance in the shown stages as the maximum strain in the fitted stress-strain relation is at 2.0. As the load would be increased further, the fibre contribution is decreasing and the reinforcement becomes the main provider of resistance.

As the shape of the force-displacement curve is analysed and explained in a qualitative way, the next step is to validate the shape in a quantitative way. This is done in the next section.

9.2.3. The model verification

The results of a FEA are highly dependent of the input parameters. Proper understanding of the applied models is therefore at the essence of achieving usable results. Small mistakes in the input can result in unexpected behaviour and major deviations in resistance. To verify the correctness of the model, it is possible to determine certain values analytical and compare them to the results from the FEA. It

should be noted that these are only indications that the model is correctly set up and even though the models compare to the analytical values, it can still be incorrect.

Cracking load $P_{c,cr}$

The first verification is the load at which cracks occur. The analytical value is determined under the assumption that the element displays linear elastic behaviour, as shown in Figure 9.21. Firstly the resulting forces are determined:

$$N_s = \epsilon_s E_s A_s = \epsilon_{c,cr} \frac{d-x}{h-x} E_s A_s \tag{9.5}$$

$$N_{ct} = \frac{1}{2} f_{ctd} b (h-x) \tag{9.6}$$

$$N_{cc} = \frac{1}{2} f_{ctd} b x \tag{9.7}$$

where:

N_s	=	–	[N]	The resulting force in the reinforcement.
N_{ct}	=	–	[N]	The resulting force of the concrete in tension.
N_{cc}	=	–	[N]	The resulting force of the concrete in compression.
$\epsilon_{c,cr}$	=	0.15	[$^0/_{00}$]	The strain at which the concrete cracks: $\frac{f_{LOP}}{\gamma_c \cdot E_c} = \frac{9.67}{1.5 \cdot 42000}$.
E_s	=	210	[GPa]	The youngs modulus of steel.
A_s	=	471	[mm^2]	The reinforcement area in the console.
h	=	80	[mm]	The height of the element.
d	=	60	[mm]	The effective height of the element.
x	=	–	[mm]	The height of the compression zone.
b	=	250	[mm]	The width of the element.

The value for x can be determined using the horizontal force equilibrium as $x = 44.2$ mm. The resulting forces than become: $N_s = 6.7$ kN; $N_{ct} = 28.9$ kN and $N_{cc} = 35.6$ kN. This results in a bending moment, $M_{c,cr}$:

$$M_{c,cr} = a_s N_s + a_{ct} N_{ct} = 1.84 \text{ kNm} \tag{9.8}$$

where:

a_s	=	45.3	[mm]	The lever arm of the resulting reinforcement force: $d - \frac{1}{3}x$.
a_{ct}	=	53.3	[mm]	The lever arm of the resulting tensile concrete force: $\frac{2}{3}(h-x) + \frac{2}{3}x$.

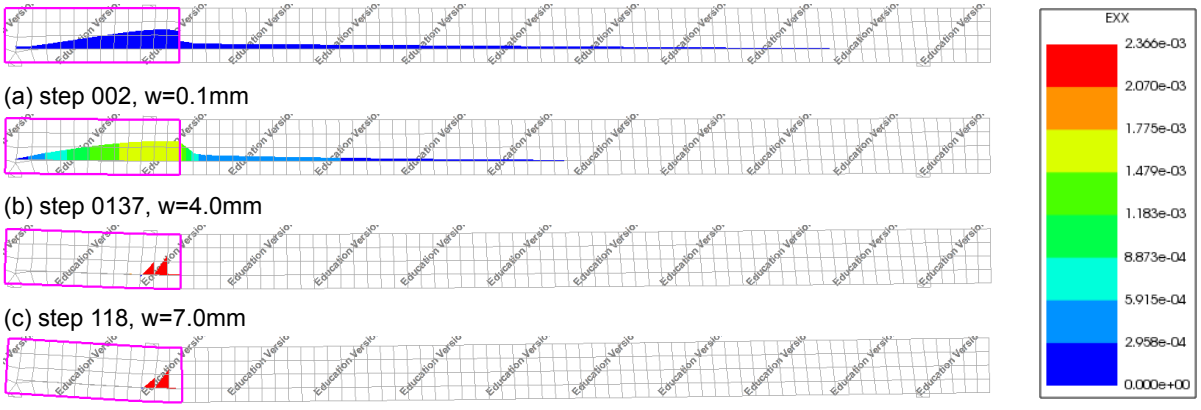

(a) step 002, w=0.1mm

(b) step 0137, w=4.0mm

(c) step 118, w=7.0mm

(d) step 195, w=12.0mm

(e) legend

Figure 9.19: The strain in the main reinforcement. The colour-scale is chosen such that a red colour indicates yielding ($\epsilon_{xx} > \epsilon_y = f_y/E_s = 0.00207$).

(a) step 002, w=0.1 mm

(b) step 037, w=2.0 mm

(c) step 118, w=7.0 mm

(d) step 195, w=12.0 mm

Figure 9.20: Strain states for marked steps. Blue is a strain below 0.0001, green below 0.1, yellow below 0.3, orange below 2.0 and black otherwise.

This cracking moment is reached at a load $P = M_{c,cr}/a \cdot (a+b)/b = 10.8$ kN for $a = 200mm$ and $b = 1155mm$. This value is significantly higher than the value found in DIANA, which is 6.8kN. This difference can be explained by the mesh-size (which resulted in 4 element over the height of the model) and that the equilibrium used by DIANA is based on the values in the integration points of the elements, while these are extrapolated to provide values at the nodes. Another factor which can be of importance is the fact that the actual strain distribution over the height of the element is not linear, as assumed for the calculation. This can be seen in Figure 9.22. Smaller steps and element sizes might provide a more accurate crack initialization, but as the most influential behaviour of CRC is the post-cracking, it is not further investigated.

Initial stiffness

The initial stiffness, before the first crack, can be determined analytically by the multi-field approach, where the element is split up into multiple fields and a differential equation is determined for each field. The model used for this approach is shown in Figure 9.23 The fields can be tied together and the unknowns can be determined by application of the boundary conditions. This derivation is done in *Maple 2018* and the code is provided in Appendix C.3. With a load of $P = 6.7$ kN, similar to the load in in step 002, the displacement at the load was determined to be 0.82 mm. Which is slightly lower than the displacement at step 002: 0.98mm.

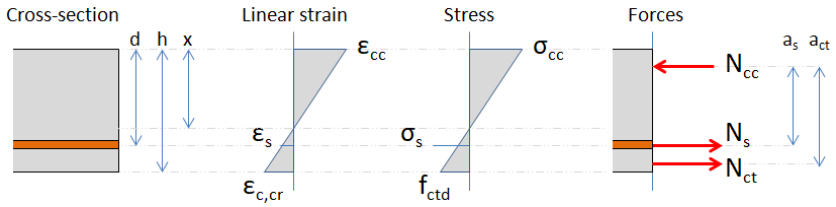

Figure 9.21: The linear elastic model used for determination of the cracking load.

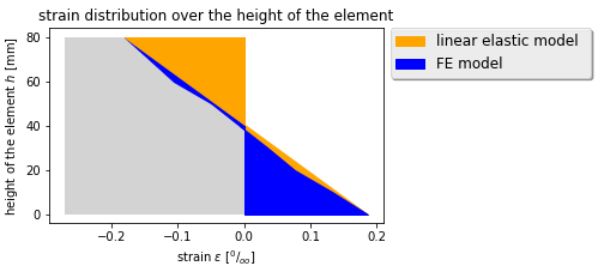

Figure 9.22: The strain distribution over the height of the element at the interface between the console and the platform.

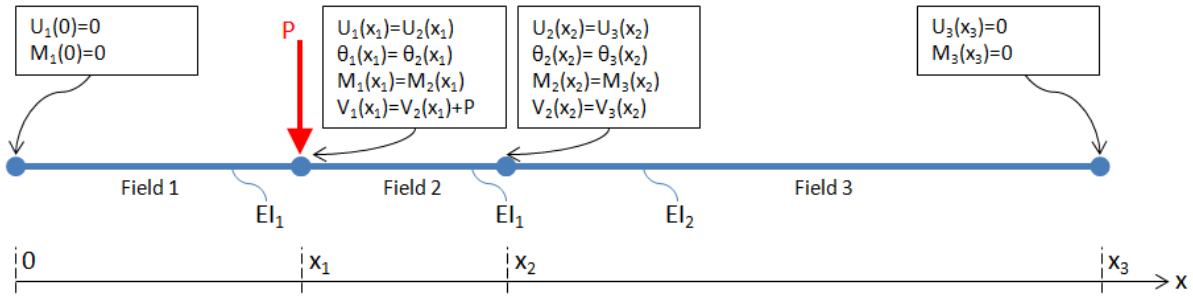

Figure 9.23: The multi-field model used for determination of the initial stiffness.

Upper value

It is possible to analytically determine the upper limit of the FE model under the assumptions of a Bernoulli beam, where planes remain straight and perpendicular to the neutral axis. When this assumption is combined with the used stress-strain relation, the FITTED_DE curve. This method is based on the a method applied in the Model code, as shown in Figure 9.24.

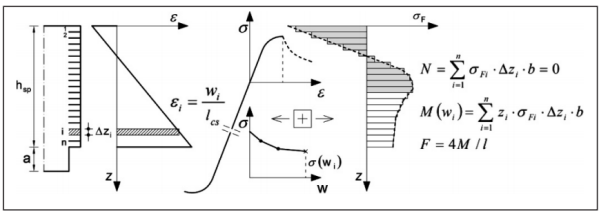

Figure 9.24: The model used for analytical upper limit. (source [20, p.145])

For a given value of the compression zone height, x, it is possible to determine the strain in the top fibre to get horizontal force equilibrium. The next step is to determine the bending moment at the given strain and the resulting load. The code used for this calculation is provided in Appendix C.4, which resulted in an upper value of $P_u = 80.0$ kN. The maximal resistance of the FE model was 77.5 kN, which is slightly below the analytical value.

Lower asymptote

The lower asymptote resembles a state where the steel fibres do not contribute any more to the resistance. In this phase the moment capacity is created by a concrete compression zone, x, and the yielding of the steel. The height of the compression zone can be determined through:

$$x = \frac{N_s}{b \cdot f_{cd} \cdot \lambda} = 13.98 \text{ mm} \tag{9.9}$$

where:

N_s	=	205.0	[kN]	The resulting force of the yielding main reinforcement: $N_s = A_s * f_y d = 471.2 * 435$.
f_{cd}	=	73.3	[MPa]	The design compresive stress for CRC: $f_{cd} = f_c k / \gamma_c = 110/1.5$.
λ	=	0.8	[-]	A reduction factor for the use of a plastic model.

With the determined value of x it is possible to determine the bending moment capacity at this point:

$$M_y = (d - \frac{1}{2}x) \cdot N_s = 10.87 \text{ kNm} \tag{9.10}$$

The resulting load is then determined to be $P = M_{c,cr}/a \cdot (a+b)/b = 63.7$ kN.

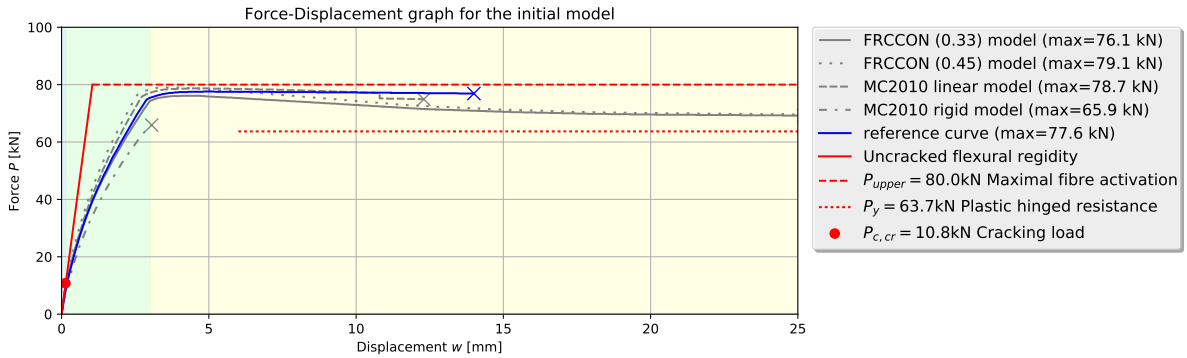

Figure 9.25: The analytical verification the load-displacement curve of the FE model.

Combining

The above analytical approaches can be combined into the figure as shown in Figure 9.25. The curve from the FE model behaves as the analytical approach predicted. Based on this information it is assumed that the model is correctly set up and provides insight in the actual behaviour of the Raqtan landing platform.

9.3. Sensitivity study

During the set up of the initial model it was required to make decisions regarding what kind of model to use. These decisions may influence the structural response and therefore have to be investigated. In this section multiple variations on the initial model are made and analysed to determine their significance.

9.3.1. Mesh size

Finite Element Analyses such as this one determine the structural response based on a stiffness matrix. The size of this matrix, and therewith the complexity of the calculations, is dependent on the number of nodes in the model. Therefore it was chosen for the initial model not to use a large amount of elements to reduce the required computation power. A coarse mesh does however influence the results. The model contains less integration points, resulting in a simplification of the actual structural response.

The mesh size is varied from elements which span the entire height of the element to a minimal of 6mm, resulting in the following steps: $80, 40, 20, 15, 10, 8$ and 6mm, while the preferred shape of the elements is kept as a square. The resulting load-deflection curves are shown in Figure 9.26.

Although the general shapes of the different meshes do resemble the initial curve, there are some deviations to be considered. First of all the results of the oversimplification by the application of 80 and 40mm elements is visible by the decrease in peak load. This is mostly due to the relatively large

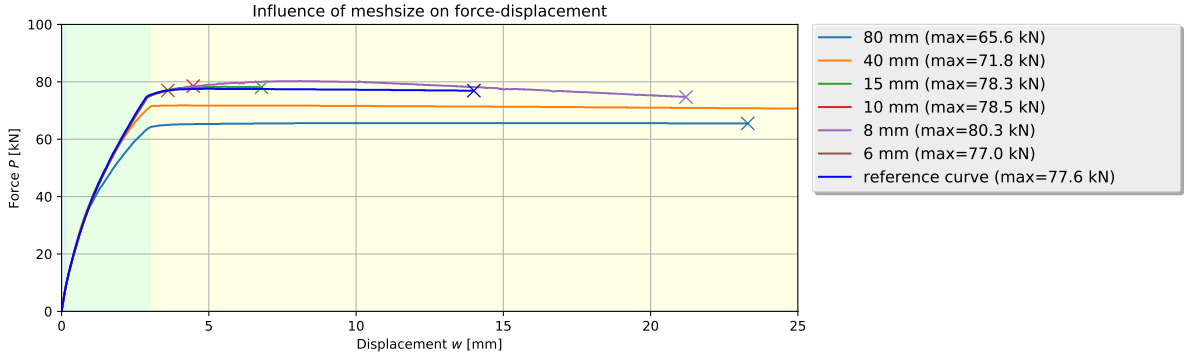

Figure 9.26: The load displacement curve for different mesh sizes.

distance between the integration points and the nodes. This behaviour is not realistic and makes these curves unfit for the validation of the model. The second deviation is in the finer meshes, which increase the peak load, but also show a clearer third transition zone. This is visual by the decrease in resistance as the displacement passes the 8mm.

This variant study showed that the actual maximal capacity might be slightly higher than the capacity found in the 20mm model. Taking the range of smooth curves (20-6mm), the model predicts a capacity within the range of 78-82 kN, which is significantly higher than the required resistance.

9.3.2. 3D model

The initial model has only two dimensions, which greatly influences the structural response. As the connection between the console and the platform is actually a disturbed region, a three dimensional analysis might provide more information regarding the actual structural behaviour. In the 2D model the console is connected to the entire width of the platform, which makes the platform side of the connection to behave stiffer than it actually would in practice. Increasing the dimensionality of the model should result in a more accurate stress distribution in the connection, which results in cracking of the platforms bottom as well. This would result in a decreased stiffness of the element as a whole, but might decrease the peak stress in the console. While the stresses are in general more spread, the stresses in the corners of the connection are significantly increased, as a results of the disturbed region.

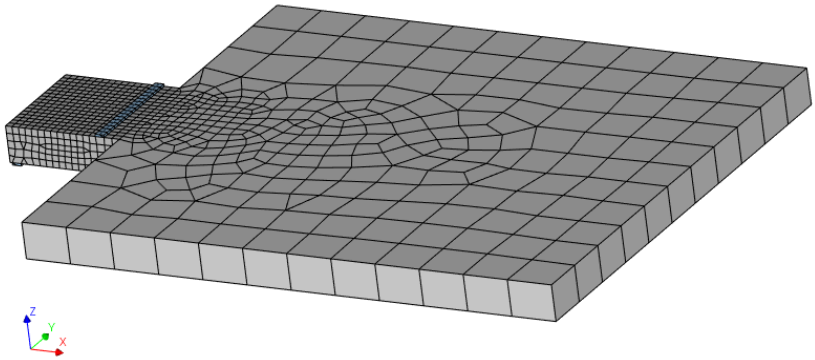

Figure 9.27: The mesh of the 3D model.

The mesh of the 3D model is shown in Figure 9.27, which shows the two different mesh sizes used: 15mm for the console and 100 mm for the platform, as the stress distributions are less critical in the platform. The reinforcement is modelled by the application of 1D lines throughout the model. The point loads and supports are replaced with line loads and supports.

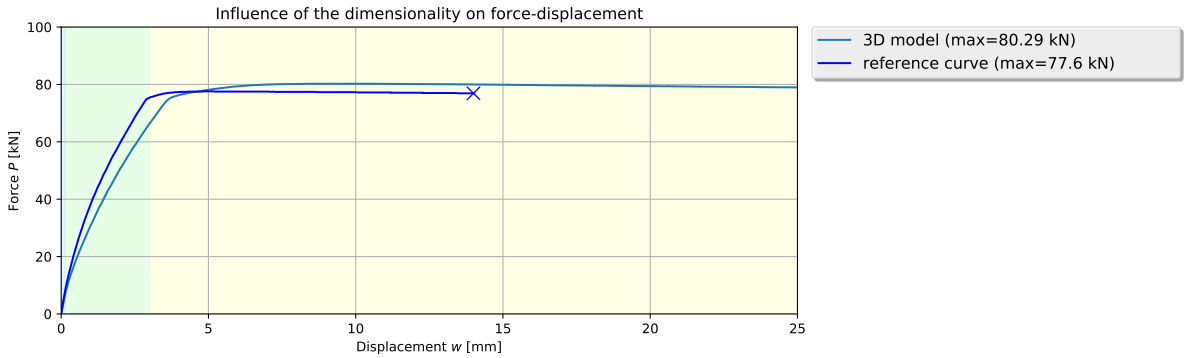

Figure 9.28: The load-displacement curve for the three dimenional model.

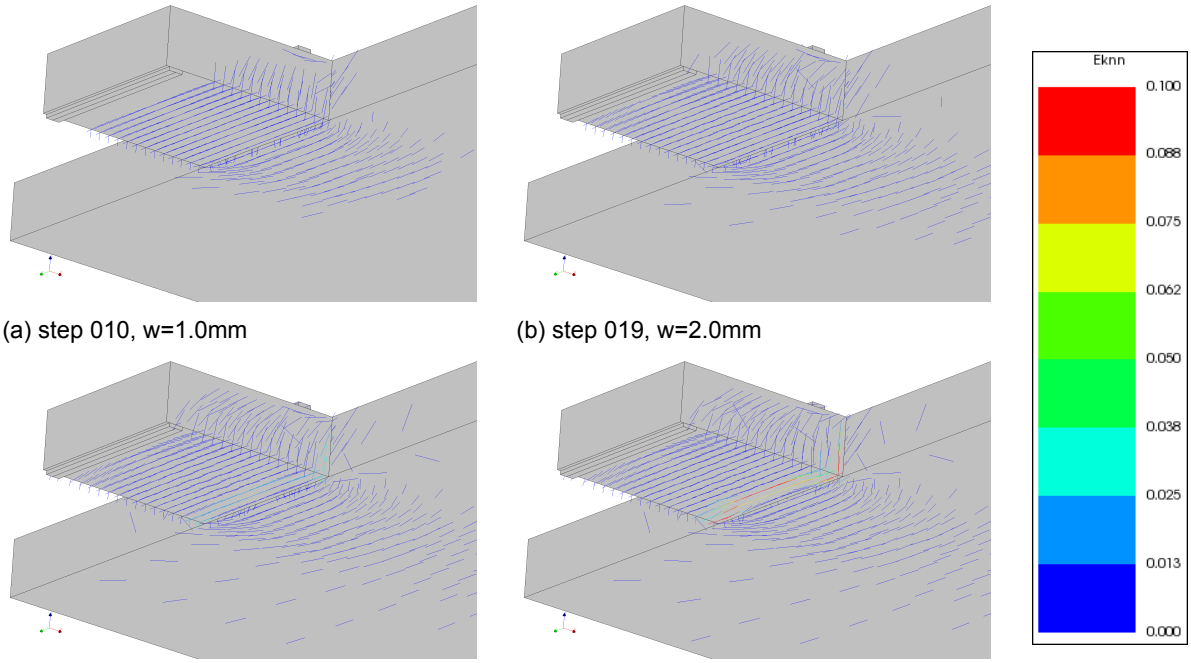

(a) step 010, w=1.0mm

(b) step 019, w=2.0mm

(c) step 037, w=4.0mm

(d) step 071, w=8.0mm

Figure 9.29: The crack pattern at multiple deformation stages seen from the bottom of the element.

The results of the model are provided in Figure 9.28. While the maximal capacity is not significantly increased, it is clearly noticeable that the stiffness of the model is decreased. This is mainly the results of increased local strains in the platform at the connection, which are caused by a decreased flexural rigidity. Figure 9.29 shows that the first cracks which occur are spread over the console and the platform. These cracks are small and remain small. As the load is further increased, see Figure 9.29c and Figure 9.29d, the crack at the connection starts to widen as the main reinforcement starts to yield. While the the entire connection is cracked it is noticeable that the crack mainly localizes at the corners.

9.3.3. Clamped connection

The application of a clamped connection does influence the structural behaviour of the landing platform, as discussed in 6.2.2. The design load is increased with 32%, but the response is also influenced. A clamped connection results in a stiffer behaviour of the console. The variation in this model is the way the model is connected on the console side. Instead of clamping the entire console, it is chosen to add a wall segment, which is clamped at the outer edges. This results in a rotational stiffness of the console which better represents the actual situation. The model is shown in Figure 9.30. The wall is designed to have the C30/37 concrete quality. As this can be modelled in different ways in DIANA it is chosen to use multiple implementations:

- **EC1992:** This model is uses the *Eurocode 2 EN 1992-1-1* material model and is in the *Concrete design codes* class. This model is chosen as it represents the implementation as expected from the Eurocode. The material properties are provided in Table 9.6.
- **IDEAL:** This model is based on the *Total strain based crack model* in the *Concrete and masonry* class. As the peak stress is reached, the resistance remains constant. This model is included as it provides and upper bound for the behaviour of the wall. The material properties are provided in Table 9.7.
- **BRITTLE:** This model is based on the *Total strain based crack model* in the *Concrete and masonry* class. As the peak stress is reached, the resistance remains constant. This model is included for the opposite reason as it provides a lower limit for the behaviour of the wall. The material properties are provided in Table 9.8.

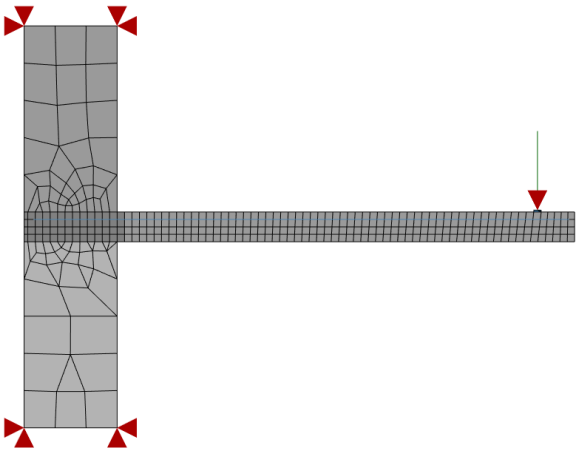

Figure 9.30: Tension models applied in the variation.

Table 9.6: Material properties for the C30/37 EC1992 model

Property		Value	
Concrete			
Concrete type		C30/37	-
Young's Modulus	E_c	33000	MPa
poisson's ratio	ν_c	0.20	-

Table 9.7: Material properties for the C30/37 IDEAL model

Property		Value	
Linear material properties			
Young's Modulus	E_c	33000	MPa
poisson's ratio	ν_c	0.20	-
Tensile behaviour			
Tensile curve		Ideal	
Tensile strength	f_{ctd}	1.33	MPa
Compressive behaviour			
Compression curve		Ideal	
Compressive strength	f_{cd}	20.0	MPa

Table 9.8: Material properties for the C30/37 BRITTLE model

Property		Value	
Linear material properties			
Young's Modulus	E_c	33000	MPa
poisson's ratio	ν_c	0.20	-
Tensile behaviour			
Tensile curve		Brittle	
Tensile strength	f_{ctd}	1.33	MPa
Residual strength	$f_{ctd,res}$	0.00	MPa
Compressive behaviour			
Compression curve		Elastic	

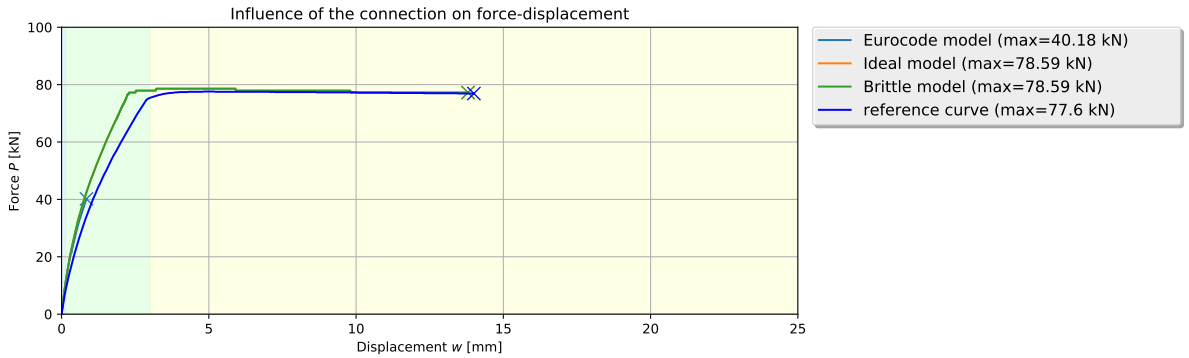

Figure 9.31: The load-displacement curve for the clamped connection. It should be noted that the different models do not influence the response and therefore the lines are on top of each other.

The results from this analysis are not directly comparable to the previously acquired results, as the applied load and deflection are now measured at the right-most support. Both values have to be scaled to gain useful results. The curve as shown in Figure 9.31 is obtained by scaling the load with a factor $200/1355 = 0.15$ and the displacement with $1355/200 = 6.78$. This graph shows the increased stiffness of the console, as the deformation is limited. The maximal load is not significantly different, as it is still based on the flexural capacity at the connection of the platform and the console. The cracking is localized in the 20mm between the wall and the platform. The stiffness of this part significantly lower than the surrounding elements, which make it prone to greater strains.

The crack pattern of the wall, as shown in Figure 9.32, shows that the wall is not only in compression, as assumed in the determination of the shear forces in the console for a clamped connection. As the connection is also able to transfer tensile forces, the actual stress distribution might result in a lower shear force, but the applied method can be used as an upper limit approach.

It should be noted that the connection between the different concrete types (the wall, the mortar and the CRC) is modelled as uncrackable. The addition of an interface in between the layers is possible, but is not expected to provide improved results. The additional information it might provide is countered by an additional uncertainty, as the exact behaviour of such an interface in a structure contains too many variables to predict precisely. It is therefore chosen not to expand the model any further.

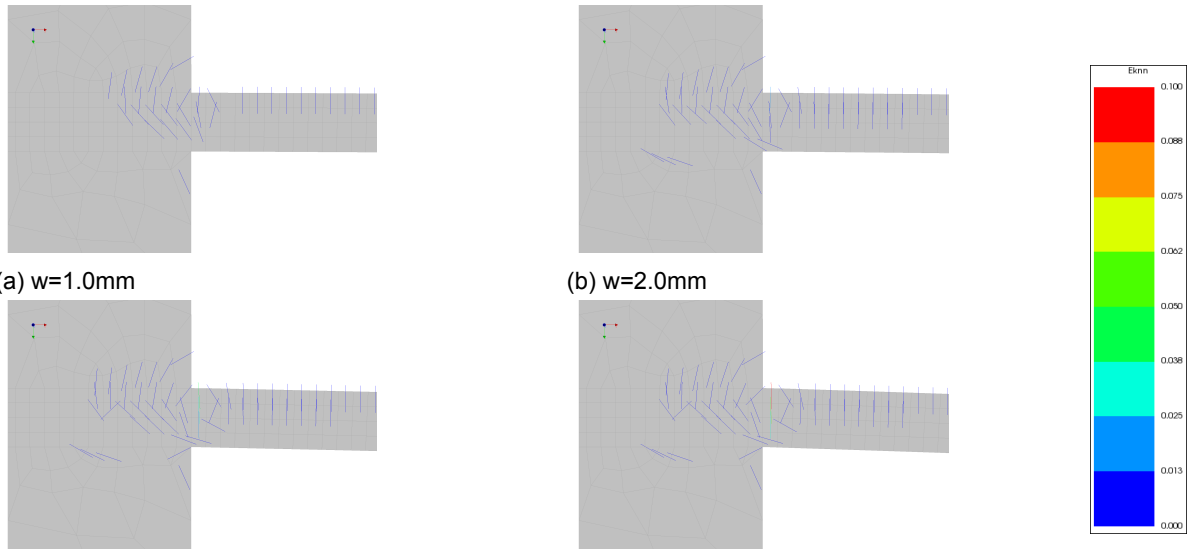

(a) w=1.0mm (b) w=2.0mm

(c) w=4.0mm (d) w=6.0mm

Figure 9.32: The crack pattern at multiple deformation stages for a clamped connection.

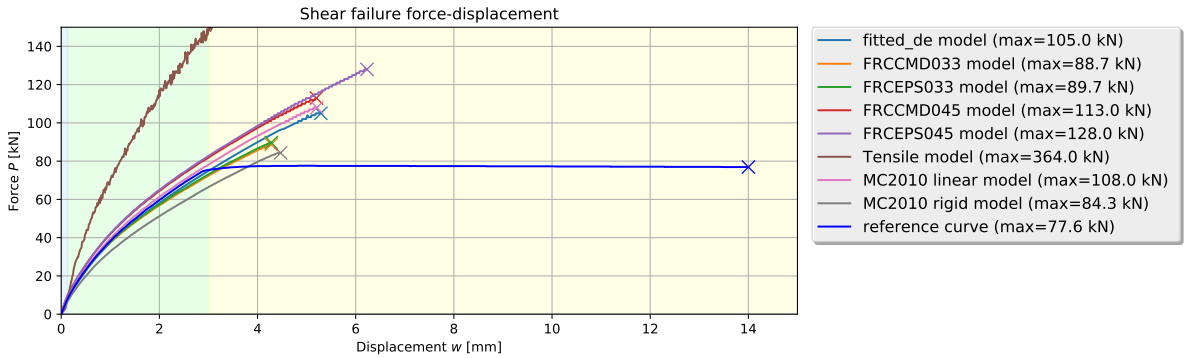

Figure 9.33: The load displacement curve for shear failure.

9.3.4. Failure mechanism

Flexural capacity was governing in the previous models. This resulted in a prediction of the actual total capacity of the element, but it does not provide much information regarding the shear capacity. As the validation study is mainly about the shear resistance it is useful to gain more insight regarding this mechanism. The models can be adapted in such a way that shear becomes governing again: by changing the stress-strain curve for the reinforcement steel to a linear one. As yielding can no longer occur, the model is forced to fail in shear. The results of this variation are shown in Figure 9.33. The variations in ultimate load between the used models is quite large ($\approx 10\%$), but is significantly higher than the ultimate load for flexural failure.

Figure 9.34 shows the principle strains in the last converged step. It clearly shows the shear failure mechanism, including the diagonal shear cracks and the splitting along the main reinforcement.

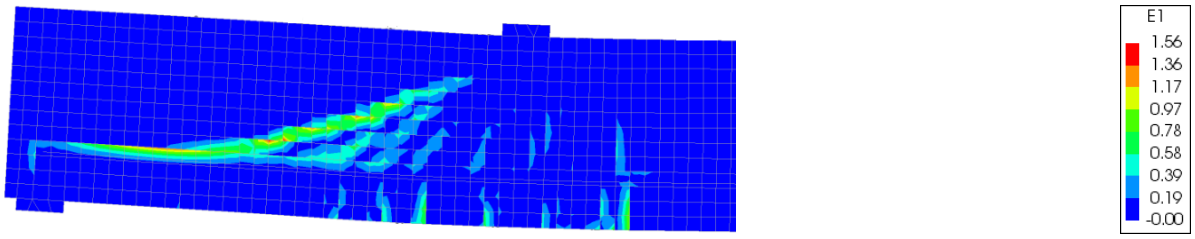

Figure 9.34: The principle strains for shear failure.

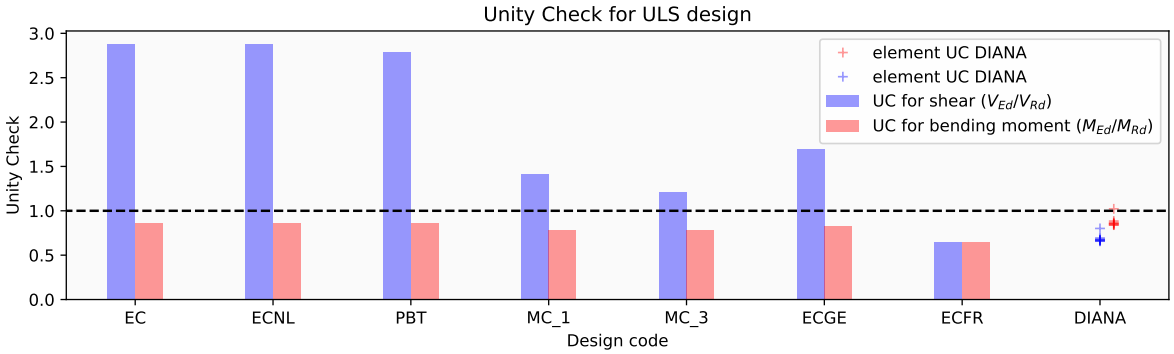

Figure 9.35: Comparison of the UC values for the applied codes and the DIANA models.

9.4. Conclusion

The capacity of the element according to the DIANA analyses is within the range of 65.9-89.6 kN. As the design value of the shear force was $57,5$ kN, this can be considered to be sufficient. An overview of the derived capacities is provided in Table 9.9. But before these values can be used as an argument to apply the actual design without the stirrups there are a few things which should be noted:

- The model is a simplification of reality and might contain imperfections. Even though the results are comparable to the analytically determined values, they might still deviate from the actual results. The assumptions on which the model is build, for example that the stress in the third direction is zero, are known to be inaccurate. Such flaws can be compensated for by applying a model safety factor. But as the significance of the flaws is unknown, it is not possible to determine the value of such a factor at this moment.
- The displayed failure behaviour is in all models the failure of the connection between the console and the platform in bending. This means that the resistance in shear is higher, but still unknown. The actual UC for shear can not be determined for the Raqtan landing platform. The failure in bending does however provide a lower limit for the shear resistance.
- Compared to the design resistance of the codes the capacity is increased. Where according to most codes the shear failure would be governing, it was actual the bending moment resistance. The predictions for this mechanism were much more in the same range as the DIANA models, as can be seen in Figure 9.35. The improvements are a result of the increased complexity of the used method of calculation, which results in a less generic approach.
- The used material tensile models not a significant influence on the bending moment capacity, but their influence on the shear capacity is significant. If these models are used to predict the shear capacity, it can be hard to determine which model provides the best prediction if no experimental data is available.

Application of a minimal amount of reinforcement is often based on the enforcement of ductile failure, as shown in the previous chapter for multiple codes. The models discussed in this chapter provide this warning mechanism as well. During the loading the model starts to deflect. Up until a deflection of 2mm at the centre support (which resembles a 13mm deflection at the cantilevering) the model has an increasing resistance. Such a deflection is already noticeable and should warn the user to unload the element. The general behaviour is shown in Figure 9.36, which contains the envelope for all the response curves.

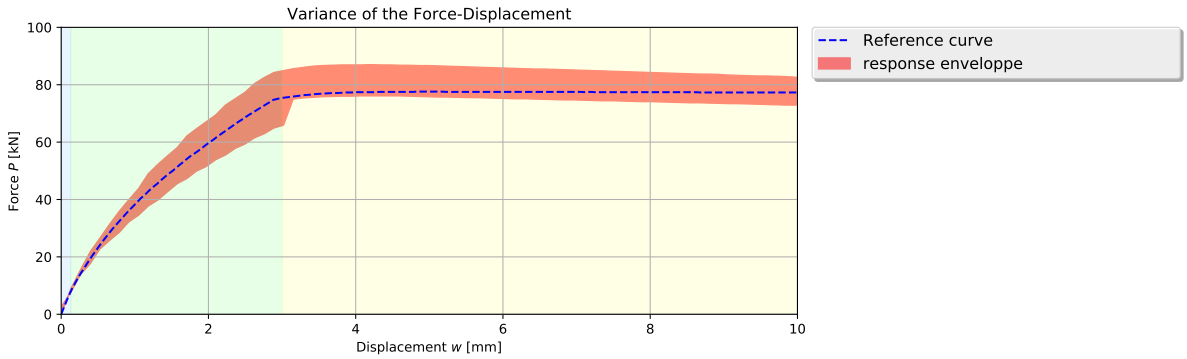

Figure 9.36: Envelope of the predicted structural response.

Table 9.9: Overview of all determined capacities.

Method		P_{Vu}		P_{Mu}		P_u		
		P_{Vm}	P_{Vd}	P_{Mm}	P_{Md}	P_{um}	P_{ud}	
FE models	Fitted_de	-	105.0	-	77.6	-	77.6	kN
	Fitted_me	141.0	-	101.0	-	101.0	-	kN
	FRCCMD033	127.0	88.7	100.0	76.1	100.0	76.1	kN
	FRCCMD045	175.0	113.0	105.0	79.1	105.0	79.1	kN
	FRCEPS033	128.0	89.7	100.0	77.0	100.0	77.0	kN
	FRCEPS045	174.0	128.0	105.0	89.6	105.0	89.6	kN
	MC2010lin	185.0	108.0	105.0	78.7	105.0	78.7	kN
	MC2010rig	104.0	84.3	97.5	65.9	97.5	65.9	kN
Design load		-	52.8	-	52.8		52.8	kN

10

Validation by testing

After validation by design codes and by FEA, the third validation which is performed in this research is the validation by testing. The purpose was to acquire information regarding the actual performance of the element under loading and use this information to determine the validity of the design without the stirrups. The Eurocode does provide a method which can be used for such a validation: *Design by testing*, where the design capacity is based on experiments rather than design principles. This method is described in Eurocode 1990 Appendix D [29]. This method formed the base for the design of this experiment, but was abandoned later on as another approach might provide more insight in the shear capacity of the elements, while the method in from the EC would only provide a design value.

This chapter will describe the experiments and its results. The chapter starts with a description of the design of the experiment and the test elements, followed by the casting and the test results. Finally the results will be analysed and conclusions will be drawn.

10.1. Design of the experiment

This section focusses on the different aspects which have to be considered during the design of the experiment. The experiment will have two main targets: determination of the actual shear resistance and determination of the actual material properties which resulted in the shear resistance. Firstly the experiment for the shear capacity will be determined and then the requirements for determining the actual material properties will be determined.

10.1.1. Design of the experiment elements

This experiment will follow the same approach as the method used by PBT and focus only on half the platform, taking into account one console and a slab with a width of 1060mm. The forces according to the Eurocode are applied at the right hand side of the model. Using only a single side of the platform for the determination of the capacity results in neglecting possible torsion in the element. It is however chosen to use this method as it is the original design method. The focus of this research is not to determine the validity of the currently used design methods but to determine the requirement of stirrups in the actual design. The model originally used to design the element is shown in Figure 10.1.

Figure 10.1: The mechanical model applied during design.

The experiment set-up will use the same model, but the centre support will be used to apply the force to the element, resulting in the configuration as shown Figure 10.2. This set-up can be tested using

a three point bending test, which is a commonly used testing rig and available in the laboratory of the Delft University of Technology.

Figure 10.2: The mechanical model applied during this thesis.

This approach results in a few changes with respect to the actual situation. The first being that according to the used code, a distributed load of 3 kN/m^2 is applied on the right span. In the experiment only a line load is applied at the centre support. As the focus is on the left span, the difference in load case does not influence the results, as both load cases would result in the same internal stresses in this span.

The platform width of the test elements is reduced from 1060mm to 500mm, as shown in Figure 10.3. Reducing the element width has a number of advantages, such as better maintainable safety during testing, as the elements mass is reduced from ±300kg to ±150kg and the elements will fit better in the testing rig. Another advantage is the reduced material usage. These concessions would not be made if the experiment results would be significantly affected by it, but the affected area still is double as wide as the console and the singularity between the console and the platform is maintained. This disturbed region (D-region) around the interface between the platform and the console plays an important role in the manner in which the stresses are introduced in the console.

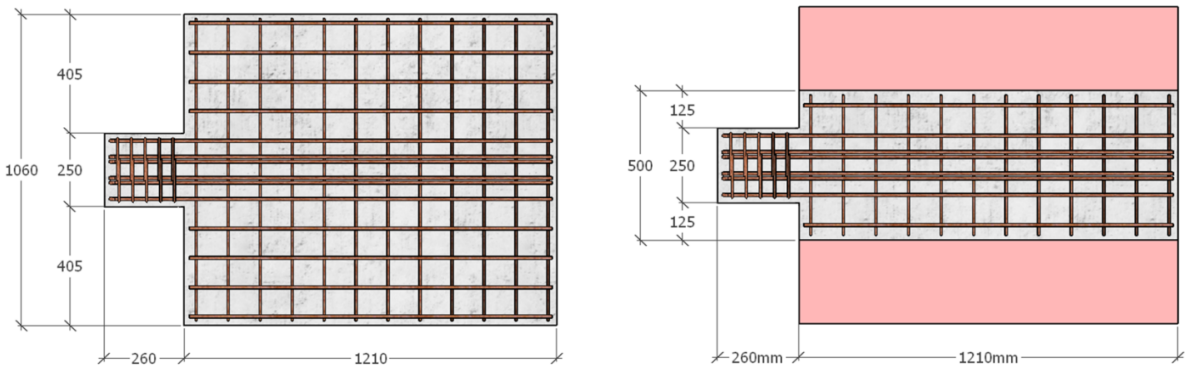

(a) Original width (b) Reduced width

Figure 10.3: Cross-section of the Raqtan landing platform with reinforcement. Figure 10.3a shows the original cross section and Figure 10.3b the reduced width.

The direction in which the loads are applied on the element is also changed. This could have an effect on the resistance, as not all loads are in the opposite direction: the load due to self-weight is still downwards. As the self-weight is now ±150kg, or ±1.5kN, this is expected to be negligible. Preliminary calculation according the code with the use of the mean material properties and without safety factors resulted in an expected capacity of 36.2kN. A preliminary DIANA run indicated a resistance about 120kN.

The element without stirrups still requires (practical) reinforcement in the console. These are determined to be $3\Phi 6-90$ both in the top and the bottom layer. This reinforcement is added as the purpose of the thesis is to determine the capacity of the element in the case the stirrups were not required. This is not the same as testing the capacity of the original element without stirrups. The mentioned practical reinforcement would be added to the design if the stirrups were not required by the codes. Details are provided in Figure 10.4.

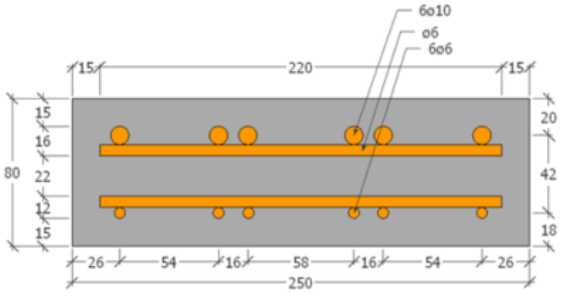

(a) Cross-section of the console with the applied reinforcement.

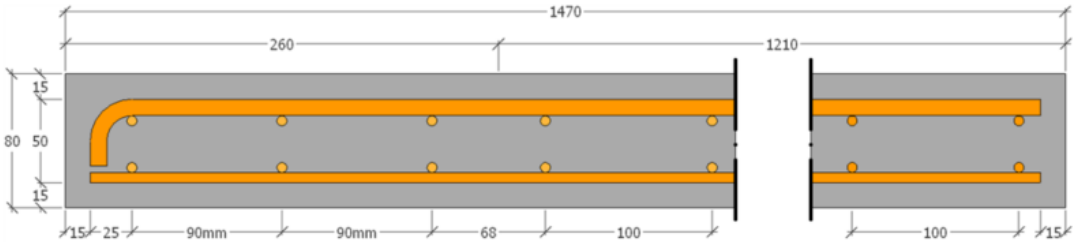

(b) Cross-section of the entire platform with the applied reinforcement.

Figure 10.4: Cross-sections of the Raqtan landing platform without stirrups.

The test consists of two types of elements: the element as it is originally designed, including the stirrups, and the element without the stirrups. The element with the stirrups is tested as a base case and serves to provide information regarding the capacity of the element and whether this is in line with the predictions by the codes. The second element has the main focus and is the modified element where the stirrups are replaced with practical reinforcement. The tests with this element should provide data in the requirement of stirrups in the Raqtan design. The details regarding the final elements can be found in Appendix A.

A final point of attention is the small margin between the left support and the edge of the element. This is only 15mm. It is chosen to use the distance as it was used in the design phase as well. It could however result in spalling of the edge. In practice, due to the clamped connection, this would result in a redistribution of the forces. When this occurs during the experiment, the support will be moved slightly inwards to resemble the redistribution. This has a negative influence on the shear capacity as the lever arm is shortened, but this would also happen when the element was placed in the original wall.

10.1.2. Testing Rig

The laboratory at the Delft University of Technology had two testing rigs available for this experiment. The first is a computer controlled hydraulic rig with a capacity of 100kN, the second one is a manually controlled hydraulic rig with a capacity of 200kN. As the expected capacity can exceed the 100kN, it is chosen to opt for the manual rig. This will result in less controlled application of the load, but provides the required capacity for the experiment. The maximal deflection for this equipment is 200mm, which is sufficient deformation for the element to be considered as having failed. This testing rig can also easily be transformer for the EC14651 experiment, which will also be performed. An overview of the rig is shown in Figure 10.5.

Multiple measurements will be taken during the tests: the elongation for failure in bending moment will be taken by two Linear Variable Differential Transformers (LVDTs) and the elongation for failure in shear will also be measured by two LVDTs. The hydraulic press measures the applied force and the resulting deflection. Finally photographs will be taken from a fixed point during the tests, which allows the use of Digital Image Correlation (DIC) to determine the strains over the side of the console.

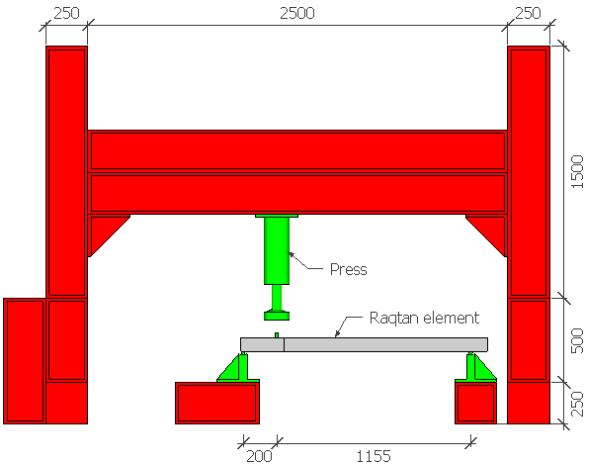

(a) Front view of the experiment rig

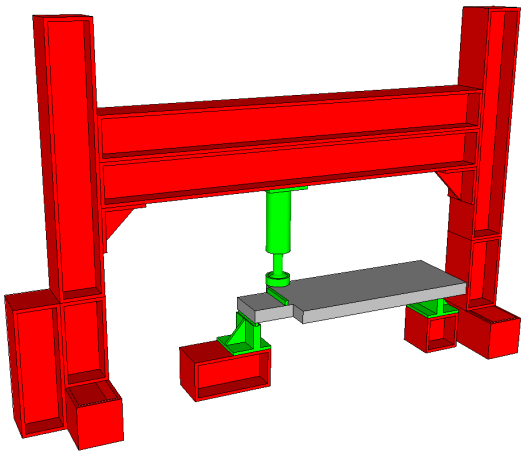

(b) Perspective view of the experiment rig

Figure 10.5: The experiment rig. The hydraulic press has a capacity of 200kN and a maximal deflection of 200mm.

10.1.3. Number of tests

Design by testing provides two methods which result is a design capacity in section EC0 section D3.1.a to determine the capacity of structures in ULS:

D7.2 This methods determines the design value by first determining the characteristic value and applying the proper safety factors. This results in:

$$X_d = \frac{\eta_d}{\gamma_m} m_x (1 - k_n V_x) \tag{10.1}$$

D7.3 This method determines the design value directly. This method uses the same formula, but without the factor γ_m. With the values for k_n being different for both methods the second methods only becomes more attractive when the coefficient of variation is small. This method requires at least four samples and is then only advantagous when the COV is lower than 3%. As this value is not known beforehand, it is decided to used the first method. The first method requires at least three samples, which is the used amount.

The element with stirrups serves as a reference case and is not used to derived design values. Therefore a single element suffices. This results in the following elements:

Table 10.1: Experiment elements.

code	Description
RAQTAN_1-A	Element with stirrups
RAQTAN_2-B	Element without stirrups
RAQTAN_3-B	Element without stirrups
RAQTAN_4-B	Element without stirrups

10.1.4. Expected failure mechanism

According to the valley of Kani, shown in Figure 10.6, an element with an a/d ratio of 3.6 results in a failure in shear [18]. The maximal achieved bending moment is expected to be 65% the bending moment capacity. It should however be noted that this prediction is based on experiments without fibres and with a reinforcement ratio of 2.8%, while the element for this experiment have a reinforcement ratio of 3.4%. The fibres are expected to have a relatively larger effect on the shear capacity than the bending moment capacity, as the element is already reinforced in to increase the bending moment capacity. Due to these influences it is important to acquire more information regarding the actual failure mechanism.

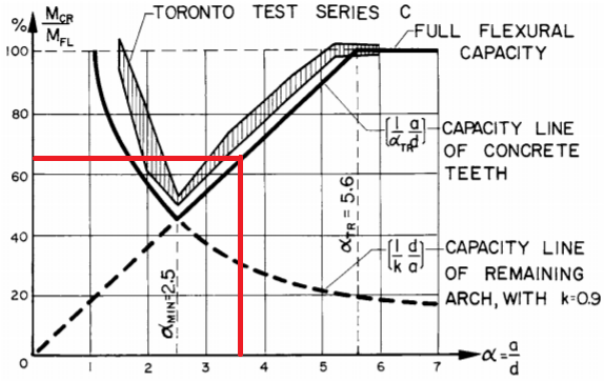

Figure 10.6: Valley of Kani. The values for this experiment are marked by the red line. Note that the mentioned k value is not the size factor, but the $z = kd$ for the internal lever arm. (source [18, p.461])

The FE models derived in the previous chapter can be used to predict the structural behaviour, but they require some modifications. The material properties should now be based on the mean values instead of the design values. These values are provided in 10.2 and 10.3

Table 10.2: Material properties for the mean DIANA

Property		**Value**	
Concrete			
Young's Modulus	E_c	50000	MPa
poisson's ratio	ν_c	0.20	-
crack orientation		*rotating*	
Tensile curve		*Variable*	
compressive curve		*Eurocode 2*	
Compressive strength	f_{cd}	130.00	MPa
Strain at f_{cd}	ϵ_{c1}	0.0026	-
Max strain	ϵ_{cu}	0.0026	-
Young's at $0.4f_{cd}$	E_c	50000	MPa

Table 10.3: Material properties for the mean DIANA

Property		**Value**	
Reinforcement			
Young's Modulus	E_s	210000	MPa
poisson's ratio	ν_s	0.25	-
yield strength	f_{yd}	500	MPa
cross-section area	A_s	471;628	mm^2
Support Plates			
Young's Modulus	E_{ss}	210000	MPa
poisson's ratio	ν_{ss}	0.25	-
yield strength	f_{syd}	500	MPa

The material properties are not the only changes. The reduced width is also included in the new models. The resulting load-displacement curves are shown in Figure 10.7. As expected the resistance based on the mean values (98-105 kN) is increased in comparison to the models based on design values (78-82 kN).

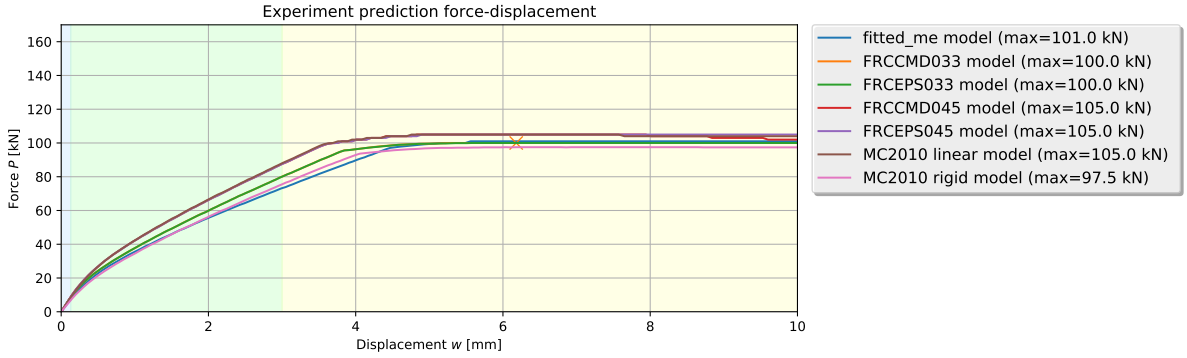

Figure 10.7: The predicted load-displacement curves for the experiment.

The models still predict failure in bending, as shown in Figure 10.8. Even though the main purpose of this experiment is to determine the shear capacity, the experiment is not rendered useless by failure in bending. The resulting ultimate capacities can still result in a design value through *design by testing*. This would result in a single value which could be used for the application of this exact design, but would not provide other insights in the actual shear capacity of the element. The research questions which were chosen at the beginning of the research were chosen such that the research would provide information regarding the actual shear capacity and not only a lower bound value. As any modification to the Raqtan design would render the found design value useless, it would not provide a broadly applicable insight in the relation of the shear capacity as predicted by the codes and the actual behaviour.

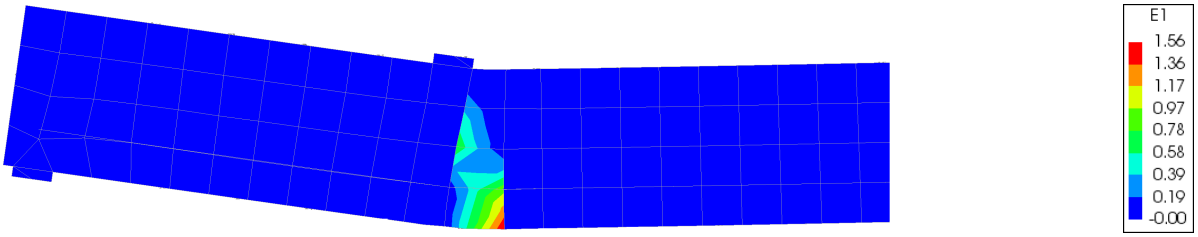

Figure 10.8: Predicted strain after failure for the FRCCMD045 model. The resulting strain pattern resembles a failure in bending.

This discussion resulted in the search for a modification of the experiment which would result in the largest possible increase of information gathered from the experiment. The possibilities were limited as the elements were already cast at this stage of the research. The next section discusses the modifications which were made to the experiment.

10.1.5. Modifications to the experiment

The purpose of these modifications is to gain more information regarding the shear capacity of the element. There are two methods considered to enforce shear failure: increasing the bending moment capacity or increasing the shear load. There are some limitations to the possible modifications which should be discussed first. The first limiting factor is the fact that the elements are already cast, which eliminates any internal changes to the elements. The second limitation is the availability of the testing rig in combination with the desire not to deviate from the original research planning to prevent extensive elongation. This resulted in a limited number of days to apply the modifications and therefore the modifications had to be made with the already available equipment and materials. Finally the increase in bending moment should not influence the shear capacity significantly, as this would result in an incomparable situation with regard to the original design. The same applies for modifications which increase the shear load in the console.

The first step is to compare the predicted shear capacity and the bending moment capacity. The shear capacity can be predicted in the same way as applied earlier in §9.3.4: by modelling the main reinforcement with a linear elastic model. The altered material properties and used models can be found in §9.3.4. The resulting force-displacement curves are shown in Figure 10.9.

The predicted range for the failure in bending is rather small based on the used models: from 97.6kN to 105kN. The applied tensile model does not seem to have a significant influence on the elements load bearing capacity. The shear models show different behaviour and the variance is larger: from 104kN to 185kN. Enforcing shear failure therefore requires an increase in bending moment capacity of up to a 100%, even though some models predict an increase of only 20% would suffice as well. This resulted in the following options being considered for the modification:

Move the support: The first modification is to move the support towards the hydraulic press, decreasing the lever arm. This modification is shown in Figure 10.11a, where the support is moved inwards by 25mm. This decreases the bending moment at the load and increases the shear load in the console. It should be noted that decreasing the lever arm too much would result in an increase in direct load transfer to the support, and therefore in an increasing shear capacity. For the mechanical models as

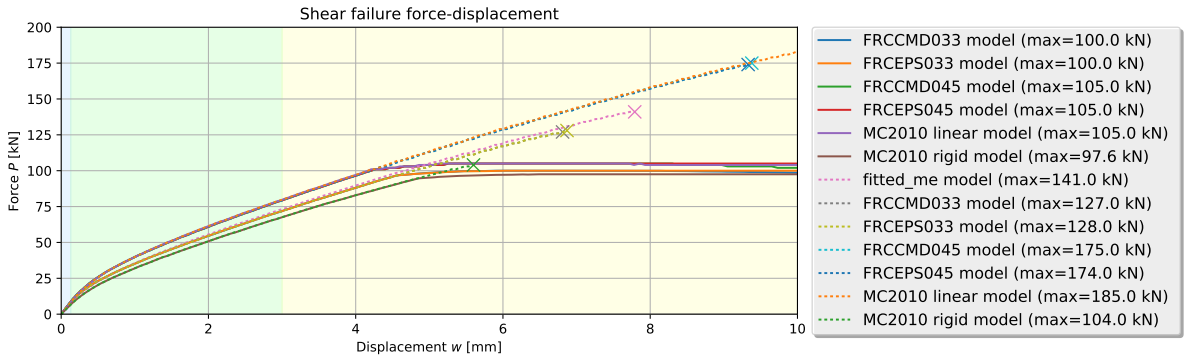

Figure 10.9: The predicted load-displacement curves for shear failure compared with the curves without intervention.

shown in Figure 10.10, the bending moment in C and the shear force in span a can be determined as:

$$M_C = \frac{P \cdot a \cdot b}{a + b} \tag{10.2}$$

$$V_a = \frac{P \cdot b}{a + b} \tag{10.3}$$

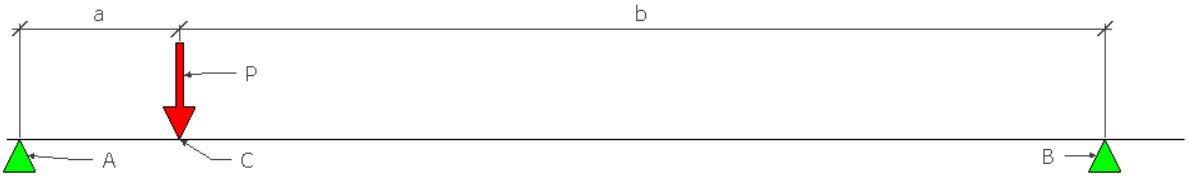

Figure 10.10: Mechanical model.

Bolt a reinforcement strip to the bottom of the element: Increasing the main reinforcement is a solution closer to the one applied in the FE analysis, as the reinforcement can handle a greater force before yielding. The laboratory has strips available with a yield strength of 500 MPa and a cross section of 10x100mm. These strips can be attached via bolts to the element, as shown in Figure 10.11b. This works fine in the platform, but the bolt connection in the console causes an interference in the zone which should fail in shear. This results in undesired side effects. Moving the bolt too far towards the end of the console would create a complex connection at the support, which is also unwanted.

Glue a reinforcement strip to the bottom of the element: To circumvent any modifications inside the console the option of glueing the reinforcement strip was considered, as shown in Figure 10.11c. Using Sicadur-30® as glue, this allows the strips to be easily connected to the element, while being able to transfer large stresses (up to 18MPa in shear stress) [38]. With this solution the area usable for the load transfer should be considered. An increase in the load resistance of 100kN would suffice according to the used models. This load would result in a transfer length of:

$$M_{add} = P_{add} \cdot \frac{a \cdot b}{a + b} = 100.000 \cdot \frac{200 \cdot 1155}{200 + 1155} = 17.0kNm \tag{10.4}$$

$$F_{strip,add} = \frac{M_{add}}{{}^1/_2 h_{strip} + {}^2/_3 \cdot h} = \frac{17000000}{{}^1/_2 10 + {}^2/_3 \cdot 80} = 292kN \tag{10.5}$$

$$l_t = \frac{F_{strip,add}}{w_{strip} \cdot f_\tau} = \frac{292000}{18 \cdot 100} = 163mm \tag{10.6}$$

This is less than the distance between the load and the support, but migth not be sufficient. Another problem to keep in mind is the occurrence of peeling of the end of the strip. The support is assumed to prevent this, as a significant portion of the load results in a compression force at the end of the strip, serving as anchorage.

Glue a reinforcement strip with corner to the bottom of the element: This addition would help to increase the load transfer zone between the strip and the element itself. It can be accomplished by welding pieces of the strip in to a reinforced corner element. This means the force in the reinforcement strip can be increased without overloading the glued connection. As the corner is not bolted, but only glued, it is expected to deform and detach from the element under loading. During this detachment the shape will still anchor the reinforcement strip. As the anchorage is ensured, it is no longer necessary to apply glue at the console. Without this glue the two elements are no longer coupled in the shear zone, thus reducing the influence on the shear capacity, while maintaining the increased bending moment capacity.

The mentioned modifications were applied to the FE models using a variety of interfaces. The glue is modelled as a perfect connection between the strip and the element, while the bolted connection is modelled as an interface with negligible shear resistance and a perfect connection at the location of the bolt. Two types of analyses were conducted in order to be able to compare the behaviours: one where the main reinforcement could not yield, resulting in the shear capacity of the modification; the other with the addition of stirrups, without yielding. Thus resulting in the bending moment capacity. The results are shown in Figure 10.12. The goal of the modifications is to increase the bending moment resistance without significantly altering the shear capacity. This is accomplished by increasing the model's horizontal-coordinate in the graph without altering its vertical-coordinate. This is best accomplished by the cornered glued connection. Therefore this approach was chosen. The models predict a capacity in the range of 105-210kN, while the testing rig has a capacity of 200kN. When this capacity is exceeded it is not possible to test the elements.

10.1.6. Sample tests

It is important to determine the properties of the test specimen as precise as possible. The material properties can differ per batch and even within a batch. The following tests will be performed to determine the significant material properties of the batch in which the elements are cast:

Cubic compressive strength There are two main ways to determine the characteristic compressive strength of the CRC batch. The cylindrical an cubic tests. In Europe the cubic test is mostly used and will be used for this experiment as well. In order to determine the characteristic value of this batch it is decided to use 3 test samples for this test. This number was later increased to six as the minimal casting volume was not met, and otherwise material would be unused.

CMOD As described in Chapter 8, the Crack Mouth Opening Displacement (CMOD) is an often used property in the determination of the shear capacity. This property is measured as described in EC14651: a notched 3 point bending test.

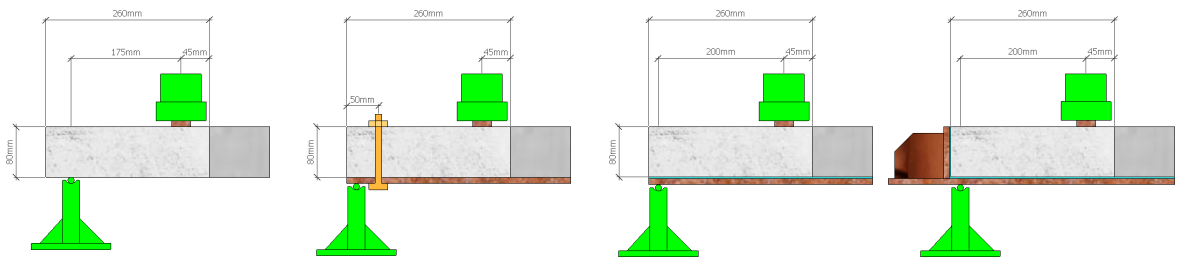

(a) Moved support. (b) Bolted strip. (c) Glued strip. (d) Glued with corner.

Figure 10.11: The considered modifications to the experiment design.

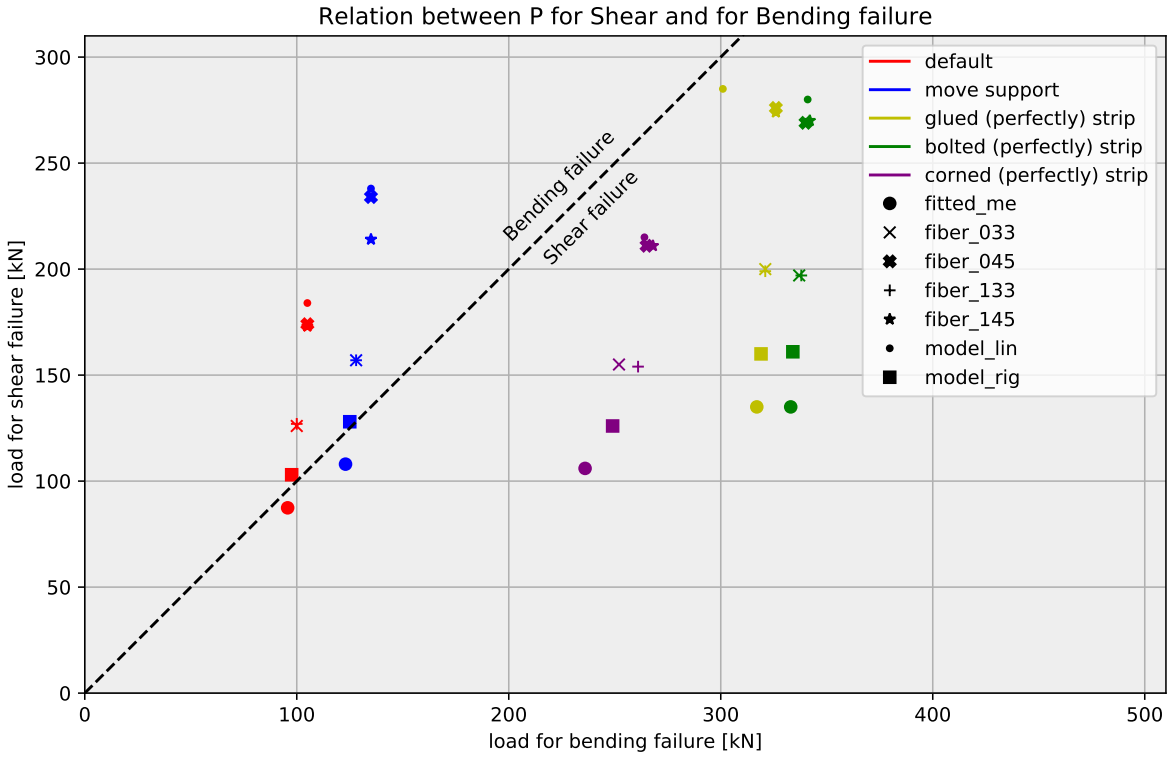

Figure 10.12: Relation between the shear and bending moment capacity for modifications.

The German guidelines require at least six of these tests in order to achieve sufficient information about the scatter in performance of the batch. It was decided to cast seven of these elements as the minimal casting volume was not met otherwise. This will provide statistically significant data into the mean and deviation of the property value for this batch.

10.2. Preparation

A number of preparations had to be made before the actual experiments could be performed. This section will explain the steps which were taken and their possible influence on the experimental results.

10.2.1. Casting

After the design of the elements was finished, the casting could be arranged. This was done in the Hi-Con factory in Hjallerup, Denmark (see Figure 10.13). After the framework and the reinforcement was made, the elements were inspected to check for any deviation from the original design.

The reinforcement in the elements without stirrups is all straight and therefore easier to be placed according to the design specifications (see Figure 10.14a), while the addition of stirrups resulted in a more complex design in the console (see Figure 10.14b and Figure 10.14c). The stirrups caused the main reinforcement to be bend slightly inwards, resulting in a smaller effective height of the cross-section. This showed that complex reinforcement detail can influence the structural response in a negative way. The small height of the stirrups also resulted in a continuous bend in the legs. This will also influence the way the stirrups respond once activated.

10.2.2. Modifying

Before the elements were tested, three were modified by adding a steel reinforcement strip to the bottom of the element. This strip has a cross-section of $10 \times 100 = 1000mm^2$ and a yield strength of approximately 500 MPa. These strips are often used in the laboratory to add reinforcement after casting.

Figure 10.13: Overview of the casting process.

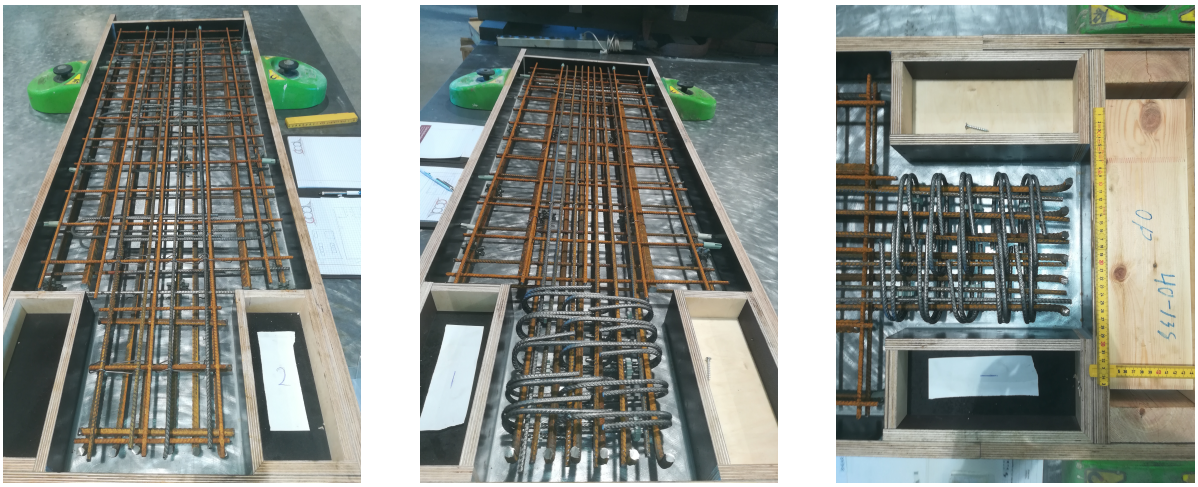

(a) Overview of reinforcement in element RAQTAN_2-B .

(b) Overview of reinforcement in element RAQTAN_1-A .

(c) Detail of reinforcement in element RAQTAN_1-A .

Figure 10.14: Reinforcement before casting.

The strips should provide maximal increase in bending moment capacity, while minimizing the influence on the shear capacity. Glueing them to the zone where shear failure is expected to occur would create a cooperation between the element and the strip. Vaseline was applied on a section between 50 and 400mm from the edge of the console to minimize the friction between the element and the strip. Sicadur-30® is applied on the rest of the contact area between the strip and the element. After placing the strip pressure is applied to join both parts. The result is shown in Figure 10.16.

10.2.3. Measuring equipment

Digital Image Correlation (DIC) is applied for the Raqtan elements. This method relates a pattern on a flat surface between different images. The strain between the markers can be determined, resulting in a strain field for the specific surface. In this case a white paint is applied on one side of the console, after which black coloured aquarium sand is glued over. This results in a high contrast surface which can be tracked digitally. During the experiment a camera will take close-ups of this surface every 5 seconds. With the use of a reference plane (a white sheet with equally distanced red dots) the images can be scaled. The digital photos will be taken with a *Nikon D5000*, with a resolution of 4288×2848 pixels (12.2 megapixel).

Linear Variable Differential Transformers (LVDTs) will be used to determine the elongation between specific points of interest. These devices can be programmed to write data at prescribed intervals. For these experiments the interval is set to every second. The experiments are planned to take between

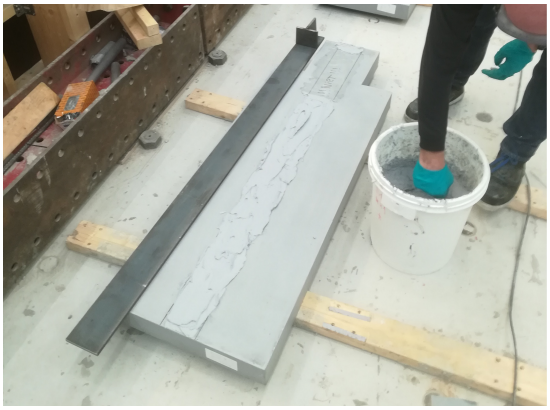

Figure 10.15: Adding The strips. The image shows the area covered in Vaseline and the area covered in Sicadur-30®.

Figure 10.16: The result of the modification. Note that the elements are upside-down.

10 to 15 minutes, resulting in 600-900 data entries. The LVDT which was supposed to measure the element's deflection was not operational. Therefore it was chosen to derive the deflection based on the images obtained for the DIC. The DIC and LVDT measurements are not coupled in time. This should be done afterwards by determining the elongation on a LVTD in the plane of the DIC.

Load The load is applied through a manually operated hydraulic press with a maximal capacity of near 200kN. The hydraulic pressure is measured and converted in to the applied load. This measurement is coupled to the LVDTs, which means the data can be easily combined.

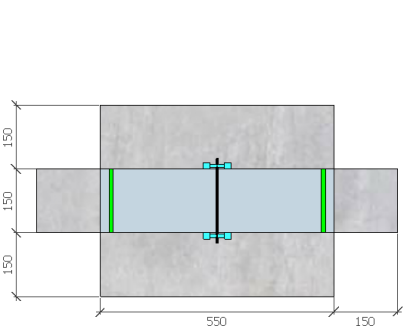

(a) equipment for the CMOD tests

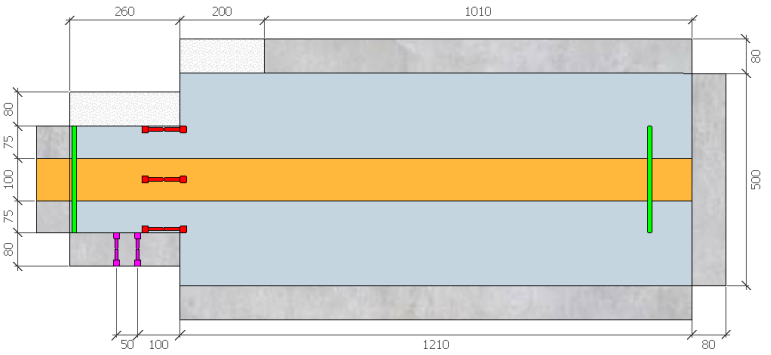

(b) equipment for the Raqtan tests

Figure 10.17: Overview of the equipment applied on the elements. The elements are viewed from the bottom and the side faces are shown as well. The LVDTs are marked in blue ($\Delta = 50mm$), purple ($\Delta = 65mm$) and red ($\Delta = 90mm$). The area used for DIC is shown as dotted white and the supports are marked green.

10.3. Results

This section describes the results of the performed experiments.

10.3.1. Compression tests (13-12-2018)

The first tests were to determine the cubical compressive strengths. For this test 6 cubes of 100x100x100 mm^3 were cast. As the sample were cast at 28th of September, this is the 76-day strength which is determined. By providing the sample dimensions, the ultimate load was automatically converted into the corresponding cylindrical compressive strength. The results are shown in Table 10.4 and the derived properties are shown in 10.5.

Table 10.4: Results for the compression tests.

Sample		001	002	003	004	005	006	-
Ultimate load	F_u	1691.4	1672.6	1736.7	1688.8	1725.3	1733.5	**kN**
Compressive strength	f_c	215.36	212.96	221.12	215.02	219.67	220.72	**MPa**

Table 10.5: Material properties based on the compression tests.

Property		Value	
Mean compressive strength	f_{cm}	217.48	MPa
Standard deviation	$f_{c\sigma}$	3.45	MPa
Characteristic compressive strength	f_{ck}	211.82	MPa
Design compressive strength	f_{cd}	141.21	MPa

10.3.2. CMOD tests (17-12-2018 and 18-12-2018)

The second material property which was tested is the relation between the load and the CMOD in a notched three-point-bending-test, according to EC14651. The testing rig is shown in Figure 10.18.

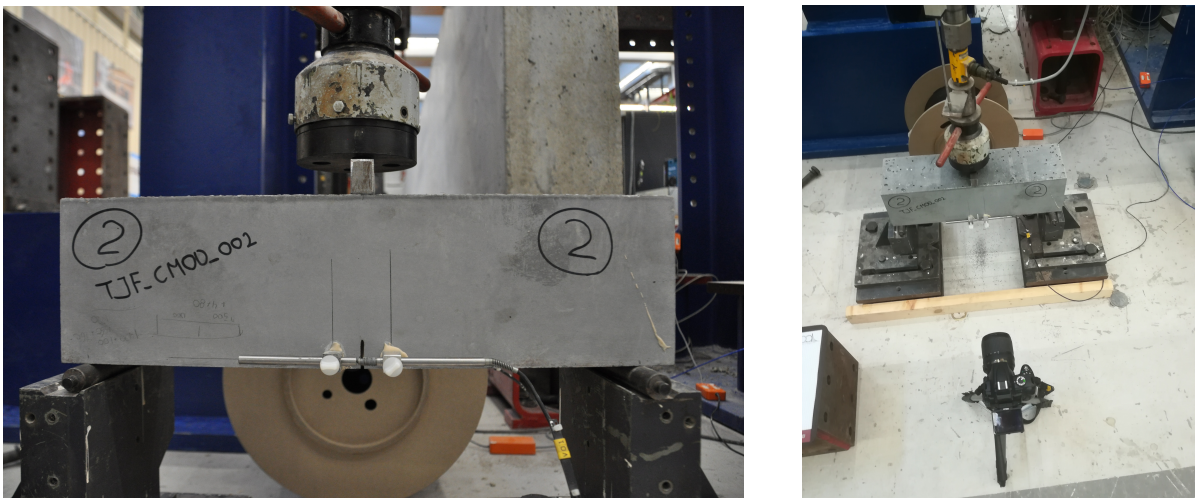

Figure 10.18: Overview of the CMOD testing rig.

The results which were obtained via the LVDTs had to be corrected for the location of the measurements on the sample. The EC14651 prescribes measurements at the bottom of the crack mouth, but it was chosen to add the LVDTs to the side of the element to protect the equipment if the sample would break. The EC14651 allows this, but the measured value has to be corrected. The resulting curves are shown in Figure 10.19 and their corresponding CMOD values can are provided in Table 10.6.

Table 10.6: Resulting CMOD values

Sample		001	002	003	004	005	006	007	μ	σ
F_{LOP}	[kN]	8.48	11.81	10.08	9.28	8.59	11.37	11.11	10.10	1.26
$F_{R,1}$	[kN]	8.77	13.81	12.50	12.30	10.93	15.52	14.80	12.65	2.16
$F_{R,2}$	[kN]	7.17	10.19	9.20	9.88	9.00	12.13	11.54	9.87	1.54
$F_{R,3}$	[kN]	5.74	6.70	6.60	8.09	6.92	8.89	8.04	7.28	1.01
$F_{R,4}$	[kN]	4.50	4.76	4.48	6.13	5.45	6.70	5.87	5.41	0.80

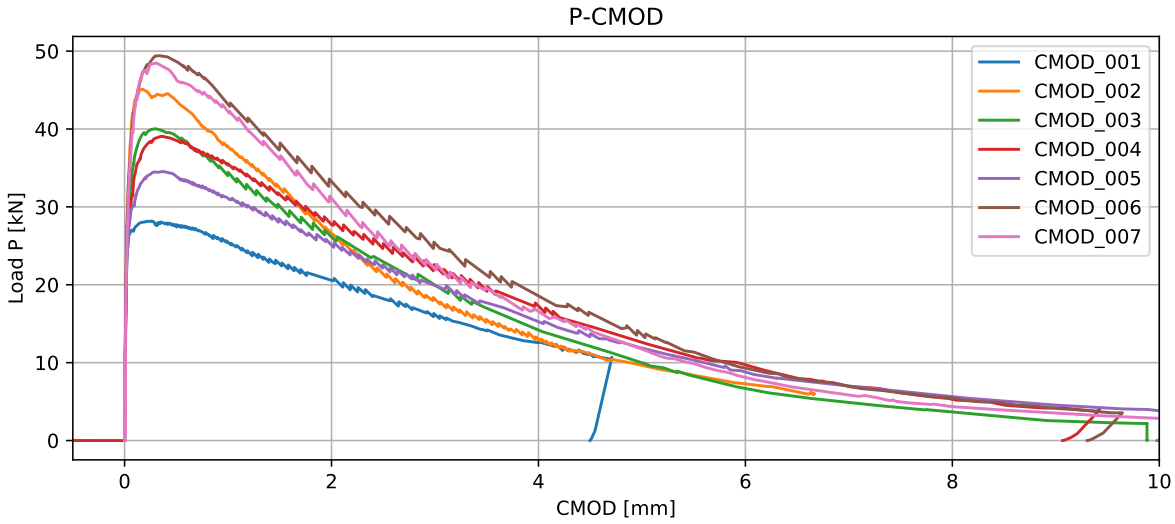

Figure 10.19: Experimental CMOD curves.

The curves can be compared to the curves for the 28 day strength, as provided in §9.1.1. This comparison is made for the mean value, the 90% interval and the design curve. The resulting curves are shown in Figure 10.20. It should be noted that the peak values are significantly increased, but so is the deviation, resulting in similar characteristic values.

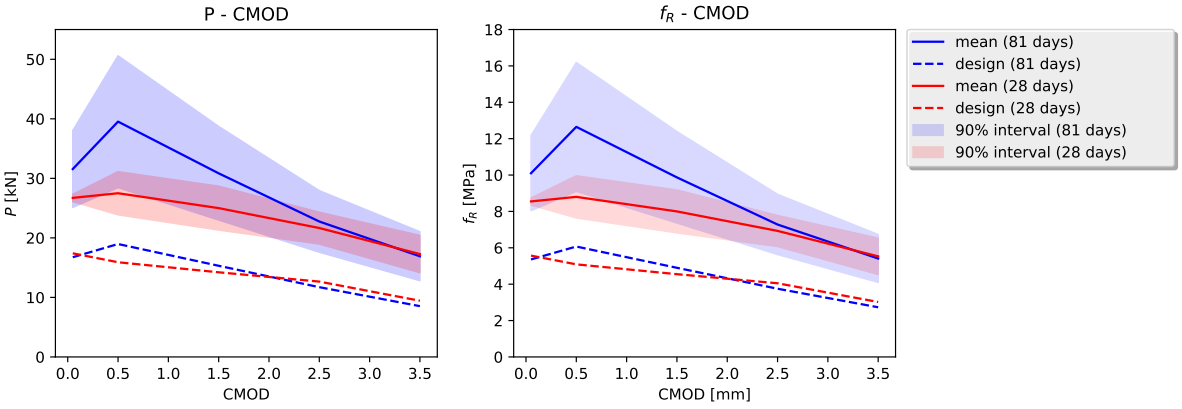

Figure 10.20: Comparison of experimental CMOD curves.

10.3.3. Main experiments: Raqtan elements

The main experiment consists of four elements: one with stirrups and three without. The different configurations and their purposes are explained below:

Test 1: **RAQTAN_4-B**, an element without stirrups and without modifications. This element was used to confirm the failure in bending moment and provide data regarding the original hypothesis that the stirrups are not required for sufficient capacity. The element failed in bending with a peak load of 100kN, which caused the other elements to be tested with modifications.

Test 2: **RAQTAN_3-B**, an element without stirrups and with an added strip of reinforcement. With the increased bending moment resistance this element was supposed to fail in shear according to the FE models. But this modification turned out to be insufficient, as the element still failed in bending at 181kN. Further modification to the other elements were not made as the testing rig was already reaching its maximum capacity. During the loading of this element the added corner in the reinforcement strip gave

way shortly after loading, at $40kN$. As this gave quite a loud response and impact to the element, the test was shortly paused to check whether all measurement equipment was still in place and unaffected.

Test 3: **RAQTAN_2-B**, an element without stirrups and with an added strip of reinforcement. It was chosen to test this element with the added strip as well, as this would provide insight in the variance of the capacity. The main difference with the previous element was that the added corner did not gave way until the peak load of 155 kN was reached.

Test 4: **RAQTAN_1-A**, an element with stirrups and without modifications. As the previous elements did not fail in shear but in bending, and as this element even has an increased shear resistance due to the application of stirrups, it was decided to remove the modification from this element. This ensured failure in bending at a peak load of 96kN, but provide information regarding the original design. The influence of the modification was removed by cutting the reinforcement plate underneath the console.

Before the data could be analysed, the measurements from the DIC and the LVDTs had to be coupled in time. This was achieved by analysing the photos taken for the DIC. An example of these photo's, the first image for the RAQTAN_4-B element, is shown in Figure 10.21.

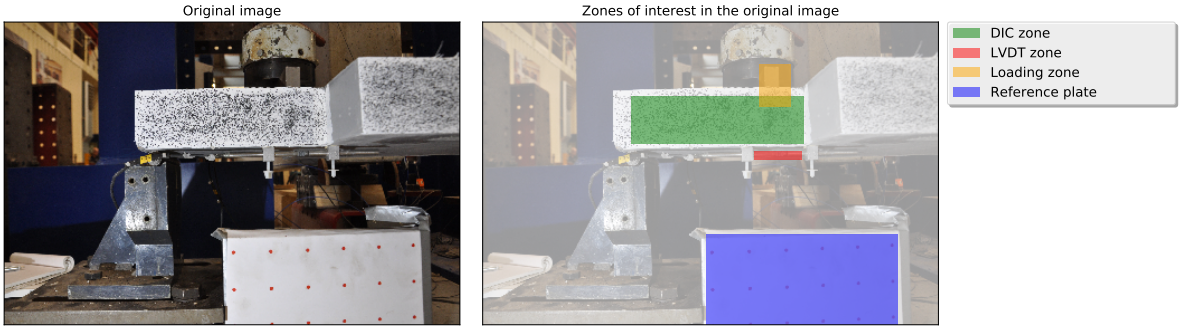

Figure 10.21: DIC image. The left image displays the multiple zones of interest.

In order to derive the elongation in the LVDT in the LVDT zone, an algorithm was written that, for each photo, analyses the image and locates the two chrome cylindrical parts of the LVDT. The intersection point of those elements is determined and the distance between the measurement part and the intersection point is determined (see Figure 10.22). The found elongation is in pixels, which can be translated in to mm using the red-dotted reference plate. The used Python code is attached in Appendix D.2. This results in a relation between time and elongation. This relation is also found in the LVDTs output, which allows the two measurements to be coupled in time. The resulting correlation for element RAQTAN_4-B is shown in Figure 10.23. The close resemblance of both lines indicate a proper correlation.

Figure 10.22: The analysis on the photos to determine the elongation. The shimmer on the metalic cylinders is traced by setting a threshold on the whiteness (right image). The direction can be determined by finding the first and the last white pixel for each cylinder (resulting in the red lines in the left image). The intersection point is located where the left red line intersects the normal to the right red line. The used Python code is attached in Appendix D.2.

The next step is to derive the deflection from the digital photos. This is done by writing an algorithm which traces the top of the loading plate in all images. The result for the first image for RAQTAN_4-B is shown in Figure 10.24. The displacement is again scaled to millimetres using the red-dotted reference plate in the image. The code can be found in Appendix D.3.

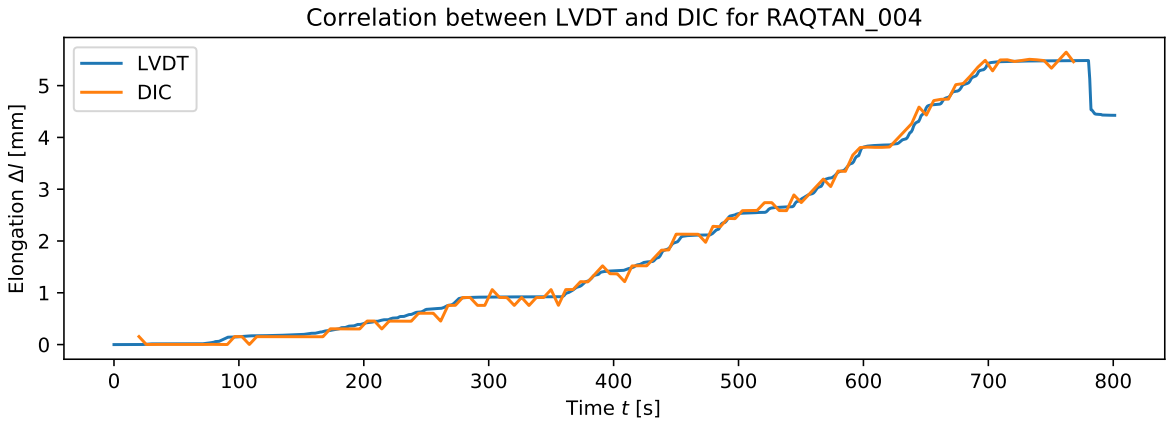

Figure 10.23: The relation between elongation according to LVDT and DIC.

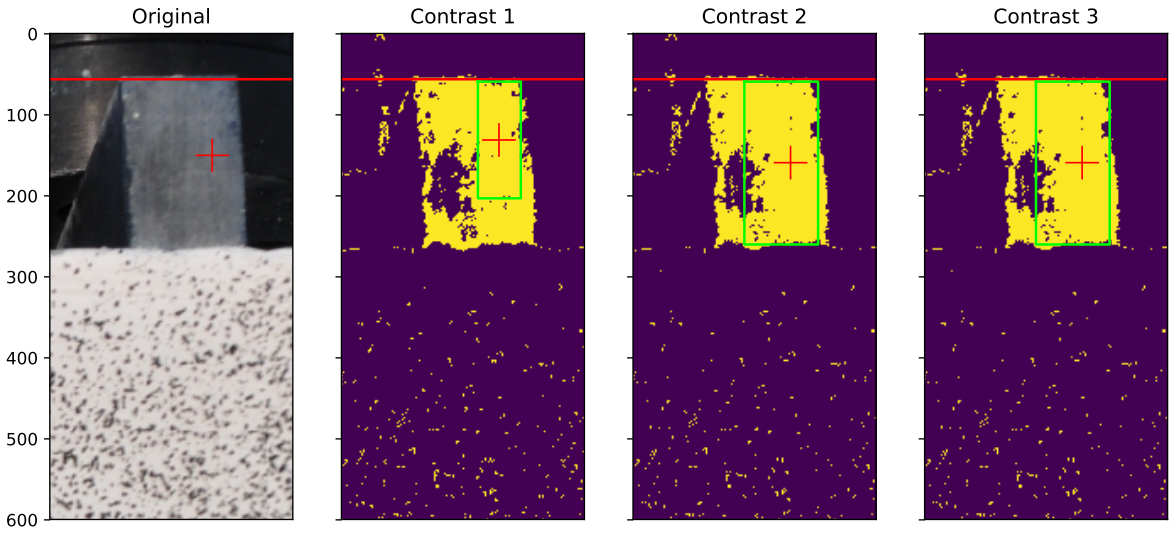

Figure 10.24: The analysis on the photos to determine the deflection. The colour of the loading plate is determined in the original image, after which a contrast is applied to all similar colours (contrast 1). A box (shown in green) with similar colour is determined. The average colour of this box is used to determine the new contrast (contrast 2). The fist row containing more than 50 pixels within the threshold is considered as the top of the loading plate (shown with a red line). The code can be found in Appendix D.3

After the different measurements (LVDT and digital imaging) were coupled in time, it became possible to plot the results. The found load-displacement curves are shown in Figure 10.25. The shape of the curves represent the shapes obtained by the FE models which failed in bending, with the deviation that the initial phase ($P < 40kN$) is rather unpredictable. This is expected to be a result of the irregularities at the element face on which the load is applied. This was the casting side, which required some force before the steel loading plate flattened the irregularities.

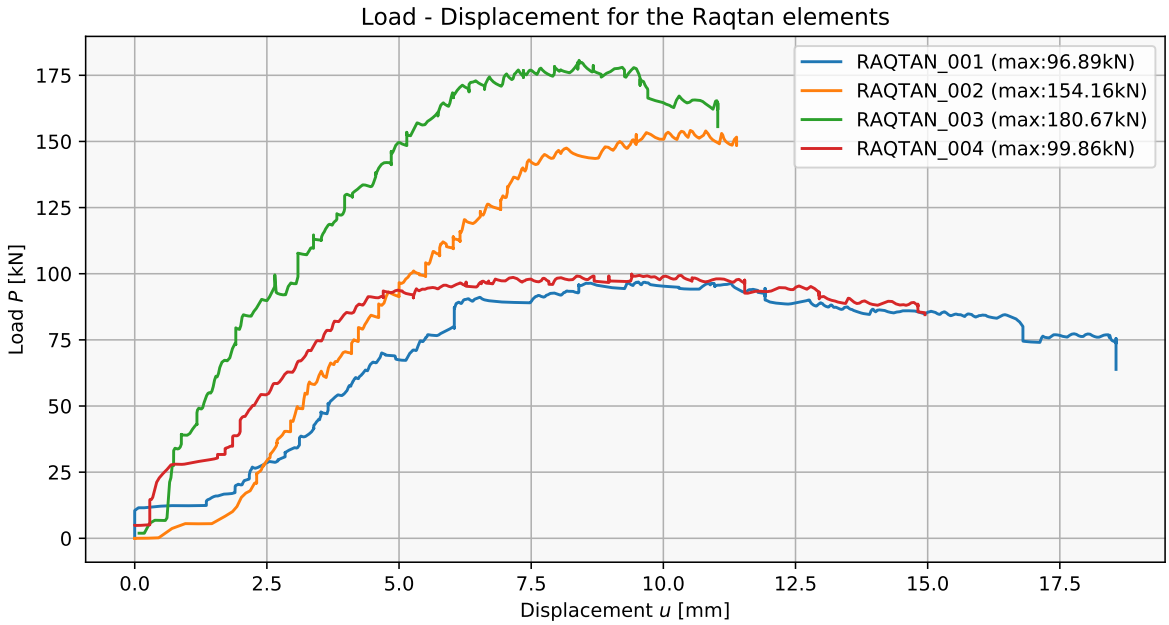

Figure 10.25: The relation between load and displacement for the Raqtan elements.

10.4. Analysis

The output is analysed in order to retrieve useful information from the experiment results.

10.4.1. LVDT measurements

The measurements from the LVDTs are shown in Figure 10.26. These graphs provide useful insight in the occurring failure mechanism. LVDT04 and LVDT05 are placed to measure the elongation over the bending crack, while LVDT01 and LVDT09 are placed to measure the elongation over the shear crack. There is a difference between these to types of elongation with multiple orders of magnitude. This clearly indicates that the shear crack does not occur and the bending crack is initiated early in the experiment and keeps expanding.

The maximal strain found in the LVDTs for shear per experiment are shown in Table 10.7. It should be noted that even the strains for shear are in the range of crack initiation:

$$\epsilon_c = \sigma_{cr}/E_c = 7.0/50000 = 1.44 \cdot 10^{-4} \tag{10.7}$$

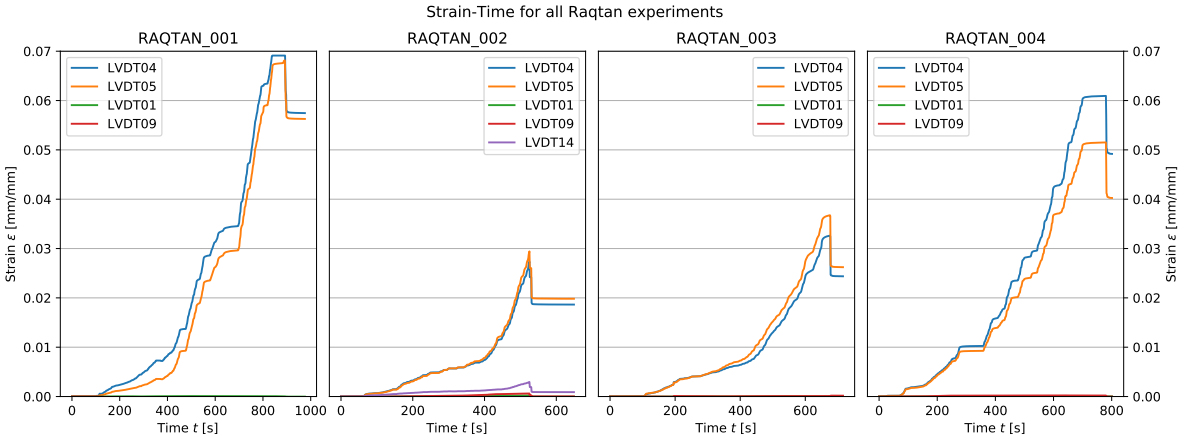

Figure 10.26: Measurements of the LVDTs.

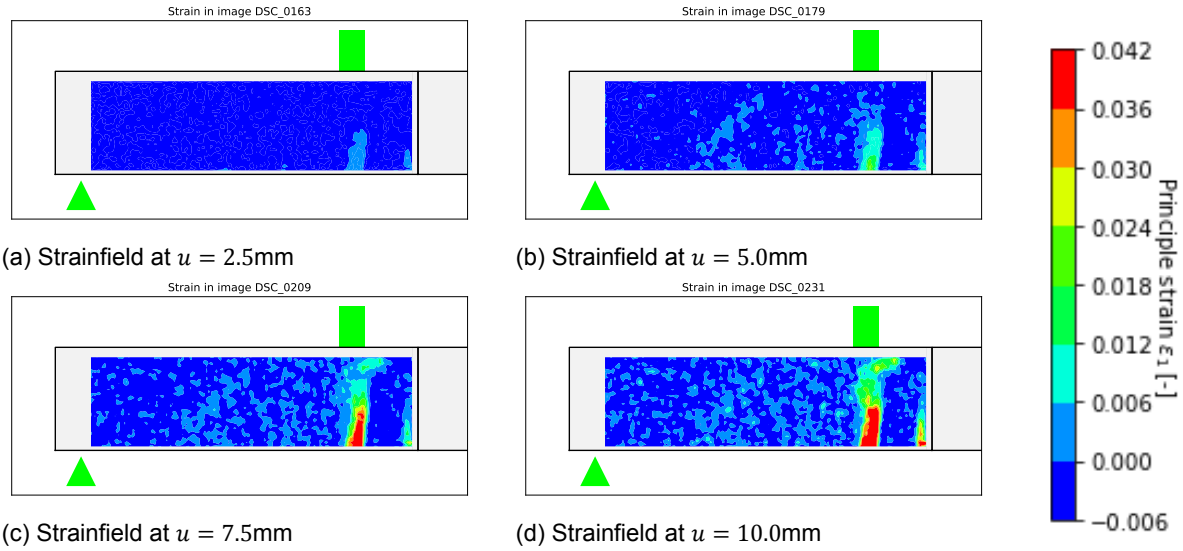

(a) Strainfield at $u = 2.5$mm

(b) Strainfield at $u = 5.0$mm

(c) Strainfield at $u = 7.5$mm

(d) Strainfield at $u = 10.0$mm

Figure 10.27: The strain field at multiple deflection stages. The images are limited to the console. The green triangle resembles the support and the green rectangle the loading plate.

This is an indication that the first invisible cracks have occurred, but not expanded significantly. The magnitude of the strain does however seem to be in dependent of the element: this can be a result of the hardening behaviour of the CRC. This will be further researched with the help of the DIC analysis.

Table 10.7: Max strain during the experiment.

Element	**Shear** [$^{mm}/_{mm}$]	**Bending** [$^{mm}/_{mm}$]
RAQTAN_1-A	$6.12 \cdot 10^{-4}$	$6.91 \cdot 10^{-2}$
RAQTAN_2-B	$6.19 \cdot 10^{-4}$	$2.94 \cdot 10^{-2}$
RAQTAN_3-B	$1.83 \cdot 10^{-4}$	$3.68 \cdot 10^{-2}$
RAQTAN_4-B	$2.44 \cdot 10^{-4}$	$6.01 \cdot 10^{-2}$

10.4.2. DIC measurements

For this analysis the photos were analysed using the opensource DIC package *pydic* as written by D. André[1]. The advantage of this package is that it is written in Python, which makes is compatible with the other scripts written for this research. The code which was written specialy for the DIC analyses of this research is provided in Appendix D.4.

The strains at multiple displacements (2.5, 5.0, 7.5 and 10.0 mm) are compared. The resulting strain fields for the RAQTAN_4-B element are shown in Figure 10.27. The bending crack is the first significant deformation which can be noted, in the middle between the support and the loading plate the formation of a diagonal shear crack can be noticed as well. At a displacement of 10.0mm a strain above 0.012 is found at the centre of this shear crack. This crack was not visible with the naked eye. Therefore it is expected to be a smeared crack, which is supported by the post-cracking peak load of CRC. The other elements showed similar behaviour. The results for the other elements are provided in Appendix E.

[1]Code can be found in https://gitlab.com/damien.andre/pydic

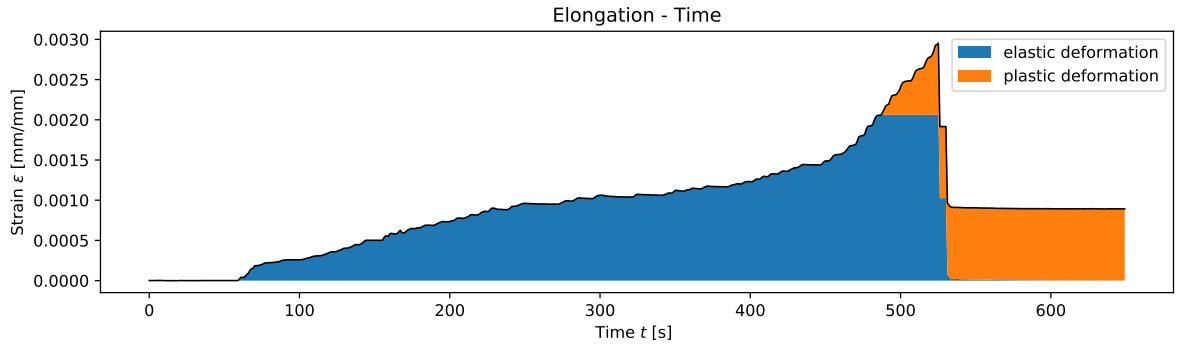

Figure 10.28: The strain in the added reinforcement strip.

10.4.3. Bending capacity with modification

The failure in bending moment can be verified by looking at the deformation in the added reinforcement strip. In RAQTAN_2-B this strain was measured and the result is shown in Figure 10.28. After unloading the element, the plastic strain remains. This indicates yielding and therefore failure in bending moment.

The modified elements, RAQTAN_2-B and RAQTAN_3-B , both failed in bending, while the FE models predicted failure in shear. Their curves are compared to their corresponding models in Figure 10.29. This graph clearly shows a differentiation between the predictions and the actual results. The first difference to notice is the different failure behaviour: the prediction was that the elements would fail in shear, while the actual failure mechanism is in bending and at a much lower ultimate load.

This can only be explained by the actual bending moment capacity being lower than the predicted one. Where the models predicted a bending moment resistance in the range of 220-260 kN (See Figure 10.12), the actual range spans at least from 155 to 180 kN. The connection at the corner of the reinforcement strip can play a major role in this deviation, as the connection at the vertical face of the element was torn apart. The fact that the strip shows plastic deformation (Figure 10.28), disputes this explanation, as the yielding results in the maximal bending moment capacity. The unpredicted behaviour of the corner would therefore only result in a lower stiffness, not in a lower ultimate load.

The difference in resistance between the two modified elements is significant as it is about 20%. While the elements are close to identical. The values can be influenced by small changes in the configuration, but for example the location of the main reinforcement and the added strip did not deviate notable. Another influencing factor could be a small deviation in the location of the supports, but as these were closely checked before loading the element it is expected that the influence can be neglected. A better explanation is found when the results are compared to the CMOD tests, where the variance in peak load was also large.

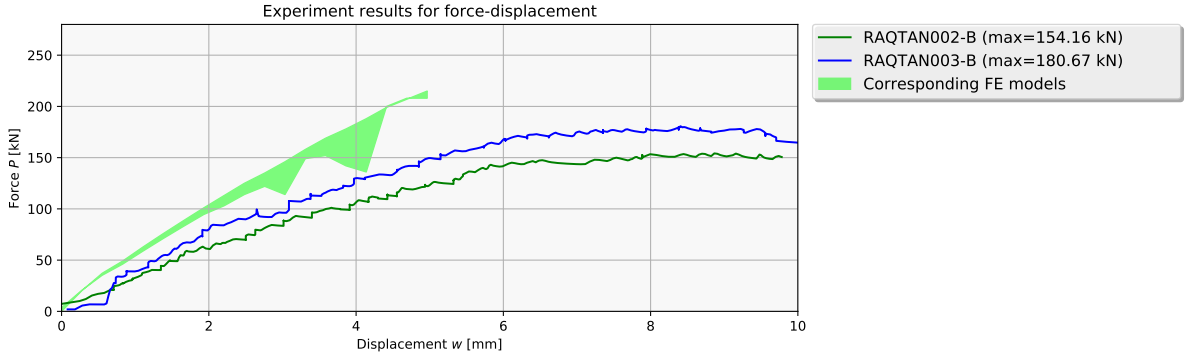

Figure 10.29: The strain in the added reinforcement strip.

10.4.4. Bending capacity without modification

The RAQTAN_1-A and RAQTAN_4-B , the ones without modification, can be compared to the FE predictions. The results are shown in Figure 10.30. The general shape shows resemblance, which is a result of a similar structural response: the failure mechanism is the same and so are the mechanisms preceding failure. The failure loads are around the lower limit as predicted by the models, but the deviation is not unexpectedly large when the variance within the models is taken in to account. The stiffness in the fibre activation zone (after crack initialization and before yielding), is lower for both experiments. This might indicate that the fibres require a larger deformation before reaching their peak resistance. Another aspect which might have caused this is the failure of the casting surface. This surface contains many irregularities, which are flattened out as the load is increased.

Both elements failed in bending. As the bending moment capacity was not influenced by the addition of stirrups, this means that both capacities (96.9kN for the RAQTAN_1-A and 99.9kN for the RAQTAN_4-B element) can be compared. While two tests is not enough to determine the design capacity according to the Eurocodes *Design by testing* method, it is possible to use the results and determine a characteristic value, which is expected to be exceeded in 95% of the tests. In order to do so, a student T-distribution is applied. This method does include the fact that the found mean value, 98.4kN, is not the true mean and compensates for this. For a normal distribution the characteristic value is found by reducing the mean with 1.64σ, but with a t-distribution with the number of tests, n, being only two, the result is penalized. The reduction factor now becomes 6.320. As a result the found characteristic values becomes:

$$P_k = \mu_P - 6.320\sigma_P = 98.4 - 6.320 \cdot 2.12 = 85.0kN \tag{10.8}$$

With a material factor of $\gamma_c = 1.5$ this would result in a design value of $P_d = P_k/\gamma_c = 56.7$ kN. The equivalent design load is $52.8kN$. Which would result in a Unity Check of $UC = 0.93$. This design value should be considered with care, as a result of the low number of tests on which the value is based. When the same calculation is made for the modified elements, which had a large different between them, the following values are found:

$$P_{k,mod} = \mu_{P,mod} - 6.320\sigma_{P,mod} = 169.5 - 6.350 \cdot 20.51 = 39.9kN \tag{10.9}$$

$$P_{d,mod} = P_{k,mod}/\gamma_c = 39.9/1.5 = 26.6kN \tag{10.10}$$

The value of the elements with extra reinforcement is lower than the original element as a result of the large spread. More test results would could provide a better insight in the actual variance and are expected to result in a better approximation of the design values.

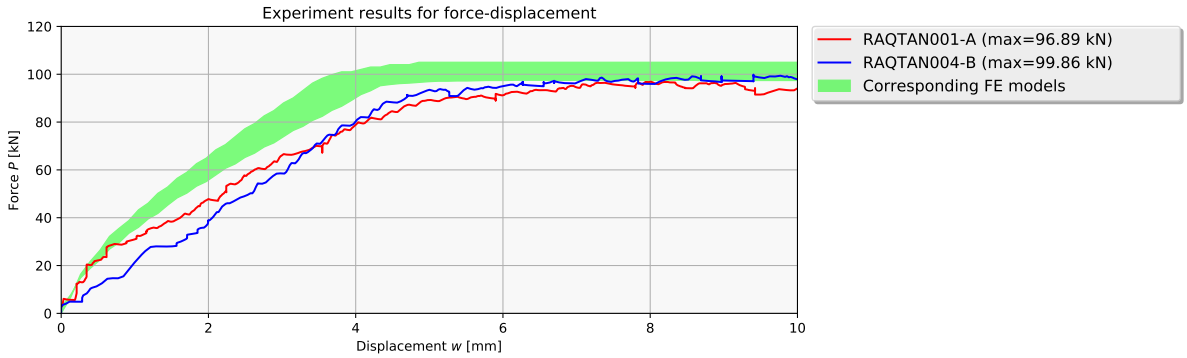

Figure 10.30: The strain in the added reinforcement strip.

10.5. Conclusions

The experiments showed that the Raqtan element fails in bending, even if the bending moment capacity is increased to 150 or 180kN by adding external reinforcement strips. While these values are reached there was no indication of failure in shear, as the characteristic diagonal cracks were not visible. The strains reached in the shear zone do however indicate the occurrence of cracking.

The found design capacity of 56.7 kN does indicate a safe design, but the UC does not allow a significant redundancy. The remark should be made that the number of experiments is low, and the significance of the statistically derived values is low. The structural response and range of values can be used to derive indications about the actual behaviour. As all the experiments showed that the bending capacity is lower than the shear capacity, the conclusion can be drawn that the bending moment is governing for the design. When this is related to the previous analyses, where the bending moment was sufficient for a safe design, this results in the overall design being sufficient for the ULS.

The capacities which were derived in this chapter based on the experiments are provided in Table 10.8. This table indicates sufficient capacity as the design capacities exceed the design loads.

Table 10.8: Overview of determined capacities.

Method		P_{Vu}		P_{Mu}		P_u		
		P_{Vm}	P_{Vd}	P_{Mm}	P_{Md}	P_{um}	P_{ud}	
Experiments	Raqtan	>184.0	>56.7	98.4	56.7	98.4	56.7	kN
Design load		-	52.8	-	52.8	-	52.8	kN

11

Validation of FE models

The data acquired from the experiments can be used to determine the accuracy of the models as created in Chapter 9 for the validation by FEA. The used tensile curves were compared to EN14651 experiments, which also resulted in curves fitted to the EN14651 experiment. These models might be overfitted and not yield accurate results for other set-ups, such as the Raqtan experiment. This chapter compares the results of the different FE models with the results from the experiments. The exact material properties, as derived in the experiments, are used in combination with the modifications as determined in the previous chapter.

Firstly the updated models will be discussed, after which the results from the models will be compared to the results from the experiments. Finally conclusions will be drawn regarding the accuracy of the models to predict the design capacity of the Raqtan element with and without stirrups.

11.1. Updated FE models

The compression strength of the model is updated to the mean value found in the compression tests: 218MPa. The properties for the *FRCCMD033*, *FRCCMD045*, *FRCEPS033* and *FRCEPS045* models are updated to correspond with the F-CMOD curves as derived in the experiments. The updated values are shown in Table 11.1. The tensile behaviour for the MC2010 linear and rigid models are redetermined as well, as shown in Table 11.2. Values which are not updated are not shown in this section, but can be found in §9.2.

Table 11.1: Material properties for the mean DIANA FRCCON models.

Property		**Value**		
Factor		0.33	0.45	
Uniaxial tensile strength	f_L	3.33	4.55	MPa
Uniaxial residual strength	f_{Ri}	4.17	5.69	MPa
Crack mouth opening at f_{Ri}	$CMOD_i$	0.50	0.50	mm
Uniaxial total strain at f_{Ri}	ϵ_i	0.10	0.10	-
Uniaxial residual strength	f_{Rj}	1.79	2.43	MPa
Crack mouth opening at f_{Rj}	$CMOD_j$	3.50	3.50	mm
Uniaxial total strain at f_{Rj}	ϵ_j	0.70	0.70	-
Uniaxial residual strength	f_{Rk}	0.01	0.01	MPa
Crack mouth opening at f_{Rk}	$CMOD_k$	8.69	8.69	mm
Uniaxial total strain at f_{Rk}	ϵ_k	1.74	1.74	-

Table 11.2: Updated material properties for the MC2010 models.

Property		**Value**	
Rigid-plastic			
Ultimate tensile strength	f_{Ftu}	2.43	MPa
Ultimate crack opening	w_u	3.15	mm
Rigid-linear			
Cracking tensile strength	f_{Fts}	5.69	MPa
Ultimate tensile strength	f_{Ftu}	0.01	MPa
Ultimate crack opening	w_u	3.15	mm

(a) The model for the RAQTAN_1-A element, with stirrups and without modifications.

(b) The model for the RAQTAN_2-B and RAQTAN_3-B elements, without stirrups and with modifications.

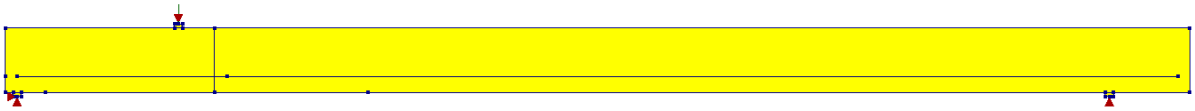

(c) The model for the RAQTAN_4-B elements, without stirrups and without modifications.

Figure 11.1: The models used for the recalibration.

The model is created in three configurations, as shown in Figure 11.1. Each model is ran with all previously defined tensile models.

11.2. Comparison

11.2.1. Load-displacement behaviour

The structural response of the actual element is compared to the behaviour of the FE models. The load-displacement curves for the experiments and the models are shown in Figure 11.2. The images for RAQTAN_1-A and RAQTAN_4-B show clear resemblance in behaviour between the model and the experiment. Both fail in bending, with a similar stiffness before the failure occurs and a similar ultimate load. When the ultimate load is considered, it is remarked that the FE models do overestimate the capacity in bending moment. For the two modified elements this is expected to be a result of the used steel reinforcement strip having a lower yielding strength then the given value of 500MPa.

11.2.2. Strainfields

The first FE model which is validated is the model for the RAQTAN_4-B . The strain field for the FEA is compared to the strainfields as derived via DIC for this element. The FE model shows a larger cracked zone, as more elements are marked red at 10mm displacement. This a result of the neglect of bondslib in the FEA. The comparison also shows that the shear capacity is underestimated in the FE, as it shows a clear strain in the shearzone, while the DIC only indicates some small dots with $\epsilon_1 > 0.006$. The strains in the bendingzone are comparable.

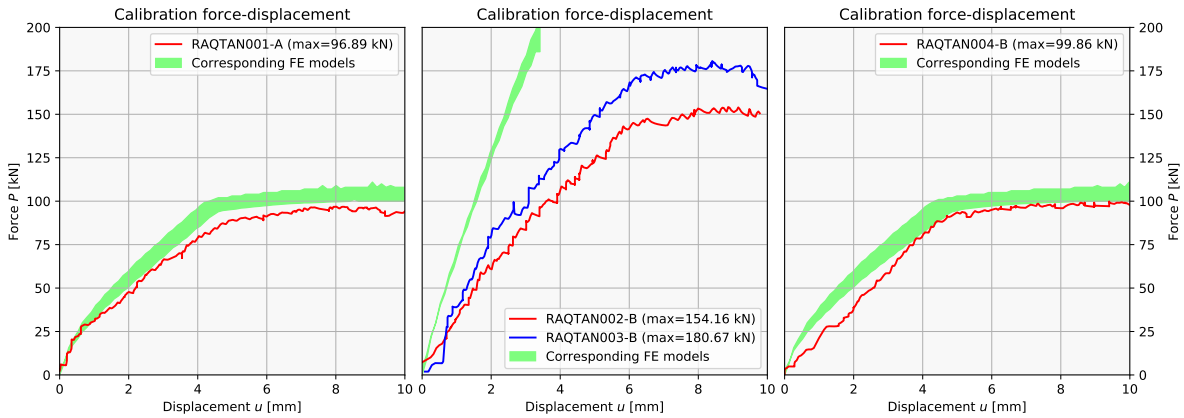

Figure 11.2: Comparison of the structural response for the calibrated models and the experiments.

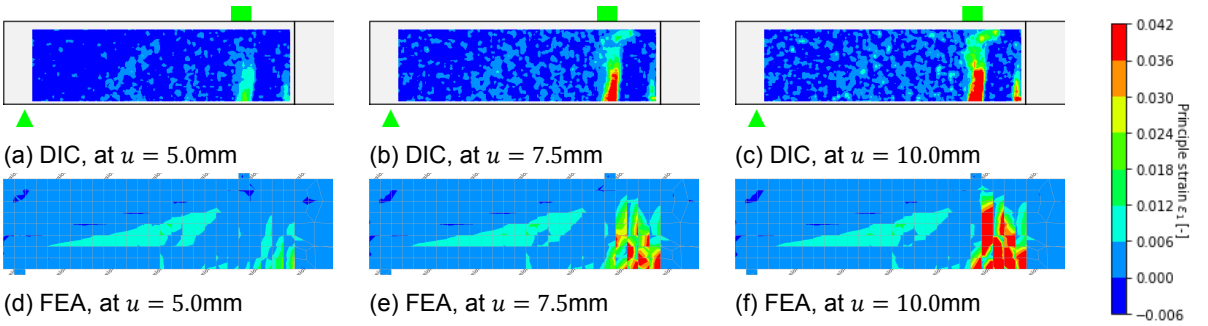

(a) DIC, at $u = 5.0$mm (b) DIC, at $u = 7.5$mm (c) DIC, at $u = 10.0$mm

(d) FEA, at $u = 5.0$mm (e) FEA, at $u = 7.5$mm (f) FEA, at $u = 10.0$mm

Figure 11.3: The strain field at multiple deflection stages for DIC and FEA compared for RAQTAN_4-B .

The models for RAQTAN_1-A show a similar comparison with the DIC results. The other models, RAQTAN_2-B and RAQTAN_3-B , failed in shear before the actual element failed in bending. The comparison of these models can be found in Appendix E. As an example the model *FRCCON045* is shown in Figure 11.4. The DIC analysis shows failure in bending, while shear strain (the diagonal strain lines) can be noted as well. The FE models show a clear failure in shear without any significant strains in the bending zone.

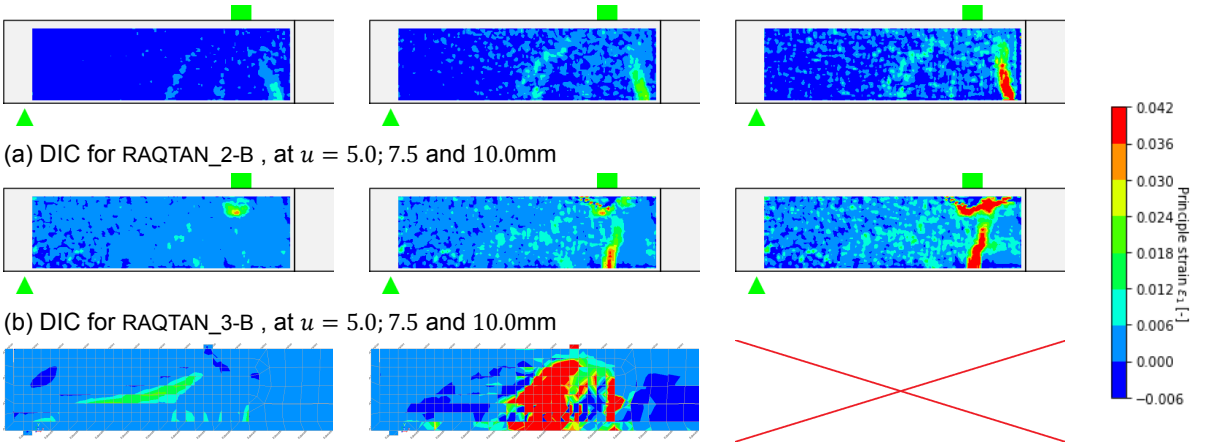

(a) DIC for RAQTAN_2-B , at $u = 5.0; 7.5$ and 10.0mm

(b) DIC for RAQTAN_3-B , at $u = 5.0; 7.5$ and 10.0mm

(c) *FRCCON045*, at $u = 5.0; 7.5$ and 10.0mm

Figure 11.4: The strain field at multiple deflection stages for DIC and FEA compared for RAQTAN_2-B and RAQTAN_3-B . A red cross indicates that shear failure occurred before the mentioned displacement is reached. The red large strains for RAQTAN_3-B just below the load plate are a result of spalling: the outer layer of the element broke away here.

11.2.3. Relation between shear and bending

As visible in Figure 11.3 and Figure 11.4, the shear strain is larger in the FE models than in the experiments. The models could be fitted, as done previously in §9.1 for the original models. This is not done as it is expected not to yield a useful improvement of the models due to a combination of factors.

As the models show a shear-strain which exceeds the actual strain in the shear region, this would require increasing the pre-ultimate tensile stiffness. As a result the stiffness for the bending moment would increase as well. As shown in Figure 11.2, the bending capacity of the models does already exceed the actual values. A further increase would result in a further deviation from the real failure mechanism. This does show a relation between the shear behaviour and the bending behaviour which does not resemble the actual relation.

11.3. Conclusions

The FE models based on the experiments mean material properties show an underestimation of the shear capacity. This can mostly be traced back to a conservative implementation of the tensile models. While the shear capacity is underestimated, the bending capacity is over estimated. For the elements without modifications this can be a result of the mean yield strength of the reinforcement bars. As the models are only based on mean values and variance within the material properties is not taken in to account. The overestimation of the bending capacity for the modified elements can be a result of the reinforcement strip have a yieldstress below the expected 500MPa.

The shear capacity is often hard to predict, as mentioned in chapter 4, as the exact mechanisms are not yet fully understood. This is supported by the underestimation of this capacity as explained in this chapter. An underestimation results in a conservative design, but a safe design. This underestimation also has some negative effects, such as a less slender design (aesthetics) or an increase in material usage (sustainability). From this point of view the models can be used to determine the safety of the Raqtan landing platform regarding shear, while it should be kept in mind that the actual shear capacity is higher.

The relation of the bending behaviour and the shear behaviour, based on the used tensile models, indicates a core problem which prevents the models to be able to predict both the shear and the bending behaviour properly. As these behaviours are both influenced by the tensile model, it is almost impossible to create a model which can predict the actual structural response accurate.

12

Comparison

The multiple validation methods which were performed in the previous part of the research resulted in multiple values for the capacity of the element. This chapter will focus on combining the found data and determine what values are useful and why so. Firstly an overview of the resulting capacities will be provided and discussed. Secondly the relation between the bending and the shear capacity is discussed for the multiple validation methods and finally the results will be combined to derive an element capacity.

12.1. The element capacity

The applied methods do result in a wide range of predictions for the bending, shear and element capacity. These values can not be directly compared, as the underlying methods differ. A complete overview is provided in Table 12.1 and a summary of the resulting ranges can be found in Table 12.2.

Table 12.1: Overview of all determined capacities. The ultimate load is provided for failure in shear, failure in bending and for the element. These values are split in design values and in mean values.

Method		P_{Vu}		P_{Mu}		P_u		
		P_{Vm}	P_{Vd}	P_{Mm}	P_{Md}	P_{um}	P_{ud}	
Codes	EC	37.1	23.4	77.5	59.4	37.1	23.4	kN
	ECNL	37.1	23.4	77.5	59.4	37.1	23.4	kN
	ECPBT	45.7	24.2	77.5	59.4	45.7	23.4	kN
	ECFR	178.6	105.2	79.4	79.4	79.4	79.4	kN
	ECGE	76.6	39.6	85.0	62.2	76.6	39.6	kN
	MC2010	73.8	47.7	88.8	65.3	73.8	47.7	kN
	MC2010a	65.3	48.3	88.8	65.3	65.3	48.3	kN
FE models	Fitted_de	-	105.0	-	77.6	-	77.6	kN
	Fitted_me	141.0	-	101.0	-	101.0	-	kN
	FRCCMD033	127.0	88.7	100.0	76.1	100.0	76.1	kN
	FRCCMD045	175.0	113.0	105.0	79.1	105.0	79.1	kN
	FRCEPS033	128.0	89.7	100.0	77.0	100.0	77.0	kN
	FRCEPS045	174.0	128.0	105.0	89.6	105.0	89.6	kN
	MC2010lin	185.0	108.0	105.0	78.7	105.0	78.7	kN
	MC2010rig	104.0	84.3	97.5	65.9	97.5	65.9	kN
Experiments	Raqtan	>184.0	>56.7	98.4	56.7	98.4	56.7	kN
Design load		-	52.8	-	52.8	-	52.8	kN

Table 12.2: Summary of all determined capacities. The range for the ultimate load is provided for failure in shear, failure in bending and for the element. These values are split in design values and in mean values.

Method	P_{Vu}		P_{Mu}		P_u		
	P_{Vm}	P_{Vd}	P_{Mm}	P_{Md}	P_{um}	P_{ud}	
Codes without fibres	37.1-178.6	23.4-105.2	77.5-88.8	59.4-79.4	37.1-79.4	23.4-79.4	kN
Codes with fibres	65.3-178.6	39.6-105.2	79.4-88.8	62.2-79.4	65.3-79.4	39.6-79.4	kN
FE models	104.0-185.0	84.3-128.0	97.5-105.0	65.9-89.6	97.5-105.0	65.9-89.6	kN
Experiments	>184.0	>56.7	98.4	56.7	98.4	56.7	kN
Design load	-	52.8	-	52.8		52.8	kN

When these ranges are compared to the experiments results, it is noted that the bending moment capacity is often predicted by the lower range values, while the shear capacity is exceeding the predictions. This is an indicator that the shear capacity as predicted by the codes results in a conservative and safe value, even when a fibre component is included.

12.2. Relation between capacity in bending and in shear

Figure 12.1 shows the capacity for both bending and shear for the design codes, the FE models and the experimental results. Many of the design codes predict insufficient shear capacity (as they are located in the zone for the design load). For the Raqtan elements the bending moment capacity of the original element (RAQTAN_1-A and RAQTAN_4-B) are shown. The shear capacity is set to be minimal equal to the failure load at the modified elements (which was 155kN for RAQTAN_2-B).

The graphs are created for the design values and the mean values, as the design values can not be directly compared to the experiments and the mean values provide an indication in the quality of the prediction. The farther the prediction is from the line for the experiment, the less valuable the prediction becomes. It should be noted that the mean value of design codes does not directly provide information regarding the accuracy of the design value, as the design guides are not derived to predict the exact values, but to predict safe values. As a result the translation from design values to mean values might not be accurate. With this remark made, the French guideline does seem to make a proper prediction for the mean value. The design value is significantly higher than the value found in the experiments, but this might be a result of the application of the material factor for concrete, $\gamma_c = 1.5$, while the bending capacity is mostly a result of the steel properties. The material factor for steel is significantly lower: $\gamma_s = 1.15$, which results in a higher design capacity based on the experiments.

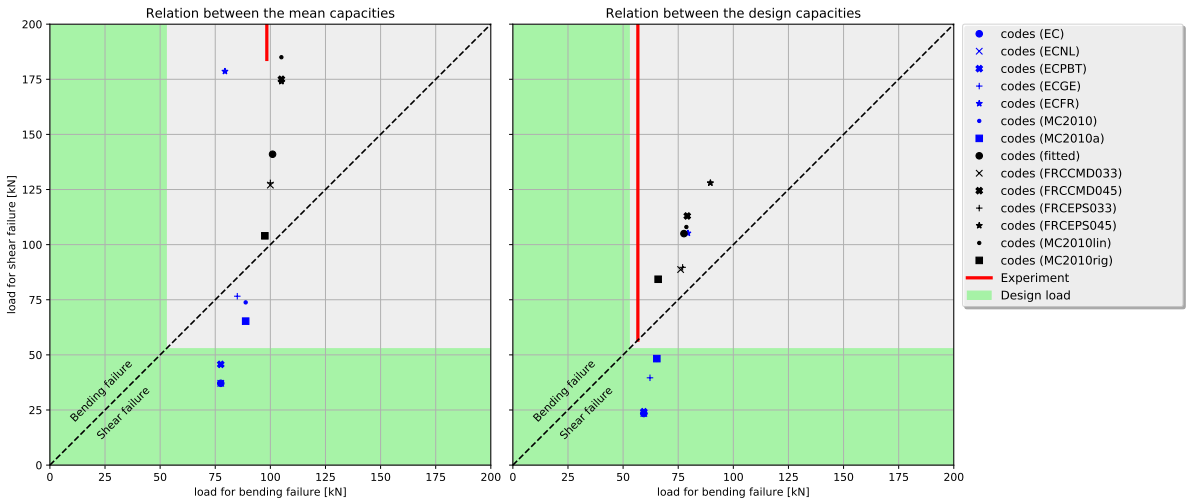

Figure 12.1: The relation between bending and shear capacity for all the derived models and experiments.

When looking at the shear capacity of the element, the vertical coordinate should be compared to the horizontal green zone for the design load. Most of the FE models are above the diagonal line. This indicates that as the load is applied, the models will fail in bending before they fail in shear. The same can be said about the experiments. It can also be seen that a more complex analysis of the capacity, such as FEA in comparison to the codes, results in a better approximation of the actual found behaviour.

The relation between the two failure mechanisms can best be described by their mutual relation. These are shown in Table 12.3. A value greater than 1 indicates failure in bending. The experiments indicate a safety factor of 1.5 with respect to the shear capacity when the bending capacity is used as a design capacity.

Table 12.3: The ratio shear over bending capacity for multiple methods.

Method	Design values	Mean values
The codes	0.39-1.32	0.48-1.98
The FEA	1.17-1.43	1.07-1.76
The experiments	>1.00	1.56-1.93

12.3. Combined capacity

Based on the information provided, it can be concluded that elements will fail in bending, as predicted by the FE models and shown in the experiments. The codes determine a Unity Check for bending in the range of 0.66-0.89, ensuring sufficient capacity for the element. The final capacity can then be determined to be at least 59.4 kN, based on the Eurocode, and 62.2 kN, based on the codes including a fibre component. As the capacity according to the Eurocode is sufficient to guarantee sufficient safety, it can be concluded that the element without stirrups meets the required level of safety as required by the Eurocode.

III

Results

13

Discussion

As a research often contains methods or assumptions which might influence the results, it is useful to discuss these factors and their influence. This chapter will focus on the remarks which should be made regarding this research in order for the results and conclusions to be properly interpreted.

The discussion is split into two parts: the first part focusses on the assumptions which were made in order to limit the scope of the research. The second part discusses the applied methodology and the limitations which this imposed.

13.1. Assumptions which influence the outcome

During the research many assumption were made. Some in order to limit the research scope, others as they are the widely accepted as valid. This section discusses the most influential assumptions and their possible impact on the results.

Mechanical model

The mechanical model which was used to analyse the structural response was based on the approach PBT used to design the original elements: a simply supported 1D beam. As the actual element is known to be subjected to 3D influences, including torsion, this resulted in a simplification. Even as this is regular practise, impact of the simplification should not be overlooked. Some FE models were used to determine the influence of this assumption, but it was later shown that the models can not be used to precisely predict the structural response with respect to shear.

The mechanical model used for the basic FE models and the experiment also translates a distributed load into a point load. This was done in such a way that the shear forces and the bending moment in the centre support were unaltered, but the influence on the landing platform was neglected. These simplifications were required in order to be able to model the application, but were not backward validated.

Bernoulli beam

Many of the calculations and checks performed in this thesis are based on the assumptions of a Bernoulli beam: planes remain straight and perpendicular to the neutral axis. This is a widely accepted assumption when shear deformation is neglected, which allows the modelling of beams in a comprehensive way. The assumption that planes remain straight is known to be false, but a lack of applicable alternatives results in this being the best approach. The actual deformation of planes results in a change in bending moment capacity and therefore the outcome of most of the made calculations.

Finite Element Method

The application of FE should always be considered critically. The computer allows us to make calculations which we could not perform ourselves, but the output is only as good as the input. A mistake in the input might be hard to spot. This was one of the reasons for FE models used in this research

to be build via Python, which resulted in an increased verifiability of the used input. But even with this increased verifiability, the models' output should be verified where possible. Efforts were made to check the correctness of the output, but it still might contain errors.

Another aspect which should be kept in mind is the application of material properties, which also largely affect the output. As shown with the multiple tensile models used for this research it is difficult to properly predict the structural response when complex materials are used.

13.2. Methodological approach

This section will discuss the aspects of the methodological approach which could be altered in order to improve the value of this thesis.

Applied codes

Multiple codes were considered during the *Validation by Codes* section, but a selection had to be made. This selection was not fully based on the models underlying the codes, but was mainly made as a result of the availability of the codes. A better selection might have provided more information regarding the applicability of the underlying models to represent an UHPFRC. The used selection is mostly based on the concrete models used by the Eurocode with extensions to incorporate a fibre component, which also limits the applied models.

Sample size

During the lab testing only two samples resulted in an actual capacity, while the two others resulted in an indication regarding the minimal shear capacity. These sample sizes are, as mentioned in the other parts of the report as well, too small to be statistically relevant. They can currently best be interpreted as providing an indication of the capacity, rather than providing an actual value. To obtain a more exact value, more elements should be tested.

Shear capacity

Stirrups are applied for three reasons: crack-width control, ductility and capacity. The first two of those are covered by the CRC as a direct result of the peak tensile resistance occurring post cracking. Therefore the focus of this thesis was mainly on the third requirement for stirrups: creating sufficient shear capacity. With the used methodology it was shown that the shear capacity is higher than the bending moment capacity, but the actual shear capacity is still unknown. The FE models provided an indication in the expected capacity, but were found to result in an underestimation. As the actual capacity is still unknown, it is currently not possible to determine the actual shear capacity. Further modifications might be made to increase the bending moment capacity and enforce failure in shear, but these enhancements do also influence the shear capacity, as shown with FE models.

Another aspect which should be discussed is the scatter in capacities. The range for the scatter in shear is usually significantly larger than the range for bending. Even though the mean shear capacity is higher than the mean bending moment capacity, this can result in the characteristic value for shear being governing for the design. As a result, the lab results might not provide sufficient information to derive a characteristic value. The lab results might indicate failure in bending, while for design and safety purposes another mechanism should be evaluated. This is also shown with the multiple FE models, which showed a small covariance for the bending moment capacity based on the different tensile models. The shear capacity of the model heavily dependent on the tensile model, showing a large covariance.

14

Conclusions

The focus of this chapter is on the answering of the research questions in order to draw conclusions. First the sub-questions will be answered, which should result in an answer to the main research question:

> *Were stirrups required in the console in the design of the Raqtan landing platform in order to obtain a level of safety as required by the Eurocode?*

The sub-questions are answered based on the information which was obtained during the research. These answers are only valid when interpreted in combination with the discussion in the previous chapter. The discussion points out some of the scope limitations and the influence of the assumptions made throughout the research.

14.1. Sub-questions

Is shear failure the governing failure mechanism for the Raqtan landing platforms when no stirrups are applied?

According to the validation by the design codes, shear would be the leading failure mechanism, with or without taking the fibres into account. The French guideline deviated from this result, mainly due to the fact that this code is based on a more complex implementation of the tensile behaviour. The French guideline has the uni-axial tensile behaviour at the base of the computations. The other models which implemented a fibre contribution were based on the flexural tensile behaviour. This flexural behaviour is transformed into a uni-axial tensile behaviour under the assumption of a Bernoulli beam. These assumptions result in rather conservative values, as more accurate values require a better understanding of the actual stress distribution. Due to this conservative translation from flexural to uni-axial tensile behaviour the models underestimate the shear capacity of the element. The direct uni-axial behaviour is closer to the behaviour which occurs under shear.

The FE analyses performed in DIANA, using design values for the material properties, predicted failure in bending for the element without stirrups for all but one of the applied models. The relation between the shear capacity and the bending moment capacity was investigated for all models and resulted in a ratio of shear capacity over bending moment capacity between 1.17 and 1.43. The codes predicted a ratio between 0.39 and 1.32. As expected the FE models can incorporate a more complex structural response, while the codes have to be on designed for the worst case scenarios. As a result the design shear capacity is significantly increased when more complex analyses are performed.

The experiments resulted in a failure in bending for all elements. Even reinforcing the elements to increase the bending moment capacity by 50-100%, did not enforce failure in shear. As a result it can be concluded that the shear capacity is significantly larger than the bending moment capacity, with a ratio of at least 1.56. This means that shear is not the governing failure mechanism for the Raqtan landing platform without stirrups.

What would the actual capacity of the Raqtan landing platform be if the stirrups are excluded from the design?
The two elements which were tested without modifications both failed just before reaching a load of 100kN (96.9 and 99.9kN). One of those elements was reinforced with stirrups, the other was not. As stated in for the previous sub-question, this resulted in bending being the governing failure mechanism and therefore the bending capacity is the overall capacity.

As the bending capacity of the two unmodified elements does not change, both values can be used to derive the actual capacity. This results in an average capacity of 98.4kN with a standard deviation of 2.12kN. A student t-distribution with a one sided 95% interval for a single degree of freedom does result in a characteristic value of 85.0 kN. The design value was determined to be 56.7kN.

When the FE models for design values are compared, they result in a shear capacity in the range of 84.3-128.0 kN and a bending capacity in the range of 65.9-89.6 kN. Based on these models the design capacity of the element is at least 65.9 kN. This indicates failure in bending, which was also the result of the experiments.

What is the actual capacity of the Raqtan landing platform without stirrups in relation to the capacity as predicted by multiple design codes?
The codes predicted capacities in the range of 23.4-79.4 kN at the centre support, while the design load is 52.8kN at this point. A large variance is found as the models on which the applied codes are based differ fundamentally. When only the codes which include a fibre contribution are considered, the range changes to 39.6-79.4 kN. The minimal value does approach the value of the design load, but still only one design guideline, the French, predicts sufficient capacity with respect to shear.

The design capacity found in the experiments is within the range of the codes, as it is 56.7kN. This should be accompanied by the remark that it is based on a small sample size of only two elements, which is too small for the Eurocode to be considered as statistically relevant. More important is the found failure mechanism. As the bending capacity is governing, this can be set as the actual capacity of the element. Without taking the fibres in to account, the Eurocode results in a design capacity of 59.4 kN, while the models including a fibre component result in capacities in the range of 62.2-79.4 kN.

The actual capacity of the Raqtan landing platform is therefore in the same range as the codes predict. This changes when only the shear capacity is considered. The codes predicted a range of 37.1-178.6kN. The values found by the EC are almost a sixth of the value as indicated by the modified elements. As these elements did not fail in shear, they only provide a lower boundary value and the actual difference between the predicted and the actual shear capacity might be even higher. It should also be noted that the models which included a fibre component also underestimated the shear capacity of the element significantly.

All in all it can be concluded that the models do predict the bending moment capacity properly, but a large underestimation is found when the shear capacity is calculated.

14.2. Main research question

The sub-questions can be combined, resulting in an answer to the main research question:

> *Were stirrups required in the console in the design of the Raqtan landing platform in order to obtain a level of safety as required by the Eurocode?*

The first conclusion with regard to the main question is regarding the influence of the stirrups on the element capacity. The FE models and the experiments resulted in the same failure mechanism for both unmodified elements: bending. As the stirrups do not significantly influence the bending capacity, it can be concluded that there is no difference in capacity of the elements.

The governing failure mechanism does provide the level of safety the Eurocode requires as the UC according to the EC for the bending capacity was 0.89. The UC check for shear indicated insufficient capacity, but the experiments showed that the actual shear capacity is significantly larger than the bending capacity, exceeding it by at least 50-100%. Therefore the UC for the actual element can be regarded equal to the UC for bending moment capacity, which is as required.

Taking all the performed research in to consideration, it can be concluded that the application of stirrups does not increase the capacity of the Raqtan landing platform and therefore a design without stirrups provides the same level of safety as the element with stirrups, which meets al requirements set by the Eurocode. Therefore the stirrups were not required in the Raqtan landing platform in order to obtain a level of safety as required by the Eurocode.

15

Recommendations

This research did provide an answer to the research questions, but during the research multiple limitations in scope, possibilities and time put restrictions on the performed work. As a result there are many untouched topics, which could provide useful insights in the structural behaviour of CRC. This chapter provides a summary of the most appealing or interesting further research opportunities, which would add value to the performed study or could build on the performed work.

Research the relation between shear and bending behaviour in the FEM
When the created FE models were compared to the actual structural response as observed in experiments, it was found that the shear capacity was underestimated and the bending capacity was overestimated. Both behaviours are coupled mainly by the implemented tensile curves. Increasing the tensile capacity resulted in an increase of both load bearing capacities and vice versa. As a result it became almost impossible to find a tensile behaviour which satisfied both capacities. This should be investigated further to properly understand, model and predict the actual structural responses and capacities of similar elements.

Investigate the true shear capacity of similar elements
The element did not fail in shear, even with the application of modifications. As a result the actual shear capacity is not found, but a lower bound value is derived. The elements for this research were already cast by the time the expectation was raised that the elements would all fail in bending, which limited the possibilities for enforcing failure in shear. By changing the configuration and dimensions earlier in the process, it might be possible to enforce the desired failure mechanism. This would provide more information regarding the predicted and the actual shear capacity and can also result in an insight in the scatter for this failure mechanism.

Further investigate shear failure in CRC elements
As discussed in chapter 4 regarding shear, a lot of research has been performed over the past decade regarding shear capacity and regarding SFRC, even on the overlapping topics. But the models derived for shear in SFRC do not properly predict the actual behaviour as found in the experiments performed for this research. It is therefore unknown what the influence of changes in dimensions and configurations are exactly. In order to be able to apply the found conclusions in practice, it is required to investigate the influence and derive a proof of concept.

Increase the number of elements tested
For this research only two elements were tested per configuration. As the difference between to similar elements was noted to be significant (20% for the modified elements), it is recommended to increase the sample size. This would result in a better indication of the actual mean values. Another advantage of increasing the number of test samples is that a design value can be statistically determined using the Appendix D of EC0: *Design by testing*.

Epilogue

As the project is finished I would like to add a personal note with regard to some ethical considerations which were made before and during the project. I think it is important for a future engineer to consider the world as something we should handle with care and preserve for future generations.

As the ever increasing amounts of research prove that the environment in which we live is affected by our presence, it is in my opinion obligatory to carefully consider the environmental impact of our actions. Even a thesis research such as this can play an important role, especially as the production chain of concrete, concerning the quantity and the effect, is one of the most polluting processes we have on earth. When handling such a material it is important to understand its influence on the global wellness. Nevertheless I still choose to research concrete as the optimization which can be achieved by better understanding the mechanical behaviour of the concrete, can result in a decrease of a project's concrete demand.

The considered class of concretes, UHPCs, has per volume a higher demand of cement, which is the main cause of the CO_2 emission in the concrete production process. But as a result of its outstanding properties the volume required for a project can be drastically decreased if the design is properly optimised. The choice for UHPC should also be based on the carbon-footprint it creates.

This research itself does not direct result in a decrease of concrete in the design of projects similar to the Raqtan project, but I hope its subsequent research will result in a better understanding of the structural response in shear zones, which can result in an optimization of the cross-section dimensions and therefore a decrease in concrete volume.

A final note which has to be made is with respect to safety. The purpose of this thesis was to reduce the unnecessary application of stirrups. This does reduce the shear capacity, which increases the probability of failure. Whenever a design is made to be on the edge of innovation, safety should be kept in high regards. The trade off between safety and innovation is a difficult one, as safety is not an absolute value, not black or white, but comes in all sorts of grey-scales. With this said, it was kept in mind during the research that removing the stirrups resulted in the removal of a certain redundancy. The modifications to the element do not result in a reduction of safety, as shear failure is not the governing mechanism.

Bibliography

[1] H. H. Bache. Introduction to compact reinforced concrete. *Nordic Concrete Research*, 6:19–33, 1987.

[2] G. L. Balázs. A historical review of shear. In *Shear and punching shear in RC and FRC elements*, volume 57, pages 1–13, 2010.

[3] B Belletti, C Damoni, Hendriks M.A.N., and A. de Boer. Validation of the Guidelines for Nonlinear Finite Element Analysis of Concrete Structures - Part: Review of results. Technical report, Rijkswaterstaat Ministerie van Infrastructuur en Milieu, 2017.

[4] E.C. Bentz and M.P. Collins. Development of the 2004 canadian strandars association (csa) a23.3 shear provisions for reinforced concrete. *Canadian Journal for Civil Engineering*, 33:521–534, 2006.

[5] M. Bøhnsdalen and J.M. Hisdal. Ultra high performance fibre reinforced concrete (UHPFRC) - state of the art. Technical report, SINTEF Building and Infrastructure, 2012.

[6] M. P. Collins, D Mitchell, P. Adebar, and Vecchio F.J. A general shear design method. *ACI Structural Journal*, 1996.

[7] Groupe de travail BFUP. Bétons fibres á ultra-hautes performances. Documents scientifiques et techniques, Association Française de Génie Civil, 2013.

[8] ECP. Commentary Eurocode 2. Technical report, European Concrete Platform, June 2008.

[9] E. Fehling, K. Bunje, and T. Leutbecher. Design relevant properties of hardened ultra high performance concrete. In *Proceedings of the international symposium on Ultra-High Performance Concrete - Heft 3*, pages 327–338, 2003.

[10] E. Fehling, M. Schmidt, J. Walraven, T. Leutbecher, and S. Fröhlich. *Ultra-High Performance Concrete UHPC: Fundamentals - Design - Examples*. Ernst & Sohn, 2014. ISBN 978-3-433-03087-5.

[11] H. Gulvanessian, J. Calgaro, and M. Holický. *Designers' Guide to Eurocode - Basis of Structural Design EN 1990 (2nd Edition)*. ICE Publishing, 2012. ISBN 978-0-7277-4171-4.

[12] K. Habel, M. Viviani, E Denarié, and E Brühwiler. Development of the mechanical properties of an ultra-high performance fiber reinforced concrete (UHPFRC). *Cement and Concrete Research*, 36, 2006.

[13] A. M. T. Hassan, Jones S. W., and G. H. Mahmud. Experimantal test methods to determine the uniaxial tensile and compressive behaviour of ultra high performance fibre reinforced concrete (UHPFRC). *Construction and Building Materials*, 37:874–882, 2012.

[14] *Ultra High Performance Concrete: Developments and Applications during 25 years*, Sept. 2004. International Symposium on UHPC.

[15] A.M. Ishtewi and E.A. Toubia. Shear capacity of fiber-reinforced concrete. In *Concrete - Innovation and Design, fib symposium*, 2015.

[16] A. Jansson. *Effect of Steel Fibres on Cracking in Reinforced Concrete*. PhD thesis, Chalmers University of Technology, Gothenburg, Sweden, 2011.

[17] D. Johnston. *Proportioning, mixing and placement of fibre-reinforced cements and concretes, Production methods and workability of concrete*. E&FN Spon, 1996.

[18] G. N. J. Kani. The riddle of shear failure and its solution. *ACI Journal*, pages 441–465, April 1964.

[19] Y. Kwak, M.O. Eberhard, W Kim, and J. Kim. Shear strength of steel fiber-reinforced concrete beams without stirrups. *ACI Structural Journal*, pages 530–538, July-August 2002.

[20] MC2010. The fib model code for concret structures 2010. Technical report, International Federation for Concrete, 2010.

[21] A. Meda, F. Minelli, G.A. Plizzari, and P. Riva. Shear behaviour of steel fibre reinforced concrete beams. *Rilem Materials and Structures*, 38:343–351, April 2005.

[22] MINISTRUCT. Final report. Technical report, Aalborg Portland A/S and Bouygues S.A. and Carl Bro Group a|s and CSIC/ICCET, 1993.

[23] MINISTRUCT. Task 5 - structural analysis. Technical report, Aalborg Portland A/S and Bouygues S.A. and Carl Bro Group a|s and CSIC/ICCET, 1996.

[24] Ø.T. Moltubakk. Nonlinear analysis of fibre reinforced concrete beams. Master's thesis, NTNU - Trontheim, Trontheim, Norway, June 2014.

[25] *Concrete Vibration Handbook*. MultiQuip, 2003.

[26] A. E. Naaman. Engineered steel fibers with optimal properties for reinforcement of cement composites. *Journal of Advanced Concrete Technology*, 1:241–252, November 2003.

[27] R. Nalta. R-317-119-W01 Raqtan calc stairs and screens. Technical report, Pieters Bouwtechniek, 2017.

[28] NEN-EN 14651+A1 (NL). Beproevingsmethode voor staalvezelbeton - meten van de buigtreksterkte (propertionaliteitsgrens (lop), reststerkte). European standard, Nederlands Normalisate Instituut, 2007.

[29] NEN-EN 1990+A1+A1/C2:2011 (nl). Eurocode: Grondslagen van het constructief ontwerp. European standard, Nederlands Normalisate Instituut, 2011.

[30] NEN-EN 1992-1-1+C2:2011 (NL). Eurocode 2: Ontwerp en berekening van betonconstructies - deel 1-1: Algemente regels en regels voor gebouwen. European standard, Nederlands Normalisate Instituut, 2011.

[31] NEN-EN 1992-1-1+C2:2011/NB:2016 (NL). Nationale bijlage bij nen-en 1992-1-1+c2 eurocode 2: Ontwerp en berekening van betonconstructies - deel 1-1: Algemente regels en regels voor gebouwen. European standard, Nederlands Normalisate Instituut, 2016.

[32] S. Norskov, R. Størup, and L.G. Hagsten. Investigation of shear design according to fib model code 2010 and underlying theories. In *Concrete - Innovation and Design, fib symposium*, pages 1–17, 2018.

[33] NF P18-710:2016-04. National addition to eurocode 2 - design of concrete structures : Specifique rules for ultra-high performance fibre-reinforced concrete (uhpfrc). European standard, Association Française de Normalisation (AFNOR), 2016.

[34] H. Pinkster. *Woordenboek Latijn/Nederlands*. Amsterdam University Press, 2003. ISBN 90-5356-607-4.

[35] Raju. Review on shear behaviour of reinforced concrete beam without transverse reinforcement. *Int. Journal of Engineering Research and Applications*, 4:116–121, April 2014.

[36] H.W. Reinhardt. *Beton als constructiemateriaal eigenschappen en duurzaamheid*. Delftse Universitaire Pers, 1998. ISBN 90-6275-165-2.

[37] V. Sigrist, E. Bentz, M.F. Ruiz, S. Foster, and A. Muttoni. Background to the fib Model Code 2010 shear provisions - part I: beams and slabs. *Structural Concrete*, pages 195–203, 2013.

[38] Sika. Productinformatieblad sikadur-30. Productinformationsheet, Sika, 2016.

[39] H. Singh. *Steel Fiber Reinforced Concrete*. Springer, 2017. ISBN 978-981-10-2506-8.

[40] E. V. Sørensen and B. Aarup. Mechanical properties of uhpfrc materials for forida wind turbine towers. Technical report, Aalborg University, 2013.

[41] R. W. Steiger. The history of concrete. *The concrete producer*, page #J950644, 1995.

[42] H. Tlemat, K. Pilakoutas, and K. Neocleous. Modelling of SFRC using inverse finite element analysis. *Materials and Structures*, 39:221–233, 2006.

[43] L. K. Turner and F. G. Collins. Carbon dioxide equivalent (CO_2) emissions: A comparison between geopolymer and opc cement concrete. *Construction and Building Materials*, 43:125–130, 2013.

[44] Ergänzungen und Änderungen zu DIN EN 1992-1-1. Deutscher ausschuss für stahlbeton. Dafstb-richtlinie - stahlfaserbeton, Deutscher Ausschuss für Stahlbeton, 2012.

[45] F. J. Vecchio and M. P. Collins. The modified compression-field theory for reinforced concrete elements subjected to shear. *ACI Journal*, pages 219–231, March-April 1986.

[46] J. Walraven. Codes of practice: Burden of inspiration? In *High Tech Concrete: Where Technology and Engineering Meet*, pages xiii–xxiv, 2017.

[47] K. Wille, N. Viet Tue, and G.J. Parra-Montesinos. Fiber distribution and orientation in UHP-FRC beams and their effect on backward analysis. *Materials and Structures*, 47:1825–1838, 2014.

[48] Y YANG. *Shear Behaviour of Reinforced Concrete Members without Shear Reinforcement*. PhD thesis, TU Delft, 2014.

Appendices

A

Design of the test elements

A.1. Original element

This is the element as originally designed.

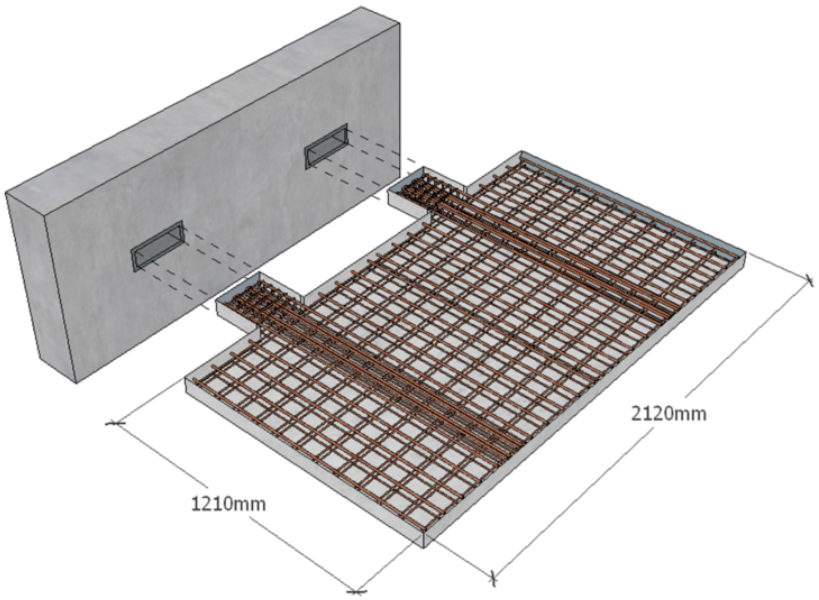

Figure A.1: Overview of the original design. (own source)

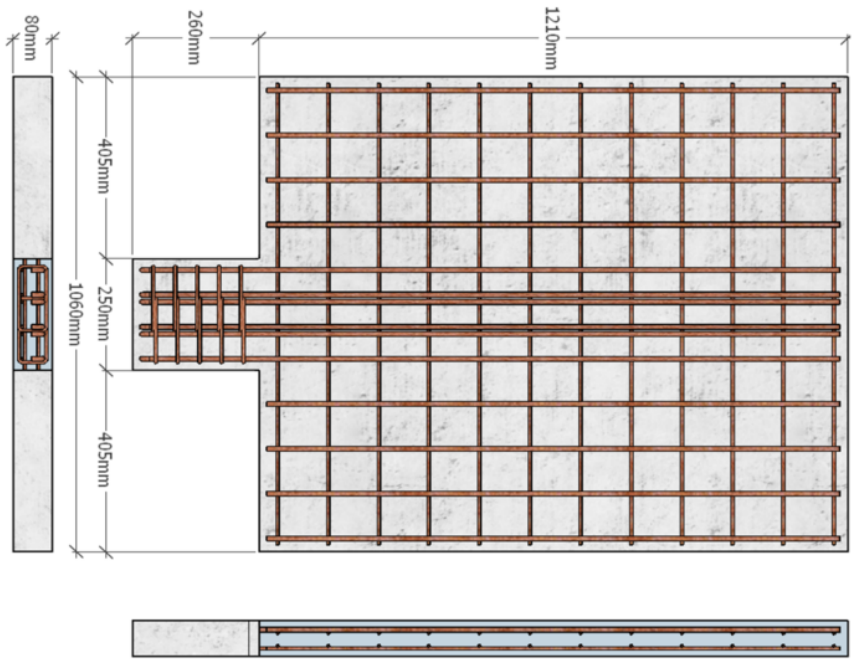

Figure A.2: Overview of the dimensions of the original design. (own source)

A.2. Element A, with stirrups

This is the element as originally designed with a reduced width of the platform. The main properties of the element are shown below.

Table A.1: Datasheet for element A

	Console		**Platform**		**Total**	
Width	250	mm	500	mm	500	mm
Height	80	mm	80	mm	80	mm
Length	260	mm	1210	mm	1470	mm
Volume	0.0052	mm^3	0.0484	mm^3	0.0536	mm^3
Reinforcement	2.3	kg	10.6	kg	12.9	kg

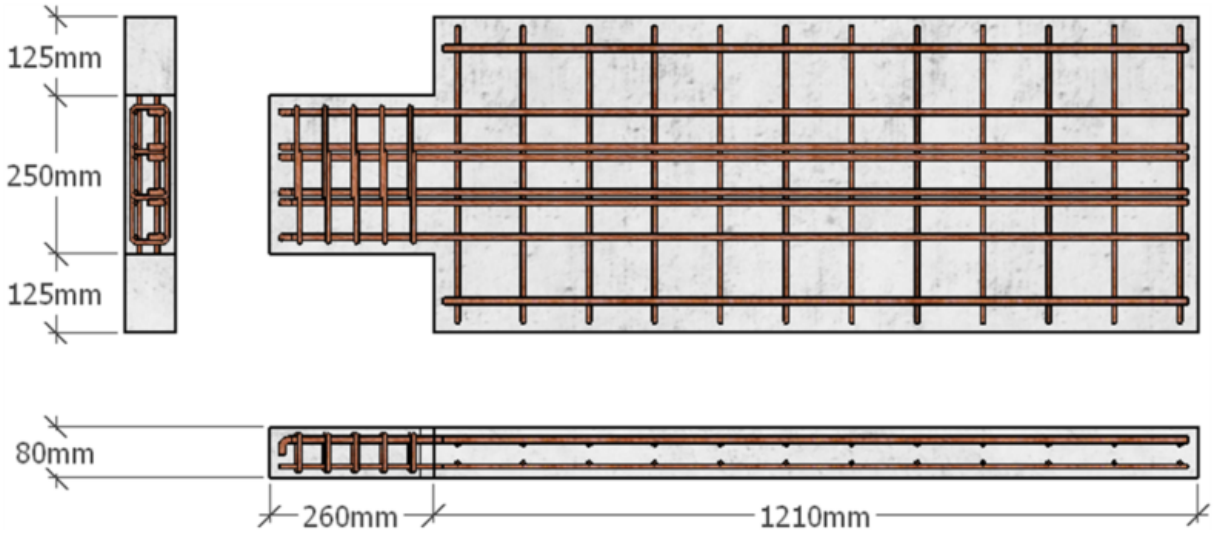

Figure A.3: Overview of the dimensions of Element A. (own source)

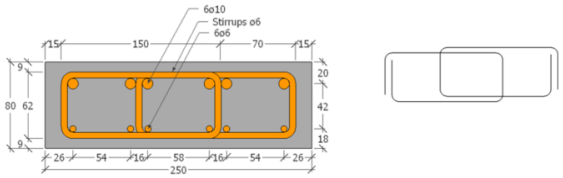

(a) Cross section of the console of Element A with the applied reinforcement.

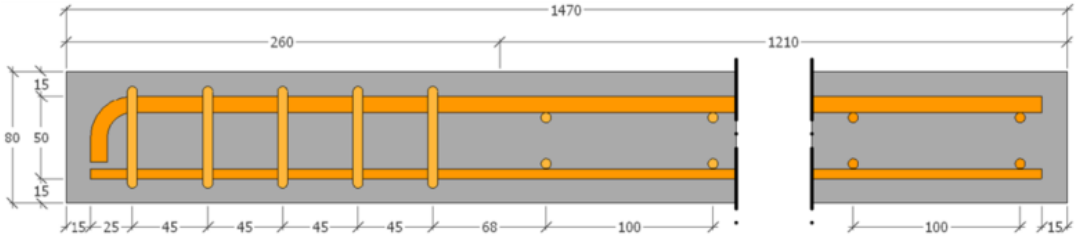

(b) Cross section of the entire platform of Element A with the applied reinforcement.

Figure A.4: Cross sections of Element A with reinforcement. (own source)

A.3. Element B, with stirrups

This is the element without the shear reinforcement with a reduced width of the platform. The main properties of the element are shown below.

Table A.2: Datasheet for element B

	Console		Platform		Total	
Width	250	mm	500	mm	500	mm
Height	80	mm	80	mm	80	mm
Length	260	mm	1210	mm	1470	mm
Volume	0.0052	mm^3	0.0484	mm^3	0.0536	mm^3
Reinforcement	1.6	kg	10.6	kg	12.3	kg

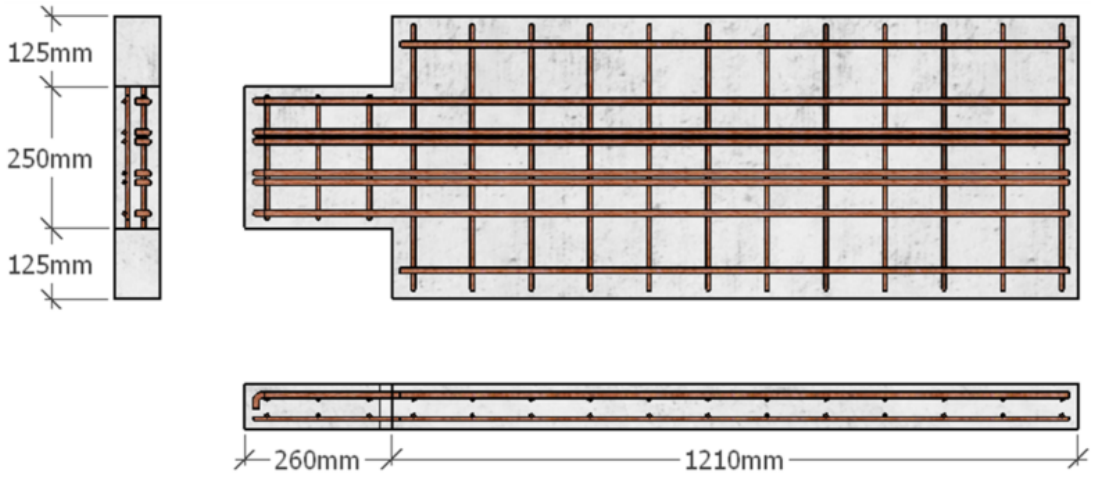

Figure A.5: Overview of the dimensions of Element B. (own source)

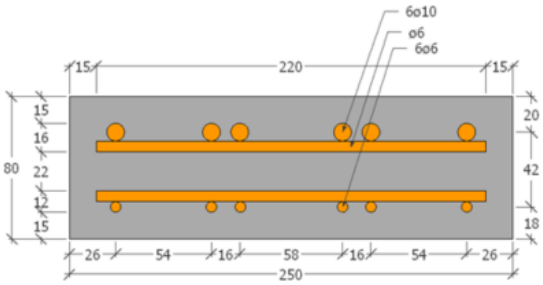

(a) Cross section of the console of Element B with the applied reinforcement.

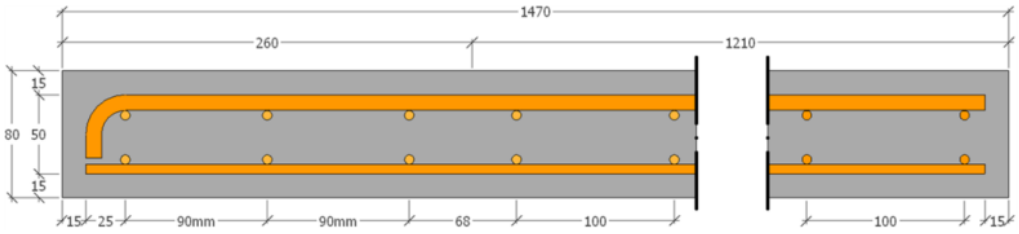

(b) Cross section of the entire platform of Element B with the applied reinforcement.

Figure A.6: Cross sections of Element B with reinforcement. (own source)

B

The design calculations

The parameters as determined in the design:

ϕ	=	10	[mm]	The bar diameter of the main longitudinal.
c	=	15	[mm]	The reinforcement cover.
n	=	6	[-]	The number of lateral bars in the console.
A_{sl}	=	471.24	[mm^2]	The area of the lateral reinforcement
s	=	45	[mm]	The distance between the stirrups
A_{sw}	=	0.00	[mm^2]	The area of the shear reinforcement per stirrup; $4 * \frac{1}{4}\pi 6^2$
d	=	60	[mm]	The active distance; $d = h - c - 0.5\phi$
b_w	=	250	[mm]	The effective width of the console.
h	=	80	[mm]	The height of the console
f_{cm}	=	130	[MPa]	The mean value of concrete compressive strength
f_{ck}	=	110	[MPa]	The characteristic value of concrete compressive strength
f_{ctm}	=	6.3	[MPa]	The mean value of concrete compressive strength
f_{ctk}	=	5.0	[MPa]	The characteristic value of concrete compressive strength
f_{yk}	=	500	[MPa]	The yield strength of the reinforcement steel

B.1. The Eurocode

Formulas in the section will be referred to as EC2F (X), where X denotes the number as found in the codes themselves. The added parameters for the Eurocode:
where:

γ_c	=	1.50	[-]	Material factor for concrete
γ_s	=	1.15	[-]	Material factor for reinforcement steel
f_{cd}	=	73.33	[MPa]	The design compressive strength of ; $\frac{f_{ck}}{\gamma_c}$
f_{yd}	=	435	[MPa]	The design yield strength of the reinforcement steel; $\frac{f_{yk}}{\gamma_s}$

B.1.1. Shear in the Eurocode

The methods to determine the shear capacity, V_{Rd}, according to the Eurocode are given in section 6.2 of Eurocode 1992. The version used for this calculation is *NEN-EN 1992-1-1+C2:2011*. Formulas in the section will be referred to as EC2F (X), where X denotes the number as found in the codes themselves. The general formula is EC2F(6.1):

$$V_{Rd} = V_{Rd,s} + V_{ccd} + V_{td} \tag{B.1}$$

As the element is not tapered, this formula is equal to:

$$V_{Rd} = V_{Rd,s} + V_{Rd,c} \tag{B.2}$$

First the resistance of the concrete is determined, $V_{Rd,c}$. This equation is the is empirically fitted to 176 testresults by König and Fischer (1995), where C_{Rd_c} was determine to have a value of 0.12 in order to have a sufficient coverage (0.0072% probability of a lower value).

$$V_{Rd,c} = \left[C_{Rd,c}k\left(100\rho_l f_{ck}\right)^{1/3} + k_1\sigma_{cp}\right]b_w d = 29.00 \text{ kN} \quad \text{(B.3)}$$

where:

$C_{Rd,c}$	=	0.12	[-]	The fitted value, detemined as $0.18/\gamma_c$
k	=	2.0	[-]	The size factor, $k = 1 + \sqrt{200/d} \leq 2.0$
ρ_l	=	0.02	[-]	The longitudinal reinforcement ratio, $\rho_l = \frac{A_s}{b_w d} \leq 0.02$
σ_{cp}	=	0	[MPa]	The prestressing stress.

This formula contained the most influential parameters, but would result in no capacity when the element contained no longitudinal reinforcement. Therefore a minimal value is introduced as well (EC2(6.2.b)):

$$V_{Rd,c} = (v_{min} + k_1\sigma_{cp})b_w d = 14.28 \text{ kN} \quad \text{(B.4)}$$

where:

v_{min}	=	1.04	[MPa]	The shearforce without longitudinal reinforcement. $v_{min} = 0.035k^{3/2}f_{ck}^{1/2}$ (*EC2F(6.3N)*)

Therefore $V_{Rd,c} = 29.00kN$.The capacity of the platform without stirrups is now determined, as $V_{Rd,s} = 0$ according *EC2F(6.8)*:

$$V_{Rd,s} = \frac{A_{sw}}{s} z f_{ywd} cot(\theta) = 0.00 \text{ kN} \quad \text{(B.5)}$$

where:

z	=	54	[mm]	The internal lever arm; $z = 0.9d$
θ	=	21.9	[°]	The angle between the compression strut and the longitudinal; $cot(\theta) = 2.5$

Resulting in a value for equation B.2 of: $29.00kN$. This value is however limited by *EC2F(6.9)*:

$$V_{Rd,max} = \frac{\alpha_{cw} b_w z v_1 f_{cd}}{cot(\theta) + tan(\theta)} = 154.46kN \quad \text{(B.6)}$$

where:

v_1	=	0.5	[-]	reductie factor voor gescheurd beton; $v_1 = 0.9 - \frac{f_{ck}}{200} \geq 0.5$
α_{cw}	=	1	[-]	A factor to include prestressing; $\alpha_{cw} = 1$ for unprestressed structures

The total shear capacity of the element is the determined to be:

$$V_{Rd} = min(V_{Rd,c} + V_{Rd,s}; V_{Rd,max}) = 29.00kN \quad \text{(B.7)}$$

B.1.2. Bending moment capacity

The model and the assumptions which can be made to determine the bending moment capacity, M_{Rd}, according to the Eurocode are given in section 6.1 of Eurocode 1992 [30].
The first mechanism to use is the yielding of the reinforcement steel. The force required for yielding is equal to:

$$N_{s,yielding} = A_s \cdot f_{yd} = 204.9 \text{ kN} \quad \text{(B.8)}$$

where:

A_s	=	471	[mm^2]	The area of the longitudinal reinforcement

In order to determine the bending moment, the distance between the steel tension force and the centre of the squared concrete compression force has to be determined. This is done by determining the height of the compression zone, x:

$$x_{yielding} = N_{s,yielding}/(b_{eff} \cdot f_c d = 11.18 \text{ mm} \quad \text{(B.9)}$$

The bending moment capacity then becomes:

$$M_{Rd,yielding} = N_{s,yielding} \cdot (h - 0.5 \cdot x_{yielding}) = 10.12 \text{ kNm} \quad \text{(B.10)}$$

The second mechanism to validate is the compression of the concrete. The maximal strain in the compression zone is determined, which results in a compressive force. This force is equal to the force in the reinforcement steel, due to horizontal equilibrium. This results in the steel strain and using a linear strain profile, the height of the compression zone, $x_{crushing}$, can be determined. The two basic equations are based on horizontal force equilibrium (Formula B.11) and geometry (Formula B.12):

$$N_{s,crushing} = F_{c,s,crushing} = \lambda x_{crushing} \eta f_{cd} b_{eff} \tag{B.11}$$

$$x_{crushing} = h \frac{\epsilon_{cu,3}}{\epsilon_s + \epsilon_{cu,3}} = h \frac{\epsilon_{cu,3}}{\frac{N_{s,crushing}}{E_s \cdot A_s} + \epsilon_{cu,3}} \tag{B.12}$$

This results in a quadratic relation of $x_{crushing}$, which yields only one positive solution:

$$x_{crushing} = 23.27 \text{ mm} \tag{B.13}$$

$$N_{s,crushing} = 341 \text{ kN} \tag{B.14}$$

This results in a maximal bending moment:

$$M_{Rd,crushing} = N_{s,crushing} \cdot (h - 0.5 \cdot x_{crushing}) = 15.59 \text{ kNm} \tag{B.15}$$

The maximal capacity then becomes:

$$M_{Rd} = min(M_{Rd,yielding}, M_{Rd,crushing}) = 10.12 \text{ kNm} \tag{B.16}$$

B.2. The Eurocode with Dutch Annex

The added parameters for the Dutch Annex:

γ_c	=	1.50	[-]	Material factor for concrete
γ_s	=	1.15	[-]	Material factor for reinforcement steel
f_{cd}	=	73.33	[MPa]	The design compressive strength of ; $\frac{f_{ck}}{\gamma_c}$
f_{yd}	=	435	[MPa]	The design yield strength of the reinforcement steel; $\frac{f_{yk}}{\gamma_s}$

B.2.1. loads in the Eurocode with Dutch Annex

This section handles the calculation as stated in Eurocode 1990 section 6.4.3.2 for a structure of type B, office space. The actual loads on the element are determined to be (see section 6.2.1): $F_G = 0.810$kN; $F_Q = 1.125$kN; $q_G = 2.290$kN/m; $q_Q = 3.180$kN/m.

$$\sum_{j\geq 1} \gamma_{G,j} G_{k,j} + \gamma_p P + \gamma_{Q,1} \phi_{0,1} Q_{k,1} + \sum_{i>1} \gamma_{Q_i} \phi_{0,i} Q_{k,i} \tag{B.17}$$

$$\sum_{j\geq 1} \xi_j \gamma_{G,j} G_{k,j} + \gamma_p P + \gamma_{Q,1} Q_{k,1} + \sum_{i>1} \gamma_{Q_i} \phi_{0,i} Q_{k,i} \tag{B.18}$$

When these values are substituted in EC0(6.10a) and EC0(6.10b) with the factors as found in the Dutch annex ($\gamma_G = 1.35$; $\gamma_Q = 1.50$; $\phi_0 = 0.50$; $\xi = 0.89$), this results in:

$$F_{6.10a} = \gamma_G F_G + \gamma_Q \phi_0 F_Q = 1.35 \cdot 0.810 + 1.50 \cdot 0.50 \cdot 1.125 = 1.94kN \tag{B.19}$$

$$q_{6.10a} = \gamma_G q_G + \gamma_Q \phi_0 q_Q = 1.35 \cdot 2.290 + 1.50 \cdot 0.50 \cdot 3.180 = 5.48kN/m \tag{B.20}$$

$$F_{6.10b} = \xi \gamma_G F_G + \gamma_Q F_Q = 0.89 \cdot 1.35 \cdot 0.810 + 1.50 \cdot 1.125 = 2.66kN \tag{B.21}$$

$$q_{6.10b} = \xi \gamma_G q_G + \gamma_Q q_Q = 0.89 \cdot 1.35 \cdot 2.290 + 1.50 \cdot 3.180 = 7.52kN/m \tag{B.22}$$

The maximal value of these is governing:

$$F_{6.10} = max(F_{6.10a}, F_{6.10b}) = max(1.94, 2.66) = 2.66kN \tag{B.23}$$

$$q_{6.10} = max(q_{6.10a}, q_{6.10b}) = max(5.48, 7.52) = 7.52kN \tag{B.24}$$

The resulting maximal bending moment, M_{Ed}, then can be determined:

$$M_{Ed,B} = b \cdot F_{6.10} + \frac{2v + l}{2} \cdot M_{6.10} \cdot l = 1.155 \cdot 2.66 + \frac{v \cdot 0 + 1.255}{2} \cdot 7.52 \cdot 1.255 = 9.00kNm \tag{B.25}$$

The reaction forces in the supports then become:

$$V_A = \frac{M_{Ed,A}}{a} = \frac{9.00}{0.2} = 44.98kN \tag{B.26}$$

$$V_B = F_{6.10} + q_{6.10} \cdot l + V_A = 2.66 + 7.52 * 1.255 + 44.98 = 57.08kN \tag{B.27}$$

Which finally results in the design shear load:

$$V_{Ed} = V_A = 44.98kN \tag{B.28}$$

B.2.2. Shear in the Eurocode with Dutch Annex

The methods to determine the shear capacity, V_{Rd}, according to the Dutch annex are equal to the general Eurocode. This combination of *NEN-EN 1992-1-1+C2:2011* and *NEN-EN 1992-1-1+C2/NB:2011* results in the same calculations as made in section B.1.1.

B.2.3. Bending moment capacity in the Eurocode with Dutch Annex

The methods to determine the bending moment capacity, M_{Rd}, according to the Dutch annex are equal to the general Eurocode. This combination of *NEN-EN 1992-1-1+C2:2011* and *NEN-EN 1992-1-1+C2/NB:2011* results in the same calculations as made in section B.1.2.

B.3. The methods used by Pieters Bouwtechniek

The added parameters for this method are:

γ_c	=	1.50	[-]	Material factor for concrete
γ_s	=	1.15	[-]	Material factor for reinforcement steel
f_{cd}	=	73.33	[MPa]	The design compressive strength of ; $\frac{f_{ck}}{\gamma_c}$
f_{ctd}	=	3.33	[MPa]	The design tensile strength: $\frac{f_{ctk}}{\gamma_c}$
f_{yd}	=	435	[MPa]	The design yield strength of the reinforcement steel; $\frac{f_{yk}}{\gamma_s}$

B.3.1. Shear in the Pieters Bouwtechniek Method

The methods to determine the shear capacity, V_{Rd}, according to this method is almost equal to the general Eurocode. Formulas B.1, B.2 and B.3 are not changed, but formula B.4 is updated to comply with the Danish national annex:

$$V_{Rd,c} = (v_{min} + k_1\sigma_{cp})b_w d = 20.63 \text{ kN} \tag{B.29}$$

where:

v_{min} = 1.50 [MPa] $v_{min} = f_c td\left(0.7 - \frac{f_{ck}}{200}\right) \geq 0.45 f_{ctd}$

Therefore $V_{Rd,c} = 29.00kN$.The capacity of the platform without stirrups is now determined (as $V_{Rd,s} = 0$). From here on the method does not deviate from the Eurocode. As the same value is determined, the further results will also be equal to those found in Appendix B.1.1.

B.3.2. Bending moment capacity in the Pieters Bouwtechniek method

The methods to determine the bending moment capacity, M_{Rd}, according to this method are equal to the general Eurocode. This combination of *NEN-EN 1992-1-1+C2:2011* and *NEN-EN 1992-1-1+C2/NB:2011* results in the same calculations as made in section B.1.2.

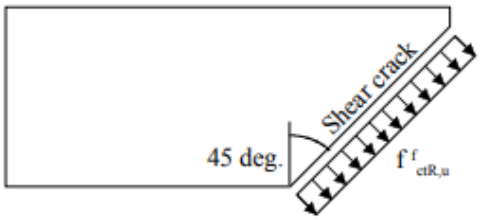

Figure B.1: The model used for the fiber contribution in the German guidelines

B.4. The Eurocode, with Dutch annex and German FRC Gruidelines

The added parameters for this method are:

γ_c	=	1.50	[-]	Material factor for concrete
γ_s	=	1.15	[-]	Material factor for reinforcement steel
f_{cd}	=	73.33	[MPa]	The design compressive strength of ; $\frac{f_{ck}}{\gamma_c}$
f_{ctd}	=	3.33	[MPa]	The design tensile strength: $\frac{f_{ctk}}{\gamma_c}$
f_{yd}	=	435	[MPa]	The design yield strength of the reinforcement steel; $\frac{f_{yk}}{\gamma_s}$

B.4.1. Shear capacity calculations

These guidelines are an extension to the Eurocode and they do include a fiber contribution. This contribution is added to the concrete resistance, $V_{Rd,c}$:

$$V_{Rd,c}^{f} = V_{Rd,c} + V_{Rd,cf} \tag{B.30}$$

The fiber contribution, $V_{Rd,cf}$, is based the ultimate resistance the fibers can offer over a crack with a $45°$ angle in ULS. The model is shown in Figure 8.10. The value for $V_{Rd,cf}$ is determined by multiplying the concrete cross section $(b_w \cdot h)$ with the stress which the fibres can take over this area, $f_{ctR,u}^{f}$. This value for stress in based on measurements of the test as prescribed in EN14651, in this case multiplied with:

$1/\gamma_{ct}^{f} = 0.80$	A material factor for steel fibers.
$\alpha_c^{f} = 0.85$	A factor to take long-term effect of the steel fibers in to account.
$\kappa_F^{f} = 1.06$	A factor to take fiber orientation in to account. This value is element specific: it is determined as $a_0/0.6$, where a_0 is 0.64 for this element, according to RSFB2012 annex L.
$\kappa_G^{f} = 1.45$	A factor to take member size in to account. This value is element specific: it is determined as $1.0 + 0.5 \cdot A_{ct}^{f} \leq 1.70$ with A_{ct}^{f} assumed to be $0.9A_c$

It should be noted that the factors which are larger than 1 result in an increased value. This is a result of the original value being determined in a stage when a reduction factor should be applied. Performing the unity check over the element results in the plot shown in Figure B.2.

B.4.2. Bending moment capacity calculations

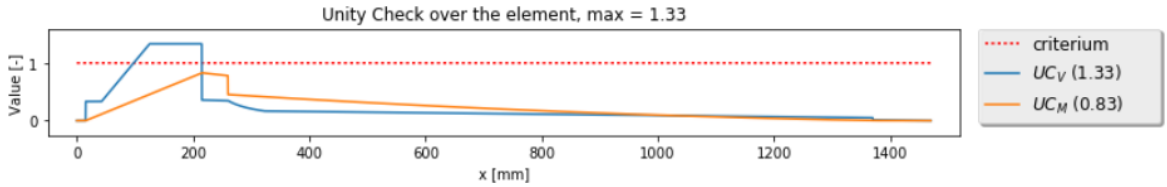

Figure B.2: The unity check performed for the German guidelines

B.5. The Eurocode, with Dutch annex and French FRC Gruidelines

The references in this section are abbreviated. NFA refers to the annex: NF P18-710. As not the entire code was available, it was complemented with the methods and values as provided in the AFGC Recommendations 2013, abbreviated as AFGC.

The added parameters for this method are: where:

γ_c	=	1.50	[-]	Partial safety factor for concrete
γ_{cf}	=	1.5	[-]	Partial safety factor for fibres, found in AFGC§2.1p80
z	=	49.5	[mm]	Leverarm of the effective height, defined as $z = 0.9d$ (ANF§6.2.2(2)).

B.5.1. Shear capacity calculations

The French national annex contains a substitute part for the determination of the shear capacity including fibres. The main formula is expanded with a fibre component NFA§6.2.1.1(2):

$$V_{Rd} = V_{Rd,c} + V_{Rd,s} + V_{Rd,f} \leq V_{Rd,max} \tag{B.31}$$

The concrete component for reinforced UHPFRC is defined as (NFA(6.201)):

$$V_{Rd,c} = \frac{0.21}{\gamma_{cf}\gamma_E} k f_{ck}^{1/2} b_w d = \frac{0.21}{1.5} \cdot 1.0 \cdot 110^{1/2} 250 \cdot 60 = 20.19kN \tag{B.32}$$

where:

k	=	1.0	[-]	A factor to incorporate prestressing: $k = 1 + 3\frac{\sigma_{cp}}{f_{ck}}$ (NFA(6.202))
$\gamma_{cf}\gamma_E$	=	1.5	[-]	This value is provided in NFA§6.2.1.2(1).

The steel component is next defined as(NFA(6.207)):

$$V_{Rd,s} = \frac{A_{sw}}{s} z f_{ywd} cot\theta = 0kN \tag{B.33}$$

The term for the fibre component is defined as (NFA(6.209)):

$$V_{Rd,f} = A_{fv}\sigma_{Rd,f} cot\theta = 12375 \cdot 3.24 \cdot cot(30°) = 69.48kN \tag{B.34}$$

where:

A_{fv}	=	12375	[mm^2]	The projection effective area $A_{vf} = b_w z = 250 \cdot 0.9 \cdot 60$ (NFA(6.212))
$\sigma_{Rd,f}$	=	3.24	[MPa]	The average design tensile stress, defined as $\sigma_{Rd,f} = \frac{1}{K\gamma_{cf}w^*}\int_0^{w^*}\sigma_f(w)dw$ (NFA(6.210)).
K	=	1.25	[-]	Fibre distribution factor, found in AFGC§2.1p80.
w^*	=	1.5	[mm]	the maximal crack width: $w^* = max(w_u; 0.3)$ (ANF(6.211)).
w_u	=	1.5	[mm]	the ultimate allowed crack width
$\int_0^{w^*}\sigma_f(w)dw$	=	9.12	[N/mm]	The area under the stress-crack width curve.
θ	=	30.0	[°]	The crack inclination angle, minimum angle is defined in NFA§6.2.1.3.

The last term to determine is the capacity of the compression struts, which for members without shear reinforcement is determined as (NFA(6.215)):

$$V_{Rd,max} = 2.3\frac{\alpha_{cc}}{\gamma_c} b_w z f_{ck}^{2/3} tan\theta = 2.3\frac{1.0}{1.5} 250 \cdot 49.5 \cdot 110^{2/3} tan(30°) = 251.51kN \tag{B.35}$$

where:

α_{cc}	=	1.00	[-]

These values are substituted in Formula B.31, resulting in:

$$V_{Rd} = 20.19 + 0.00 + 69.48 = 89.67 \leq 251.51kN \tag{B.36}$$

B.6. The ModelCode2010

Formulas in the section will be referred to as MC-F(X), where X denotes the number as found in the codes themselves. The added parameters for the Eurocode:

where:

γ_c	=	1.50	[-]	Material factor for concrete
γ_s	=	1.15	[-]	Material factor for reinforcement steel
f_{cd}	=	73.33	[MPa]	The design compressive strength of ; $\frac{f_{ck}}{\gamma_c}$
f_{yd}	=	435	[MPa]	The design yield strength of the reinforcement steel; $\frac{f_{yk}}{\gamma_s}$

B.6.1. Shearcapacity according to the ModelCode2010 LoAI

The methods to determine the shear capacity, V_{Rd}, according to the ModelCode are given in section 7.7.3 of ModelCode2010. The general formula for an element without shear reinforcement is MC-F(7.7-5):

$$V_{Rd,F} = \left[\frac{0.18}{\gamma_c} \cdot k \cdot \left(100 \cdot \rho_l \cdot \left\{1 + 7.5 \cdot \frac{f_{Ftuk}}{f_{ctk}}\right\} \cdot f_{ck}\right)^{1/3} + k_1\sigma_{cp}\right] \cdot b_w \cdot d \tag{B.37}$$

where:

k	=	2.0	[-]	The size factor, $k = 1 + \sqrt{200/d} \leq 2.0$
ρ_l	=	0.034	[-]	The longitudinal reinforcement ratio, $\rho_l = \frac{A_s}{b_w d}$
f_{Ftuk}	=	0	[MPa]	The characteristic value of the fibre tensile stress in ULS.
σ_{cp}	=	0	[MPa]	The prestressing stress.

The value for f_{Ftuk} has to be determined using an ultimate crack width of $w_u = 1.5$mm and the characteristic results of EN14651 tests in equation MC-F(5.6-6):

$$f_{Ftu} = f_{Fts} - \frac{w_u}{CMOD_3}(f_{Fts} - 0.5f_{R3} + 0.2f_{R1}) \geq 0 = 2.63 \text{ MPa} \tag{B.38}$$

where:

f_{Fts}	=	4.00	[MPa]	tensile capacity of the fibre in SLS, $f_{Fts} = 0.45f_{R1}$
$CMOD_3$	=	2.5	[mm]	The Crack Mouth Opening
f_{R1}	=	–	[MPa]	The stress at CMOD=0.5mm
f_{R3}	=	–	[MPa]	The stress at CMOD=2.5mm

Which results in a shear capacity of $V_{Rd,F} = 40.63$ kN, this value is already higher thant the minimal, as determined in *MC-F(7.7-6)* to be:

$$V_{Rd,Fmin} = (v_{min} + k_1\sigma_{cp})b_w d = 14.28 \text{ kN} \tag{B.39}$$

where:

v_{min}	=	1.04	[MPa]	The shearforce without longitudinal reinforcement. $v_{min} = 0.035k^{3/2}f_{ck}^{1/2}$

B.6.2. Shearcapacity according to the ModelCode2010, alternative

The Model Code does provide an alternative methods, which is less based on empirically fitting and more based on the GSFA as derived by Sigrist. The fibre component in this case is a result of solving a set of equations, depending on the relation between the crack inclination angle, the longitudinal strain and the loads.

The MC provides the following formula for the fibre component (MC(7.7-7)):

$$V_{Rd,F} = \frac{1}{\gamma_f}(k_v\sqrt{f_{ck}} + k_f f_{Ftuk} cot\theta)zb_w \tag{B.40}$$

where:

k_f	=	0.8	[-]	Provided in MC§7.7.3.2.2
k_v	=	–	[-]	Provided as: $k_v = \frac{0.4}{1+1500\epsilon_x}\frac{1300}{1000+k_{dg}z}$ (MC(7.7-8))
k_{dg}	=	1.00	[-]	The aggregate size influence parameter. For a maximum aggregate size of less than 16mm this value is 1.0 (MC§7.7.3.2.2)

There are some restraints on the crack inclination angle as well (MC(7.7-10)):

$$\theta_{min} \leq \theta \leq 45° \tag{B.41}$$

where:

θ_{min} = – [°] The minimum inclination angle, defined as: $29° + 7000\epsilon_x$ (MC(7.7-11))

The relation between the longitudinal strain and the applied loads is defined as (MC(7.3-16)):

$$\epsilon_x = \frac{1}{2E_sA_s}\left(\frac{M_{Ed}}{z} + V_{Ed} + N_{Ed}\left(\frac{1}{2} \mp \frac{\Delta e}{z}\right)\right) \tag{B.42}$$

The relation between the applied load, P_{Ed} and the bending, normal and shear forces for this design are defined as:

$$N_{Ed} = 0 \tag{B.43}$$

$$V_{Ed} = \frac{P_{Ed}b}{a+b} \tag{B.44}$$

$$M_{Ed} = \frac{P_{Ed}ab}{a+b} \tag{B.45}$$

The purpose is to find the maximal capacity, firstly based on the shear capacity. Therefore the equation provided have to be solves for:

$$V_{Ed} = V_{Rd} \tag{B.46}$$

This is most easily solved by implementing all the equations in an Excel sheet and using the *goal-seek method* (*Data>Tools>What-If>Goal Seek*). Resulting in a maximal value for $V_{Rd} = 41.1$ kN.

C

Other calculations

C.1. Determining the maximal shear load

The influence of the connection should not be underestimated as the difference between a clamped of a double-hinged connection is significant. This section will determine the maximal shear force to resist a bending moment M_{Ed} in comparison for the two connection types for the Raqtan landing platform connection.

For the double hinged connection the maximal shear force occurs between the hinges. With a lever arm a, the reaction force in the left support becomes M_{Ed}/a. Determining the maximal shear with a clamped connection is more complicated. Assuming the model as shown in plaatje!!!!, it can be shown by moment equilibrium that:

$$M_{Ed} = \frac{2}{3}a\frac{1}{2}av_a - \frac{1}{3}a\frac{1}{2}av_b = \frac{2}{6}a^2v_a - \frac{1}{6}a^2v_b \tag{C.1}$$

The vertical force equilibrium then enforces:

$$\frac{1}{2}av_b - \frac{1}{2}av_a - V_{Ed} = 0 \tag{C.2}$$

$$v_b = \frac{2}{a}(\frac{1}{2}av_a + V_{Ed}) \tag{C.3}$$

Substitution then results in:

$$M_{Ed} = \frac{2}{6}a^2v_a - \frac{1}{6}a^2(\frac{2}{a}(\frac{1}{2}av_a + V_{Ed})) = \frac{1}{6}a^2v_a - \frac{2}{6}aV_{Ed} \tag{C.4}$$

from this it follows that:

$$v_a = \frac{6}{a^2}(M_{Ed} + \frac{2}{6}aV_{Ed}) = \frac{6}{a^2}M_{Ed} + \frac{2}{a}V_{Ed} \tag{C.5}$$

$$v_b = \frac{6}{a^2}M_{Ed} + \frac{4}{a}V_{Ed} \tag{C.6}$$

determine the shear force over a:

$$V(x) = v_a x - \frac{v_b + v_a}{2a} x^2 \tag{C.7}$$

$$= (\frac{6}{a^2} M_{Ed} + \frac{2}{a} V_{Ed}) x - \frac{\frac{6}{a^2} M_{Ed} + \frac{4}{a} V_{Ed} + \frac{6}{a^2} M_{Ed} + \frac{2}{a} V_{Ed}}{2a} x^2 \tag{C.8}$$

$$= (\frac{6}{a^2} M_{Ed} + \frac{2}{a} V_{Ed}) x - (\frac{6}{a^3} M_{Ed} + \frac{6}{2a^2} V_{Ed}) x^2 \tag{C.9}$$

(C.10)

determine the maximal by determining the peak location:

$$V'(x) = (\frac{6}{a^2} M_{Ed} + \frac{2}{a} V_{Ed}) - 2(\frac{6}{a^3} M_{Ed} + \frac{6}{2a^2} V_{Ed}) x \qquad = 0 \tag{C.11}$$

$$x = \frac{(3aM_{Ed} + a^2 V_{Ed})}{(6M_{Ed} + 3aV_{Ed})} \tag{C.12}$$

With the distance a now being the maximal available 240 mm, and the loads given as $V_{Ed} = 11.91$ kN and $M_{Ed} = 8.69$ kNm, it follows that $x = 114.4$ mm. Substitution of these values in $V(x)$ results in the maximal shear force as $V_{max,clamped} = V(114.4) = 57.5$ kN for the clamped model and $V_{max,hinged} = 43.5$ kN. Applying the clamped connection results in an increase of 32.2% in the shear force.

C.2. Determining the flexural rigidity of the element

This section shows the calculations used to determine the flexural rigidity of the element, EI. As the cross-section of the element differs between the console and the platform this results in two value, respectively EI_1 and EI_2. Their values are determined using the following Python 3.0 code:

```
import numpy as np

E_s,E_c     = 210000,  42000
l1, l2      =    200,   1155
h,  d, b, l =     80,     60,  [250,1060],  l1+l2
phi,n       =     10, [6,14]
for i in [0,1]:
    # determine the neutral axis, part concrete
    I_c = 1/12*b[i]*h**3
    A_c = b[i]*h
    a_c = 1/2*h
    # determine the neutral axis, part steel
    I_s = n[i]*1/64*np.pi*phi**4
    A_s = n[i]*1/4*np.pi*phi**2
    a_s = h-d
    # determine the neutral axis
    a    = (A_s*a_s*E_s+A_c*a_c*E_c)/(A_s*E_s+A_c*E_c)
    # determine the flexural rigidity
    EI   = E_c*I_c+E_c*A_c*(a_c-a)**2+E_s*I_s+E_s*A_s*(a_s-a)**2
    print('The flexural rigidity, EI_%s is : %s Nmm^2' % (i,EI))
```

```
The flexural rigidity, EI_0 is : 484030670555.59753 Nmm^2
The flexural rigidity, EI_1 is : 1987702476081.3062 Nmm^2
```

The result is a flexural rigidity of $EI_1 = 484 \cdot 10^9$ Nmm^2 for the console and $EI_2 = 1987 \cdot 10^9$ Nmm^2 for the platform.

C.3. Initial stiffness FE model

The following code is used to determine the initial stiffness of the model, using *Maple2018*. The input is provided in SI units and their values are based on the provided dimension and the results of the flexural rigidity is as determined in Appendix C.2:

```
restart;

--- The input parameters ----------
P := 13300 : l1 := 200 : l2 := 45 : l3 := 1155 : l := l1 + l2 + l3 : x1 := l1 : x2 := l1 + l2 : x3 := l1 + l2 + l3 :
EI1 := 484030670555 : EI2 := 1987702476081 :

--- Determine the differential equations ----------
DV1 := EI1·diff(w(x), x$4) : DV2 := EI2·diff(w(x), x$4) :
w1 := subs(_C1 = C1, _C2 = C2, _C3 = C3, _C4 = C4, rhs(dsolve(DV1, w(x)))):
w2 := subs(_C1 = C5, _C2 = C6, _C3 = C7, _C4 = C8, rhs(dsolve(DV1, w(x)))):
w3 := subs(_C1 = C9, _C2 = C10, _C3 = C11, _C4 = C12, rhs(dsolve(DV2, w(x)))):
```

$$w_1 := \frac{1}{6} C_1 x^3 + \frac{1}{2} C_2 x^2 + C_3 x + C_4$$

$$w_2 := \frac{1}{6} C_5 x^3 + \frac{1}{2} C_6 x^2 + C_7 x + C_8$$

$$w_3 := \frac{1}{6} C_9 x^3 + \frac{1}{2} C_{10} x^2 + C_{11} x + C_{12} \quad (1)$$

```
Φ1 := -diff(w1, x) : κ1 := diff(Φ1, x) : M1 := EI1·κ1 : V1 := diff(M1, x) :
Φ2 := -diff(w2, x) : κ2 := diff(Φ2, x) : M2 := EI1·κ2 : V2 := diff(M2, x) :
Φ3 := -diff(w3, x) : κ3 := diff(Φ3, x) : M3 := EI2·κ3 : V3 := diff(M3, x) :

--- Apply the boundary conditions ----------
x := 0 : eq1 := w1 = 0 : eq2 := M1 = 0 :
x := x1 : eq3 := w1 = w2 : eq4 := Φ1 = Φ2 : eq5 := M1 = M2 : eq6 := V1 = V2 + P :
x := x2 : eq7 := w2 = w3 : eq8 := Φ2 = Φ3 : eq9 := M2 = M3 : eq10 := V2 = V3 :
x := x3 : eq11 := w3 = 0 : eq12 := M3 = 0 :

--- Solve the system ----------
sol := solve({eq1, eq2, eq3, eq4, eq5, eq6, eq7, eq8, eq9, eq10, eq11, eq12}, {C1, C2, C3, C4, C5, C6, C7, C8, C9, C10, C11, C12}) : assign(sol) :
x := 'x': with(plots) : p1 := plot(-w1, x = 0..x1) : p2 := plot(-w2, x = x1..x2) : p3 := plot(-w3, x = x2..x3) : display(p1, p2, p3);
```

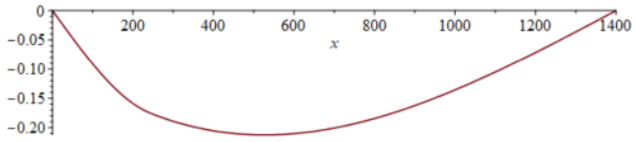


```
--- Determine the displace at the load for the given load P ----------
displacement := subs(x = x1, w1)
```

$$displacement\_at\_P := \frac{1456539453227061765000}{9162942498679240747571} \quad (2)$$

at 5 digits →

$$0.15896 \quad (3)$$

C.4. Upper value

The following Python 3.0 code is used to determine an upper value for the load resistance, based on a linear elastic strain distribution. Using the integrale over the height for the stress, resulting in the load resistance.

```
# IMPORTS ###################################
import numpy as np
import matplotlib.pyplot as plt
import scipy.optimize as opt
```

```
# INPUT #####################################
E_c, E_s = 42000, 210000
l_1, l_2 =   200,   1155
d, h, b  =    60,     80, 250
phi, n   =    10,      6
A_s      = n*1/4*np.pi*phi**2
f_y      = 500/1.15
eps_s    = f_y/E_s
```

```
# BASIC METHODS #############################
def interpolate(x1,x2,y1,y2,x): return (x-x1)/(x2-x1)*(y2-y1) + y1
def integral(f,van,tot,n=1000):
    area = 0
    delta = (tot-van)/n
    ips   = np.linspace(van+0.5*delta,tot-0.5*delta,n)
    for ip in ips: area += f(ip)*delta
    return area
```

```
# Devine the Stress-Strain relations #########
def stress_steel(strain):
    stresses = [0, f_y,   f_y]
    strains  = [0, eps_s, 3.0]
    for i in range(len(stresses)-1):
        if strain<strains[i+1]: return interpolate(strains[i],strains[i+1],stresses[i],stresses[i+1],strain)
    return 0
def stress_CRC(strain):
    stresses = [  0, 0, 9.67/1.5,       8.89/1.5, 7/1.5, 0.0]
    strains  = [-10, 0, 9.67/1.5/42000, 0.1,      0.5,   0.8]
    for i in range(len(stresses)-1):
        if strain<strains[i+1]: return interpolate(strains[i],strains[i+1],stresses[i],stresses[i+1],strain)
    return 0
```

```
# Determine the resulting forces #############
def N_cc_(x,eps_c):  return b*1/2*x*eps_c*E_c
def N_st_(x,eps_c):  return A_s*stress_steel(eps_c/x*(d-x))
def N_ct_(x,eps_c):  return b*integral(stress_CRC,0,eps_c/x*(h-x))
```

```
# Determine the horizonal force equilibrium ##
def get_equilibrium(x): return lambda eps: equilibrium(x,eps)
def equilibrium(x,eps): return N_cc_(x,eps) - N_st_(x,eps) - N_ct_(x,eps)
```

```
# Determine the bending moment ###############
def stress_M(x,x1,eps): return x1*stress_CRC(eps/x*x1)
def moment(x,eps_c):
    N_s  = N_st_(x,eps_c)
    a_s  = d-1/3*x
    return N_s*a_s + b*integral(lambda x1: stress_M(x,x1,eps_c),0,h-x)
```

```
# Determine the strain-moment relation ######
x                 = np.linspace(h,1,100)
eps_c = np.zeros(len(x))
eps_t = np.zeros(len(x))
M = np.zeros(len(x))
P = np.zeros(len(x))
# , eps_t, M, P = [np.zeros(len(x))]*4

for i in range(len(x)):
    eps_c[i] = opt.root(get_equilibrium(x[i]),0.002).x[0]     # the strain in compression at x=x[i]
    M[i]     = moment(x[i],eps_c[i])                          # the bending moment at x=x[i]
    P[i]     = M[i]/l_1*(l_1+l_2)/l_2                         # the load at x=x[i]
    eps_t[i] = eps_c[i]/x[i]*(h-x[i])                         # the strain in tension at x=x[i]

print('max P:%s kN'  % round(max(P/1000),2))
```

```
max P:95.34 kN
```

```
plt.figure(figsize=(15,3))
plt.title('strain at bottom fibre - resistance')
plt.xlabel('strain $\epsilon$ [$^0/_{00}$]')
plt.ylabel('load $P$ [kN]')
plt.plot(eps_t,[a/1000 for a in P])
plt.show()
```

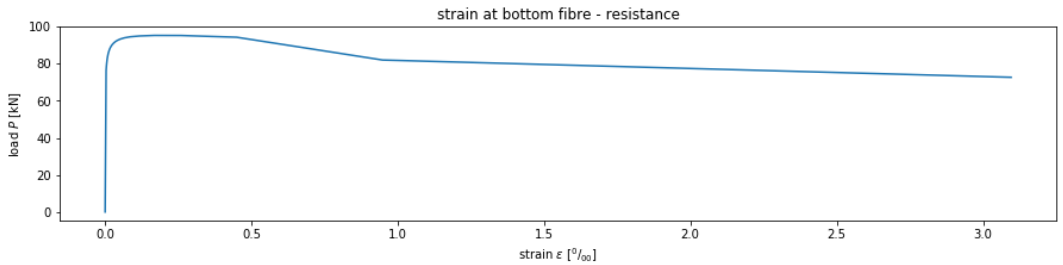

D

Python code

This appendix contains the python code which is used throughout the research. It is developed for Python 3.6.0 and Anaconda 4.3.0 (64-bit). The packages which are used are default packages or can be installed with *pip*. If the package has to be downloaded, the source is provided.

D.1. Code for the 2D models in DIANA

The following code can run by DIANA to create all the predictive 2D models, including those for the modification study. The last blocks can be put after hashes to prevent all the models from being run.

```
def model_setup(config):
    # settings
    config.FEM_name  = '%s_%s' % (config.project,config.FEM)
    config.folder    = '%s - ' % config.FEM_name
    if config.clamped:
        config.folder += "C0" if config.wall_type=='EC'      else ""
        config.folder += "C1" if config.wall_type=='ideal'   else ""
        config.folder += "C2" if config.wall_type=='brittle' else ""
    config.folder += "Y" if config.yielding   else ""
    config.folder += str(config.reinforce).replace(" ","").replace("'","") if config.reinforce  else ""
    config.folder += "M" if config.mean       else ""
    config.folder += "A" if config.con_arclen else ""
    config.folder += "B" if config.stirrups   else ""
    config.folder += "L" if config.con_linese else ""
    config.folder += "I" if config.incr_inte  else ""
    config.folder += "R" if config.rota_crac  else ""
    config.folder += "F" if config.con_force  else ""
    config.folder += "D" if config.con_displ  else ""
    config.folder += "E" if config.con_energ  else ""
    config.folder += "S" if config.small_pla  else ""
    config.folder += '%s - %s-%s-%s' % (config.mesh_size,config.tensi_model,config.compr_model,config.tag)
    # Dimensions: [h,b,l,n]
    config.block_h = 80
    config.block_1 = [ 250, 260,6,'Block_1']
    config.block_2 = [ 500,1210,8,'Block_2'] if config.small_pla else [1060,1210,12,'Block_2']
    # Support plates
    config.sup_l = [15,215,1370]
    if config.FEM == '2D_008': config.sup_l = [65,215,1370]
    config.sup_w = 20
    config.sup_h = 5
    config.wall_h = 500
    # other
    pi       = 3.14159265359
    gamma_cf = 1.5
    config.analyse = "Analysis"
    # material properties
    # FRCCON CMOD model
    f_te = [9.97, 10.19,0.5, 6.45,3.5, 8.69] if config.mean else [9.58/1.5, 8.61/1.5,0.5, 5.32/1.5,3.5, 8.36]
    config.crc_fiber_030 = [f_te[0]*0.30, f_te[1]*0.30,f_te[2], f_te[3]*0.30,f_te[4], 0.001,f_te[5], f_te[5]]
    config.crc_fiber_033 = [f_te[0]*0.33, f_te[1]*0.33,f_te[2], f_te[3]*0.33,f_te[4], 0.001,f_te[5], f_te[5]]
    config.crc_fiber_045 = [f_te[0]*0.45, f_te[1]*0.45,f_te[2], f_te[3]*0.45,f_te[4], 0.001,f_te[5], f_te[5]]
    # FRCCON strain model
    f_te = [ 9.97, 10.27,0.1, 8.08, 0.5, 0.01,1.5, 5.0 ] if config.mean else [ 6.52, 6.07,0.1, 4.82, 0.5, 0.01,1.5, 5.0 ]
    config.crc_fiber_130 = [f_te[0]*0.30, f_te[1]*0.30,f_te[2], f_te[3]*0.30,f_te[4], f_te[5]*0.30,f_te[6], f_te[7]]
    config.crc_fiber_133 = [f_te[0]*0.33, f_te[1]*0.33,f_te[2], f_te[3]*0.33,f_te[4], f_te[5]*0.33,f_te[6], f_te[7]]
    config.crc_fiber_145 = [f_te[0]*0.45, f_te[1]*0.45,f_te[2], f_te[3]*0.45,f_te[4], f_te[5]*0.45,f_te[6], f_te[7]]
    # MC2010 linear model
    config.crc_model_lin = [0.0,0.0,  0.0001,4.58,  0.9,0.04,  0.95,0.01,  1.0,0.0]
    if not config.mean: config.crc_model_lin = [0.0,0.0,  0.0001,2.58,  0.3,1.77,  0.3,0.0,  1.0,0.0]
    # MC2010 rigid model
    config.crc_model_rig = [0.0,0.0,  0.0001,2.69,  0.9,2.68,  0.91,0.0,  1.0,0.0]
    if not config.mean: config.crc_model_rig = [0.0,0.0,  0.0001,1.58,  0.3,1.58,  0.3,0.0,  1.0,0.0]
    # based on the tensile model
    if config.tensi_model == 'multi_ten': config.crc_multi = [0.0,0.0, 0.00014,23.33, 0.040237, 39.433, 0.100138, 39.433,
      0.200084, 14.0, 0.300056, 9.333, 0.800000, 0.0]
```

```
    # curves fitted to CMOD-P curve
    if config.tensi_model == 'multi_001': config.crc_multi = [0.0,0.0, 0.0001,4.00,  1.8,0.02,  1.9,0.01,  10.0,0.001]    #
     expands the ultimate strain
    if config.tensi_model == 'multi_002': config.crc_multi = [0.0,0.0, 0.0001,3.50,  2.8,0.02,  5.9,0.01,  10.0,0.001]    #
     expands the ultimate strain
    if config.tensi_model == 'multi_003': config.crc_multi = [0.0,0.0, 0.0001,3.80,  2.8,0.02,  5.9,0.01,  10.0,0.001]    #
     expands the ultimate strain
    if config.tensi_model == 'multi_004': config.crc_multi = [0.0,0.0, 0.0001,3.20,  2.8,0.02,  5.9,0.01,  10.0,0.001]    #
     expands the ultimate strain
    if config.tensi_model == 'multi_005': config.crc_multi = [0.0,0.0, 0.0001,3.30,  2.3,0.02,  5.9,0.01,  10.0,0.001]    #
     expands the ultimate strain
    if config.tensi_model == 'multi_006': config.crc_multi = [0.0,0.0, 0.0001,3.30,  2.0,0.02,  5.9,0.01,  10.0,0.001]    #
     expands the ultimate strain
    if config.tensi_model == 'multi_007': config.crc_multi = [0.0,0.0, 0.0001,3.40,  2.0,0.02,  5.9,0.01,  10.0,0.001]    #
     expands the ultimate strain
    if config.tensi_model.startswith('multi'):
        config.tensi_model = 'multi' # runs the multi-linear input
        if not config.mean: config.crc_multi[1::2] = [stress/1.5 for stress in config.crc_multi[1::2]]
    # the inverse analysis curve
    if config.tensi_model == 'fitted_me': config.tensi_model,config.crc_multi = 'multi', [0.0,0.0, 0.0001,3.50,  2.8,0.02,
     5.9,0.01,  10.0,0.001]
    if config.tensi_model == 'fitted_ch': config.tensi_model,config.crc_multi = 'multi', [0.0,0.0, 0.0001,3.40,  2.0,0.02,
     5.9,0.01,  10.0,0.001]
    if config.tensi_model == 'fitted_de': config.tensi_model,config.crc_multi = 'multi', [0.0,0.0, 0.0001,2.27,  2.0,0.02,
     5.9,0.01,  10.0,0.001]
    # other material properties
    config.cover         = 15
    config.crc_E         =  50000.00  if config.mean else  42000
    config.crc_poisson   =      0.20
    config.crc_f_c       =    130.00  if config.mean else (110/1.5)
    config.steel_E       = 210000.00  if config.mean else 200000
    config.steel_poisson =      0.25
    config.steel_f_y     =    550.00  if config.mean else    435
    config.rebar_E       = 210000.00  if config.mean else 200000
    config.rebar_d       =     10.00
    config.rebar_A       = 1/4.0*pi*config.rebar_d**2
    if config.reinforce: config.plate_h,config.plate_t,config.plate_f_y,config.plate_type     = config.reinforce

    return config

def model_load(config):
    openProject("%s%s/%s/Project.dpf" % (config.home,config.path,config.folder))

def model_generate(config):
    print('generate project')
    newProject( "../%s/%s/%s" % (config.path,config.folder,config.FEM_name), 10 )
    saveProjectAs( "%s%s/%s/Project.dpf" % (config.home,config.path,config.folder))
    print('RUNNING:%s'%config.tensi_model)
    print('FOLDER:%s'%print(config.folder))
    setModelAnalysisAspects( [ "STRUCT" ] )
    setModelDimension( "2D" )
    setDefaultMeshOrder( "QUADRATIC" )
    setDefaultMesherType( "HEXQUAD" )
    setUnit( "LENGTH", "MM" )
    setUnit( "FORCE", "N" )

def model_build(config):
    model_generate(config)
    model_build_objects(config)
    model_build_materials(config)
    model_build_datasets(config)
    model_build_geometries(config)
    model_build_loads(config)
    model_build_BC(config)
    model_build_mesh(config)

def model_build_objects(config):
    print("CREATING OBJECTS")
    l = 1335-50*2 # 400<l<1335
    x = 25
    if config.reinforce:
        if config.plate_type == 'S': x = 30
        if config.plate_type == 'C': x = -45
    createSheet( config.block_1[3],  [[0,0,0],[x+50,0,0],
                                      [config.block_1[1],0,0],
                                      [config.block_1[1],config.block_h,0],
                                      [0,config.block_h,0]])
    createSheet( config.block_2[3],  [[config.block_1[1],0,0],[x+50+l,0,0],
                                      [config.block_1[1]+config.block_2[1],0,0],
                                      [config.block_1[1]+config.block_2[1],config.block_h,0],
                                      [config.block_1[1],config.block_h,0]])
    createSheet( "Support R", [[config.sup_l[2]-0.5*config.sup_w,0,0],
                               [config.sup_l[2]+0.5*config.sup_w,0,0],
                               [config.sup_l[2]+0.5*config.sup_w,-config.sup_h,0],
                               [config.sup_l[2],-config.sup_h,0],
                               [config.sup_l[2]-0.5*config.sup_w,-config.sup_h,0]] )
    createLine( "Rebar_1",     [config.cover,config.cover+0.5*config.rebar_d,0],
                               [config.block_1[1]+config.block_2[1]-config.cover,config.cover+0.5*config.rebar_d,0])
    createLine( "Rebar_2",     [config.cover+config.block_1[1],           config.cover+0.5*config.rebar_d,0],
                               [config.block_1[1]+config.block_2[1]-config.cover,config.cover+0.5*config.rebar_d,0])

    if config.stirrups:
        locs = [15,40,85,130,175,220]
        for i in range(len(locs)): createLine( "Stirrup_%s"%(i+1), [locs[i],config.cover-0.5*6,0],[locs[i], config.block_h-
     config.cover+0.5*6,0])
```

```
    if config.clamped:
        createSheet( "Wall_1"  , [[-10,0,0],[240,0,0],[240,    -config.wall_h,0],[-10,    -config.wall_h,0]])
        createSheet( "Wall_2"  , [[-10,0,0],[  0,0,0],[  0,config.block_h,0],[-10,config.block_h,0]])
        createSheet( "Wall_3"  , [[-10,config.block_h,0],
                                  [-10,config.block_h+config.wall_h,0],
                                  [240,config.block_h+config.wall_h,0],
                                  [240,config.block_h,0]])
    else:
        x = -10 if config.reinforce and (config.plate_type == 'C') else 0
        createSheet( "Support L", [[config.sup_l[0]-0.5*config.sup_w,x,0],
                                   [config.sup_l[0]+0.5*config.sup_w,x,0],
                                   [config.sup_l[0]+0.5*config.sup_w,-config.sup_h+x,0],
                                   [config.sup_l[0],-config.sup_h+x,0],
                                   [config.sup_l[0]-0.5*config.sup_w,-config.sup_h+x,0]] )
        createSheet( "Loadplate", [[config.sup_l[1]-0.5*config.sup_w,config.block_h,0],
                                   [config.sup_l[1]+0.5*config.sup_w,config.block_h,0],
                                   [config.sup_l[1]+0.5*config.sup_w,config.block_h+config.sup_h,0],
                                   [config.sup_l[1],config.block_h+config.sup_h,0],
                                   [config.sup_l[1]-0.5*config.sup_w,config.block_h+config.sup_h,0]] )
    if config.reinforce:
        x = 25
        if config.plate_type == 'S': x = 30
        if config.plate_type == 'C':
            createSheet( 'add1', [[-10,-10,0],[      0,-10,0],[      0, 80,0],[-10, 80,0]])
            createSheet( 'add2', [[  0,  0,0],[25+50+l,  0,0],[25+50+l,-10,0],[  0,-10,0]])
        else:
            createSheet( 'add1', [[x     ,0,0],[x+50     ,0,0],[x+50     ,-config.plate_h,0],[x     ,-config.plate_h,0]])
            createSheet( 'add2', [[x+50  ,0,0],[x+50+l   ,0,0],[x+50+l   ,-config.plate_h,0],[x+50  ,-config.plate_h,0]])
        createSheet( 'add3', [[x+50+l,0,0],[x+50+l+50,0,0],[x+50+l+50,-config.plate_h,0],[x+50+l,-config.plate_h,0]])

    fitAll()

def model_build_materials(config):
    print("CREATING MATERIALS")
    addMaterial( "CRC", "CONCR", "TSCR", [] )
    setParameter( "MATERIAL", "CRC", "LINEAR/ELASTI/YOUNG",  config.crc_E       )
    setParameter( "MATERIAL", "CRC", "LINEAR/ELASTI/POISON", config.crc_poisson )
    # crack model
    if config.rota_crac: setParameter( MATERIAL, "CRC", "MODTYP/TOTCRK", "ROTATE" )
    # tensile model
    if config.tensi_model == 'multi':
        setParameter( MATERIAL, "CRC", "TENSIL/TENCRV", "MULTLN" )
        setParameter( MATERIAL, "CRC", "TENSIL/EPSIGT", config.crc_multi )
    if config.tensi_model == 'model_lin':
        setParameter( MATERIAL, "CRC", "TENSIL/TENCRV", "MULTLN" )
        setParameter( MATERIAL, "CRC", "TENSIL/EPSIGT", config.crc_model_lin )
    if config.tensi_model == 'model_rig':
        setParameter( MATERIAL, "CRC", "TENSIL/TENCRV", "MULTLN" )
        setParameter( MATERIAL, "CRC", "TENSIL/EPSIGT", config.crc_model_rig )
    if config.tensi_model == 'fiber_030':
        setParameter( "MATERIAL", "CRC", "TENSIL/TENCRV", "FRCCON" )
        setParameter( "MATERIAL", "CRC", "TENSIL/FRCCMD", config.crc_fiber_030 )
    if config.tensi_model == 'fiber_033':
        setParameter( "MATERIAL", "CRC", "TENSIL/TENCRV", "FRCCON" )
        setParameter( "MATERIAL", "CRC", "TENSIL/FRCCMD", config.crc_fiber_033 )
    if config.tensi_model == 'fiber_045':
        setParameter( "MATERIAL", "CRC", "TENSIL/TENCRV", "FRCCON" )
        setParameter( "MATERIAL", "CRC", "TENSIL/FRCCMD", config.crc_fiber_045 )
    if config.tensi_model == 'fiber_130':
        setParameter( "MATERIAL", "CRC", "TENSIL/TENCRV", "FRCCON" )
        setParameter( MATERIAL, "CRC", "TENSIL/FRCTYP", "STRAIN" )
        setParameter( MATERIAL, "CRC", "TENSIL/FRCEPS", config.crc_fiber_130 )
    if config.tensi_model == 'fiber_133':
        setParameter( "MATERIAL", "CRC", "TENSIL/TENCRV", "FRCCON" )
        setParameter( MATERIAL, "CRC", "TENSIL/FRCTYP", "STRAIN" )
        setParameter( MATERIAL, "CRC", "TENSIL/FRCEPS", config.crc_fiber_133 )
    if config.tensi_model == 'fiber_145':
        setParameter( "MATERIAL", "CRC", "TENSIL/TENCRV", "FRCCON" )
        setParameter( MATERIAL, "CRC", "TENSIL/FRCTYP", "STRAIN" )
        setParameter( MATERIAL, "CRC", "TENSIL/FRCEPS", config.crc_fiber_145 )
    if config.tensi_model == 'brittle':
        setParameter( "MATERIAL", "CRC", "LINEAR/ELASTI/YOUNG", config.crc_E )
        setParameter( "MATERIAL", "CRC", "LINEAR/ELASTI/POISON", config.crc_poisson )
        setParameter( "MATERIAL", "CRC", "TENSIL/TENCRV", "BRITTL" )
        setParameter( "MATERIAL", "CRC", "TENSIL/TENSTR", 3.33 )
        setParameter( "MATERIAL", "CRC", "TENSIL/RESTST", 0.1 )

    # compression model
    if config.compr_model == 'EC2':
        setParameter( "MATERIAL", "CRC", "COMPRS/COMCRV", "EC2" )
        setParameter( "MATERIAL", "CRC", "COMPRS/COMSTR", config.crc_f_c )
        setParameter( "MATERIAL", "CRC", "COMPRS/EPSC1",  config.crc_f_c/config.crc_E )
        setParameter( "MATERIAL", "CRC", "COMPRS/EPSCU",  config.crc_f_c/config.crc_E )
        setParameter( "MATERIAL", "CRC", "COMPRS/YOUNCM", config.crc_E )
    if config.compr_model == 'MC1990':
        setParameter( MATERIAL, "CRC", "COMPRS/COMCRV", "MC1990" )
        setParameter( MATERIAL, "CRC", "COMPRS/COMSTR", config.crc_f_c )

    if config.clamped:
        walls = ["Wall_1","Wall_2","Wall_3"]
        # addMaterial( "C30/37", "CONCDC", "EN1992", [ "PLASTI", "ELASTI", "CRACKI" ] )
        # setParameter( MATERIAL, "C30/37", "MC90CO/NORMAL/CLASS", "C30/37" )

        if config.wall_type == 'EC1992':
            addMaterial( "C30/37", "CONCDC", "EN1992", [ "TOTCRK" ] )
```

```
            setParameter( "MATERIAL", "C30/37", "EC2CON/NORMAL/FACTOR/SFSTIF", 1 )
            setParameter( "MATERIAL", "C30/37", "EC2CON/NORMAL/FACTOR/SFTENS", 1.5 )
            setParameter( "MATERIAL", "C30/37", "EC2CON/NORMAL/FACTOR/SFCOMP", 1.5 )

        if config.wall_type == 'ideal':
            addMaterial( "C30/37", "CONCR", "TSCR", [] )
            setParameter( "MATERIAL", "C30/37", "LINEAR/ELASTI/YOUNG", 34000 )
            setParameter( "MATERIAL", "C30/37", "LINEAR/ELASTI/POISON", 0.2 )
            setParameter( "MATERIAL", "C30/37", "TENSIL/TENCRV", "CONSTA" )
            setParameter( "MATERIAL", "C30/37", "TENSIL/TENSTR", 20 )

        if config.wall_type == 'brittle':
            addMaterial( "C30/37", "CONCR", "TSCR", [] )
            setParameter( "MATERIAL", "C30/37", "LINEAR/ELASTI/YOUNG", 34000 )
            setParameter( "MATERIAL", "C30/37", "LINEAR/ELASTI/POISON", 0.2 )
            setParameter( "MATERIAL", "C30/37", "TENSIL/TENCRV", "BRITTL" )
            setParameter( "MATERIAL", "C30/37", "TENSIL/TENSTR", 20 )
            setParameter( "MATERIAL", "C30/37", "TENSIL/RESTST", 0.01 )

    if config.reinforce:
        addGeometry( "interface_GEO", "LINE", "STLIIF", [] )
        setParameter( "GEOMET", "interface_GEO", "LIFMEM/THICK", config.plate_t)
        addMaterial( "interface_MAT", "INTERF", "ELASTI", [] )
        setParameter( "MATERIAL", "interface_MAT", "LINEAR/IFTYP", "LIN2D" )
        setParameter( "MATERIAL", "interface_MAT", "LINEAR/ELAS2/DSNY", 1000*config.rebar_E/config.plate_t )
        setParameter( "MATERIAL", "interface_MAT", "LINEAR/ELAS2/DSSX", 1000*config.rebar_E/config.plate_t if config.
      plate_type=='G' else 0)
        createConnection( "INTERFACE", "INTER", "SHAPEEDGE" )
        setParameter( "GEOMETRYCONNECTION", "INTERFACE", "MODE", "AUTO" )
        attachTo( "GEOMETRYCONNECTION", "INTERFACE", "SOURCE", "Block_1", [[ 170, 0, 0 ]] )
        attachTo( "GEOMETRYCONNECTION", "INTERFACE", "SOURCE", "Block_2", [[ 370, 0, 0 ]] )
        attachTo( "GEOMETRYCONNECTION", "INTERFACE", "SOURCE", "add2", [[ 280, 0, 0 ]] )
        setElementClassType( "GEOMETRYCONNECTION", "INTERFACE", "STLIIF" )
        assignMaterial( "interface_MAT", "GEOMETRYCONNECTION", "INTERFACE" )
        assignGeometry( "interface_GEO", "GEOMETRYCONNECTION", "INTERFACE" )
        setParameter( "GEOMETRYCONNECTION", "INTERFACE", "FLIP", False )
        resetElementData( "GEOMETRYCONNECTION", "INTERFACE" )


        addMaterial( "Plate", "STEEDC", "N6720B", [] )
        setParameter( "MATERIAL", "Plate", "N6720B/PLTYPE", "PLASTI" )
        setParameter( "MATERIAL", "Plate", "N6720B/GRADE", "FEB500" )
        setParameter( "MATERIAL", "Plate", "N6720B/PLASTI/FEB500/YLDSTR", config.plate_f_y )
        setParameter( "MATERIAL", "Plate", "N6720B/POISON", 0.3 )

        # addMaterial( "Plate", "STEEDC", "EN1993", [] )
        # setParameter( "MATERIAL", "Plate", "EURO93/EN931/GRADE", "S%s"%config.plate_f_y )
        # setParameter( "MATERIAL", "Plate", "EURO93/EN931/NTHICK", "MAX40" )
        # setParameter( "MATERIAL", "Plate", "EURO93/YOUNG", config.rebar_E )
        # setParameter( "MATERIAL", "Plate", "EURO93/POISON", 0.3 )

    if config.FEM == '2D_009':
        addMaterial( "Stirrups", "REINFO", "LINEAR", [] )
        setParameter( "MATERIAL", "Stirrups", "LINEAR/ELASTI/YOUNG", config.rebar_E )


    addMaterial( "Steel", "MCSTEL", "ISOTRO", [] )
    setParameter( "MATERIAL", "Steel", "LINEAR/ELASTI/YOUNG", config.steel_E )
    setParameter( "MATERIAL", "Steel", "LINEAR/ELASTI/POISON", config.steel_poisson )

    if config.yielding:
        addMaterial( "Rebar", "REINFO", "UNIAXI", [] )
        setParameter( "MATERIAL", "Rebar", "ELASTI/EPSSIG", [ 0, 0, config.steel_f_y/config.rebar_E, config.steel_f_y, 0.1,
      config.steel_f_y ] )
        setParameter( MATERIAL, "Rebar", "ELASTI/ELASTI/YOUNG", config.rebar_E )
    else:
        addMaterial( "Rebar", "REINFO", "LINEAR", [] )
        setParameter( "MATERIAL", "Rebar", "LINEAR/ELASTI/YOUNG", config.rebar_E )

def model_build_datasets(config):
    print("CREATING DATASETS")
    if config.incr_inte:
        addElementData( "dataset" )
        setParameter( DATA, "dataset", "INTEGR", "HIGH" )
        assignElementData( "dataset", SHAPE, [ config.block_1[3],config.block_2[3],"Support R" ] )
        if config.clamped: assignElementData( "dataset", SHAPE, ["Wall_1","Wall_2","Wall_3"] )
        else:              assignElementData( "dataset", SHAPE, [ "Support L", "Loadplate"] )

def model_build_geometries(config):
    print("CREATING GEOMETRIES")
    for block in [config.block_1,config.block_2]:
        addGeometry( block[3], "SHEET", "MEMBRA", [] )
        setParameter( "GEOMET", block[3], "THICK", block[0] )

        clearReinforcementAspects( [ block[3] ] )
        setElementClassType( [ block[3] ], "MEMBRA" )
        assignMaterial( "CRC", "SHAPE", [ block[3] ] )
        assignGeometry( block[3], "SHAPE", [ block[3] ] )
        resetElementData( "SHAPE", [ block[3] ] )

    if config.clamped:
        walls = ["Wall_1","Wall_2","Wall_3"]
        clearReinforcementAspects( walls )
        setElementClassType( walls, "MEMBRA" )
        assignMaterial( "C30/37", SHAPE, walls )
        assignGeometry( "Block_1", SHAPE, walls )
```

```
        resetElementData( SHAPE, walls )

        supports = ["Support R"]
    else:
        supports = [ "Support L", "Loadplate", "Support R" ]

    clearReinforcementAspects( supports )
    setElementClassType( supports, "MEMBRA" )
    assignMaterial( "Steel", "SHAPE", supports )
    assignGeometry( config.block_1[3], "SHAPE", supports )
    resetElementData( "SHAPE", supports )

    if config.reinforce:
        blokken = ['add1','add2','add3']
        clearReinforcementAspects( blokken )
        setElementClassType( blokken, "MEMBRA" )
        assignMaterial( "Plate", "SHAPE", blokken )

        addGeometry( "plate_GEO", "SHEET", "MEMBRA", [] )
        setParameter( "GEOMET", "plate_GEO", "THICK", config.plate_t )
        assignGeometry( "plate_GEO", "SHAPE", blokken )
        resetElementData( "SHAPE", blokken )

    if config.stirrups:
        addGeometry( "Stirrups", "RELINE", "REBAR", [] )
        setParameter( "GEOMET", "Stirrups", "REIEMB/CROSSE", (1/4)*3.14159265359*6**2*4)
        stirrups = ['Stirrup_1','Stirrup_2','Stirrup_3','Stirrup_4','Stirrup_5','Stirrup_6']
        setReinforcementAspects( stirrups )
        if config.FEM == '2D_009':      assignMaterial( "Stirrups", "SHAPE", stirrups )
        else:                           assignMaterial( "Rebar", "SHAPE", stirrups )
        assignGeometry( "Stirrups", "SHAPE", stirrups )
        resetElementData( "SHAPE", stirrups )
        setReinforcementDiscretization( stirrups, "ELEMENT" )

    addGeometry( "Rebar_1", "RELINE", "REBAR", [] )
    setParameter( "GEOMET", "Rebar_1", "REIEMB/CROSSE", config.rebar_A*config.block_1[2])
    setReinforcementAspects( [ "Rebar_1" ] )
    assignMaterial( "Rebar", "SHAPE", [ "Rebar_1" ] )
    assignGeometry( "Rebar_1", "SHAPE", [ "Rebar_1" ] )
    resetElementData( "SHAPE", [ "Rebar_1" ] )
    setReinforcementDiscretization( [ "Rebar_1" ], "ELEMENT" )

    addGeometry( "Rebar_2", "RELINE", "REBAR", [] )
    setParameter( "GEOMET", "Rebar_2", "REIEMB/CROSSE", config.rebar_A*(config.block_2[2]-config.block_1[2]))
    setReinforcementAspects( [ "Rebar_2" ] )
    assignMaterial( "Rebar", "SHAPE", [ "Rebar_2" ] )
    assignGeometry( "Rebar_2", "SHAPE", [ "Rebar_2" ] )
    resetElementData( "SHAPE", [ "Rebar_2" ] )
    setReinforcementDiscretization( [ "Rebar_2" ], "ELEMENT" )

def model_build_loads(config):
    print("ADD LOADS")
    addSet( "GEOMETRYLOADSET", "loadcase_1" )
    createPointLoad( "P", "loadcase_1" )
    setParameter( "GEOMETRYLOAD", "P", "LODTYP", "DEFORM" )
    setParameter( "GEOMETRYLOAD", "P", "DEFORM/TR/VALUE", -1 )
    setParameter( "GEOMETRYLOAD", "P", "DEFORM/TR/DIRECT", 2 )
    if config.clamped:
        setParameter( "GEOMETRYLOAD", "P", "DEFORM/TR/VALUE", 1 )
        attach( "GEOMETRYLOAD", "P", "Support R", [[ config.sup_l[2], -config.sup_h, 0 ]] )
    else:
        setParameter( "GEOMETRYLOAD", "P", "DEFORM/TR/VALUE", -1 )
        attach( "GEOMETRYLOAD", "P", "Loadplate", [[ config.sup_l[1], config.block_h+config.sup_h, 0 ]] )

def model_build_BC(config):
    print("ADD BOUNDARY CONDITIONS")
    addSet( "GEOMETRYSUPPORTSET", "supports_1" )
    createPointSupport( "fix_x", "supports_1" )
    setParameter( "GEOMETRYSUPPORT", "fix_x", "AXES", [ 1, 2 ] )
    setParameter( "GEOMETRYSUPPORT", "fix_x", "TRANSL", [ 1, 0, 0 ] )
    setParameter( "GEOMETRYSUPPORT", "fix_x", "ROTATI", [ 0, 0, 0 ] )
    createPointSupport( "fix_y", "supports_1" )
    setParameter( "GEOMETRYSUPPORT", "fix_y", "AXES", [ 1, 2 ] )
    setParameter( "GEOMETRYSUPPORT", "fix_y", "TRANSL", [ 0, 1, 0 ] )
    setParameter( "GEOMETRYSUPPORT", "fix_y", "ROTATI", [ 0, 0, 0 ] )

    if config.clamped:
        attach( "GEOMETRYSUPPORT", "fix_x", "Wall_1",    [[ -10, -config.wall_h, 0 ]] )
        attach( "GEOMETRYSUPPORT", "fix_x", "Wall_1",    [[ 240, -config.wall_h, 0 ]] )
        attach( "GEOMETRYSUPPORT", "fix_x", "Wall_3",    [[ -10, config.sup_h+config.wall_h, 0 ]] )
        attach( "GEOMETRYSUPPORT", "fix_x", "Wall_3",    [[ 240, config.sup_h+config.wall_h, 0 ]] )
        attach( "GEOMETRYSUPPORT", "fix_y", "Wall_1",    [[ -10, -config.wall_h, 0 ]] )
        attach( "GEOMETRYSUPPORT", "fix_y", "Wall_1",    [[ 240, -config.wall_h, 0 ]] )
        attach( "GEOMETRYSUPPORT", "fix_y", "Wall_3",    [[ -10, config.sup_h+config.wall_h, 0 ]] )
        attach( "GEOMETRYSUPPORT", "fix_y", "Wall_3",    [[ 240, config.sup_h+config.wall_h, 0 ]] )
        attach( "GEOMETRYSUPPORT", "fix_y", "Support R", [[ config.sup_l[2], -config.sup_h, 0 ]] )
    else:
        x = -10 if config.reinforce and (config.plate_type == 'C') else 0
        attach( "GEOMETRYSUPPORT", "fix_x", "Support L", [[ config.sup_l[0], -config.sup_h+x, 0 ]] )
        attach( "GEOMETRYSUPPORT", "fix_y", "Support L", [[ config.sup_l[0], -config.sup_h+x, 0 ]] )
        attach( "GEOMETRYSUPPORT", "fix_y", "Loadplate", [[ config.sup_l[1], config.block_h+config.sup_h, 0 ]] )
        attach( "GEOMETRYSUPPORT", "fix_y", "Support R", [[ config.sup_l[2], -config.sup_h, 0 ]] )

def model_build_mesh(config):
    print("CREATE MESH")
    if config.clamped:
```

```
        elements = [ "Wall_1","Wall_3" ]
        setElementSize(  elements, 100 )
        setMesherType(   elements, "HEXQUAD" )
        elements = [ config.block_1[3],config.block_2[3], "Support R","Wall_2" ]
    else:
        elements = [ config.block_1[3],config.block_2[3], "Loadplate", "Support L", "Support R" ]
    if config.reinforce:
        elements += ['add1','add2','add3']
    setElementSize(  elements, config.mesh_size )
    setMesherType(   elements, "HEXQUAD" )
    generateMesh( [] )

def model_run_create(config):
    print("CREATE ANALYSIS")
    addAnalysis(config.analyse)
    addAnalysisCommand( config.analyse, "NONLIN", "Structural nonlinear" )
    def temp(a,b): setAnalysisCommandDetail( config.analyse, "Structural nonlinear", a,b)
    temp("EXECUT(1)/LOAD/STEPS/EXPLIC/SIZES", config.steps )
    addAnalysisCommandDetail( config.analyse, "Structural nonlinear", "EXECUT(1)/LOAD/STEPS/EXPLIC/ARCLEN" )
    temp("EXECUT(1)/LOAD/STEPS/EXPLIC/ARCLEN", config.con_arclen )
    temp("EXECUT(1)/ITERAT/MAXITE", config.max_iterations )
    temp("EXECUT(1)/ITERAT/CONVER/DISPLA/TOLCON", 0.001 )
    temp("EXECUT(1)/ITERAT/CONVER/DISPLA/TOLCON", 0.04 )
    temp("EXECUT(1)/ITERAT/CONVER/FORCE/TOLCON",  0.04 )
    temp("EXECUT(1)/ITERAT/CONVER/FORCE",  config.con_force )
    temp("EXECUT(1)/ITERAT/CONVER/ENERGY", config.con_energ )
    temp("EXECUT(1)/ITERAT/CONVER/SIMULT", True )
    temp("EXECUT(1)/ITERAT/METHOD/NEWTON/TYPNAM", "MODIFI" )
    renameAnalysisCommandDetail( config.analyse, "Structural nonlinear", "OUTPUT(1)", "Output" )
    temp("OUTPUT(1)/SELTYP", "USER" )
    addAnalysisCommandDetail( config.analyse, "Structural nonlinear", "OUTPUT(1)/USER" )
    temp("EXECUT(1)/ITERAT/CONVER/DISPLA", config.con_displ )
    temp("EXECUT(1)/ITERAT/LINESE", config.incr_inte)

def model_run_output(config):
    def add(output): addAnalysisCommandDetail( config.analyse, "Structural nonlinear", "OUTPUT(1)/USER/%s" % output )
    add("DISPLA(1)/TOTAL/TRANSL/GLOBAL" )
    add("STRESS(1)/TOTAL/CAUCHY/PRINCI" )
    add("STRESS(2)/TOTAL/CAUCHY/LOCAL" )
    add("STRESS(3)/CRACK/CAUCHY/LOCAL" )
    add("STRAIN(1)/TOTAL/GREEN/GLOBAL" )
    add("STRAIN(2)/TOTAL/GREEN/VONMIS" )
    add("STRAIN(4)/TOTAL/TRACTI/GLOBAL" )
    add("STRAIN(5)/TOTAL/TRACTI/LOCAL" )
    add("STRAIN(6)/CRACK/GREEN" )
    add("STRAIN(7)/CRKWDT/GREEN" )
    add("STRAIN(8)/TOTAL/GREEN/PRINCI" )
    add("FORCE(1)/REACTI/TRANSL/GLOBAL" )

def model_run(config):
    model_run_create(config)
    model_run_output(config)
    model_save(config)
    print("RUN THE ANALYSIS")
    runSolver(config.analyse)
    setViewSettingValue( "view setting", "RESULT/DEFORM/MODE", "ABSOLU" )
    setResultPlot( "vectors", "Reaction Forces/node", "FBY" )

def model_save(config):
    print("SAVE THE GENERATED MODEL")
    saveProjectAs( "%s%s/%s/Project.dpf" % (config.home,config.path,config.folder) )
    exportModel("Model.dat", 10 )
    saveAnalysisCommands( config.analyse, "Analyse_commands.dcf")

def model_import(config):
    print('NOT IMPLEMENTED!!')

def model_export(config):
    print('EXPORTING DATA')
    mm = 0.1
    cases = resultCases(config.analyse,'Output')
    nodes = nodesTable(config.analyse)
    if config.clamped: nodes  = findNearestNodes([(config.sup_l[2],-config.sup_h,0)])
    else:              nodes = list(filter(lambda x: abs (x[1] - config.block_l[1]) < mm, nodes))
    table = [ config.analyse, 'Output', 'Cauchy Total Stresses', 'S1']
    exportResultsToCSV( 'sigma_xx.csv', table, cases, [1] )

    if config.clamped:  nodes  = findNearestNodes([(config.sup_l[2],-config.sup_h,0)])
    else:               nodes  = findNearestNodes([(config.sup_l[1],config.block_h+config.sup_h,0)])
    table = [ config.analyse, 'Output', 'Reaction Forces']
    exportResultsToCSV( 'ReactionForces.csv', table, cases, nodes )

    if config.clamped: return

    print('EXPORTING IMAGES')
    vp_angle = 1
    vp_dir = (0.0,1.0,0.0)

    vp_pos = ((config.block_l[1]+config.block_2[1])/2/1000,config.block_h/2/1000,16)
    vp_height = 0.188
    vp_fp  = (vp_pos[0],vp_pos[1],0.0)
    cvp1 = ( vp_pos[0],vp_pos[1],vp_pos[2],vp_dir[0],vp_dir[1],vp_dir[2],vp_fp[0],vp_fp[1],vp_fp[2],vp_angle,vp_height)
    setViewPoint(cvp1)

    vp_pos = ((config.block_l[1])/2/1000,config.block_h/2/1000,16)
    vp_fp  = (vp_pos[0],vp_pos[1],0.0)
```

```
    vp_height = 0.08/75*config.block_h
    cvp2 = ( vp_pos[0],vp_pos[1],vp_pos[2],vp_dir[0],vp_dir[1],vp_dir[2],vp_fp[0],vp_fp[1],vp_fp[2],vp_angle,vp_height)
    setViewPoint(cvp2)

    for i in [-2,-1]:
        setResultCase('%s/Output/%s' % (config.analyse,cases[i]))
        png_W = 4000
        png_H = 1000

        def plot(titel,soort,data,richting):
            setResultPlot(soort,data,richting)
            setViewPoint(cvp1)
            writeToPng( "img_%s_step_%s.png" % (titel,i), png_W, png_H)
            setViewPoint(cvp2)
            writeToPng( "img_%s_step_%s_Detail.png" % (titel,i), png_W, png_H)

        setViewPoint(cvp1)
        writeToPng( "img_mesh.png" , png_W, png_H )
        setViewPoint(cvp2)
        writeToPng( "img_mesh_Detail.png" , png_W, png_H )

        showView( "RESULT" )
        setViewSettingValue( "view setting", "RESULT/TITLE/SHOW", True )
        setViewSettingValue( "view setting", "RESULT/LEGEND/SHOW", True )
        plot('Rein_Strain_EXX','contours','Reinforcement Total Strains/node','EXX')
        plot('Rein_Strain_Sxx','contours','Reinforcement Cauchy Total Stresses/node','Sxx')
        plot('Total_Strain_E1','contours','Total Strains/node','E1')
        plot('Total_Stress_S1','contours','Cauchy Total Stresses/node','S1')
        plot('Total_Stress_Sxx','contours','Cauchy Total Stresses/node','Sxx')
        plot('Total_Stress_Syy','contours','Cauchy Total Stresses/node','Syy')
        plot('Crack_Strain','cracks','Crack Strains/mappedcrack','Eknn')


def analyse_model(config,do_diana):
    config = model_setup(config)
    if do_diana.load:  model_load(config)
    if do_diana.build: model_build(config)
    if do_diana.run:   model_run(config)
    if do_diana.imp:   model_import(config)
    if do_diana.exp:   model_export(config)
    print('Finished')

def analyse_models(config,do_diana):
    for prop in vars(config):
        if isinstance(vars(config)[prop], list):
            for item in vars(config)[prop]:
                b = copier(config)
                b.__dict__[prop] = item
                analyse_models(b,do_diana)
            return
    analyse_model(config,do_diana)

def model_import(config):
    addAnalysis(config.analyse)
    loadResults(config.analyse,'%s.dnb'% config.analyse)

class env():
    def __init__(self): return

def copier(config):
    temp = env()
    for prop in vars(config): temp.__dict__[prop] = vars(config)[prop]
    return temp

config = env()
config.home           = '__PATH_WHERE_TO_STORE_ALL_OUTPUT_FOLDERS/'
config.path           = 'PBT317-119 Raqtan'
config.project        = 'Raqtan 01'
config.FEM            = '2D_007'
config.steps          = '0.05(400)'
config.tag            = 'W'

config.small_pla      = False   # boolean
config.stirrups       = False   # boolean
config.clamped        = False   # False/'EC'/'ideal'/'brittle'
config.reinforce      = False   # False/ [t,f_yk]
config.mean           = False   # boolean
config.yielding       = True    # boolean
config.incr_inte      = True    # boolean
config.con_arclen     = True    # boolean
config.con_linese     = True    # boolean
config.con_force      = True    # boolean
config.con_displ      = True    # boolean
config.con_energ      = False   # boolean
config.rota_crac      = True    # boolean
config.plane_strain   = False   # boolean

config.tensi_model    = 'fitted_de'
config.compr_model    = 'default'
config.mesh_size      = 20
config.max_iterations = 1000

do_diana = env()
t,f = True,False
do_diana.build  = t
do_diana.load   = f
```

```
do_diana.run    = t
do_diana.imp    = f
do_diana.exp    = t

####################################
#### TEST RUN ######################
####################################
analyse_models(config,do_diana)

####################################
#### VARY TENSILE MODEL ############
####################################
temp                = copier(config)
temp.tensi_model    = ['fitted_de','fiber_033','fiber_045','multi_fib','model_lin','model_rig','multi_007','multi_ten','
    fitted_ch']
temp.steps          = '0.01(400)'
temp.max_iterations = 999
temp.tensi_model    = ['brittle']
analyse_models(temp,do_diana)

####################################
#### VARY MESH SIZE ################
####################################
temp                = copier(config)
temp.mesh_size      = [80,40,15,10,8,6]
analyse_models(temp,do_diana)

####################################
#### VARY CLAMPED ################
####################################
temp                = copier(config)
temp.clamped        = True
temp.wall_type      = ['EC','ideal','brittle']
temp.steps          = '0.1(3000)'
temp.tag            = 'F'
analyse_models(temp,do_diana)

####################################
#### VARY YIELDING MODEL ###########
####################################
temp                = copier(config)
temp.steps          = '0.01(1000)'
temp.tensi_model    = ['fiber_033','fiber_045','fiber_133','fiber_145','model_lin','model_rig','multi_ten','fitted_de']
temp.yielding       = False
temp.mesh_size      = 10
analyse_models(temp,do_diana)
temp.tensi_model    = ['fitted_de']
temp.mesh_size      = 6
analyse_models(temp,do_diana)

####################################
#### MEAN EXPERIMENTAL MODEL #######
####################################
temp                = copier(config)
temp.tensi_model    = ['fitted_de','fiber_033','fiber_045','fiber_133','fiber_145','model_lin','model_rig','multi_ten']
temp.mean           = True
temp.small_pla      = True
temp.yielding       = False
analyse_models(temp,do_diana)
temp.yielding       = True
analyse_models(temp,do_diana)

####################################
#### MEAN IMPROVED EXP. MODEL ######
####################################
temp                = copier(config)
temp.mean           = True
temp.small_pla      = True
temp.reinforce      = (10,100,500,'G') # b = bolted, s = separated, g = glued
temp.reinforce      = [(10,100,235,'G'), (10,100,235,'B')] # b = bolted, s = separated, g = glued, L= long glued, l = long
    bolted
temp.tag            = 'A' # using EC model for steel
temp.tag            = 'B' # using plastic model for steel
temp.tensi_model    = ['fitted_me','fiber_033','fiber_045','fiber_133','fiber_145','model_lin','model_rig','multi_ten']
analyse_models(temp,do_diana)

####################################
#### MEAN IMPROVED EXP. MODEL ######
####################################
temp                = copier(config)
temp.mean           = True
temp.small_pla      = True
temp.tag            = 'S'
temp.FEM            = '2D_008'
temp.tensi_model    = ['fitted_de','fiber_033','fiber_045','fiber_133','fiber_145','model_lin','model_rig','multi_007']

analyse_models(temp,do_diana)
temp.yielding       = False
analyse_models(temp,do_diana)
temp.yielding       = True
temp.stirrups       = True   # met beugels
analyse_models(temp,do_diana)

temp.FEM            = '2D_007'
analyse_models(temp,do_diana)
```

```
# met gelijmde plaat V
temp.tensi_model    = ['fiber_033','fiber_045','fiber_133','fiber_145','model_lin','model_rig','multi_007']
temp.tensi_model    = ['fitted_de']
temp.reinforce      = (10,100,500,'G')
temp.yielding       = False
temp.stirrups       = False
temp.FEM            = '2D_009' # beugels vloeien niet
analyse_models(temp,do_diana)
met gelijmde plaat M
temp.yielding       = True
temp.stirrups       = True
analyse_models(temp,do_diana)

# met geboutte plaat V
temp.tensi_model    = ['fitted_de','fiber_033','fiber_045','fiber_133','fiber_145','model_lin','model_rig','multi_007']
temp.reinforce      = (10,100,500,'B')
temp.yielding       = False
temp.stirrups       = False
temp.FEM            = '2D_009' # beugels vloeien niet
analyse_models(temp,do_diana)
met geboutte plaat M
temp.yielding       = True
temp.stirrups       = True
analyse_models(temp,do_diana)

# do all models for the cornerd strengthening
# DETERMINE BASE CASE
temp.tensi_model    = ['fitted_de','fiber_033','fiber_045','fiber_133','fiber_145','model_lin','model_rig','multi_007']
temp.FEM            = '2D_010'
temp.reinforce      = (10,100,500,'C')
analyse_models(temp,do_diana)
# DETERMINE M
temp.yielding       = True
temp.stirrups       = True
analyse_models(temp,do_diana)
# DETERMINE V
temp.FEM            = '2D_009' # beugels vloeien niet
temp.yielding       = False
temp.stirrups       = False
analyse_models(temp,do_diana)
```

D.2. Code for the derivation of the elongation

The following code was developed to trace the elongation measured in the LVDT visible in the reference plane. This LVDT was tracked as is could be used to place the image on the timeline of the LVDT measurements.

```
#######################################################
### IMPORTS ###########################################
#######################################################
import matplotlib.pyplot as plt
import pandas as pd
import cv2
import numpy as np
from scipy.misc import imread
import os
import warnings
%matplotlib inline
warnings.filterwarnings("ignore")

#######################################################
### DEFAULTS ##########################################
#######################################################
class env():
    def __init__(self): return
def get_path(n):      return conv.folder+'DSC_0%s.jpg'%n
def no_ticks():       plt.yticks([]),plt.xticks([])
def plot_line(p1,p2): plt.plot([p1[0],p2[0]],[p1[1],p2[1]],'r-')

#######################################################
### SETTINGS ##########################################
#######################################################
folder = '__PATH_TO_PROJECT_FOLDER__/'
# for run 1
settings_1 = env()
settings_1.label   = 'DIC_0001'
settings_1.folder  = folder + '20181220 Testdag 4 - RAQTAN1/RAQTAN001/Main run/'
settings_1.limx    = [2455,2900]
settings_1.limy    = [1030,1300]
settings_1.filter  = 130
settings_1.example = 475
settings_1.images  = [472,585]
settings_1.scalers = [1947,2316]
settings_1.scale   = 50/(settings_1.scalers[1]-settings_1.scalers[0])
settings_1.h_init  = [60,60]
settings_1.h_exam  = [60,60]
settings_1.margin  = 40
# for run 2
settings_2 = env()
settings_2.label   = 'DIC_0002'
settings_2.folder  = folder + '20181219 Testdag 3 - RAQTAN4-3-2/RAQTAN002 - Default + Strip/Main run/'
settings_2.limx    = [2350,2800]
settings_2.limy    = [1170,1400]
settings_2.filter  = 130
settings_2.example = 377
settings_2.example = 455
settings_2.images  = [377,457]
settings_2.scalers = [1822,2212]
settings_2.scale   = 50/(settings_2.scalers[1]-settings_2.scalers[0])
settings_2.h_init  = [80,80]
settings_2.h_exam  = [80,80]
settings_2.h_exam  = [147.5, 152.0]
settings_2.margin  = 20
# for run 3
settings_3 = env()
settings_3.label   = 'DIC_0003'
settings_3.folder  = folder + '20181219 Testdag 3 - RAQTAN4-3-2/RAQTAN003 - Default + Strip/Main run/'
settings_3.limx    = [2430,2900]
settings_3.limy    = [1170,1400]
settings_3.filter  = 100
settings_3.example = 278
settings_3.images  = [278,376]
settings_3.scalers = [2017,2357]
settings_3.scale   = 50/(settings_3.scalers[1]-settings_3.scalers[0])
settings_3.h_init  = [70,70]
settings_3.h_exam  = [70,70]
settings_3.margin  = 20
# for run 4
settings_4 = env()
settings_4.label   = 'DIC_0004'
settings_4.folder  = folder + '20181219 Testdag 3 - RAQTAN4-3-2/RAQTAN004 - Default/03 Final run/'
settings_4.limx    = [2550,3000]
settings_4.limy    = [1220,1400]
settings_4.filter  = 120
settings_4.example = 206
settings_4.images  = [136,266]
settings_4.scalers = [2140,2491]
settings_4.scale   = 50/(settings_4.scalers[1]-settings_4.scalers[0])
settings_4.h_init  = [20,20]
settings_4.h_exam  = [80,80]
settings_4.margin  = 20

#######################################################
### SELECT WHICH RUN TO DO ############################
#######################################################
```

```
conv = settings_1

#######################################################
### VERIFY THE SELECTION ##############################
#######################################################
img = cv2.imread(get_path(conv.example))

img_0 = [i[conv.limx[0]:conv.limx[1]] for i in img[conv.limy[0]:conv.limy[1]]]
img_1 = [[min(i) for i in row] for row in img_0]
img_2 = [[i>conv.filter  for i in row] for row in img_1]
img_3 = [[1 if i else 0 for i in row] for row in img_2]

plt.figure(figsize=(20,10))
plt.subplot(131),plt.imshow(img_0),no_ticks()
plt.subplot(132),plt.imshow(img_1,cmap='hot',interpolation='nearest'),no_ticks()
plt.subplot(133),plt.imshow(img_2,cmap='hot',interpolation='nearest'),no_ticks()
plt.show()

plt.figure(figsize=(20,10))
plt.subplot(133),plt.imshow(img_2,cmap='hot',interpolation='nearest')
plt.show()

#######################################################
### PREP THE METHODS ##################################
#######################################################
def filter_h(h,ys):
    rs=[]
    for y in ys: rs += [y] if y<h+conv.margin and y>h-conv.margin else []
    return rs

def find_light_in(column,img):
    rows=[]
    for i in range(len(img)): rows += [i] if img[i][column] == 1 else []
    return rows

def line_finder(img,h):
    x1,y1 = 0,find_light_in(0,img)
    y1 = filter_h(h[0],y1)
    y1 = np.mean(y1)
    h[0] = y1

    x2,y2 = 0,find_light_in(0,img)
    y2_   = y2

    h1 = h[0] # houd alles binnen de range
    while len(y2_)>0 and x2+1<len(img):
        y2,x2 = y2_,x2+1
        y2_ = find_light_in(x2+1,img)
        y2_ = filter_h(h1,y2_)
        h1 = np.mean(y2_)
        rows = []
        for y in y2_:
            if y-1 in y2 or y in y2 or y+1 in y2: rows += [y]
        y2_ = rows
    y2 = np.mean(y2)

    x3,y3 = len(img[0])-1,find_light_in(len(img[0])-1,img)
    y3 = filter_h(h[1],y3)
    y3 = np.mean(y3)
    h[1] = y3

    x4,y4 = x3,find_light_in(x3,img)
    y4_   = y4

    h1 = h[1] # houd alles binnen de range
    while len(y4_)>0 and x4>0:
        y4,x4 = y4_,x4-1
        y4_ = find_light_in(x4-1,img)
        y4_ = filter_h(h1,y4_)
        h1 = np.mean(y4_)
        rows = []
        for y in y4_:
            if y-1 in y4 or y in y4 or y+1 in y4: rows += [y]
        y4_ = rows
    y4 = np.mean(y4)

    return [x1,y1],[x2,y2],[x3,y3],[x4,y4],h

p1,p2,p3,p4,h = line_finder(img_3,conv.h_exam)
print(p1,p2,p3,p4,h)

plt.figure(figsize=(20,3))
plt.subplot(121),plt.imshow(img_0),plot_line(p1,p2),plot_line(p3,p4)
plt.fill([0,20,20,0],[h[0]-conv.margin,h[0]-conv.margin,h[0]+conv.margin,h[0]+conv.margin],'lime',alpha=1.0,)
plt.fill([conv.limx[1]-conv.limx[0],conv.limx[1]-conv.limx[0]-20,conv.limx[1]-conv.limx[0]-20,conv.limx[1]-conv.limx[0]],[h
      [0]-conv.margin,h[0]-conv.margin,h[1]+conv.margin,h[1]+conv.margin],'lime',alpha=1.0,)
no_ticks()
plt.subplot(122),plt.imshow(img_2,cmap='hot',interpolation='nearest'),no_ticks()
plt.show()

#######################################################
### VERIFY THE SCALERS ################################
#######################################################
scale,scalers = conv.scale,conv.scalers
van,tot       = int(0.9*scalers[0]),int(1.1*scalers[1])
```

```
img__ = cv2.imread(get_path(conv.example))
img__ = [i[van:tot] for i in img__[int(0.7*len(img__)):]]
img__ = [[min(i) for i in row] for row in img__]

print(scale)

plt.figure(figsize=(20,20))
plt.imshow(img__, cmap='hot', interpolation='nearest')
plt.plot([scalers[0]-van,scalers[0]-van],[0,len(img__)-1],color='lime')
plt.plot([scalers[1]-van,scalers[1]-van],[0,len(img__)-1],color='lime')
plt.show()

#######################################################
### PREP THE ANALYSIS METHODS #########################
#######################################################
def line(p1, p2):
    A = (p1[1] - p2[1])
    B = (p2[0] - p1[0])
    C = (p1[0]*p2[1] - p2[0]*p1[1])
    return A, B, -C

def intersection(L1, L2):
    D  = L1[0] * L2[1] - L1[1] * L2[0]
    Dx = L1[2] * L2[1] - L1[1] * L2[2]
    Dy = L1[0] * L2[2] - L1[2] * L2[0]
    if D != 0:
        x = Dx / D
        y = Dy / D
        return x,y
    else: return False

def determine_length(p1,p2,p3,p4):
    dx = p3[0]-p4[0]
    dy = p3[1]-p4[1]
    p5 = [p4[0]-dy,p4[1]+dx]

    L1 = line(p1, p2)
    L2 = line(p4, p5)

    xr,yr = intersection(L1, L2)
    lx,ly = xr-p2[0],yr-p2[1]
    l = (lx**2+ly**2)**0.5*conv.scale
    return l,[xr,yr]

l,R = determine_length(p1,p2,p3,p4)

plt.figure(figsize=(10,5))
plt.imshow(img_0),plot_line(p1,p2),plot_line(p3,p4)
plt.plot([R[0]],[R[1]],'+',color='lime',ms=10),no_ticks()
plt.show()
print('length is %s mm'%round(l,3))

#######################################################
### RUN THE ANALYSIS ##################################
#######################################################
ls = []
h  = conv.h_init
for step in range(conv.images[0],conv.images[1]):
    # handle the image
    img_0 = cv2.imread(get_path(step))
    img_0 = [i[conv.limx[0]:conv.limx[1]] for i in img_0[conv.limy[0]:conv.limy[1]]]
    img_1 = [[min(i) for i in row] for row in img_0]
    img_2 = [[i>conv.filter for i in row] for row in img_1]
    img_3 = [[1 if i else 0 for i in row] for row in img_2]
    # search the lines
    p1,p2,p3,p4,h = line_finder(img_3,h)
    l,R = determine_length(p1,p2,p3,p4)
    # store the data
    ls += [l]
    # plot the results
    plt.figure(figsize=(20,6))
    plt.subplot(121)
    plt.imshow(img_0)
    plt.plot([p1[0],p2[0]],[p1[1],p2[1]],'r-')
    plt.plot([p3[0],p4[0]],[p3[1],p4[1]],'r-')
    plt.plot([R[0]],[R[1]],'+',color='lime',ms=10)
    plt.fill([0,20,20,0],[h[0]-conv.margin,h[0]-conv.margin,h[0]+conv.margin,h[0]+conv.margin],'lime',alpha=1.0,)
    plt.fill([conv.limx[1]-conv.limx[0],conv.limx[1]-conv.limx[0]-20,conv.limx[1]-conv.limx[0]-20,conv.limx[1]-conv.limx
      [0]],[h[0]-conv.margin,h[0]-conv.margin,h[1]+conv.margin,h[1]+conv.margin],'lime',alpha=1.0,)
    plt.yticks([])
    plt.xticks([])
    plt.subplot(122)
    plt.imshow(img_2, cmap='hot', interpolation='nearest')
    plt.yticks([])
    plt.xticks([])
    plt.show()
    print('length at step %s is %s mm (h=%s)'%(step,round(l,3),h))

#######################################################
### PLOT THE RESULTS ##################################
#######################################################
plt.figure(figsize=(15,5))
plt.plot(ls)
plt.show()
```

D.3. Code for the derivation of the displacement

The following code was developed to trace the loadblock in the DIC images. The displacement can be derived in mm per image.

```
#######################################################
### IMPORTS ###########################################
#######################################################
import matplotlib.pyplot as plt
import pandas as pd
import cv2
import numpy as np
from scipy.misc import imread
import os
import warnings
%matplotlib inline
warnings.filterwarnings("ignore")

#######################################################
### DEFAULTS ##########################################
#######################################################
class env():
    def __init__(self): return
def get_path(n):      return conv.folder+'DSC_0%s.jpg'%n
def no_ticks():       plt.yticks([]),plt.xticks([])
def clean(image):
    for i in range(3): image[i] = image[i]-image[i]%30
    return image
def plotter(n,images,show=True):
    for i in range(len(images)):
        plt.subplot(100+n*10+i+1)
        plt.imshow(images[i])
    if show: plt.show()

#######################################################
### SETTINGS ##########################################
#######################################################
folder = '__PATH_TO_PROJECT_FOLDER__/'
# for run 1
settings_1 = env()
settings_1.label     = 'DIS_0001'
settings_1.folder    = folder + '20181220 Testdag 4 - RAQTAN1/RAQTAN001/Main run/'
settings_1.xlim      = [2500,2800]
settings_1.ylim      = [ 150, 750]
settings_1.example   = 475
settings_1.images    = [472,585]
settings_1.scalers   = [1947,2316]
settings_1.center    = [2700,300]
settings_1.margin    = 20
settings_1.tresshold = 50
# for run 2
settings_2 = env()
settings_2.label     = 'DIS_0002'
settings_2.folder    = folder + '20181219 Testdag 3 - RAQTAN4-3-2/RAQTAN002 - Default + Strip/Main run/'
settings_2.xlim      = [2300,2600]
settings_2.ylim      = [ 275, 800]
settings_2.example   = 377
settings_2.images    = [377,457]
settings_2.scalers   = [1822,2212]
settings_2.center    = [2450,450]
settings_2.margin    = 20
settings_2.tresshold = 50
# for run 3
settings_3 = env()
settings_3.label     = 'DIS_0003'
settings_3.folder    = folder + '20181219 Testdag 3 - RAQTAN4-3-2/RAQTAN003 - Default + Strip/Main run/'
settings_3.xlim      = [2550,2775]
settings_3.ylim      = [ 400, 900]
settings_3.example   = 278
settings_3.images    = [278,376]
settings_3.scalers   = [2017,2357]
settings_3.center    = [2675,500]
settings_3.margin    = 25
settings_3.tresshold = 50
# for run 4
settings_4 = env()
settings_4.label     = 'DIS_0004'
settings_4.folder    = folder + '20181219 Testdag 3 - RAQTAN4-3-2/RAQTAN004 - Default/03 Final run/'
settings_4.xlim      = [2600,2900]
settings_4.ylim      = [ 400, 900]
settings_4.example   = 206
settings_4.images    = [136,266]
settings_4.scalers   = [2140,2491]
settings_4.center    = [2700,575]
settings_4.margin    = 15
settings_4.tresshold = 50

path = folder + '20181219 Testdag 3 - RAQTAN4-3-2/RAQTAN004 - Default/03 Final run/'

#######################################################
### SELECT WHICH RUN TO DO ############################
#######################################################
conv = settings_1
conv.scale = 50/(conv.scalers[1]-conv.scalers[0])
```

```
#######################################################
### PREP THE METHODS ##################################
#######################################################
def create_images(step):
    img_0 = cv2.imread(get_path(step))
    img_1 = [row[conv.xlim[0]:conv.xlim[1]] for row in img_0[conv.ylim[0]:conv.ylim[1]]]
    return img_1

def find_block(img,center,color):
    xmin,xmax,ymin,ymax=center[0],center[0],center[1],center[1]
    while img[center[1]][xmin] == color and xmin>0:             xmin -= 1
    while img[center[1]][xmax] == color and xmax<len(img[0])-1: xmax += 1
    while img[ymin][center[0]] == color and ymin>0:             ymin -= 1
    while img[ymax][center[0]] == color and ymax<len(img)-1:    ymax += 1
    return xmin,xmax,ymin,ymax

def get_average_color(img,xmin,xmax,ymin,ymax):
    block_1 = [ row[xmin:xmax] for row in img[ymin:ymax]]
    R = np.mean([[i[0]   for i in row] for row in block_1])
    G = np.mean([[i[1]   for i in row] for row in block_1])
    B = np.mean([[i[2]   for i in row] for row in block_1])
    return [R,G,B]

def within_margin(mean_color,color):
    A = color[0]>mean_color[0]-conv.margin and color[0]<mean_color[0]+conv.margin
    B = color[1]>mean_color[1]-conv.margin and color[1]<mean_color[1]+conv.margin
    C = color[2]>mean_color[2]-conv.margin and color[2]<mean_color[2]+conv.margin
    return A and B and C

def find_height(step,center,first):
    img_1 = create_images(step)                                     # the local image
    center_0 = [center[0]-conv.xlim[0],center[1]-conv.ylim[0]]       # the local center
    # find the block                                                ########################
    color = img_1[center_0[1]][center_0[0]]                         # the color at the center
    img_2 = [[within_margin(color,i) for i in row] for row in img_1] # local compliance with color
    xmin1,xmax1,ymin1,ymax1 = find_block(img_2,center_0,True)       # the box which complies
    center_1 = [int((xmin1+xmax1)/2),int((ymin1+ymax1)/2)]
    # second round
    mean_color_1 = get_average_color(img_1,xmin1,xmax1,ymin1,ymax1)
    img_3 = [[within_margin(mean_color_1,i) for i in row] for row in img_1]
    xmin2,xmax2,ymin2,ymax2 = find_block(img_3,center_1,True)
    xmin2,xmax2,ymin2,ymax2 = min(xmin1,xmin2),max(xmax1,xmax2),min(ymin1,ymin2),max(ymax1,ymax2)
    center_2 = [int((xmin2+xmax2)/2),int((ymin2+ymax2)/2)]
    # determine the heighest occurance within the limits
    img_4 = img_3.copy()
    first = int(first/conv.scale)
    cutoff = 40
    if first>cutoff: img_4[:first-cutoff] = [[False]*len(img_4[0])]*(first-cutoff)
    first = np.argmax([sum(row)>conv.tresshold for row in img_4])
    # plot it all
    plt.figure(figsize=(15,15))
    plotter(5,[img_1,img_2,img_3,img_4],show=False)
    plt.subplot(151),plt.plot([center_0[0]],[center_0[1]],'r+',ms=20)
    plt.title('Original')
    plt.xticks([])
    plt.plot([0,conv.xlim[1]-conv.xlim[0]-1],[first,first],'r')
    plt.subplot(152),plt.plot([center_1[0]],[center_1[1]],'r+',ms=20)
    plt.title('Contrast 1')
    plt.xticks([]),plt.yticks([0,100,200,300,400,500,600],['','','','','','',''])
    plt.plot([0,conv.xlim[1]-conv.xlim[0]-1],[first,first],'r')
    plt.plot([xmin1,xmax1,xmax1,xmin1,xmin1],[ymin1,ymin1,ymax1,ymax1,ymin1],'lime')
    plt.subplot(153),plt.plot([center_1[0]],[center_2[1]],'r+',ms=20)
    plt.title('Contrast 2')
    plt.xticks([]),plt.yticks([0,100,200,300,400,500,600],['','','','','','',''])
    plt.plot([0,conv.xlim[1]-conv.xlim[0]-1],[first,first],'r')
    plt.plot([xmin2,xmax2,xmax2,xmin2,xmin2],[ymin2,ymin2,ymax2,ymax2,ymin2],'lime')
    plt.subplot(154),plt.plot([center_1[0]],[center_2[1]],'r+',ms=20)
    plt.title('Contrast 3')
    plt.xticks([]),plt.yticks([0,100,200,300,400,500,600],['','','','','','',''])
    plt.plot([0,conv.xlim[1]-conv.xlim[0]-1],[first,first],'r')
    plt.plot([xmin2,xmax2,xmax2,xmin2,xmin2],[ymin2,ymin2,ymax2,ymax2,ymin2],'lime')
    plt.savefig('raqtan_deflector.png', bbox_inches='tight')
    plt.savefig('raqtan_deflector.pdf', bbox_inches='tight')
    plt.show()
    # return the results
    center = [center_2[0]+conv.xlim[0],center_2[1]+conv.ylim[0]]
    first  = round(conv.scale*first,3)
    return first,center

#######################################################
### RUN THE ANALYSIS ##################################
#######################################################
ls = []
center = conv.center
first  = 0
for step in range(conv.images[0],conv.images[1]):
    first,center = find_height(step,center,first)
    ls += [first]
    print('At step %s the first is at %s mm and the center is %s'%(step,first,center))
plt.figure(figsize=(20,5))
plt.plot(ls)
plt.show()
```

D.4. Code for DIC analyses

The following code was used to analyse the digital photos which were taken during the experiments. The code refers to the *pydic* file, which was developed by D. André[1].

```
########################################
### Load all resources #################
########################################
import numpy as np
import os
import cv2
import matplotlib as m
import pandas as pd
from matplotlib import pyplot as plt
from scipy import stats
import imp
########################################
### Define methods #####################
########################################
def find_images(data,init_image,path):
    data = pd.read_csv(data)                                    # load the data
    data.DIS = [float(v) for v in data.DIS.values]              # convert to floats
    u0 = data.DIS.values[[a[-3:]==str(init_image) for a in data.photo.values]][0]
    images = [init_image]                                      # the target photos
    for u in [2.5,5,7.5,10]:
        i = len(data.DIS.values) - sum(data.DIS.values>=u+float(u0))
        images += [int(data.photo[i][-3:])]
        photo = data.photo[i]
    return [path+'/DSC_0%s.jpg'%n for n in images]
def plotter_line(x1,x2,y1,y2,color):       plt.plot([x1,x1,x2,x2,x1],[y1,y2,y2,y1,y1],color)
def plotter_fill(x1,x2,y1,y2,color): plt.fill([x1,x1,x2,x2,x1],[y1,y2,y2,y1,y1],color,alpha=0.1)
def plotter(field,code,number,tag):
    field = [[field[a][b] for a in range(len(field))] for b in range(len(field[0]))]
    vmin,vmax = -0.005714,0.04

    plt.figure(figsize=(15,4))
    plt.xticks([]),plt.yticks([])
    plotter_line(1220,3050, 680,1200,'k')
    plotter_fill(1220,1400, 680,1200,'grey')
    plotter_fill(3020,3050, 680,1200,'grey')
    plotter_fill(1400,3020, 680, 700,'grey')
    plotter_fill(1400,3020,1150,1200,'grey')
    plotter_line(3050,5000, 680,1200,'k')
    plotter_fill(3050,5000, 680,1200,'grey')
    x,y,s = 1350,650,150
    plt.fill([x,x-s/2,x+s/2],[y,y-s,y-s],'lime')
    x,y,w,h = 2650,1200,130,210
    plt.fill([x,x+w,x+w,x],[y,y,y+h,y+h],'lime')

    x1,x2             = 1400,3020
    y1,y2             = 700,1150
    x = list(np.linspace(x1,x2,len(field[0])))
    y = list(np.linspace(y2,y1,len(field)))
    z = [[max(vmin,min(vmax,v)) for v in vs] for vs in field]

    a = plt.contourf(x,y,z,cmap=cmap,vmin=vmin,vmax=vmax)
    plt.title('Strain in image %s'%code)
    plt.axis('scaled')
    plt.xlim(1000,3300)
    plt.savefig('raqtan_FEM_DIC_%s_%s.pdf'%(tag,number), bbox_inches='tight')
    plt.savefig('raqtan_FEM_DIC_%s_%s.png'%(tag,number), bbox_inches='tight')
    plt.show()
def displayer(pydic,images,tag):
    for i in range(len(pydic.grid_list)):
        field  = pydic.grid_list[i].strain_xy
        code   = images[i].split('/')[-1].split('.')[0]
        number = code[5:]
        print(code,number)
        plotter(field,code,number,tag)
########################################
### Defaults ###########################
########################################
fullpath = '__PATH_TO_PYDIC__/pydic-master/'
correl_wind_size = (80,80) # the size in pixel of the correlation windows
correl_grid_size  = (10,10) # the size in pixel of the interval (dx,dy) of the correlation grid
interpolation     = 'raw' #
save_image        = True
scale_disp        = 1
scale_grid        = 1
cmap = m.colors.ListedColormap(['#0000FF', '#0091FF','#00FFDA', '#00FF48', '#48FF00', '#DAFF00', '#FF9100','#FF0000']) #
    matches with DIANA
########################################
### For RAQTAN_004 #####################
########################################
pydic = imp.load_source('pydic', fullpath +'pydic.py')
path = fullpath + 'examples/RAQTAN004'
area_of_intersest = [(1400,700),(3020,1150)]  # (x1,y1),(x2,y2)
images            = find_images('DIS_0004.csv',141,path)
# and read the result file for computing strain and displacement field from the result file
pydic.init(path+'/DSC_0*61.jpg', correl_wind_size, correl_grid_size, path+"/result.dic",img_list=images,area_of_intersest=
    area_of_intersest)
pydic.read_dic_file(path+'/result.dic', interpolation=interpolation, save_image=save_image, scale_disp=scale_disp,
```

[1]Code can be found in https://gitlab.com/damien.andre/pydic, the code was downloaded at 28-12-2018

```
                    scale_grid=scale_grid,meta_info_file=path+'/meta-data.txt')
displayer(pydic,images,'004')
########################################
### For RAQTAN_003 #####################
########################################
pydic = imp.load_source('pydic', fullpath +'pydic.py')
path = fullpath + 'examples/RAQTAN003'
area_of_intersest = [(1300,650),(3000,1140)]  # (x1,y1),(x2,y2)
images            = find_images('DIS_0003.csv',279,path)
# and read the result file for computing strain and displacement field from the result file
pydic.init(path+'/DSC_0*61.jpg', correl_wind_size, correl_grid_size, path+"/result.dic",img_list=images,area_of_intersest=
    area_of_intersest)
pydic.read_dic_file(path+'/result.dic', interpolation=interpolation, save_image=save_image, scale_disp=scale_disp,
                    scale_grid=scale_grid,meta_info_file=path+'/meta-data.txt')
displayer(pydic,images,'003')
########################################
### For RAQTAN_002 #####################
########################################
pydic = imp.load_source('pydic', fullpath +'pydic.py')
path = fullpath + 'examples/RAQTAN002'
area_of_intersest = [(1000,630),(2850,1140)]  # (x1,y1),(x2,y2)
images            = find_images('DIS_0002.csv',378,path)
# and read the result file for computing strain and displacement field from the result file
pydic.init(path+'/DSC_0*61.jpg', correl_wind_size, correl_grid_size, path+"/result.dic",img_list=images,area_of_intersest=
    area_of_intersest)
pydic.read_dic_file(path+'/result.dic', interpolation=interpolation, save_image=save_image, scale_disp=scale_disp,
                    scale_grid=scale_grid,meta_info_file=path+'/meta-data.txt')
displayer(pydic,images,'002')
########################################
### For RAQTAN_001 #####################
########################################
pydic             = imp.load_source('pydic', fullpath +'pydic.py')
path              = fullpath + 'examples/RAQTAN001'
area_of_intersest = [(1200,500),(2950,1000)]  # (x1,y1),(x2,y2)
images            = find_images('DIS_0001.csv',475,path)
# and read the result file for computing strain and displacement field from the result file
pydic.init(path+'/DSC_0*61.jpg', correl_wind_size, correl_grid_size, path+"/result.dic",img_list=images,area_of_intersest=
    area_of_intersest)
pydic.read_dic_file(path+'/result.dic', interpolation=interpolation, save_image=save_image, scale_disp=scale_disp,
                    scale_grid=scale_grid,meta_info_file=path+'/meta-data.txt')
displayer(pydic,images,'001')
```

D.5. Code for the validation models in DIANA

The following code can run by DIANA to create the models for the validation with respect to the experimental results. The last blocks can be put after hashes to prevent all the models from being run.

```
def model_setup(config):
    # settings
    config.FEM_name  = '%s_%s' % (config.project,config.FEM)
    config.folder    = '%s - ' % config.FEM_name
    config.folder += "Y" if config.yielding   else ""
    config.folder += "+" if config.reinforce  else ""
    config.folder += "M" if config.mean       else ""
    config.folder += "A" if config.con_arclen else ""
    config.folder += "B" if config.stirrups   else ""
    config.folder += "L" if config.con_linese else ""
    config.folder += "I" if config.incr_inte  else ""
    config.folder += "R" if config.rota_crac  else ""
    config.folder += "F" if config.con_force  else ""
    config.folder += "D" if config.con_displ  else ""
    config.folder += "E" if config.con_energ  else ""
    config.folder += '%s - %s-%s-%s' % (config.mesh_size,config.tensi_model,config.compr_model,config.tag)
    # Dimensions: [h,b,l,n]
    config.block_h = 80
    config.block_1 = [ 250, 260,6,'Block_1']
    config.block_2 = [ 500,1210,8,'Block_2']
    # Support plates
    config.sup_l = [15,215,1370]
    config.sup_w = 20
    config.sup_h = 5
    config.wall_h = 500
    # other
    pi       = 3.14159265359
    gamma_cf = 1.5
    config.analyse = "Analysis"
    # material properties
    # FRCCON CMOD model
    f_te = [9.97, 10.19,0.5, 6.45,3.5, 8.69] if config.mean else [9.58/1.5, 8.61/1.5,0.5, 5.32/1.5,3.5, 8.36]
    config.crc_fiber_030 = [f_te[0]*0.30, f_te[1]*0.30,f_te[2], f_te[3]*0.30,f_te[4], 0.001,f_te[5], f_te[5]]
    config.crc_fiber_033 = [f_te[0]*0.33, f_te[1]*0.33,f_te[2], f_te[3]*0.33,f_te[4], 0.001,f_te[5], f_te[5]]
    config.crc_fiber_045 = [f_te[0]*0.45, f_te[1]*0.45,f_te[2], f_te[3]*0.45,f_te[4], 0.001,f_te[5], f_te[5]]
    # FRCCON strain model
    f_te = [ 9.97, 10.27,0.1, 8.08, 0.5, 0.01,1.5, 5.0 ] if config.mean else [ 6.52, 6.07,0.1, 4.82, 0.5, 0.01,1.5, 5.0 ]
    config.crc_fiber_130 = [f_te[0]*0.30, f_te[1]*0.30,f_te[2], f_te[3]*0.30,f_te[4], f_te[5]*0.30,f_te[6], f_te[7]]
    config.crc_fiber_133 = [f_te[0]*0.33, f_te[1]*0.33,f_te[2], f_te[3]*0.33,f_te[4], f_te[5]*0.33,f_te[6], f_te[7]]
    config.crc_fiber_145 = [f_te[0]*0.45, f_te[1]*0.45,f_te[2], f_te[3]*0.45,f_te[4], f_te[5]*0.45,f_te[6], f_te[7]]
    # MC2010 linear model
    config.crc_model_lin = [0.0,0.0,  0.0001,4.58,  0.9,0.04,  0.95,0.01,  1.0,0.0]
    if not config.mean: config.crc_model_lin = [0.0,0.0,  0.0001,2.58,  0.3,1.77,  0.3,0.0,  1.0,0.0]
    # MC2010 rigid model
    config.crc_model_rig = [0.0,0.0,  0.0001,2.69,  0.9,2.68,  0.91,0.0,  1.0,0.0]
    if not config.mean: config.crc_model_rig = [0.0,0.0,  0.0001,1.58,  0.3,1.58,  0.3,0.0,  1.0,0.0]
    # based on the tensile model
    if config.tensi_model == 'multi_ten': config.crc_multi = [0.0,0.0, 0.00014,23.33, 0.040237, 39.433, 0.100138, 39.433,
      0.200084, 14.0, 0.300056, 9.333, 0.800000, 0.0]
    # curves fitted to CMOD-P curve
    if config.tensi_model == 'multi_001': config.crc_multi = [0.0,0.0, 0.0001,4.00,  1.8,0.02,  1.9,0.01,  10.0,0.001]    #
      expands the ultimate strain
    if config.tensi_model == 'multi_002': config.crc_multi = [0.0,0.0, 0.0001,3.50,  2.8,0.02,  5.9,0.01,  10.0,0.001]    #
      expands the ultimate strain
    if config.tensi_model == 'multi_003': config.crc_multi = [0.0,0.0, 0.0001,3.80,  2.8,0.02,  5.9,0.01,  10.0,0.001]    #
      expands the ultimate strain
    if config.tensi_model == 'multi_004': config.crc_multi = [0.0,0.0, 0.0001,3.20,  2.8,0.02,  5.9,0.01,  10.0,0.001]    #
      expands the ultimate strain
    if config.tensi_model == 'multi_005': config.crc_multi = [0.0,0.0, 0.0001,3.30,  2.3,0.02,  5.9,0.01,  10.0,0.001]    #
      expands the ultimate strain
    if config.tensi_model == 'multi_006': config.crc_multi = [0.0,0.0, 0.0001,3.30,  2.0,0.02,  5.9,0.01,  10.0,0.001]    #
      expands the ultimate strain
    if config.tensi_model == 'multi_007': config.crc_multi = [0.0,0.0, 0.0001,3.40,  2.0,0.02,  5.9,0.01,  10.0,0.001]    #
      expands the ultimate strain
    if config.tensi_model.startswith('multi'):
        config.tensi_model = 'multi' # runs the multi-linear input
        if not config.mean: config.crc_multi[1::2] = [stress/1.5 for stress in config.crc_multi[1::2]]
    # the inverse analysis curve
    if config.tensi_model == 'fitted_me': config.tensi_model,config.crc_multi = 'multi', [0.0,0.0, 0.0001,3.50,  2.8,0.02,
      5.9,0.01,  10.0,0.001]
    if config.tensi_model == 'fitted_ch': config.tensi_model,config.crc_multi = 'multi', [0.0,0.0, 0.0001,3.40,  2.0,0.02,
      5.9,0.01,  10.0,0.001]
    if config.tensi_model == 'fitted_de': config.tensi_model,config.crc_multi = 'multi', [0.0,0.0, 0.0001,2.27,  2.0,0.02,
      5.9,0.01,  10.0,0.001]
    # other material properties
    config.cover         = 15
    config.crc_E         =  50000.00  if config.mean else  42000
    config.crc_poisson   =      0.20
    config.crc_f_c       =    218.00  if config.mean else (110/1.5)
    config.steel_E       = 210000.00  if config.mean else 200000
    config.steel_poisson =      0.25
    config.steel_f_y     =    550.00  if config.mean else    435
    config.rebar_E       = 210000.00  if config.mean else 200000
    config.rebar_d       =     10.00
    config.rebar_A       = 1/4.0*pi*config.rebar_d**2
    config.plate_f_y     =    500.00
    return config

def model_load(config):
    openProject("%s%s/%s/Project.dpf" % (config.home,config.path,config.folder))
```

```
def model_generate(config):
    print('generate project')
    newProject( "../%s/%s/%s" % (config.path,config.folder,config.FEM_name), 10 )
    saveProjectAs( "%s%s/%s/Project.dpf" % (config.home,config.path,config.folder))
    print('RUNNING:%s'%config.tensi_model)
    print('FOLDER:%s'%print(config.folder))
    setModelAnalysisAspects( [ "STRUCT" ] )
    setModelDimension( "2D" )
    setDefaultMeshOrder( "QUADRATIC" )
    setDefaultMesherType( "HEXQUAD" )
    setUnit( "LENGTH", "MM" )
    setUnit( "FORCE", "N" )

def model_build(config):
    model_generate(config)
    model_build_objects(config)
    model_build_materials(config)
    model_build_datasets(config)
    model_build_geometries(config)
    model_build_loads(config)
    model_build_BC(config)
    model_build_mesh(config)

def model_build_objects(config):
    print("CREATING OBJECTS")
    h_corner = 20
    createSheet( 'Block_1',    [[0,0,0],[50,0,0],[260,0,0],[260,80,0],[0,80,0],[0,h_corner,0]])
    createSheet( 'Block_2',    [[260,0,0],[450,0,0],[1470,0,0],[1470,80,0],[260,80,0]])
    createSheet( "Loadplate", [[210,80,0],[220,80,0],[220,85,0],[215,85,0],[210,85,0]])
    if config.reinforce:
      createSheet( "Support L", [[10,-10,0],[10,-15,0],[15,-15,0],[20,-15,0],[20,-10,0]])
      createSheet( "Support R", [[1365,-10,0],[1365,-15,0],[1370,-15,0],[1375,-15,0],[1375,-10,0]])
      createSheet( 'Reinforce', [[0,0,0],[0,h_corner
     ,0],[-1,80,0],[-10,80,0],[-10,-10,0],[1470,-10,0],[1470,0,0],[450,0,0],[50,0,0]])
    else:
      createSheet( "Support R", [[1365,0,0],[1365,-5,0],[1370,-5,0],[1375,-5,0],[1375,0,0]])
      createSheet( "Support L", [[10,0,0],[10,-5,0],[15,-5,0],[20,-5,0],[20,0,0]])
    createLine( "Rebar_1",      [15,20,0],[1455,20,0])
    createLine( "Rebar_2",      [275,20,0],[1455,20,0])

    if config.stirrups:
      locs = [40,85,130,175,220]
      for i in range(len(locs)): createLine( "Stirrup_%s"%(i+1), [locs[i],12,0],[locs[i], 68,0])

    fitAll()

def model_build_materials(config):
    print("CREATING MATERIALS")
    addMaterial( "CRC", "CONCR", "TSCR", [] )
    setParameter( "MATERIAL", "CRC", "LINEAR/ELASTI/YOUNG",  config.crc_E       )
    setParameter( "MATERIAL", "CRC", "LINEAR/ELASTI/POISON", config.crc_poisson )
    # crack model
    if config.rota_crac: setParameter( MATERIAL, "CRC", "MODTYP/TOTCRK", "ROTATE" )
    # tensile model
    if config.tensi_model == 'multi':
        setParameter( MATERIAL, "CRC", "TENSIL/TENCRV", "MULTLN" )
        setParameter( MATERIAL, "CRC", "TENSIL/EPSIGT", config.crc_multi )
    if config.tensi_model == 'model_lin':
        setParameter( MATERIAL, "CRC", "TENSIL/TENCRV", "MULTLN" )
        setParameter( MATERIAL, "CRC", "TENSIL/EPSIGT", config.crc_model_lin )
    if config.tensi_model == 'model_rig':
        setParameter( MATERIAL, "CRC", "TENSIL/TENCRV", "MULTLN" )
        setParameter( MATERIAL, "CRC", "TENSIL/EPSIGT", config.crc_model_rig )
    if config.tensi_model == 'fiber_030':
        setParameter( "MATERIAL", "CRC", "TENSIL/TENCRV", "FRCCON" )
        setParameter( "MATERIAL", "CRC", "TENSIL/FRCCMD", config.crc_fiber_030 )
    if config.tensi_model == 'fiber_033':
        setParameter( "MATERIAL", "CRC", "TENSIL/TENCRV", "FRCCON" )
        setParameter( "MATERIAL", "CRC", "TENSIL/FRCCMD", config.crc_fiber_033 )
    if config.tensi_model == 'fiber_045':
        setParameter( "MATERIAL", "CRC", "TENSIL/TENCRV", "FRCCON" )
        setParameter( "MATERIAL", "CRC", "TENSIL/FRCCMD", config.crc_fiber_045 )
    if config.tensi_model == 'fiber_130':
        setParameter( "MATERIAL", "CRC", "TENSIL/TENCRV", "FRCCON" )
        setParameter( MATERIAL, "CRC", "TENSIL/FRCTYP", "STRAIN" )
        setParameter( MATERIAL, "CRC", "TENSIL/FRCEPS", config.crc_fiber_130 )
    if config.tensi_model == 'fiber_133':
        setParameter( "MATERIAL", "CRC", "TENSIL/TENCRV", "FRCCON" )
        setParameter( MATERIAL, "CRC", "TENSIL/FRCTYP", "STRAIN" )
        setParameter( MATERIAL, "CRC", "TENSIL/FRCEPS", config.crc_fiber_133 )
    if config.tensi_model == 'fiber_145':
        setParameter( "MATERIAL", "CRC", "TENSIL/TENCRV", "FRCCON" )
        setParameter( MATERIAL, "CRC", "TENSIL/FRCTYP", "STRAIN" )
        setParameter( MATERIAL, "CRC", "TENSIL/FRCEPS", config.crc_fiber_145 )
    if config.tensi_model == 'brittle':
        setParameter( "MATERIAL", "CRC", "LINEAR/ELASTI/YOUNG", config.crc_E )
        setParameter( "MATERIAL", "CRC", "LINEAR/ELASTI/POISON", config.crc_poisson )
        setParameter( "MATERIAL", "CRC", "TENSIL/TENCRV", "BRITTL" )
        setParameter( "MATERIAL", "CRC", "TENSIL/TENSTR", 3.33 )
        setParameter( "MATERIAL", "CRC", "TENSIL/RESTST", 0.1 )

    # compression model
    if config.compr_model == 'EC2':
        setParameter( "MATERIAL", "CRC", "COMPRS/COMCRV", "EC2" )
        setParameter( "MATERIAL", "CRC", "COMPRS/COMSTR", config.crc_f_c )
```

```
        setParameter( "MATERIAL", "CRC", "COMPRS/EPSC1",  config.crc_f_c/config.crc_E )
        setParameter( "MATERIAL", "CRC", "COMPRS/EPSCU",  config.crc_f_c/config.crc_E )
        setParameter( "MATERIAL", "CRC", "COMPRS/YOUNCM", config.crc_E )
    if config.compr_model == 'MC1990':
        setParameter( MATERIAL, "CRC", "COMPRS/COMCRV", "MC1990" )
        setParameter( MATERIAL, "CRC", "COMPRS/COMSTR", config.crc_f_c )

    if config.reinforce:
        addGeometry( "interface_GEO", "LINE", "STLIIF", [] )
        setParameter( "GEOMET", "interface_GEO", "LIFMEM/THICK", 100)
        addMaterial( "interface_MAT", "INTERF", "ELASTI", [] )
        setParameter( "MATERIAL", "interface_MAT", "LINEAR/IFTYP", "LIN2D" )
        setParameter( "MATERIAL", "interface_MAT", "LINEAR/ELAS2/DSNY", 1000*config.rebar_E/100 )
        setParameter( "MATERIAL", "interface_MAT", "LINEAR/ELAS2/DSSX", 0)
        createConnection( "INTERFACE", "INTER", "SHAPEEDGE" )
        setParameter( "GEOMETRYCONNECTION", "INTERFACE", "MODE", "AUTO" )
        attachTo( "GEOMETRYCONNECTION", "INTERFACE", "SOURCE", "Block_1", [[ 170, 0, 0 ]] )
        attachTo( "GEOMETRYCONNECTION", "INTERFACE", "SOURCE", "Block_2", [[ 370, 0, 0 ]] )
        attachTo( "GEOMETRYCONNECTION", "INTERFACE", "SOURCE", "add2", [[ 280, 0, 0 ]] )
        setElementClassType( "GEOMETRYCONNECTION", "INTERFACE", "STLIIF" )
        assignMaterial( "interface_MAT", "GEOMETRYCONNECTION", "INTERFACE" )
        assignGeometry( "interface_GEO", "GEOMETRYCONNECTION", "INTERFACE" )
        setParameter( "GEOMETRYCONNECTION", "INTERFACE", "FLIP", False )
        resetElementData( "GEOMETRYCONNECTION", "INTERFACE" )

        addMaterial( "Plate", "STEEDC", "N6720B", [] )
        setParameter( "MATERIAL", "Plate", "N6720B/PLTYPE", "PLASTI" )
        setParameter( "MATERIAL", "Plate", "N6720B/GRADE", "FEB500" )
        setParameter( "MATERIAL", "Plate", "N6720B/PLASTI/FEB500/YLDSTR", config.plate_f_y )
        setParameter( "MATERIAL", "Plate", "N6720B/POISON", 0.3 )

    addMaterial( "Steel", "MCSTEL", "ISOTRO", [] )
    setParameter( "MATERIAL", "Steel", "LINEAR/ELASTI/YOUNG", config.steel_E )
    setParameter( "MATERIAL", "Steel", "LINEAR/ELASTI/POISON", config.steel_poisson )

    if config.yielding:
        addMaterial( "Rebar", "REINFO", "UNIAXI", [] )
        setParameter( "MATERIAL", "Rebar", "ELASTI/EPSSIG", [ 0, 0, config.steel_f_y/config.rebar_E, config.steel_f_y, 0.1,
     config.steel_f_y ] )
        setParameter( MATERIAL, "Rebar", "ELASTI/ELASTI/YOUNG", config.rebar_E )
    else:
        addMaterial( "Rebar", "REINFO", "LINEAR", [] )
        setParameter( "MATERIAL", "Rebar", "LINEAR/ELASTI/YOUNG", config.rebar_E )

def model_build_datasets(config):
    print("CREATING DATASETS")
    if config.incr_inte:
        addElementData( "dataset" )
        setParameter( DATA, "dataset", "INTEGR", "HIGH" )
        assignElementData( "dataset", SHAPE, ['Block_1','Block_2',"Support R","Support L", "Loadplate"] )

def model_build_geometries(config):
    print("CREATING GEOMETRIES")
    for block in [config.block_1,config.block_2]:
        addGeometry( block[3], "SHEET", "MEMBRA", [] )
        setParameter( "GEOMET", block[3], "THICK", block[0] )

        clearReinforcementAspects( [ block[3] ] )
        setElementClassType( [ block[3] ], "MEMBRA" )
        assignMaterial( "CRC", "SHAPE", [ block[3] ] )
        assignGeometry( block[3], "SHAPE", [ block[3] ] )
        resetElementData( "SHAPE", [ block[3] ] )

    supports = [ "Support L", "Loadplate", "Support R" ]

    clearReinforcementAspects( supports )
    setElementClassType( supports, "MEMBRA" )
    assignMaterial( "Steel", "SHAPE", supports )
    assignGeometry( config.block_1[3], "SHAPE", supports )
    resetElementData( "SHAPE", supports )

    if config.reinforce:
        blokken = ['Reinforce']
        clearReinforcementAspects( blokken )
        setElementClassType( blokken, "MEMBRA" )
        assignMaterial( "Plate", "SHAPE", blokken )

        addGeometry( "plate_GEO", "SHEET", "MEMBRA", [] )
        setParameter( "GEOMET", "plate_GEO", "THICK", 100 )
        assignGeometry( "plate_GEO", "SHAPE", blokken )
        resetElementData( "SHAPE", blokken )

    if config.stirrups:
        addGeometry( "Stirrups", "RELINE", "REBAR", [] )
        setParameter( "GEOMET", "Stirrups", "REIEMB/CROSSE", (1/4)*3.14159265359*6**2*4)
        stirrups = ['Stirrup_1','Stirrup_2','Stirrup_3','Stirrup_4','Stirrup_5']
        setReinforcementAspects( stirrups )
        assignMaterial( "Rebar", "SHAPE", stirrups )
        assignGeometry( "Stirrups", "SHAPE", stirrups )
        resetElementData( "SHAPE", stirrups )
        setReinforcementDiscretization( stirrups, "ELEMENT" )

    addGeometry( "Rebar_1", "RELINE", "REBAR", [] )
    setParameter( "GEOMET", "Rebar_1", "REIEMB/CROSSE", config.rebar_A*config.block_1[2])
    setReinforcementAspects( [ "Rebar_1" ] )
    assignMaterial( "Rebar", "SHAPE", [ "Rebar_1" ] )
```

```
    assignGeometry( "Rebar_1", "SHAPE", [ "Rebar_1" ] )
    resetElementData( "SHAPE", [ "Rebar_1" ] )
    setReinforcementDiscretization( [ "Rebar_1" ], "ELEMENT" )

    addGeometry( "Rebar_2", "RELINE", "REBAR", [] )
    setParameter( "GEOMET", "Rebar_2", "REIEMB/CROSSE", config.rebar_A*(config.block_2[2]-config.block_1[2]))
    setReinforcementAspects( [ "Rebar_2" ] )
    assignMaterial( "Rebar", "SHAPE", [ "Rebar_2" ] )
    assignGeometry( "Rebar_2", "SHAPE", [ "Rebar_2" ] )
    resetElementData( "SHAPE", [ "Rebar_2" ] )
    setReinforcementDiscretization( [ "Rebar_2" ], "ELEMENT" )

def model_build_loads(config):
    print("ADD LOADS")
    addSet( "GEOMETRYLOADSET", "loadcase_1" )
    createPointLoad( "P", "loadcase_1" )
    setParameter( "GEOMETRYLOAD", "P", "LODTYP", "DEFORM" )
    setParameter( "GEOMETRYLOAD", "P", "DEFORM/TR/VALUE", -1 )
    setParameter( "GEOMETRYLOAD", "P", "DEFORM/TR/DIRECT", 2 )
    setParameter( "GEOMETRYLOAD", "P", "DEFORM/TR/VALUE", -1 )
    attach( "GEOMETRYLOAD", "P", "Loadplate", [[ config.sup_l[1], config.block_h+config.sup_h, 0 ]] )

def model_build_BC(config):
    print("ADD BOUNDARY CONDITIONS")
    addSet( "GEOMETRYSUPPORTSET", "supports_1" )
    createPointSupport( "fix_x", "supports_1" )
    setParameter( "GEOMETRYSUPPORT", "fix_x", "AXES", [ 1, 2 ] )
    setParameter( "GEOMETRYSUPPORT", "fix_x", "TRANSL", [ 1, 0, 0 ] )
    setParameter( "GEOMETRYSUPPORT", "fix_x", "ROTATI", [ 0, 0, 0 ] )
    createPointSupport( "fix_y", "supports_1" )
    setParameter( "GEOMETRYSUPPORT", "fix_y", "AXES", [ 1, 2 ] )
    setParameter( "GEOMETRYSUPPORT", "fix_y", "TRANSL", [ 0, 1, 0 ] )
    setParameter( "GEOMETRYSUPPORT", "fix_y", "ROTATI", [ 0, 0, 0 ] )

    x = -10 if config.reinforce else 0
    attach( "GEOMETRYSUPPORT", "fix_x", "Support L", [[ config.sup_l[0], -config.sup_h+x, 0 ]] )
    attach( "GEOMETRYSUPPORT", "fix_y", "Support L", [[ config.sup_l[0], -config.sup_h+x, 0 ]] )
    attach( "GEOMETRYSUPPORT", "fix_y", "Loadplate", [[ config.sup_l[1], config.block_h+config.sup_h, 0 ]] )
    attach( "GEOMETRYSUPPORT", "fix_y", "Support R", [[ config.sup_l[2], -config.sup_h+x, 0 ]] )

def model_build_mesh(config):
    print("CREATE MESH")
    elements = [ config.block_2[3], "Loadplate", "Support L", "Support R" ]
    if config.reinforce: elements += ['Reinforce']
    setElementSize(  elements, config.mesh_size )
    setElementSize(  [config.block_1[3]], 10 )
    setMesherType(   elements+[config.block_1[3]], "HEXQUAD" )
    generateMesh( [] )

def model_run_create(config):
    print("CREATE ANALYSIS")
    addAnalysis(config.analyse)
    addAnalysisCommand( config.analyse, "NONLIN", "Structural nonlinear" )
    def temp(a,b): setAnalysisCommandDetail( config.analyse, "Structural nonlinear", a,b)
    temp("EXECUT(1)/LOAD/STEPS/EXPLIC/SIZES", config.steps )
    addAnalysisCommandDetail( config.analyse, "Structural nonlinear", "EXECUT(1)/LOAD/STEPS/EXPLIC/ARCLEN" )
    temp("EXECUT(1)/LOAD/STEPS/EXPLIC/ARCLEN", config.con_arclen )
    temp("EXECUT(1)/ITERAT/MAXITE", config.max_iterations )
    temp("EXECUT(1)/ITERAT/CONVER/DISPLA/TOLCON", 0.001 )
    temp("EXECUT(1)/ITERAT/CONVER/DISPLA/TOLCON", 0.04 )
    temp("EXECUT(1)/ITERAT/CONVER/FORCE/TOLCON",  0.04 )
    temp("EXECUT(1)/ITERAT/CONVER/FORCE",  config.con_force )
    temp("EXECUT(1)/ITERAT/CONVER/ENERGY", config.con_energ )
    temp("EXECUT(1)/ITERAT/CONVER/SIMULT", True )
    temp("EXECUT(1)/ITERAT/METHOD/NEWTON/TYPNAM", "MODIFI" )
    renameAnalysisCommandDetail( config.analyse, "Structural nonlinear", "OUTPUT(1)", "Output" )
    temp("OUTPUT(1)/SELTYP", "USER" )
    addAnalysisCommandDetail( config.analyse, "Structural nonlinear", "OUTPUT(1)/USER" )
    temp("EXECUT(1)/ITERAT/CONVER/DISPLA", config.con_displ )
    temp("EXECUT(1)/ITERAT/LINESE", config.incr_inte)

def model_run_output(config):
    def add(output): addAnalysisCommandDetail( config.analyse, "Structural nonlinear", "OUTPUT(1)/USER/%s" % output )
    add("DISPLA(1)/TOTAL/TRANSL/GLOBAL" )
    add("STRESS(1)/TOTAL/CAUCHY/PRINCI" )
    add("STRESS(2)/TOTAL/CAUCHY/LOCAL" )
    add("STRESS(3)/CRACK/CAUCHY/LOCAL" )
    add("STRAIN(1)/TOTAL/GREEN/GLOBAL" )
    add("STRAIN(2)/TOTAL/GREEN/VONMIS" )
    add("STRAIN(4)/TOTAL/TRACTI/GLOBAL" )
    add("STRAIN(5)/TOTAL/TRACTI/LOCAL" )
    add("STRAIN(6)/CRACK/GREEN" )
    add("STRAIN(7)/CRKWDT/GREEN" )
    add("STRAIN(8)/TOTAL/GREEN/PRINCI" )
    add("FORCE(1)/REACTI/TRANSL/GLOBAL" )

def model_run(config):
    model_run_create(config)
    model_run_output(config)
    model_save(config)
    print("RUN THE ANALYSIS")
    runSolver(config.analyse)

def model_save(config):
    print("SAVE THE GENERATED MODEL")
    saveProjectAs( "%s%s/%s/Project.dpf" % (config.home,config.path,config.folder) )
```

```
    exportModel("Model.dat", 10 )
    saveAnalysisCommands( config.analyse, "Analyse_commands.dcf")

def model_import(config):
    print('NOT IMPLEMENTED!!')

def model_export(config):
    print('EXPORTING DATA')
    mm = 0.1
    cases = resultCases(config.analyse,'Output')
    nodes = nodesTable(config.analyse)
    nodes = list(filter(lambda x: abs (x[1] - config.block_1[1]) < mm, nodes))
    table = [ config.analyse, 'Output', 'Cauchy Total Stresses', 'S1']
    exportResultsToCSV( 'sigma_xx.csv', table, cases, [1] )

    nodes  = findNearestNodes([(config.sup_1[1],config.block_h+config.sup_h,0)])
    table = [ config.analyse, 'Output', 'Reaction Forces']
    exportResultsToCSV( 'ReactionForces.csv', table, cases, nodes )

    print('EXPORTING IMAGES')
    setResultPlot( "contours", "Total Strains/node", "E1" )
    setViewSettingValue( "view setting", "RESULT/DEFORM/MODE", "OFF" )
    setViewSettingValue( "view setting", "RESULT/TITLE/SHOW", False )
    setViewSettingValue( "view setting", "RESULT/LEGEND/SHOW", False )
    setResultPlot( "contours", "Total Strains/node", "E1" )
    setViewSettingValue( "view setting", "RESULT/CONTOU/LEGEND", "DISCRE" )
    setViewSettingValue( "view setting", "RESULT/CONTOU/AUTRNG", "LIMITS" )
    setViewSettingValue( "view setting", "RESULT/CONTOU/LIMITS/MINVAL", -0.006 )
    setViewSettingValue( "view setting", "RESULT/CONTOU/LIMITS/BOUNDS", "CLAMP" )
    setViewSettingValue( "view setting", "RESULT/CONTOU/LIMITS/MAXVAL", 0.042 )

    cvp1 = ( 0.13604597, 0.048823687, 16.111854, 0, 1, 0, 0.13604597, 0.048823687, -2.7755576e-17, 0.65078904, 0.090460861)
      # with margins
    cvp1 = ( 0.15078169, 0.040121712, 16.111854, 0, 1, 0, 0.15078169, 0.040121712, -8.3266727e-17, 0.33395768, 0.046420725)
    cvp1 = ( 0.16052275, 0.033672337, 16.111866, 0, 1, 0, 0.17052275, 0.033672337, 1.2252505e-05, 0.40408879, 0.056169077) #
      for raqtan 2 en 3
    setViewPoint(cvp1)

    cases = resultCases(config.analyse,'Output')
    targets = [2.5,5.0,7.5,10.0]
    for case in cases:
      if len(targets)==0:break
      if float(case.split(" ")[3][:-1])>targets[0]:
        setResultCase('%s/Output/%s' % (config.analyse,case))
        print(targets[0],case)
        # writeToPng( "Raqtan_FEM_%s_%smm.png"%(config.tag,str(targets[0]).replace(".","")), 1147, 556) # with margins
        writeToPng( "Raqtan_FEM_%s_%s_%smm.png"%(config.tensi_model,config.tag,str(targets[0]).replace(".","")), 924, 284)
        targets = targets[1:]

def analyse_model(config,do_diana):
    config = model_setup(config)
    if do_diana.load:  model_load(config)
    if do_diana.build: model_build(config)
    if do_diana.run:   model_run(config)
    if do_diana.imp:   model_import(config)
    if do_diana.exp:   model_export(config)
    print('Finished')

def analyse_models(config,do_diana):
    for prop in vars(config):
        if isinstance(vars(config)[prop], list):
            for item in vars(config)[prop]:
                b = copier(config)
                b.__dict__[prop] = item
                analyse_models(b,do_diana)
            return
    analyse_model(config,do_diana)

def model_import(config):
    addAnalysis(config.analyse)
    loadResults(config.analyse,'%s.dnb'% config.analyse)

class env():
    def __init__(self): return

def copier(config):
    temp = env()
    for prop in vars(config): temp.__dict__[prop] = vars(config)[prop]
    return temp

config = env()
config.home           = '__PATH_TO_THE_FOLDER_WHERE_TO_STORE_THE_RESULT_FOLDERS__/'
config.path           = '01 FEM/PBT317-119 Raqtan'
config.project        = 'Raqtan Cali'
config.FEM            = '2D_001'
config.steps          = '0.05(250)'
config.tag            = '004'

config.stirrups       = False   # boolean
config.reinforce      = False   # boolean
config.mean           = True    # boolean
config.yielding       = True    # boolean
config.incr_inte      = True    # boolean
config.con_arclen     = True    # boolean
config.con_linese     = True    # boolean
config.con_force      = True    # boolean
```

```
config.con_displ      = True    # boolean
config.con_energ      = False   # boolean
config.rota_crac      = True    # boolean
config.plane_strain   = False   # boolean

config.tensi_model    = 'fitted_me'
config.compr_model    = 'default' # default,EC2
config.mesh_size      = 20
config.max_iterations = 1000

do_diana = env()
t,f = True,False
do_diana.build  = t
do_diana.load   = f
do_diana.run    = t
do_diana.imp    = f
do_diana.exp    = t

####################################
#### Test run ######################
####################################
analyse_models(config,do_diana)

####################################
#### RAQTAN004 #####################
####################################
temp                = copier(config)
temp.tensi_model    = ['fitted_me','fiber_033','fiber_045','fiber_133','fiber_145','model_lin','model_rig']
analyse_models(temp,do_diana)

####################################
#### RAQTAN002 #####################
####################################
temp                = copier(config)
temp.tensi_model    = ['fitted_me','fiber_033','fiber_045','fiber_133','fiber_145','model_lin','model_rig']
temp.tag            = '003'
temp.reinforce      = True
analyse_models(temp,do_diana)

####################################
#### RAQTAN001 #####################
####################################
temp                = copier(config)
temp.tensi_model    = ['fitted_me','fiber_033','fiber_045','fiber_133','fiber_145','model_lin','model_rig']
temp.tag            = '001'
temp.stirrups       = True
analyse_models(temp,do_diana)
```

E

Validation of FE models

For this part the DIANA models were set up to resemble the experiments as close as possible. This was accomplished by implementing multiple modifications. First of all the material properties were updated to correspond with the values derived from lab tests: The CMOD curve and the compression strength were updated. The configuration of the elements was also set to the exact tested configuration, as shown in Figure E.1. The results of the FE models were compared to the output from the DIC analysis and the load-deflection curve found in the experiments. This appendix only visually compares the results, for the discussion the reader is referred to Chapter 11.

(a) The model for the RAQTAN_1-A element, with stirrups and without modifications.

(b) The model for the RAQTAN_2-B and RAQTAN_3-B elements, without stirrups and with modifications.

(c) The model for the RAQTAN_4-B elements, without stirrups and without modifications.

Figure E.1: The models used for the recalibration.

E.1. Load-displacement curves

The load-displacement curves for the Raqtan elements and their corresponding FE models are shown below.

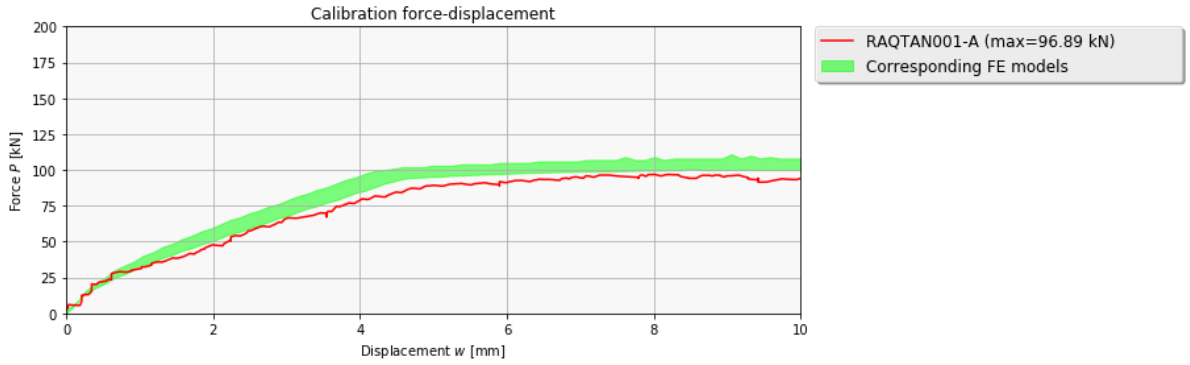

Figure E.2: Validation of FE model RAQTAN_1-A : Load-displacement .

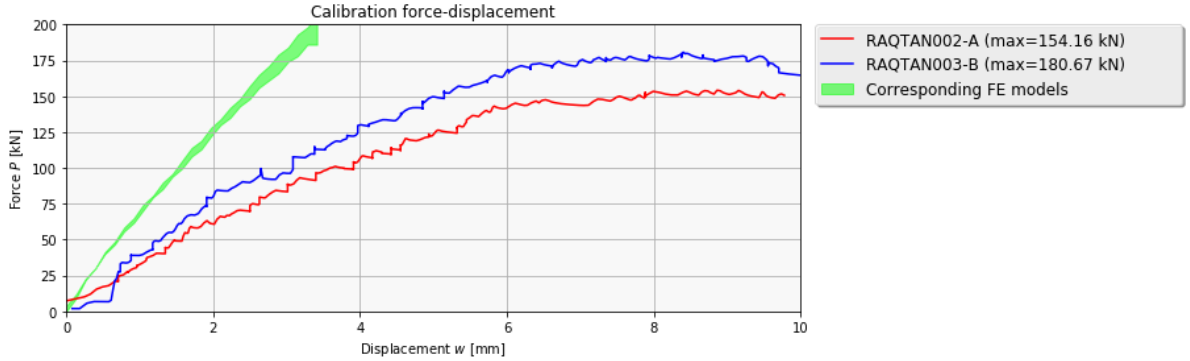

Figure E.3: Validation of FE model RAQTAN_2-B and RAQTAN_3-B : Load-displacement .

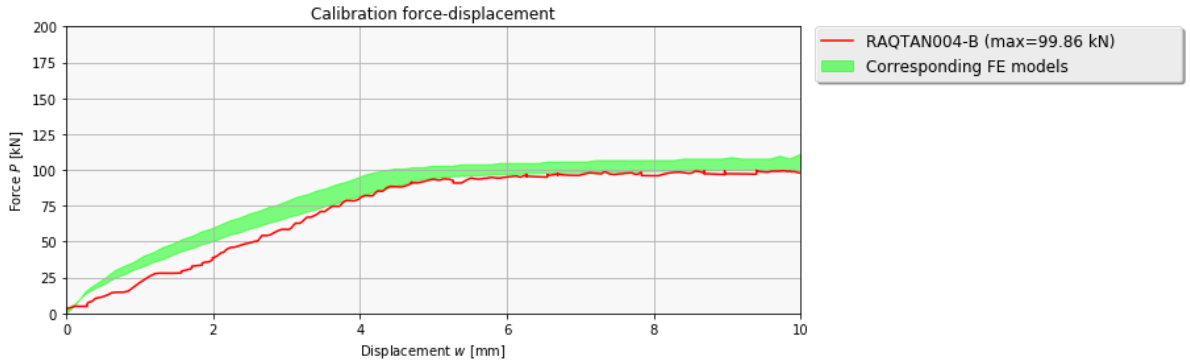

Figure E.4: Validation of FE model RAQTAN_4-B : Load-displacement .

E.2. Strain fields

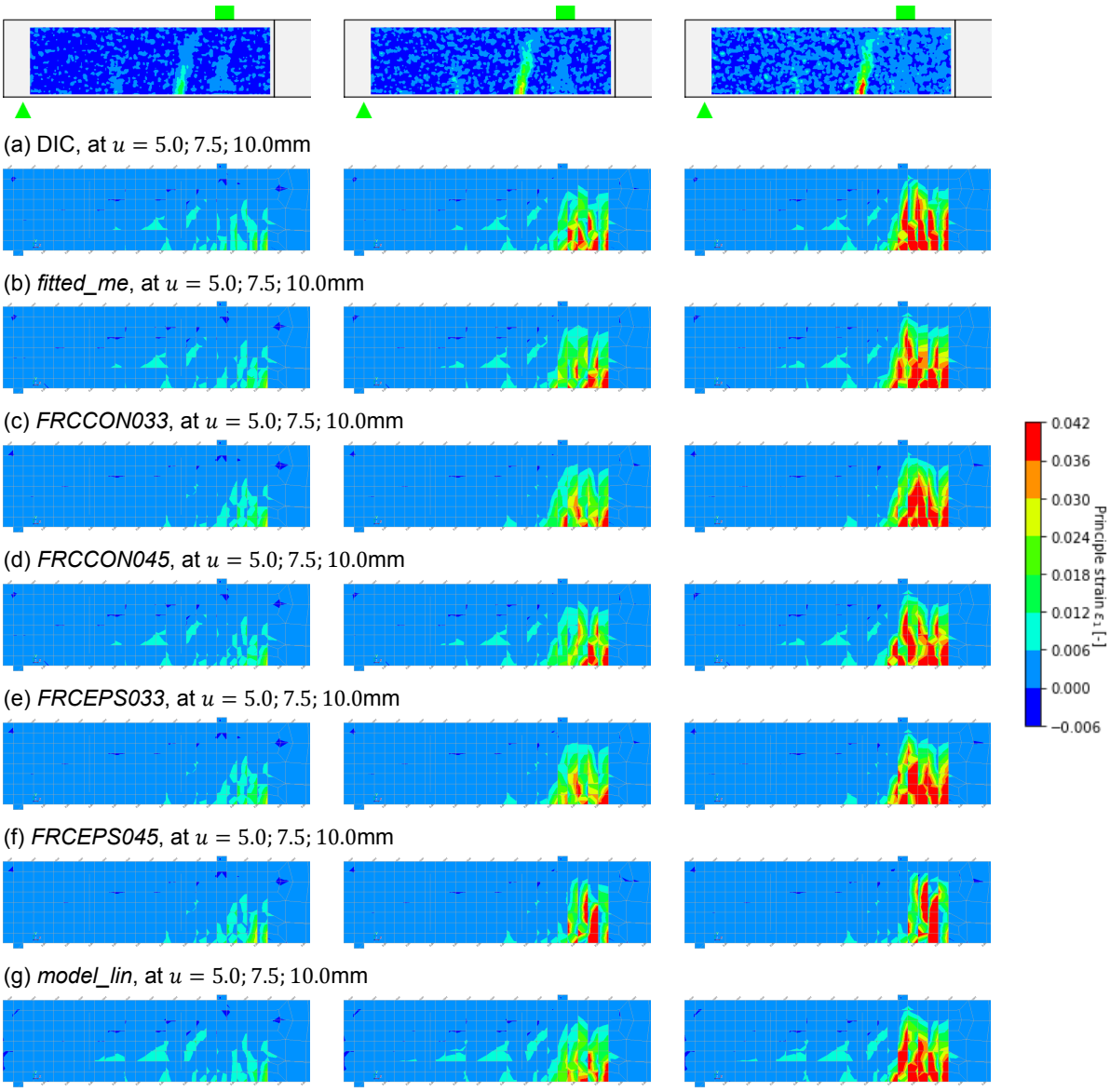

(a) DIC, at $u = 5.0; 7.5; 10.0$mm

(b) *fitted_me*, at $u = 5.0; 7.5; 10.0$mm

(c) *FRCCON033*, at $u = 5.0; 7.5; 10.0$mm

(d) *FRCCON045*, at $u = 5.0; 7.5; 10.0$mm

(e) *FRCEPS033*, at $u = 5.0; 7.5; 10.0$mm

(f) *FRCEPS045*, at $u = 5.0; 7.5; 10.0$mm

(g) *model_lin*, at $u = 5.0; 7.5; 10.0$mm

(h) *model_rig*, at $u = 5.0; 7.5; 10.0$mm

Figure E.5: The strain field at multiple deflection stages for DIC and FEA compared for RAQTAN_1-A .

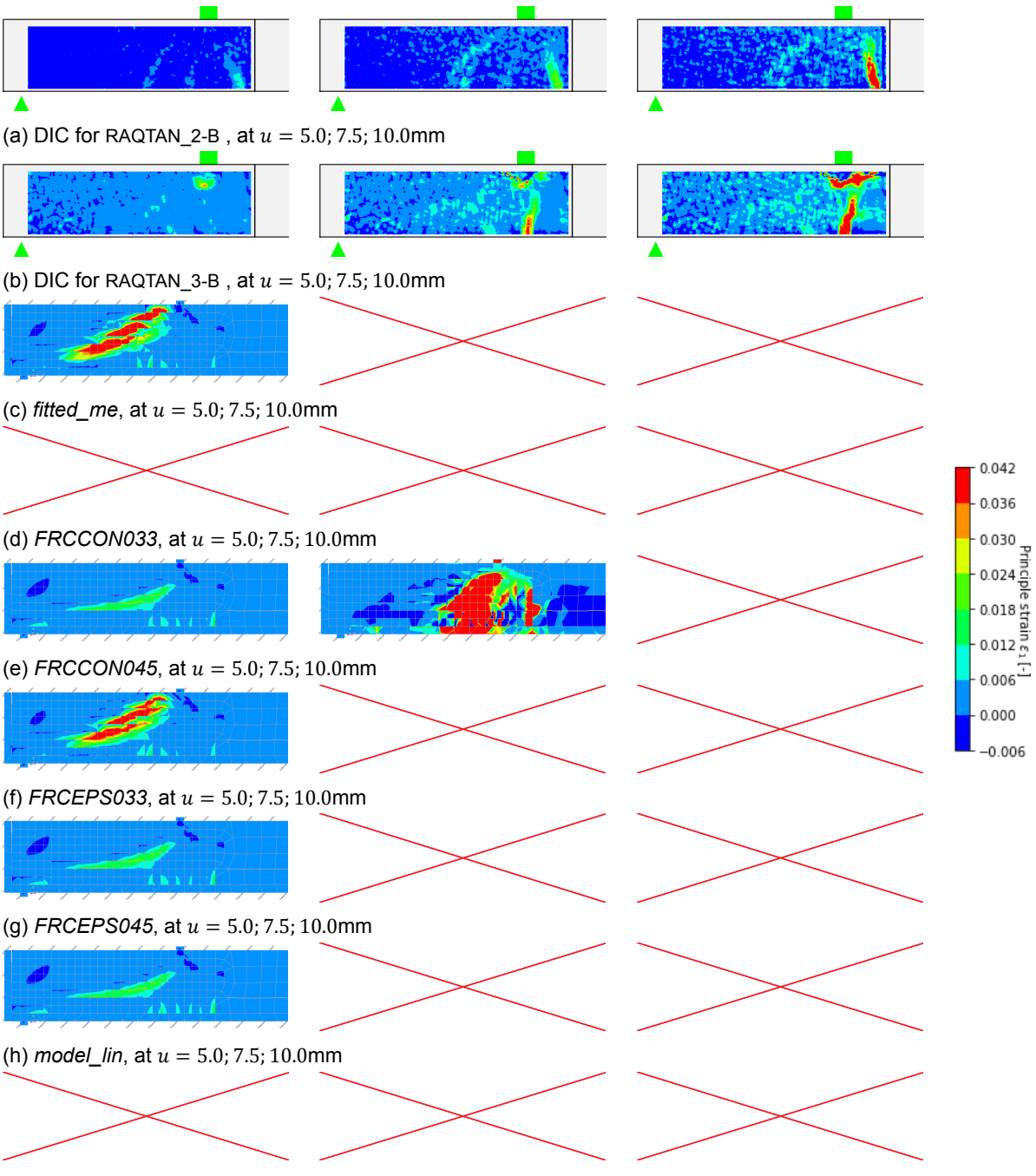

(a) DIC for RAQTAN_2-B , at $u = 5.0; 7.5; 10.0$mm

(b) DIC for RAQTAN_3-B , at $u = 5.0; 7.5; 10.0$mm

(c) *fitted_me*, at $u = 5.0; 7.5; 10.0$mm

(d) *FRCCON033*, at $u = 5.0; 7.5; 10.0$mm

(e) *FRCCON045*, at $u = 5.0; 7.5; 10.0$mm

(f) *FRCEPS033*, at $u = 5.0; 7.5; 10.0$mm

(g) *FRCEPS045*, at $u = 5.0; 7.5; 10.0$mm

(h) *model_lin*, at $u = 5.0; 7.5; 10.0$mm

(i) *model_rig*, at $u = 5.0; 7.5; 10.0$mm

Figure E.6: The strain field at multiple deflection stages for DIC and FEA compared for RAQTAN_2-B and RAQTAN_3-B . A red cross means that shear failure occurred before the mentioned displacement is reached.

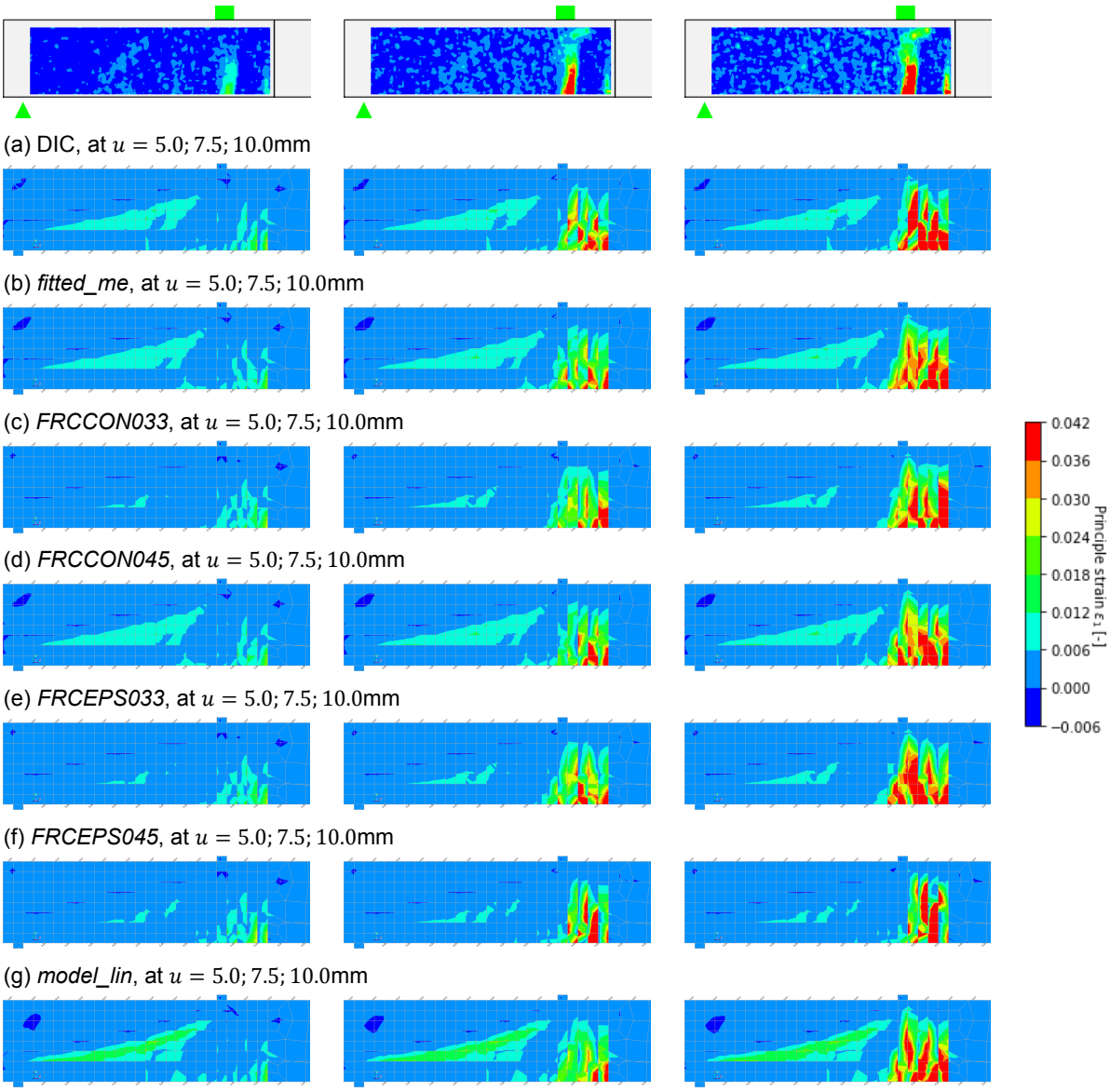

(a) DIC, at $u = 5.0; 7.5; 10.0$mm

(b) *fitted_me*, at $u = 5.0; 7.5; 10.0$mm

(c) *FRCCON033*, at $u = 5.0; 7.5; 10.0$mm

(d) *FRCCON045*, at $u = 5.0; 7.5; 10.0$mm

(e) *FRCEPS033*, at $u = 5.0; 7.5; 10.0$mm

(f) *FRCEPS045*, at $u = 5.0; 7.5; 10.0$mm

(g) *model_lin*, at $u = 5.0; 7.5; 10.0$mm

(h) *model_rig*, at $u = 5.0; 7.5; 10.0$mm

Figure E.7: The strain field at multiple deflection stages for DIC and FEA compared for RAQTAN_4-B .